Axial, Shear and Moment Interaction of Single Plate "Shear Tab" Connections

by

Scott L. Thompson

A Report Submitted to the Faculty of the

Milwaukee School of Engineering

in Partial Fulfillment of the

Requirements for the Degree of

Master of Science in Structural Engineering

Milwaukee, Wisconsin

May 2009

Abstract

The construction and engineering fields have long used simple shear connections such as single plates, single angles, and t-sections as supports for framing members in steel framed structures due to their relative simplicity and cost effectiveness of fabrication and erection. Historically these connections have been thought to support vertical shear loads exclusively; however, knowledge of their ability to support axial forces and moments has been speculated but seldom verified.

The purpose of this research is to provide observations and numerical verification of the single plate "Shear Tab" connection's ability to support the combination of shear, axial, and moment forces as a result of a simulated column failure. This research presents a historical background of the single plate connection's development along with providing insight into the connection's ability to utilize catenary action as an inherent secondary load transfer mechanism.

Nine full scale tests simulating an interior column failure have been conducted for various depths of single plate connections. Shear, axial, and moment forces, as well as beam end rotation values have been derived from experimentally measured strain and deflection data to provide numerical evidence of the various observed connection rupture failures. A preliminary bolt force analysis technique has been developed to provide an understanding of the connection's behavior prior to failure as well as to provide comparisons between the observed failure mechanisms and those expected using the current steel specification.

This research has shown the single plate connection has a low level ability to transform from a shear and flexural response to catenary tension. The experimental data suggest the shear tab connection alone could not support its intended design level shear load in the event of a catastrophic loss of a supporting column.

Acknowledgments

The completion of this research was not possible without the assistance and donations of many organizations and people. I would like thank the American Institue of Steel Construction Foundation and US Steel Corporation for providing the financial backing neccasary for the success of this project. I would also like to thank Germantown Iron and Steel for their donation of fabrication time and materials. I want to thank the Milwaukee School of Engineering for the use of the laboratory facilities as well as the wonderful professors and faculty which make MSOE a top university.

I want to say a big thank you to my advisor Professor Chris Raebel for his ongoing support, motivation, and donation of time and knowledge throught the extent of this research. Thank you to Chris Foley, Ph.D., at Marquette University for his enthusiam and donation of test equipment. Thank you to H. Peter Huttelmaier, Ph.D., and Richard Devries, Ph.D. at MSOE as well as my collegues at Computerized Strucutral Design for their knowledge and guidance throughout this research.

I would like to thank Adam Friedman and Matthew Johnson for their dedication, knowledge, and friendship as they worked alongside me on their own repsective research.

I would like to express my great appreciation to my parents, Richard and Merna, to whom I am eternally grateful for their sacrifices throughout my life which allowed me to complete this research. I also want to thank Kelly, Julie, Corey, as well as my family and friends for their own unique encouragement which helped push me through this process.

Last, but certainly not least, thank you to my wife, Heather, for her tireless love, support, and understanding throughout this process; and the sacrifice of weekends which allowed me to complete this project. You have served as a great motivator and cofidant throughout this project. I love you; you can have your husband back now.

Table of Contents

List of Figures

List of Tables

Nomenclature

Symbols

a = horizontal distance from the bolt line to the weld line, inch.

a_c = distance from column flange to column centerline, inch.

c_n = distance from strain gage ‘n’ to the neutral axis of the supported beam.

d = nominal bolt diameter, inch.

d_b = bolt diameter, inch.

d_{bg} = depth of the bolt group, inch.

d_{max} = maximum distance from the bolt group centroid to the beam flange, inch.

e = natural logarithm equal to 2.71828…

e_b = bolt design eccentricity, inch.

e_w = eccentricity taken as ‘n’ bolts in inches from the weld line.

f_t = applied normal tension stress, ksi.

f_v = applied normal shear stress, ksi.

g = horizontal distance from the face of support to supported beam end, inch.

h = hole pattern depth.

h_a = vertical distance from beam support to column support ‘A’, inch.

h_b = vertical distance from beam support to column support ‘B’, inch.

k_s = elastic rotational stiffness

n = number of bolts.

t = thickness of the connected material, inch.

y = vertical deflection at failed column, inch.

x_b = horizontal distance from the true pin connection to the bolt line, inch.

x_f = horizontal distance from the true pin connection to the supporting column flange, inch.

x_{sg} = horizontal distance from the true pin connection to the strain gage, inch.

A = cross sectional area, in.^{2}.

A_{gv} = gross shear area, in.^{2}.

A_{nv} = net shear area, in.^{2}.

A_{nt} = net tension area, in.^{2}.

C = eccentricity coefficient per the ICOR method analysis.

E = Modulus of elasticity of steel, 29,000 ksi.

F = applied shear force, kips.

F_t = maximum principal tensile stress based on material capacity, ksi.

F_u = specified minimum tensile strength of the connected material, ksi.

F_v = maximum principal shear stress based on material capacity, ksi.

$H_{mx,n}$ = horizontal bolt force component due to measured moment ICOR analysis, kips.

$H_{my,n}$ = vertical bolt force component due to measured moment ICOR analysis, kips.

I_x = strong axis moment of inertia, in.^{4}.

L = framing bay width, inch.

L_b = distance between the centerlines of the beam supports, inch.

L_c = clear edge distance in the direction of force between the edge of the hole and the edge of the adjacent hole or the edge of the connected material, inch.

L_{eh} = horizontal distance from the center of bolt to plate edge, inch.

L_{ev} = vertical distance from the center of bolt to plate edge, inch.

L_{sg} = horizontal distance from the true pin connection to the strain gages, inch.

L_w = Whitmore Section length, inch.

M = theoretic moment in the connection, kip-inch.

M^* = intermediate non-dimensional moment value.

M_b = flexural force at the bolt line, kip-inch.

M_M = measured moment, kip-inch.

$M_{M,\,max}$ = maximum connection moment capacity based on a moment only ICOR analysis, kip-inch.

M_{ref} = reference moment based on a pure moment applied to a connection with all bolts loaded to their maximum capacity, kip-inch.

M_y = yield moment, kip-inch.

N = normal force, kips.

P = applied axial force, kips.

P_x = horizontal axial force component at each bolt, kips.

P_y = vertical axial force component at each bolt, kips.

R_a = horizontal reaction at support ‘A’, kips.

R_b= horizontal reaction at support ‘B’, kips.

ϕR_{bst} = LRFD block shear rupture capacity in the direction of the applied tensile force, kips.

ϕR_{bsv} = LRFD block shear rupture capacity in the direction of the applied shear force, kips.

R = nominal shear strength of one bolt at deformation Δ, kips.

R_v = resultant bolt line shear force of applied shear and measured axial force, kips.

$R_{v,\,max}$ = ultimate connection shear capacity base the number of bolts times the ultimate experimental bolt shear value, kips.

R_T = Vertical reaction at the true pin connection, kips.

R_u = resultant shear vector, kips.

R_{ult} = ultimate shear strength of one bolt, kips.

R_y = Vertical reaction at the true pin connection for side ‘x’, kips.

T = pure catenary tensile force, kips.

T_u = factored tension force using LRFD load combinations, kips.

U_{bs} = factor of 1.0 for uniform tension stress.

$V_{b\ max,n}$ = resultant bolt shear force due to the forces at the point of the maximum measured moment, kips.

V_u = factored shear force using LRFD load combinations, kips.

$V_{mx,n}$ = horizontal bolt force component due to the eccentric shear ICOR analysis, kips.

$V_{my,n}$ = vertical bolt force component due to the eccentric shear ICOR analysis, kips.

Δ = theoretical maximum bolt deformation equal to 0.34 inches.

Δ_n = vertical deflection measured by DWT at time step ‘n’, inch.

ϕ = LRFD safety factor taken as 0.75 for shear and 0.9 for tension.

ϕ^* = free end rotation of the beam divided by ϕ_{ref}, radians.

ϕ_{ref} = beam end rotation reference angle, radians.

θ_g = maximum beam end rotation associated with connection failure, radians.

$\theta_{g,\ max}$ = maximum beam end rotation prior to beam flange binding, radians.

θ_n = beam end rotation at time step ‘n’, radians.

θ_p = maximum beam end rotation associated with the connections maximum flexural capacity as a result of excess bolt or bearing deformations, radians.

μ^{-6} = experimentally measured microstrain.

σ_n = stress at strain gage ‘n’, ksi.

Abbreviations

in	Inch
lbs	Pounds
kips	1000 pounds
ksi	Kips per square inch
psi.	Pounds per square inch
AISC	American Institute of Steel Construction
ASD	Allowable Strength Design
ASTM	American Society of Testing and Material
BGAF	Bolt Group Action Factor
CSEC	Construction Science and Engineering Center
DWT	Draw Wire Transducer
FEMA	Federal Emergency Management Agency
KSI	Kips Per Square Inch
ICOR	Instantaneous Center of Rotation
LRFD	Load Factor and Resistance Design
MSOE	Milwaukee School of Engineering
NIST	National Institute of Standards and Technology
RCC	Reduced Component Connection
RCSC	Reduced Coarse Shell Connection

Chapter 1

INTRODUCTION

1.1 Background

Current design and construction practices in the steel construction industry utilize the concept of simply supported framing to simplify member and connection design. As a framing member is subjected to typical loads, such as gravity loads, the ends of the framing members rotate as the beam deflects vertically. Allowing the ends of the framing members to rotate, the transfer of moment from one framing member to another is eliminated resulting in an idealized transfer of shear forces exclusively. Doing so, designers are able to simplify design by reducing the type and complexity of connection design. Figure 1.1 shows a simplified illustrative comparison of the framing member moment distribution under uniform loading for fixed and simple end conditions.

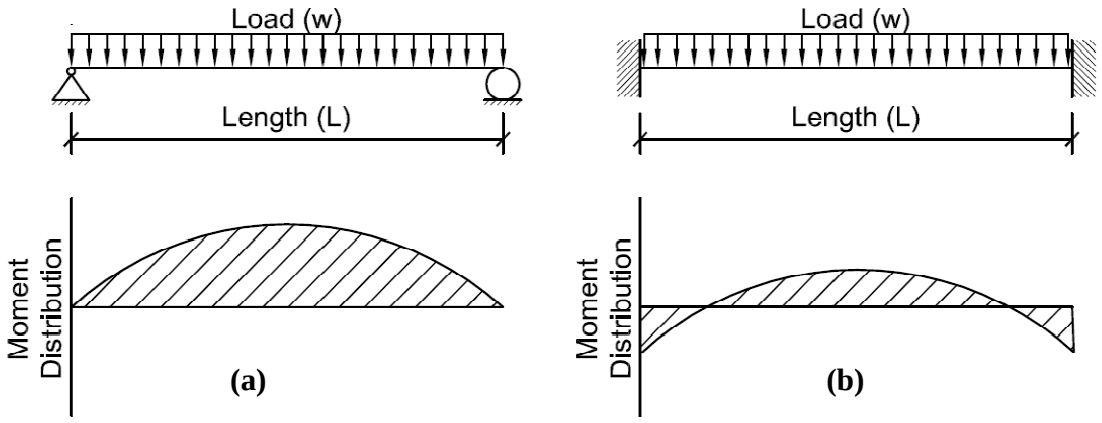

Figure 1.1: Typical Moment Distribution Due to Different Beam End Restraint Conditions [1].
(a) Pinned-Roller Simple End Support; (b) Fixed-Fixed End Support

Several key advantages exist by eliminating the transfer of moment from secondary framing members to primary framing members including reduced engineering, fabrication, and erection costs. Standard connections, categorized as simple connections,

have been developed which allow for this simple support assumption at the beam ends. The behavior of these connections subjected to gravity load conditions has been well documented and researched during the course of steel construction history. The current American Institute of Steel Construction (AISC) design manual, *Steel Construction Manual, 13th Edition*, provides specific design requirements that aid designers' understanding of the behavior of simple connections to ensure the characteristic behavior of simple end supports is maintained [2].

1.2 Single-Plate Connections

One of the least complex forms of simple connections utilized in the steel construction industry is the single-plate. This connection requires little fabrication and installation time because of the limited number of parts required for fabrication and installation. As the name implies, the single-plate connection is made of a single high strength steel plate welded to a primary framing member, *i.e.* column or girder, and bolted to the web of the secondary member. The current AISC manual presents two different forms of single-plate connections. The most common connection is the "Conventional Configuration", also referred to as a "shear tab" or "finplate" connection [2]. Shown in Figure 1.2, the "Conventional Configuration," referred to as a "shear tab" from this point forward, utilizes one row of vertical bolts at the supported member's web. The shear tab is attached to the flange or web of a supporting column or to the web of a supporting primary girder. The second form of single-plate connection, the "Extended Configuration", is unlimited in the number vertical bolt rows [2]. The "Extended Configuration" will not be further investigated as it is outside the scope of this report.

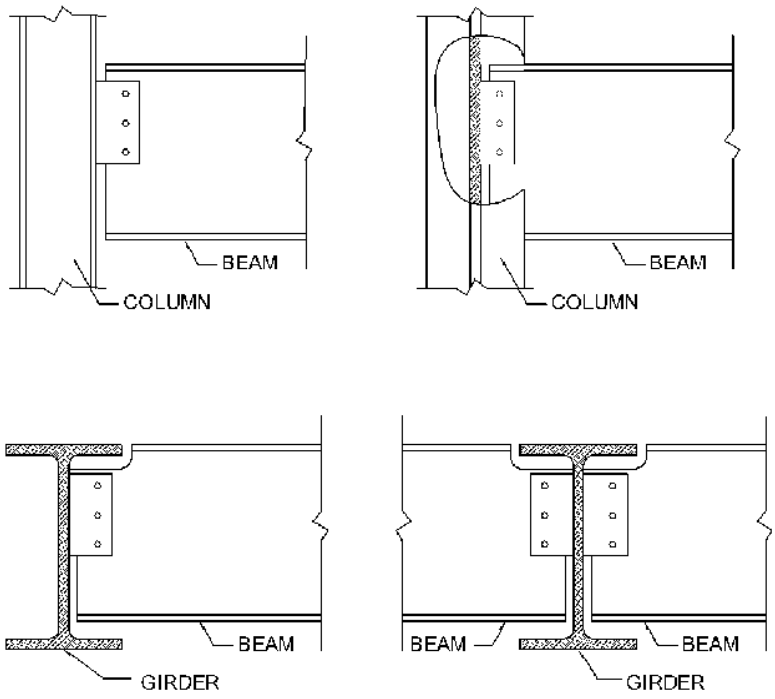

Figure 1.2: Typical Shear Tab Configurations [3].

1.3 Scope of Research

As Figure 1.2 shows, the shear tab connection is a versatile and relatively simple connection to design, fabricate, and erect. The behavior of this connection under gravity loads has been well documented and researched over the past forty years [3]. Yet, an important question was presented by Jim DeStefano of DeStefano Associates in a November 2006 *STRUCTURE* magazine article, entitled "Detailing to Prevent Progressive Collapse", pertaining to the current understanding of the behavior of simple shear connections subjected to unexpected forces [4]. Discussing the events of progressive collapse occurring at the World Trade Center Towers in New York City, New York on September 11, 2001, DeStefano stated, "we as a [engineering] profession don't really know how to design buildings to resist progressive collapse. We can't even

agree on what progressive collapse is or what we should call it." [4] The increasing threat of planned destruction as a result of terroristic activities requires designers to think beyond typical gravity and lateral load cases. DeStefano believes the recent rise in terrorism threats has produced a situation in which, "the most likely perceived terrorist event is a car bomb removing an exterior column." [4] While hopefully rare, Destafano raises concern pertaining to the ability of a structure to withstand the loss of a load bearing column without initiating progressive collapse resulting in the catastrophic loss of human life.

The most likely solution to this problem is through the phenomenon of catenary action allowing the supported structure to bridge over the loss of a load bearing column. The intent of this research is to provide background information into the development of the shear tab connection and its intended function. The interaction of shear and tension forces combined with beam end rotation will be examined to better understand the rotational ductility limits of the shear tab connection. Doing so, this research will provide a basis of understanding of the shear tab connection's ability to handle the unexpected forces and deflections resulting from the loss of a load bearing column and whether catenary action can be achieved as an effective alternative load path.

Chapter 2

LITERATURE REVIEW

2.1 Overview

The characteristic behavior of the shear tab connection has been well studied and researched with respect to gravity load conditions [3]. Limit states for design due to vertical shear loads have been formulated and tested proving the capabilities and predictability of the connection. Also, research time has been well spent understanding the rotational characteristics occurring during the applications of gravity loads [3]. Yet, limited research has been invested into the possibility of unexpected forces transferred through the shear tab connection. Namely, understanding the interaction of shear and tension combined with the connection's inherent moment capacity has largely been neglected.

This literature review describes the information currently available pertaining to the unit behavior of shear tab connections as well as the behavior of the individual connection components. A review of past research describing the shear tab connection's behavior subjected to gravity loading is provided, along with its correlation to the current AISC design manual requirements. Furthermore, applicable research pertaining to abnormal loading conditions and force interaction is described providing insight into the need for the current research.

2.2 Previous Shear Tab Research

Progressive collapse of steel structures may be able to take advantage of catenary action by using ductile girder to column connections which have the ability to handle

beam end rotations and resist high axial loads. Some experts recommend avoiding seat connections and one sided connections due to their inherent physical limitations [4]. Yet for existing structures with one sided connections such as shear tabs this assumption holds little value when trying to understand the performance and capability of an existing structure. Before an understanding of how catenary action affects the characteristic behavior of shear tab connections, an review of past research is required to understand the intended behavior of shear tab connections when designed per the current AISC design requirements.

2.2.1 The Analysis and Design of Single Plate Framing Connections.

Research by Richard *et al.* [5] in 1980 looked to verify the design specifications of the time through testing two, three, five, and seven bolt shear tab connections. Richard *et al.* looked to validate 1968 Canadian research by Lipson [6] which concluded the shear tab connection's ductility is derived from bolt deformation, plate and/or beam web hole distortion, and out-of-plane bending of the plate and/or beam web. Richard *et al.* [5] also conducted research to determine if sizeable moment capacities could be developed in the shear tab connection. The research maintained significant moment capacity could be developed at the supported beam ends by varying the bolt number, size, configuration, thickness of plate and/or beam web, beam span to depth ratio, and loading.

The end moments generated by the shear tab connections were evaluated by constructing a comparison between a "beam line" generated on a moment-rotation curve. Figure 2.1 provides the typical relationship between moment and rotation where the vertical axis represents the beam fixed end moment while the horizontal axis represents the simple span beam end rotation. A linear relationship between moment and rotation

was defined for the particular beam while the moment-rotation curve was generated using analytical and experimental data. The intersection of the two lines represented the moment-rotation capacity of the shear tab connection.

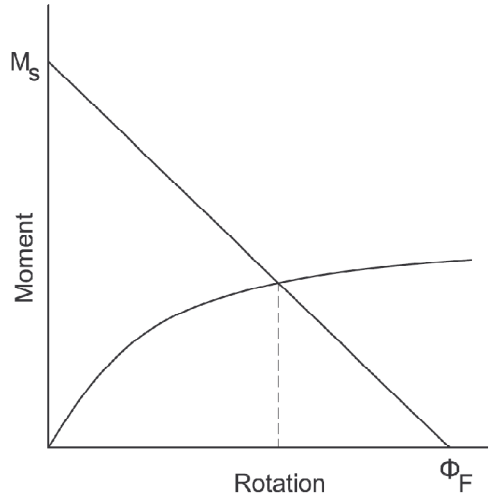

Figure 2.1: Shear Tab Idealized Moment-Rotation Interaction Diagram [5].

Richard *et al.* utilized finite element modeling for two, three, five, and seven bolt shear tab connections to develop a theoretical equation to determine moment-rotation curves for various connection configurations. The testing variable was limited to the eccentricity versus the connection bolt pattern height, where the eccentricity was taken as the distance from the weld line to the bolt line. Richard *et al.* [5] formulated a theoretical equation for the shear tab connection moment, M, shown as,

$$M = M^{*}\left[1-\left(1-\frac{e}{h}\right)^{3.9}\right]M_{ref}, \tag{1}$$

based on non-dimensional values,

$$M^{*} = \frac{60\phi^{*}}{\left[1+\left(\frac{60\phi^{*}}{1.1}\right)^{\frac{2}{3}}\right]^{\frac{3}{2}}}, \tag{2}$$

and,

$$\phi_{ref} = \frac{0.3 \text{ in}}{\left[\frac{(n-1)(3 \text{ in})}{2}\right]} \quad (3)$$

where

M = moment in the connection,

M_{ref} = reference moment based on a pure moment being applied to a connection with all bolts loaded to their maximum capacity,

M^* = intermediate non-dimensional moment value,

ϕ^* = free end rotation of the beam divided by a reference value ϕ_{ref},

n = number of bolts,

e = eccentricity of load (horizontal distance from weld line to bolt line),

h = bolt pattern depth (center to center distance from the top to bottom bolt).

The finite element results for the shear tab connections indicated key connection characteristics. First, the results indicated virtually all connection ductility originates from the deformation of the bolts as well as the deformation of the bolt holes in the plate and/or beam web. Also, the outer bolts showed two levels of behavior. During initial loading, as moments in the connection increased, the forces on the outer bolts were nearly horizontal. As loading continued, these forces rotated to near vertical until max bolt forces were reached. According to Richard *et al.*, this behavior indicated a shift in the connection eccentricity allowing the connection to carry more vertical shear.

Seven full scale experimental tests were conducted to verify the finite element results and the validity of Equation (1). The experimental testing used a load cell to

measure the applied load at the end of a cantilevered stub beam and measured the beam end rotations using rotation bars at the weld interface of the connection. The connection material tested included 1/4 inch ASTM A36 plate with 3/4 inch diameter ASTM A325 bolts. The experimental testing indicated maximum beam end rotations of 0.06 and 0.045 radians for the three and five bolt connections, respectively. Figures 2.2 and 2.3 depict the theoretical and experimental moment-rotation curves for the three and five bolt connections, respectively.

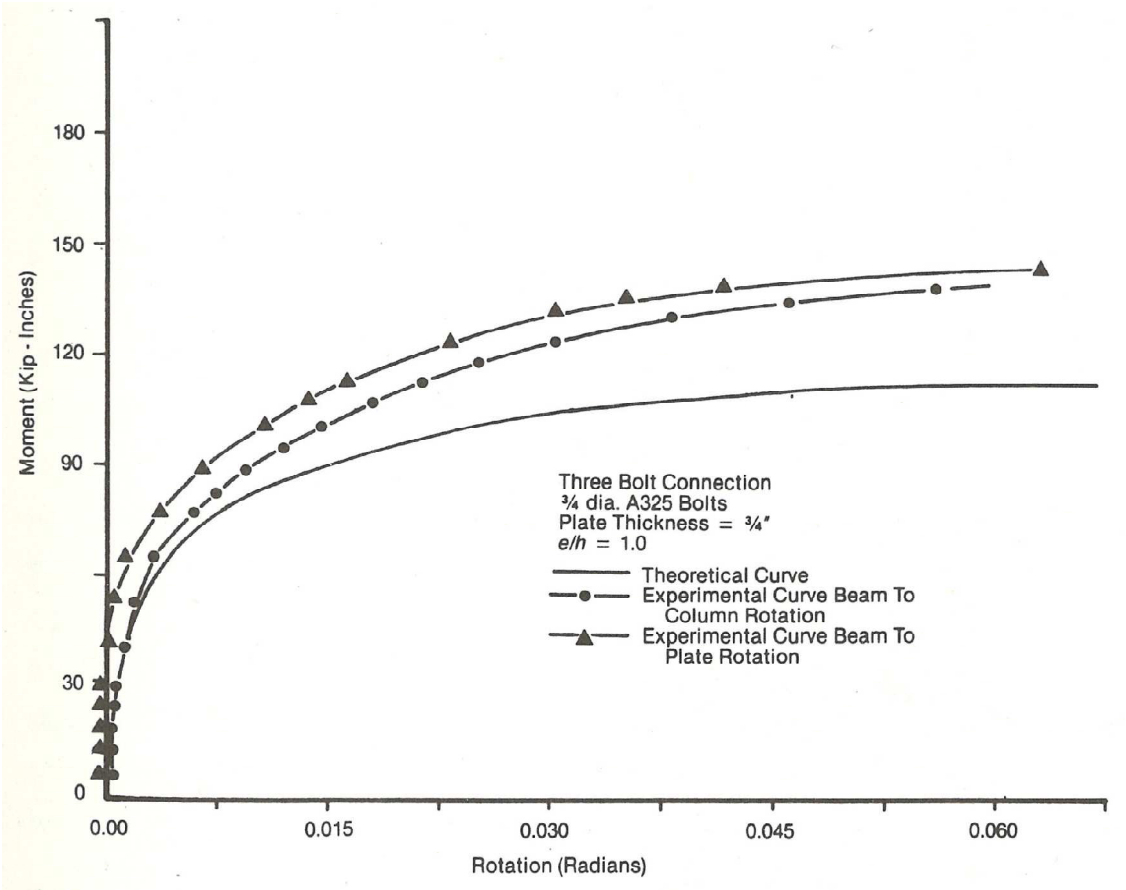

Figure 2.2: Theoretical and Experimental Beam Line Curves for Three Bolt Connections [5].

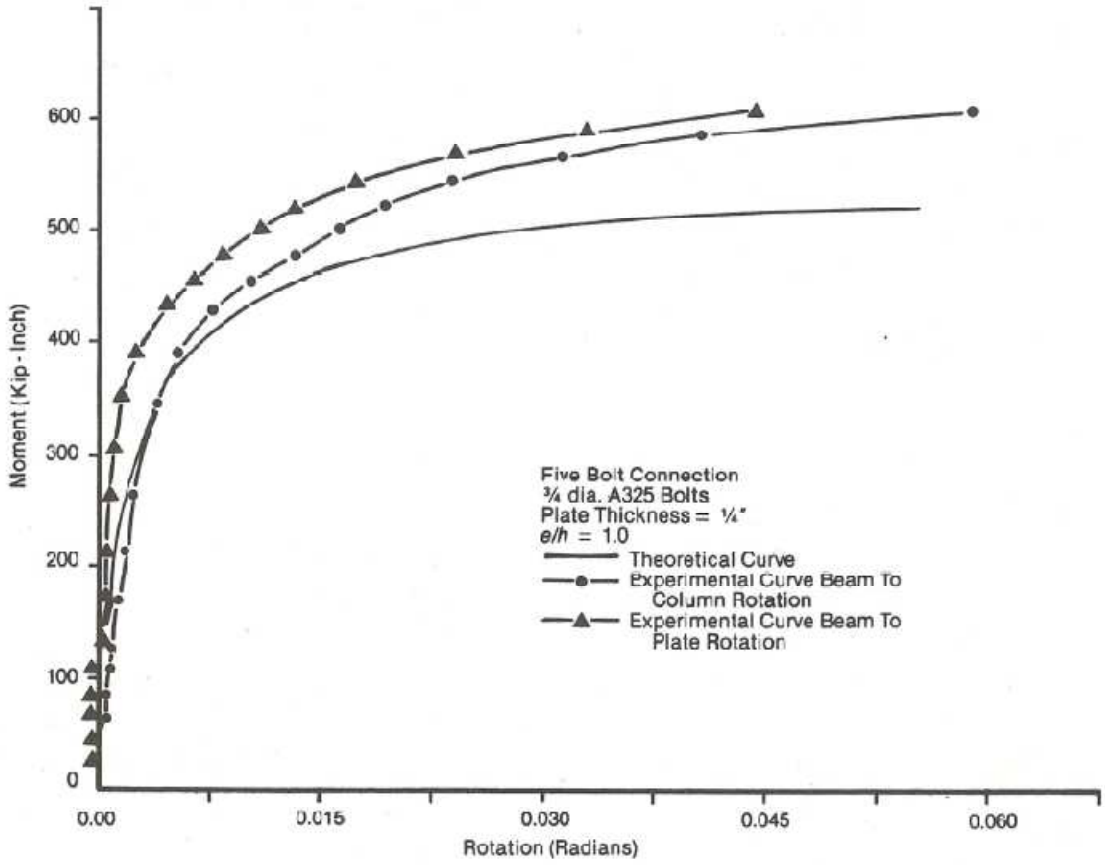

Figure 2.3: Theoretical and Experimental Beam Line Curves for Five Bolt Connections [5].

The analytical analysis and experimental verification performed by Richard *et al.* produced a relationship between an analytical model and experimental results. Richard *et al.* provided an approximate equation to determine the moment and rotation capacities for shear tab connections. The results also established the behavior of the bolts as the connections are subjected to rotation. However, the results were based on a maximum rotation of 0.06 radians and did not include destructive testing. Further research in 1989 by Astaneh *et al.* [7] developed formulas and design specifications which were eventually adopted by the *AISC Steel Construction Manual 3rd Edition* [8] and which disagreed with Richard *et al.* findings.

2.2.2 Design of Single Plate Shear Connections.

Research by Astaneh *et al.* [7] developed a design standard in which shear strength, rotational flexibility, and ductility were considered. Figure 2.4 provides an illustration of the test setup used by Astaneh *et al.* The testing incorporated one load cell near the connection to apply direct shear while another load cell was placed near the supported beam end imparting the beam end rotations about the shear tab connection. The experimental testing was conducted on five full scale specimens with two lots of materials. The first lot used 3/4 inch diameter ASTM A325 bolts, 3/8 inch ASTM A36 plate, and ASTM A36 beams while the other group used 3/4 inch diameter ASTM A490 bolts, 3/8 ASTM A36 plate, and Grade 50 beam material.

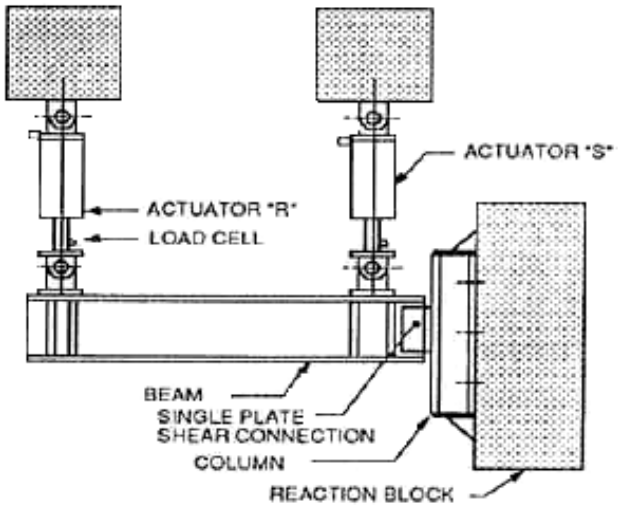

Figure 2.4: Astaneh *et al.* Experimental Test Setup [7].

Astaneh *et al.* created a standard shear-rotation relationship which described the beam's behavior and the corresponding effects of the connection to develop design equations for the shear tab connection. Shown in Figure 2.5, three distinct phases of the shear versus rotation relationship were used to describe the characteristic behavior of the connection and supported beam. In phase one, segment "ab" depicts the elastic behavior

in the beam during the applied loading. To develop this line, Astaneh *et al.* assumed the yield moment of the beam, M_y, corresponded to a beam end rotation of 0.02 radians. The corresponding shear value when the beam reached M_y was then taken as $4M_y/L$ where L is taken as the beam span length. As loading increased, inelastic behavior began as the beam reached its plastic moment, M_p. Depicted as segment "bc", the beam is assumed to reach the full plastic moment as the beam end rotation reached 0.03 radians with a corresponding shear of $4M_p/L$. Finally, segment "cd" represents increased beam capacity due to strain hardening where the beam end rotation is assumed to reach 0.1 radians.

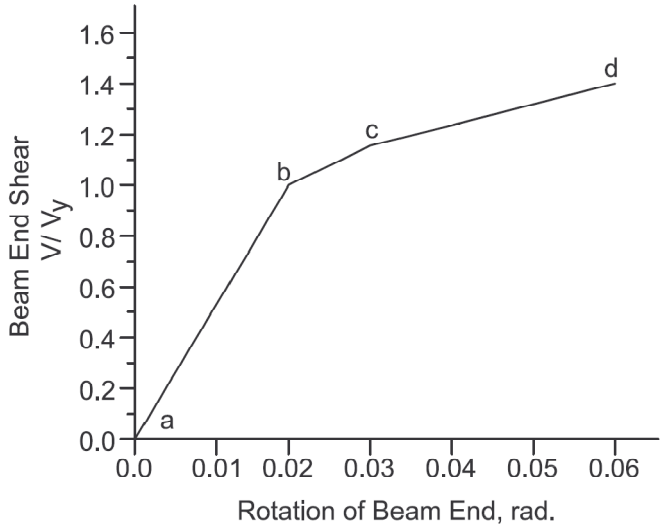

Figure 2.5: Simply Supported Beam End Shear-Rotation Relationship [7].

The destructive testing by Astaneh *et al.* provided key insight into the shear tab connection's behavior during gravity loading. First, the bolts exhibited sudden fracture. The researchers discovered that the bolts of the tested connection exhibited inelastic deformations prior to fracture as well as significant bearing in the plate and beam web holes. Furthermore, the development of Figure 2.5 corresponded with the development of three expected phases of the shear tab's behavior. Initially, the connection is thought to

act as a short cantilever where moment capacity rapidly increases. As load is increased, shear yielding in the connection generally controls resulting in component failure of the connection. Finally, if fracture has not occurred in the plate or bolt components, large deformations cause the shear tab to act as a diagonal member of a truss with shear and diagonal tension effects. Provided the bolts and welds of the shear tab connection have the capacity and/or ductility to withstand the shear yielding phase, the connection's ability to transfer the combination of shear and tensile forces is important in quantifying the ability of the connection to handle unexpected forces due to column collapse. This concept is further discussed in Section 2.5.

Specifically, Astaneh *et al.* observed characteristic limits of the connections within the three phases of connection behavior. Shear yielding on the gross area of the plate was clear to have occurred uniformly throughout the section. As part of this shear yielding effect, signs of local buckling occurred on the plate bottom edge as a result of stiffness loss. However, this limit was outside the limits of the research and was suggested to best be avoided by limiting the distance between the weld and bolt lines to one-half the length of the connection plate. Another observation was the change in the connection's rotational ductility based on the number of bolts in the connection. For a seven bolt connection the rotational ductility of 0.026 radians was nearly half the rotational ductility of the three and five bolt connections of 0.05 radians. The ductility was observed to be controlled by the design of the bolts in the connections. Before bolt fracture occurred, tolerable shear deformation of the bolt shank as well as the bolt holes was evident. Based on previous research by Astaneh and Nadar [9], tolerable bolt hole deformations occurred when the connection plate thickness was limited to one-half the

diameter of the bolts plus 1/16 inch for ASTM A325 bolts and ASTM A36 plate materials. These tolerable deformations provided the connection with increased rotational ductility.

The results of Astaneh *et al.'s* testing culminated in the formation of five limits states which controlled the capacity of the shear tab connection. Shear failure of the bolts was calculated [7] using an eccentrically applied shear load analysis where the eccentricity, e_b, as shown as

$$e_b = (n-1)(1.0) - a \tag{4}$$

where,

e_b = bolt design eccentricity,

n = number of bolts in the connection,

a = distance from the bolt line to the weld line.

The weld design was required to resist a similar eccentrically applied shear where the eccentricity, e_w, was taken as the number of bolts, *n*, in inches away from the weld line. The minimum weld thickness was recommended to be equal to 3/4 the thickness of the connecting plate to ensure plate yielding occurred prior to weld yielding. Further connection limits were based on existing limits specified in the AISC *Manual of Steel Construction 8th Edition* [10] for gross shear yield of the plate, net area fracture of the plate, and bearing failure in the plate and beam web.

2.3 AISC 13th Edition Design Provisions

2.3.1 Verification of a New Single Plate Shear Connection Design Model.

Research by Baldwin Metzger in 2006 [3] conducted experimental tests to prove the adequacy of the AISC *Manual of Steel Construction 13th Edition* specification [2]. The research provided a thorough investigation into the development of the shear tab connection and how the AISC 13th Edition adapted prior research. Among the investigated research, Baldwin Metzger summarized the findings of Richard *et al.* [5] and Astaneh *et al*. [7]. Baldwin Metzger also presented research into Astaneh's role in the definition of the shear tab eccentricity as it applied to the AISC 3rd [8] and AISC 13th Editions [2]. The research showed eccentricity could be ignored for connections with three or more bolts if a twenty percent reduction factor, known as the "bolt group action factor" (BGAF), was applied to the bolt capacity. The AISC 13th Edition utilizes this reduction in the tabulated value of nominal bolt stress to "account for non-uniform load distributions in connections." [2] The investigation by Baldwin Metzger concluded that bolts toward the ends of shear splice plate connections exhibited higher stress levels than those of bolts near the center of the connection for connections up to a length of 50 inches. Research by Creech [11] indicated the BGAF factor was not applicable to single plate shear connections based on the assumption that framing connections such as the shear tab do not experience this same occurrence.

The experimental phase of Baldwin Metzger's research tested the compatibility of the analytical values of connection capacity prescribed by the AISC 13th Edition [2] with those found through experimentation. Four full scale tests were conducted using three, four, five, and seven bolt connections all abiding by the geometric parameters specified

by the AISC 13th Edition [2]. The test setup utilized a supported beam with two point loads supplied at the beams third points by hydraulic rams. One end of the beam used a true roller support while the other end of the beam was supported by a shear tab specimen to a supporting test column flange. The test measured the applied force using load cells at the roller support while measuring the beam end rotation using linear potentiometers.

Analytical nominal capacities of Baldwin Metzger's experiment were based on the provisions prescribed in the AISC 13th Edition [2]. These values are based on the use of 3/8 inch ASTM A36 plate material, ASTM A992 Grade 50 support steel, and ASTM A325 bolts with the threads included in the shear plane. The weld line was based on 5/8 times the plate thickness rather than 3/4 times the plate thickness as prescribed by Astaneh [7]. The applicable limit state capacitates are shown in Table 2.1.

Table 2.1: Baldwin Metzger Analytical Nominal Capacities [3].

Bolts	Bolt Shear Rupture (Kips)	Bolt Shear Rupture (No BGAF)[1] (Kips)	Plate Shear Yielding (Kips)	Plate Shear Rupture (Kips)	Plate Block Shear (Kips)	Plate Bearing (Kips)	Beam Bearing (Kips)
3	64.0	80	96	86	100	113	137
4	84.8	106	129	117	131	156	206
5	106	133	163	148	162	200	257
7	148	186	231	210	224	288	446

--[1] Not a permitted limit state according to procedure in the AISC 13th Edition Manual.

The outcome of Baldwin Metzger's experimental tests resulted in the failure of two of the four connections. The three and four bolt connections did not fail before lateral torsional buckling of the test beam occurred. After reconfiguration of the testing apparatus, failure of the five and seven bolt connections occurred due to bolt shear rupture. Table 2.2 provides the experimental ultimate shear load and beam end rotation measured for Baldwin Metzger's four tested connections.

Table 2.2: Baldwin Metzger Experimental Results [3].

Test	Columns of Bolts	Bolts	Maximum Connection Shear (kips)	Maximum Connection Rotation (radians)	Connection Failure Mode
1	1	3	81	0.032	--[1]
2	1	4	110	0.027	--[1]
3	1	5	146	0.03	Bolt Shear
4	1	7	173	0.018	Bolt Shear

--[1] Test beam failure occurred prior to connection failure.

The results of Baldwin Metzger's tests corresponded well with 1989 research by Astaneh. The maximum connection rotation of approximately 0.03 radians measured by Baldwin Metzger is consistent with Astaneh's assumption of the maximum beam end rotation of 0.03 radians during the shear yielding phase. The results also show the decreased rotational ductility evident for seven bolts versus the three, four, and five bolt connections as was concluded by Astaneh [7]. Comparing Table 2.1 and Table 2.2, the conservative nature of the current specification is evident. The bolt shear rupture capacities for analytical values with no BGAF more closely match the experimental values than do the nominal bolt shear rupture capacities. The research by Baldwin Metzger provides a clear logical progression of the history of shear tab research and how the current AISC 13th Edition Manual compares to experimental values.

2.3.2 AISC Manual of Steel Construction 13th Edition Specification.

The "Conventional Configuration", or shear tab connection as it has been defined, is the focus of this research. The shear tab connection design requires that six geometric connection properties are met to utilize the provisions of the AISC 13th Edition Specification [2], including:

1) One single vertical column of bolts with at least two but no more than twelve rows of bolts
2) The horizontal distance from the weld line to the bolt line must be less than or equal to 3 1/2 inches;
3) The use of standard or horizontal short slotted holes;
4) The horizontal edge distance must be greater than or equal to twice the bolt diameter, d_b, for both the plate and beam web;
5) The vertical edge distance, L_{ev}, must meet AISC Table J3.4;
6) Either the plate or beam web must be less than or equal to d_b plus 1/16 inches.

As previously discussed by Astaneh [7], the shear tab connection's rotational ductility is derived from the ability of the bolt line to undergo tolerable deformations in the connecting material. To ensure this, the AISC 13th Edition limits the plate thickness based on the diameter of the bolts and by requiring minimum edge distances to prevent the possibility of bolt bearing tearouts from occurring during typical beam end rotations.

Eccentric effects on the bolt line have been altered in the AISC 13th Edition to reflect the research of Creech [11]. Connections with up to nine rows of bolts are not required to be designed for eccentric effects due to the AISC 13th Edition's [2] use of the BGAF. Creech showed the twenty percent reduction in allowable bolt shear stress does not apply to shear tab connections with fewer than ten rows of bolts [11]. For connections with ten through twelve rows of bolts, a 1.25 multiplier is required when calculating the eccentricity coefficient, C, as described per the AISC 13th Edition Specification [2]. The bolt group eccentricity, e_b, is given by

$$e_b = (n-4) \tag{5}$$

where

e_b = bolt design eccentricity,

n = number of bolts in one vertical row.

Comparing Equation (4) provided by Astaneh [7] and Equation (5) provided in the AISC 13th Edition, for ten rows of bolts with a three inch distance from the bolt line to the weld line, both equations produce a design eccentricity of six inches.

Weld design requirements for the AISC 13th Edition utilize a required weld size of 5/8 times the plate thickness versus the 3/4 times the plate thickness specified by Astaneh. The AISC Committee on Manuals and Textbooks determined weld thickness should be based on weld fracture rather than weld yielding [12]. As was verified by Baldwin Metzger [3], the requirement of 5/8 times the plate thickness provides the shear yielding limit state of the plate will control before weld fracture for pure moment, pure shear, or the combination of shear and moment.

Further limits states for the design of the shear tab connection are highlighted in the design example of Appendix A. These design checks include bolt shear, block shear rupture, bolt bearing, shear yielding and shear rupture of the plate. The AISC 13th Edition does not require a check for plate buckling due to only minor evidence that local buckling occurs in select conditions of shear tab connections.

2.4 Interaction of Shear, Tension, and Rotation

The shear tab connection's ability to handle vertical shear loads has been well researched and documented. The findings have been useful for maximizing the connection's capabilities due to expected gravity load conditions. However, the

introduction of incidental tensile forces and their interaction with gravity load induced shear forces has largely been undeveloped by the “Conventional Configuration” provisions of the current AISC design specification. The AISC 13th Edition does not account for incidental tension or the combination of tension and shear in simple shear connections. Analytical and experimental research has been conducted providing some insight and approximate design limitations to account for the combination of shear and tension forces.

2.4.1 Combined Shear and Tension Stresses.

Based on the provisions of the AISC Allowable Stress Design (ASD) *Manual of Steel Construction 8th Edition* [10], evaluating shear and tension stresses individually for members where maximum stresses of shear and tension do not occur simultaneously is acceptable. According to analytical research by Goel [13], designing connections separately for shear and tension stresses leads to grossly un-conservative results. Goel provided an analytical comparison of different models of the combination of maximum shear and tension stresses. The first comparison Goel made was using maximum principal stress criterion. Goel stated, “the maximum principal stress theory can be justified in design situations where the failure mode is governed by brittle fracture, such as fatigue loading.” [13] Goel related the normal tension and shear stress to the maximum principal stress [13] shown as

$$\frac{1}{2}\left[\frac{f_t}{F_t}+\sqrt{\left(\frac{f_t}{F_t}\right)^2+\frac{16}{9}\left(\frac{f_v}{F_v}\right)^2}\right]=1 \qquad (6)$$

where,

f_t = applied normal tension stress,

f_v = applied normal shear stress,

F_t = maximum principal tensile stress based on material capacity,

F_v = maximum principal shear stress based on material capacity.

As Figure 2.6 shows, for low levels of tension force, Equation (6) can result in nearly a fifty percent overstress. This model indicates the maximum principal stress theory is not applicable for limit states controlled by yielding.

Goel's second comparison utilized the combination of the Von Mises' yield criterion and a four-thirds safety factor per the AISC 8th Edition [10] to develop an interaction equation [13] which is

$$\left(\frac{f_t}{F_t}\right)^2 + \frac{4}{3}\left(\frac{f_v}{F_v}\right)^2 = 1. \quad (7)$$

The interaction curve for Equation (7) shown on Figure 2.6 indicates a conservative limit for the maximum shear stress, f_v, of $0.866F_v$ for the situation where low levels of normal tension stress are present. Goel then compared a straight line interaction of shear and tension stress [13] shown as

$$\frac{f_t}{F_t} + \frac{f_v}{F_v} = 1. \quad (8)$$

As Figure 2.6 indicates, Equation (8) is largely conservative compared to Equation (7) for most ranges. The combination of Equation (7) and Equation (8) led Goel to the develop a final interaction equation [13] for combined shear and tension stresses shown as

$$\frac{f_t}{F_t} + \left(\frac{f_v}{F_v}\right)^2 = 1. \quad (9)$$

The interaction curve of Equation (9) depicts an equation which largely follows Von Mises' yield criterion while having similar end limits of 1.0 as in Equation (8).

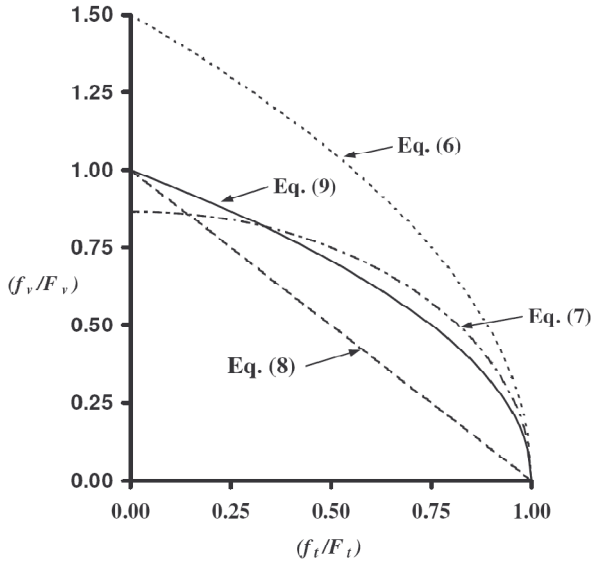

Figure 2.6: Shear and Tension Stress Interaction Curve Comparisons [13].

Goel's empirical equation for the interaction of shear and tension, given by Equation (9), provides a simple interaction equation which can be effectively incorporated in the design and analysis of shear tab connections while providing an equation which corresponds well to the accepted Von Mises yield criterion.

2.4.2 Simple Beam Connections under Shear and Axial Loads.

The design of shear tab connections subject to shear and tensile forces requires adequacy checks for many limit states. As outlined in Appendix A and B, these limit states are required to be checked independently for both shear and tension cases. As Goel observed, ignoring the interaction of these applied forces can result in an un-conservative connection design [13]. Further complicating these designs are design checks such as bolt bearing and block shear rupture. The AISC 13th Edition [2] does not address how to design bolt bearing and block shear rupture for combined shear and tension forces. Tamboli [14] provides an analytical design approach for these connections.

The design equation for the connection strength due to bolt bearing per the AISC 13th Edition Specification [2] requires a designer to calculate both bolt bearing and bolt tearout capacities for each connection ply using

$$R_n = 1.2 L_c t F_u \leq 2.4 d t F_u \tag{10}$$

where

L_c = clear edge distance in the direction of the force between the edge of the hole and the edge of the adjacent hole or the edge of the connected material in inches,

t = thickness of connected material in inches,

d = nominal bolt diameter in inches,

F_u = specified minimum tensile strength of connected material.

According to Tamboli [14] the correct method for determining the clear edge distance is to determine the magnitude and direction of the resultant force vector, R_u, based on the applied shear and tension forces. The resultant vector is then applied at the resultant angle from the center of each bolt. The clear edge distance can be taken as the distance from the center of the bolt to the edge of the material less one-half the diameter of the bolt. Figure 2.7 provides an illustration of Tamboli's recommendation. As a conservative method, Tamboli suggests designers use L_c as the lesser distance in the direction of the vertical and horizontal components [14].

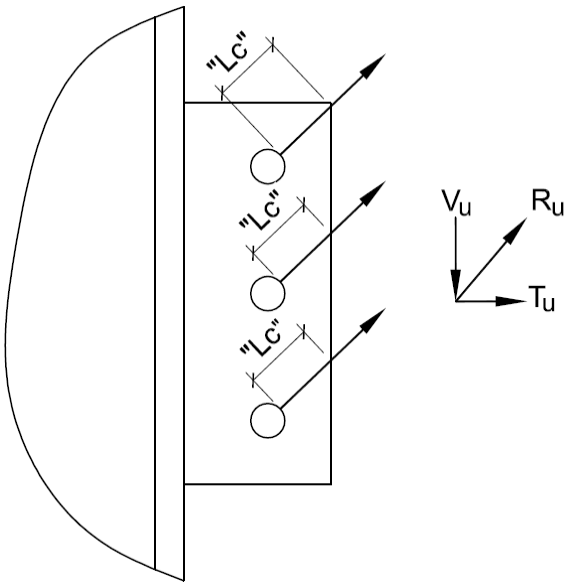

Figure 2.7: Clear Edge Distance, L_c, due to Combined Shear and Tension [14].

Tamboli also discusses the design of block shear rupture in connections subject to shear and tension. According to Tamboli, the most efficient and conservative way to design for block shear rupture is to treat R_u as the design shear force. Tamboli also suggests a more involved analysis utilizing the Von Mises yield criterion. Tamboli suggests an elliptical interaction equation [14] in which

$$\left(\frac{V_u}{\phi R_{bsv}}\right)^2 + \left(\frac{T_u}{\phi R_{bst}}\right)^2 \leq 1 \qquad (11)$$

where

V_u = factored shear force using LRFD load combinations,

T_u = factored tension force using LRFD load combinations,

ϕR_{bsv} = block shear rupture capacity in direction of shear,

ϕR_{bst} = block shear rupture capacity in direction of tension.

The block shear rupture capacities are based on the AISC 13th Edition Specification [3] shown as

$$\phi R_n = \phi\left[\left(0.6F_u A_{nv} + U_{bs} F_u A_{nt}\right) \le \left(0.6F_y A_{gv} + U_{bs} F_u A_{nt}\right)\right] \quad (12)$$

where

ϕ = LRFD safety factor taken as 0.75,

F_u = specified minimum tensile strength of connected material,

A_{gv} = gross area subject to shear,

A_{nv} = net area subject to shear,

A_{nt} = net area subject to tension,

U_{bs} = 1.0 for uniform tension stress.

Equation (11), presented by Tamboli, requires Equation (12) to be calculated for both the shear and tensile directions. The gross and net areas must be calculated for each direction to determine the block shear rupture design strength. Figures 2.8 and 2.9 provide illustrations of the block shear rupture design components for the shear and tension directions, respectively.

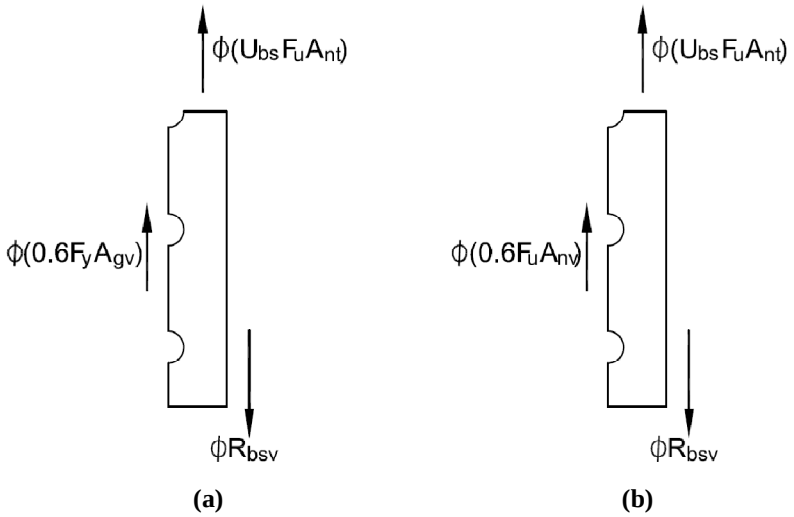

Figure 2.8: Block Shear Rupture Subject to Shear [14].
a) Failure due to combined shear yield and tension rupture
b) Failure due to combined shear rupture and tension rupture.

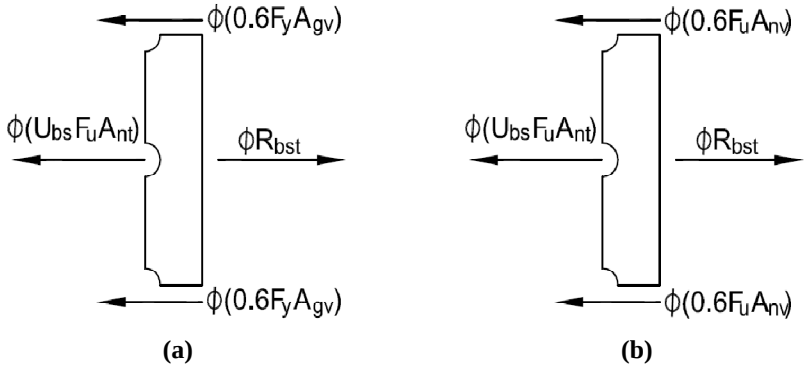

Figure 2.9: Block Shear Rupture Subject to Tension [14].
a) Failure due to combined shear yield and tension rupture
b) Failure due to combined shear rupture and tension rupture

Tamboli's methods for calculating component capacities for bearing, tearout, and block shear rupture due to the combination of shear and tension forces offer the designer a practical and simple design equation. In practice, the process of calculating block shear as presented in Equation (11) would be inefficient, as it requires more calculation time with a less conservative result. However, for experimental purposes, Equation (11) provides a useful comparison value when determining possible failure mechanisms which occur during destructive testing.

2.4.3 Simple Beam Connections in Combined Shear and Tension.

Guravich and Dawe [15] experimentally tested shear tab connections behavior when subjected to combined shear and tension forces. The National Building Code of Canada requires that structures are designed to provide a level of structural integrity which prevents the initiation of progressive collapse. Simple shear connections are required to have the ability to transfer vertical shear and incidental tension forces. However, the Canadian steel design standard CAN/CSA-S16-01 [16] and the AISC 3rd Edition [8] do not specifically provide guidelines for the design of connections subject to

combined shear and tension forces. While specifications do exist for the design of bolts and welds subject to combined forces, little guidance exists for the design of other connection components.

The experiments conducted by Guravich and Dawe tested eleven shear tab connections using 3/4 inch ASTM A325 diameter bolts with 3/8 inch ASTM A36 shear plates. The testing was conducted on two and three bolt connections using an assembly of hydraulic rams which provided stability as well as the applied shear and tensile forces. Guravich and Dawe specifically constructed the test so a rotation of 0.03 radians was initially imposed on the connection. After this initial rotation, no additional rotation was introduced into the connection. The forces were applied using an inverted “T” frame, where the shear force was transferred horizontally as close to the connection as possible, while the tension force was applied vertically at the end of the test beam. The testing specifically looked at the capacity of the connection by eliminating potential test beam failure modes through the use of stiffeners and doubler plates on the beam web. Load was applied using four different benchmarks including pure shear, fifty percent of the factored shear strength, one hundred percent of the factored shear strength, and pure tension.

The results of Guravich and Dawe’s testing provided several behavioral characteristics. During two pure shear tests, out-of-plane buckling occurred in the connecting plate. However, the connections did not meet the AISC specification requirement which requires the connection’s overall length to be greater than one-half the supported beam’s clear web depth, T, to reduce the likelihood of an out-of-plane buckling failure mode. The research also found plastic bolt bearing deformations occurred in the direction of the resultant force R_u. These results were typical with the analytical

expressions presented by Goel [13] for determining bolt bearing capacity. An average ratio of 0.94 was found comparing the applied resultant force to the plate bearing capacity indicating the bolt bearing limit state due to combined shear and tension was a good predictor of the shear tab connection capacity.

The testing conducted by Guravich and Dawe looked into the effects of combined shear and tension forces on shear tab connections. The research determined bolt shear and plate bearing are proper design capacities which generally control the connection capacity. The research also inadvertently proved the importance of the overall connection length provisions. However, the research by Guravich and Dawe did not look at the combined effects of shear, tension, and moment. The testing configuration specifically enacted a static rotation and measured the amount of tension which could be transferred after a predetermined shear load was applied. While the applied rotation agrees with previous research by Astaneh *et al.* [7] for typical beam end rotations subject to gravity loading scenarios, the introduction of severe beam end rotations produced by a supporting member failure was not researched. The testing was also limited by only analyzing two and three bolt connections and did not address nor compare the influence of full web depth connections.

2.4.4 FEMA-355D: State of the Art Report on Connection Performance.

In response to the 1994 Northridge Earthquake in Los Angeles, California, the Federal Emergency Management Agency (FEMA) funded a large undertaking under the name of the SAC Joint Venture to research steel framed structures subjected to cyclical loadings as a result of earthquakes. FEMA-355D was developed to present “the current

state of knowledge with regard to cyclic inelastic behavior of beam-column connections that have been employed in moment-resisting steel frame structures." [17] While cyclical loading as a result of seismic events is out of the scope of this report, FEMA-355D produced valuable research studying the behavior of shear tab connections subjected to combinations of shear and rotation resulting in plastic deformation and connection failure.

The research by the partners of the SAC Joint Venture suggested two distinct rotational characteristics exist in the behavior of shear tab connections. First, the rotational limit, θ_p, exists at which the connections moment capacity peaks as a result of excess bolt or bearing deformations. Second, the ultimate rotational limit, θ_g, occurs when the connection loses the ability to support the applied vertical shear load. Both rotational limits result in plastic deformation; however, the ultimate rotational limit provides insight into the ultimate capacity of the shear tab connection. The experimental analysis presented in FEMA-355D used the geometrical properties shown in Figure 2.10 to determine the plastic rotational capacity of shear tab connections.

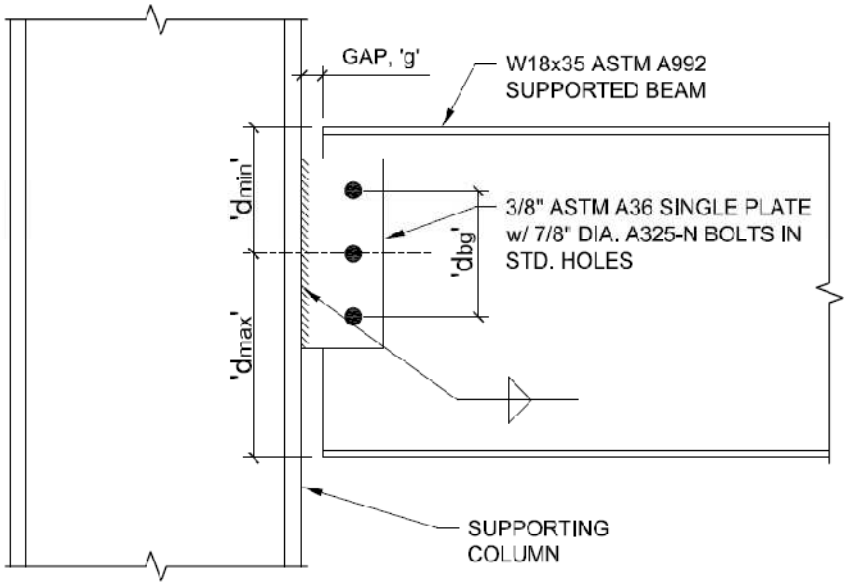

Figure 2.10: FEMA-355D Rotational Limits Controlling Connection Geometry [17].

Two plastic rotation limits were used to characterize the expected beam end rotations. First, the maximum plastic beam end rotation was established to characterize the maximum beam end rotation the connection could withstand prior to failure. The mean average [17] of the test data yielded

$$\theta_g = \left(0.15 - 0.0036 * d_{bg}\right) \pm (0.015 - 0.0011 * d_{bg}) \quad (13)$$

where θ_g is the beam end rotation in radians, and d_{bg} is the connection depth in inches. The second half of Equation (13) represents the experimentally based standard deviation. An upper bound maximum geometric beam end rotation limit [17],

$$\theta_{g,max} = \frac{g}{d_{max}} - 0.02, \quad (14)$$

was established to account for binding which may occur when large beam end rotations cause the supported beam flange to become pinned against the supporting column flange where g is the beam end gap dimension in inches and d_{max} is the distance from the center of the bolt group to the extreme supported beam flange.

As a result of the plastic rotational limits determined by the experimental research of FEMA-355D, an elastic rotational stiffness equation was derived which described the initial rotational stiffness having a direct correlation to the depth of the connections. The elastic rotational stiffness, k_s, increased linearly with respect to connection depth, yielding

$$k_s = 28000 * (d_{bg} - 5.6) \quad (15)$$

where k_s is in units of kip-in/radian. Equation (15) represents approximately fifty to seventy-five percent of the maximum achieved rotational resistance measured during testing. However, the rotational stiffness observed during the experimental testing was as low as ten percent of the supported beam stiffness. The research presented by FEMA-

355D suggested the low rotational stiffness of shear tab connections requires modeling of the connection to be considered a rotational spring element. Yet, as the connection stiffness is supplemental to the overall connection requirements, the elastic stiffness of the connection presented in Equation (15) provides a beneficial stiffness to the overall structure. Equation (15) provides an accurate description of the early stages of the shear tab connections' behavior when subjected to the combination of shear and rotation.

The research specifically stated the use of Equation (13) was only valid provided the horizontal edge distances of the single plate and supported beam web were such that the bolt group was allowed to reach its ultimate plastic moment capacity. Shown in Figure 2.11, the connections plastic moment capacity was estimated to be equal to the shear strength of the bolt group analyzed with the threads excluded from the shear plane and without the use of safety factors. Based on the experimental results obtained by the research of FEMA-355D using 7/8 inch diameter ASTM A325 bolts and 3/8 inch ASTM A36 plate material, the estimated plastic moment capacity was within ten percent of the measured moment capacity.

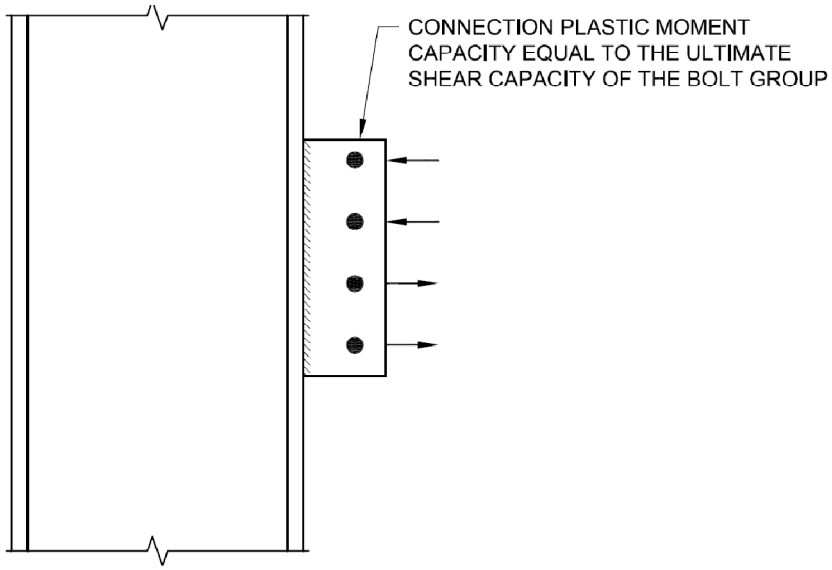

Figure 2.11: FEMA-355D Estimated Connection Plastic Moment Capacity [17].

While the development of Equation (13) may well represent the findings of the specific analysis conducted by the researchers of the SAC Joint Venture Group, the equation may not represent a true guideline for the expected rotational limits for shear tab connections. Restricting the connection rotational failure to a bolt shear failure rather than bolt bearing or bolt tearout failure for either the single plate or beam web indicates sufficient thicknesses and edge distances are required to develop the full shear capacity of the bolt group. Current design practices do not necessarily account for this occurrence. The shear tab design protocol per the AISC 13th Edition Specification [2] provides the minimum edge distance requirements based on the diameter of the fasteners used. The edge distance does not limit the connections limiting failure state to bolt shear failure as several other limit states including bolt bearing and bolt tearout of the connecting plate and supported beam web may control.

2.5 Catenary Action

When damage occurs within a structure, the design intent is to prevent the initiation of progressive collapse and catastrophic structure loss. In the event of a structural failure of an occupied structure, the design must allow patrons adequate time to exit the structure to prevent the likelihood of fatalities. An example of such an occurrence is the loss of a column. Members framing to this column are subject to loads which were not accounted for in the original connection design. The ability of the connection to bridge over the lost column is believed to be largely controlled by catenary action and the connecting elements' ability to transfer the resulting tensile forces.

2.5.1 Behavior of Bolted Beam-Column Connections under Catenary Action in Damaged Steel Structures.

Girhammar [18] tested the phenomenon of catenary action experimentally using bolted end plates and bolted heel connections. Girhammar looked into the statics of catenary action, investigated the capacities of the tested connections, and presented a design theory and systematic design procedure for each of the connections. The functionality of the bolted heel plate is a Swiss version of what is commonly known as an un-stiffened seat connection, where a supported beam rests on a plate which is bolted to the supporting member. The bolted end plate tested was a semi-rigid connection with a designed moment capacity. Girhammar's research into the type of connections is valid for this report in terms of the test setup and the statics for a simply supported member subject to catenary forces. The physical results and conclusions pertaining to the specific connections will not be discussed in length as they generally do not apply to the shear tab connection and the scope of this research.

The test setup utilized by Girhammar's research is an important aspect in understanding the behavior of catenary action and a connections ability to bridge over a damaged column. Girhammar's test setup shown in Figure 2.12 utilized two equally spaced bays with simply supported connections at both exterior columns as well as at each side of the interior column. Because of the destructive nature of the testing, the test arrangement was laid parallel to the ground to prevent the collapse of the structure upon failure. The exterior columns were idealized to have fully restrained connections preventing both axial and rotational movements. The interior column simulated the destroyed column and served as the point of load application, F, for the testing.

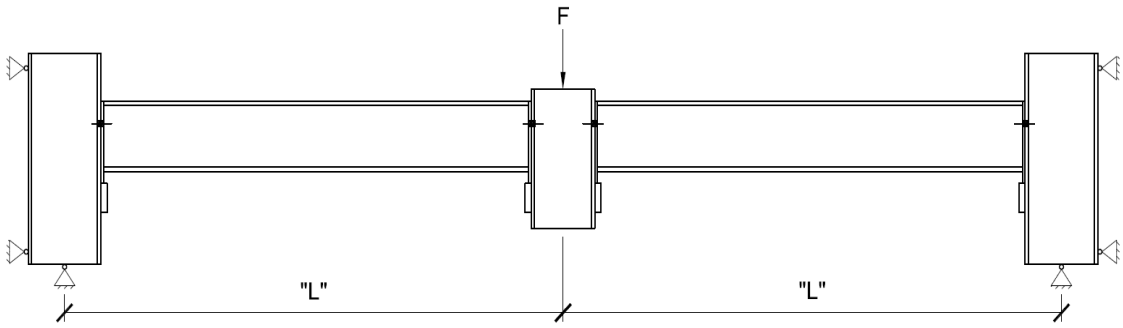

Figure 2.12: Test Arrangement for Simple Supports Subject to Catenary Action [18].

The bay length, L, used in the Girhammar experiment was approximately sixteen feet in length. Because of this, large deflections at the interior column were generated which exceeded the stroke of the hydraulic ram. This inherent test deficiency required the ram assembly to be adjusted multiple times during testing. Testing measurements included deflection of the interior column, strain gage readings of the beam flanges near the connections to determine moment distribution in the beam, strain gage readings of the bolts to determine the normal load on the bolts, and applied force from the hydraulic ram.

Girhammar provided a breakdown of the static force distribution of the system in Figure 2.13 assuming a symmetric test system about the applied load.

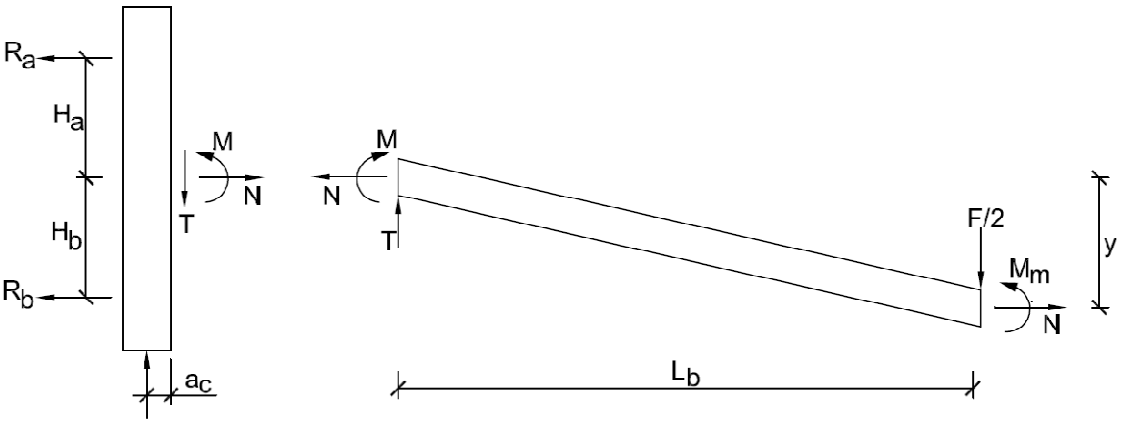

Figure 2.13: Static Free Body Diagram for Beam and Supporting Column [18].

A static equilibrium equation was derived [18] for one-half of the tested system to provide the normal force, N, caused by the applied force, F, shown as

$$N = \frac{\left(\frac{FL_b}{2} + M - M_m\right)}{y} . \quad (16)$$

Assuming a true catenary state where no moment is present, Equation (16) can be simplified to

$$N = \frac{FL_b}{2y} . \quad (17)$$

In pure catenary the shear force, T, can be taken as,

$$T = \frac{F}{2} . \quad (18)$$

Summing the horizontal forces to zero, the supporting column reaction at support A is equal to

$$R_A = \frac{\left(Nh_B + R_C a_C - M\right)}{(h_A + h_B)} . \quad (19)$$

Similarly, the supporting column reaction at B is equal to

$$R_B = \frac{\left(Nh_B - R_C a_C + M\right)}{(h_A + h_B)} . \quad (20)$$

Assuming during catenary action the moment capacity within the beam to column connection has been released and h_A is equal to h_B, the reactions at A and B can be simplified to

$$R_A = R_B = \frac{N}{2} . \quad (21)$$

Girhammar's simple statics model can be used to predict the normal forces present when catenary action occurs as a result of an applied vertical load. This process can also be used to ensure load measurement devices provide accurate data during elastic stages of load application by maintaining equilibrium in the test system where the sum-of-forces is equal to zero. Furthermore, the pure catenary response can be used to

determine the maximum tensile force occurring at the connections. Doing so, maximum forces can be developed for the initial design of the tested connections and for the verification of testing apparatuses. Girhammar's model and test methodology will be used as the experimental test model for the research conducted for this report .

2.5.2 Robustness of Composite Floor Systems with Shear Connections: Modeling, Simulation, and Evaluation.

As part of the National Institute of Standards and Technology's (NIST) study of events leading to progressive collapse, Sadek *et al.* [19] conducted analytical research similar to the experimental research of Girhammar [18] studying the characteristic behavior of shear tab beam to column connections when subjected to a simulated column collapse. Sadek *et al.* studied two specific scenarios using a multitude of modeling techniques. First, an understanding of the connection's behavior and failure modes was studied by isolating the modeling to a planar frame model comprised of a supported beam, supporting column, and a single plate connection. The information obtained from this isolated model was then used to develop a three dimensional multi-bay framing system incorporating the contributions of steel deck and a wire mesh reinforced concrete slab component to determine analytical values of the robustness of the total floor system when subjected to a simulated slow rate column failure.

The analytical modeling was based on a prototype steel framed building designed by NIST comprised of twenty by thirty foot bays using W16X26 ASTM A992 beams and W14X74 ASTM A992 columns connected by the shear tab connection shown in Figure

2.14. All models were analyzed using a twenty foot span with one connection modeled as a true pin connection opposite of the research specimen.

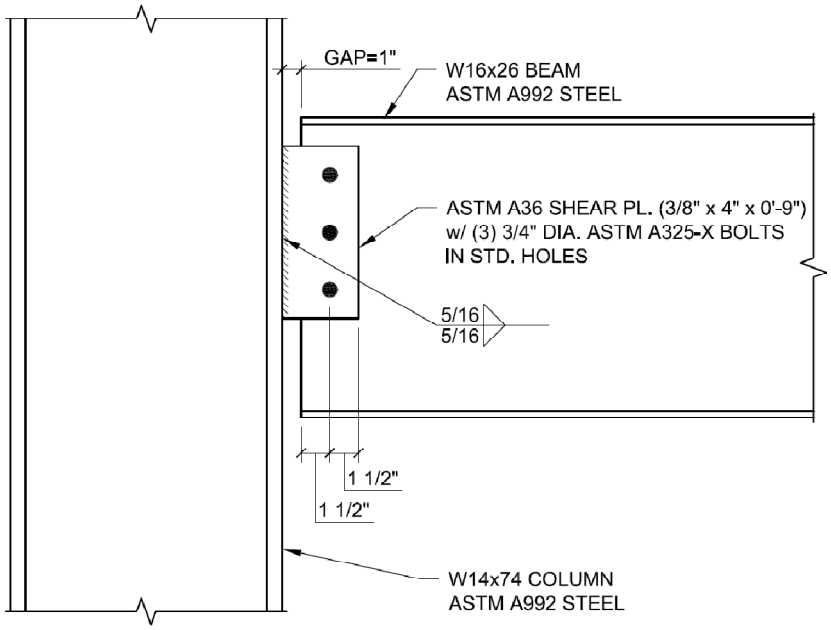

Figure 2.14: NIST Theoretical Test Assembly for Shear Tab Connections [19].
-- Reproduced image, converted to Imperial units

Due to the lack of experimental data available to describe the shear tab connection's response to column failure, three finite element models of various degrees of complexity were used to describe the isolated connection's behavior allowing the researchers the ability to narrow down the size of model required for the overall system model. The finite element modeling techniques incorporated high fidelity, reduced component, and reduced coarse shell connection models. The more complex high fidelity model shown in Figure 2.15(a) incorporated contact surfaces between the beam web, bolts, and shear plate. This model provided the baseline data used to develop the less complex modeling scenarios. The high fidelity model showed the connections flexural stiffness controlled the early stages of load transfer through a force couple created by bolt bearing about the neutral axis of the bolt group. As the column reached approximately

1/2 inch of vertical deflection or 0.002 radians of beam end rotation, the connection moved towards cable-like or catenary behavior. This transition point was one-tenth of the elastic rotational limit described by Astaneh [7] for the elastic rotational range of shear tab connections for shear only tests. Failure occurred due to large catenary forces at approximately twenty-one inches of vertical deflection or 0.088 radians of beam end rotation as a result of bolt bearing tearout of the supported W16 beam web. Substantial plastic deformation was also exhibited in the single plate bolt holes as well as the connecting bolts while the overall supported W16 beam remained in the elastic state.

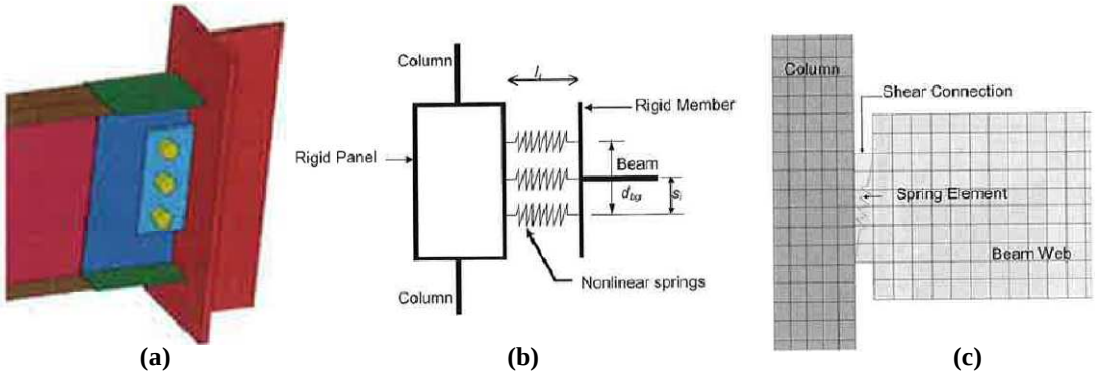

Figure 2.15: Illustration of Different Complexities of Finite Element Models [19].
(a) High fidelity connection model; (b) Reduced component connection model;
(c) Reduced coarse shell connection model.

Based on the results of the high fidelity connection model, a reduced component connection (RCC) model was created simulating the connection strength using non-linear springs and rigid supports. Shown in Figure 2.15(b), three non-linear springs simulated the behavior of the contact surfaces of the high fidelity model. The initial elastic stiffness of the springs was based on the research of the SAC Joint Venture Group [17] with a yield and rupture point established using the AISC 13th Edition Specification [2] limit states for axially loaded connecting elements. The spring's inelastic deformation limit, θ_g, was established using the plastic rotation limits of Equation (13). An additional 0.02

radians was added to the plastic rotational limits to account for elastic deformation. The combination of the two values resulted in a total rotational deformation limit of

$$\theta_g = \left(0.17 - 0.0036 * d_{bg}\right). \quad (22)$$

The approximate total rotational deformation for each spring element was estimated at 0.14 radians. This approximation is interesting due to the fact that the calculated controlling ultimate capacity of the connection was determined to be a bearing tearout failure of the beam web.

The final finite element model utilized the aspects of the previous models to produce the most simplistic of the three models. The reduced coarse shell connection (RCSC) model shown if Figure 2.15(c) utilized a connecting element with a width equal to the supported beam web and a thickness equal to the horizontal edge distance shown in Figure 2.14. The elastic-inelastic characteristics were represented by a spring element based on the behavior of the spring elements utilized in the RCC model. The model required less detail yet maintained the same strength and rotational ductility characteristics exhibited by the more intensive modeling methods.

The data accumulated from the three finite element models were used to model various three-dimensional framing systems subjected to a simulated column failure. The research analyzed three states of a steel framed structure including framing only, framing plus a secured metal deck, and finally, a detailed model including a composite concrete slab. The framing only scenario is pertinent as the remaining scenarios are beyond the scope of this research. Figure 2.16 provides the response of the simulated column failure for the framing only (columns restrained) scenario with a peak displacement of

approximately twenty-four inches which results in a beam end rotation of approximately 0.98 radians.

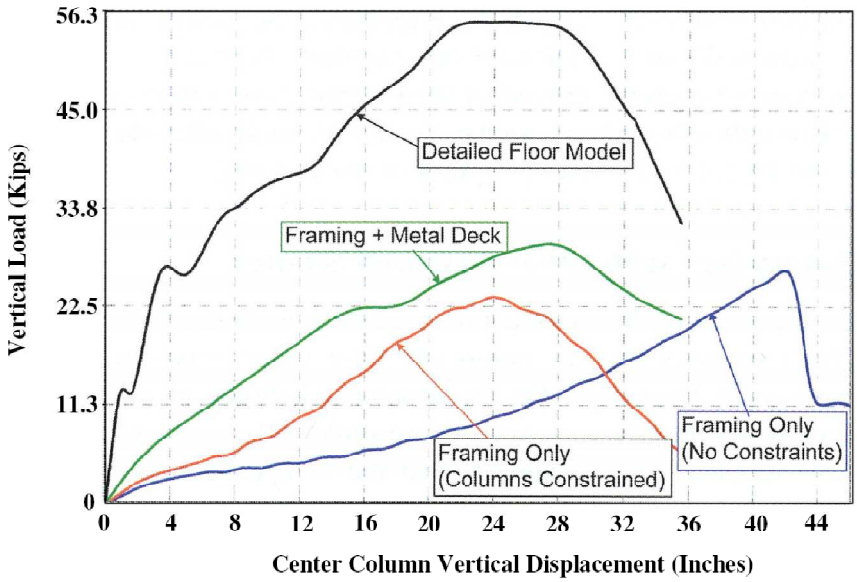

Figure 2.16: Analytical Floor Model Analysis Comparisons [19].

The three finite element modeling methods simulated a column failure which caused the connections to exceed their flexural capacity. The connection progressed to cable-like catenary action due to large rotational deformations as a result of vertical deflections which caused the bolts to plow through the connecting material of the supported beam web. The actual peak beam end rotation of 0.088 radians was significantly less than estimated beam end rotation of 0.14 radians determined using Equation (22). Sadek *et al.* attributed this difference due to the inherent variation in load transfer mechanisms of flexure and catenary action. The research described in FEMA-355D [17] reported a flexural failure mechanism as a result of the connection's plastic rotational capacity being exceeded by an internal force couple about the centroid of the bolt group. The connection ductility was based on depth of the connection and the distance from the outermost bolt to the bolt group centroid. The analytical models created

by Sadek *et al.* [19] determined though flexure limits initially control, the column failure created a tensile failure mechanism where the ductility was based on the connections ability to stretch. The research by Sadek *et al*. concluded for the particular tested scenario bolt bearing tearout of the beam web was the controlling limit state. The beam web tearout failure contradicts the criterion established for Equation (13) by FEMA-355D [17]. The research stated Equation (13) and therefore Equation (22) were only valid provided the edge distances and element thicknesses were such that bolt shear rupture was the controlling limit state [17]. This discrepancy will be further investigated by this research to determine which method most accurately depicts the ultimate plastic beam end rotation limit when subjected to catenary forces introduced by column failure.

2.6 Structural High Strength Bolt Behavior

2.6.1 Guide to Design Criteria for Bolted and Riveted Joints.

Previous research has shown the bolt shear rupture capacity for shear tab connections is the pivotal link for determining the connections' capabilities to transfer various forces. Kulak *et al.* [20] conducted direct shear tests which established the base line data for the shear strength of high strength structural steel fasteners adopted by the AISC 13th Edition Specification [2]. The testing utilized two separate jigs to determine a mean ultimate shear stress as a percentage of the ultimate tensile strength for ASTM A325 high strength bolts. Shown in Figure 2.17, a compression and tension shear jig made of like materials applied load, P, to high strength bolts in double shear. The compressive jig produced higher ultimate shear stress capacities than the tension jig because the tension jig's lap plates pried away from the main connection plate. This

prying action caused additional flexural stresses to develop in the bolts which the compressive jig tests did not observe.

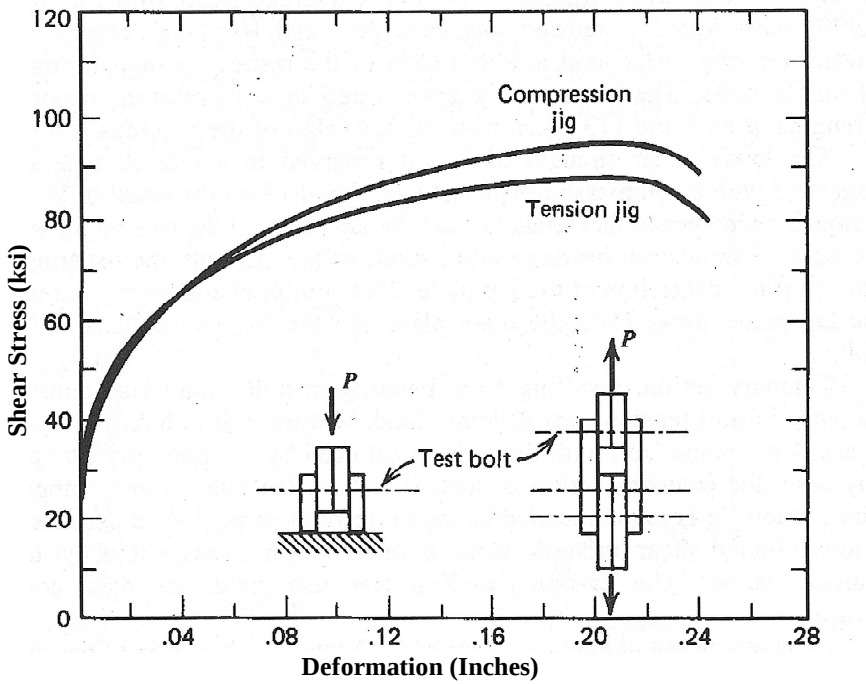

Figure 2.17: Ultimate Shear Stress versus Deformation for ASTM A325 Bolts Tested in Compression and Tension Jigs [20].

Kulak *et al.* determined the ASTM A325 high strength bolts subjected to shear through the tension jig reached an average ultimate shear stress of 80.1 kips-per-square-inch (ksi) equal to sixty-two percent of the ultimate tensile capacity. The compressive tests reached and average ultimate shear stress of 86.5 ksi equaling sixty-eight percent of the ultimate tensile capacity. Kulak *et al.*'s research also suggested the lower bound experimental values obtained by the tension type jig be used in practice to prevent un-conservative designs. The research conducted by Kulak *et al.* can be used to establish ultimate bolt shear forces which can be expected during experimentation.

Chapter 3

Experimental Testing

3.1 Experimental Overview

The purpose of the experimentation was to capture the shear tab's characteristic behavior when subjected to unexpected forces caused by the failure of a supporting column. A total of nine full scale tests were conducted at the Milwaukee School of Engineering (MSOE) Construction Science and Engineering Center (CSEC) laboratory on three, four, and five bolt shear tab connections designed per the "Conventional Configuration" procedure described per the 2005 AISC Specification 13th Edition [2].

The connection properties were chosen to simulate common connection configurations typically found in steel framed structures. Furthermore, the current experimental testing was conducted in conjunction with similar testing of WT simple shear connection specimens by Friedman [22] as well as single angle simple shear connection specimens by Johnson [23]. Connection geometries were selected which were within the allowable provisions of the current connection design specifications while allowing the use of a single test apparatus setup for all testing.

Figure 3.1 shows the typical test system configuration. The testing simulated a planar two bay framing system of equal lengths consisting of two exterior columns, one interior column, and two supported beams. The exterior beam connections were connected with fabricated true pin connections at the exterior column flanges. The interior beam connections were connected with similar shear tab test specimens at each flange of the interior column. The test system did not include steel deck or concrete slab connections as the goal of the research was to isolate the shear tab's response to extreme

loading conditions. A hydraulic cylinder connected to the interior stub column simulated load and displacements occurring as if the column had been compromised. A complete description of the test apparatus and test specimens is provided in Section 3.3.

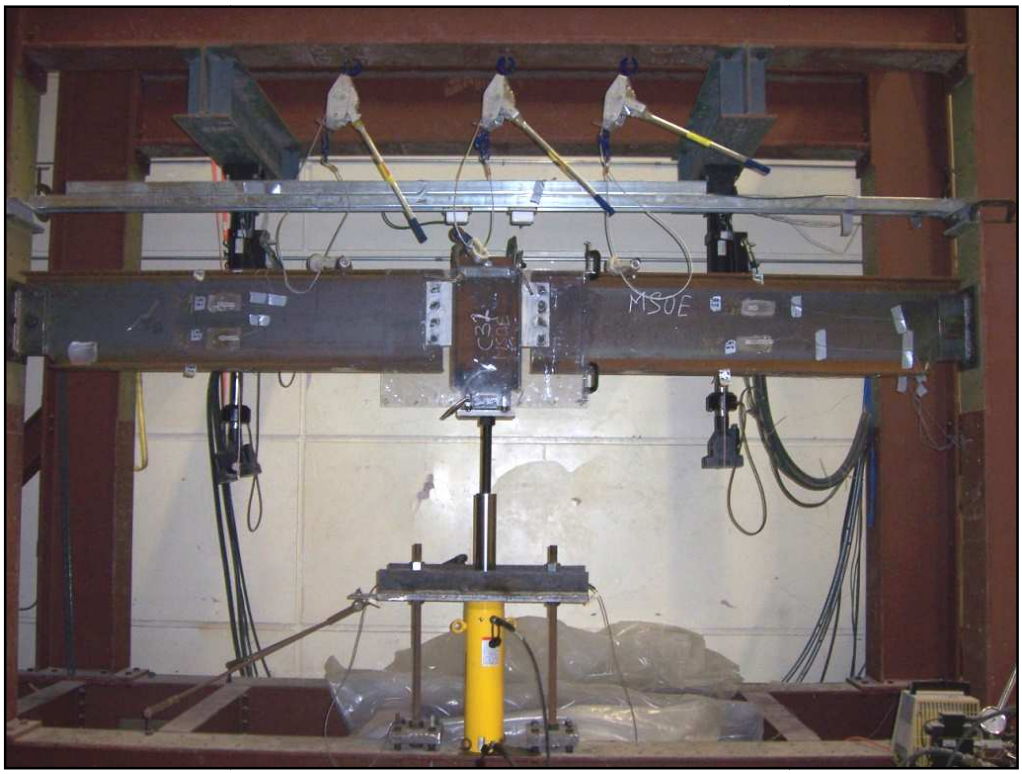

Figure 3.1: Typical Test System Configuration Prior to Testing.

The goal of the simulated column failure was to induce tensile forces in the shear tab connections not accounted for in the "Conventional Configuration" design as well as to generate beam end rotations exceeding current design standards of 0.03 radians assumed for simply supported framing. Research is presented providing experimental data depicting the shear tab's characteristic behavior when subjected to a combination of shear, tension, and moment as a result of a simulated column failure. Furthermore, the robustness of the shear tab connection and the connection's ability to reach a catenary state is investigated.

3.2 Test Specimens

3.2.1 Test Specimen Geometry

A total of eighteen connection specimens were designed per the provisions of the 2005 AISC 13th Edition Specification using connection length as the sole varying parameter in the specimens' geometry. Three lots of six connections consisting of three, four, and five bolt connections were chosen to provide a full range of connection depths which fit within the available web depth of the test beams.

The connections were designed with the maximum allowed bolt offset dimension of 3 1/2 inches to reduce the possibility of the test beams' top flange from binding against the test column as the specimens were expected to be subjected to large beam end rotations. The connection plate material was limited to 3/8 inch ASTM A36 material along with 3/4 inch diameter A325 bolts with the threads excluded from the shear plane to keep within the load capabilities of the MSOE CSEC test frame. In accordance with Table J3.4 of the 2005 AISC 13th Edition Specification [2], a vertical and horizontal edge distance of two times the bolt diameter equal to 1 1/2 inches was selected. A three inch center to center bolt spacing as well as three inch punch-down dimension from the beam top flange to the center of the first bolt hole was selected in keeping within current industry standard practices. Figures 3.2 through 3.4 depict the connection geometry and naming convention used for the three, four, and five bolt tests, respectively.

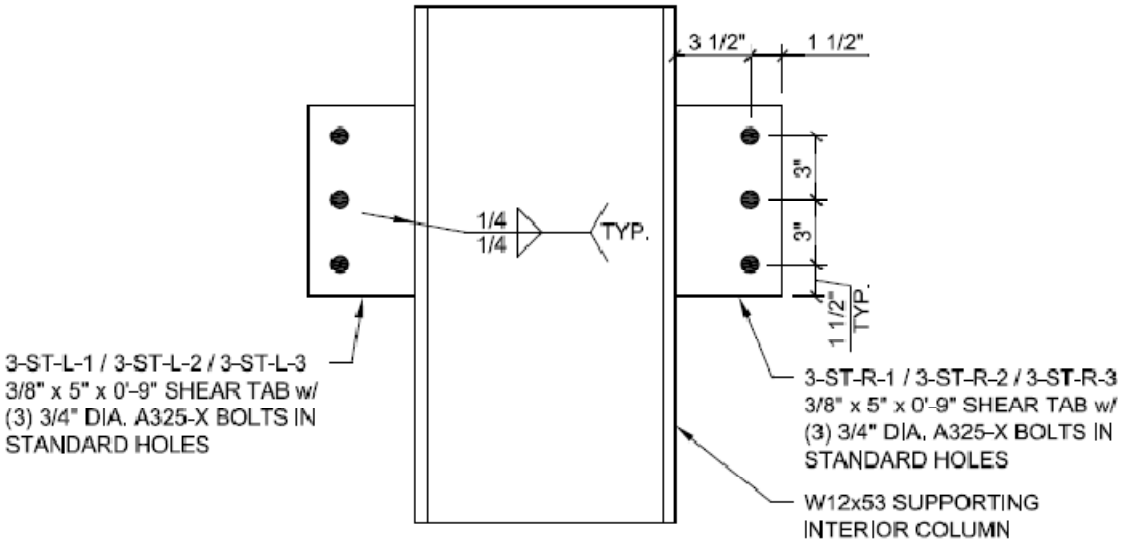

Figure 3.2: Typical Three Bolt Shear Tab Connection Geometry.

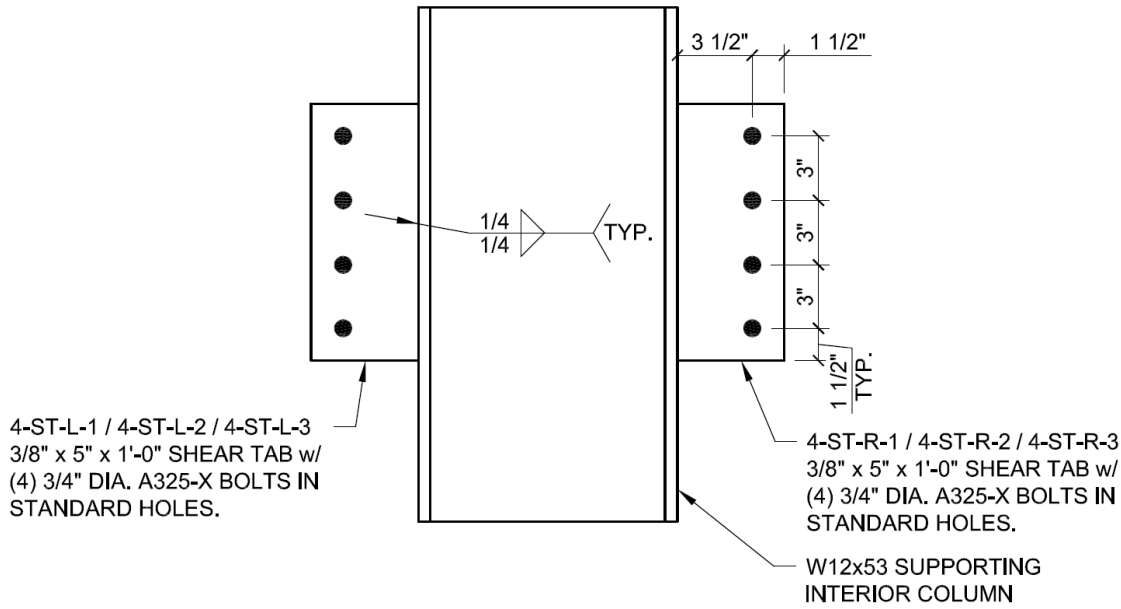

Figure 3.3: Typical Four Bolt Shear Tab Connection Geometry.

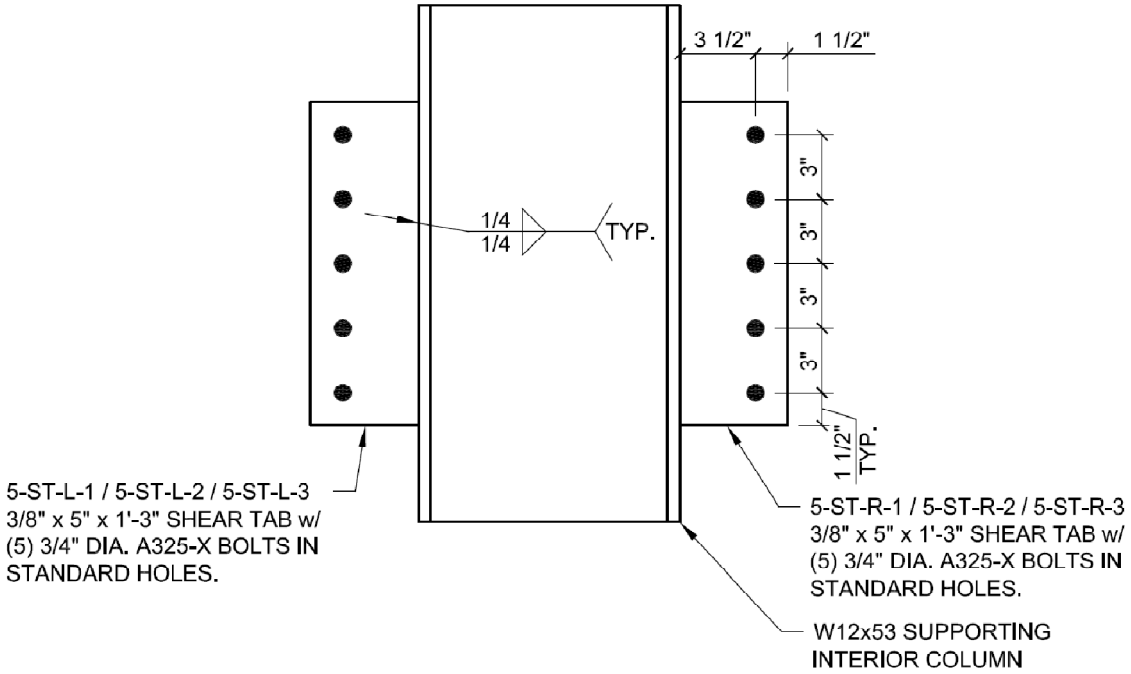

Figure 3.4: Typical Five Bolt Shear Tab Connection Geometry.

3.2.2 Connection Design Capacities

Two controlling limit states were determined for two load scenarios. First, the governing limit state was calculated for the connection's capacities per the AISC 13th Edition Specification [2] "Conventional Configuration" guidelines without the use of the specified safety factors for a vertical shear only load case. A complete example of the required connection limit states due to shear only is provided in Appendix A.

The second limit state was calculated for the connection's capacity as a "Hanger" or tension only connection per the design equations of Chapter J of the AISC 13th Edition Specification [2] without the use of the specified safety factors. A complete example of the required limit states for the tension only scenario is provided in Appendix B. Summaries of the connection capacities for the three, four, and five bolt connections are provided in Tables 3.1 and 3.2.

Based on the analytical research by Sadek *et al.* [19] the connection failures were expected to result from a combination of bolt shear and bolt bearing rupture failures due to large beam end rotations and the introduction of large catenary forces as the interior column deflected vertically.

Table 3.1: "Conventional Configuration" Single Plate Un-Factored Shear Capacities per AISC 13th Edition Limit States [2].

Single Plate "Conventional Configuration" Ultimate Shear Capacity				
Connection Limit State	**AISC 13th Equation**	**3 Bolt Shear Tab**	**4 Bolt Shear Tab**	**5 Bolt Shear Tab**
Single Bolt Shear Rupture (kips/bolt)	J3-1	26.5	26.5	26.5
Shear Plate Single Bolt Tearout (kips/bolt)	J3-6b	35.7	35.7	35.7
Shear Plate Single Bolt Bearing (kips/bolt)	J3-6b	48.9	48.9	48.9
Beam Web Single Bolt Tearout (kips/bolt)	J3-6b	-	-	-
Beam Web Single Bolt Bearing (kips/bolt)	J3-6b	43.9	43.9	43.9
Bolt Shear Rupture (kips)	J3-1	79.5	106.0	132.5
Shear Plate Bolt Bearing (kips)	J3-6b	133.6	182.4	231.4
Beam Web Bolt Bearing (kips)	J3-6b	131.6	175.6	219.5
Weld Shear Rupture (kips)	J2-4	129.9	174.4	219.0
Base Metal Shear Rupture (kips)	J4-4	114.2	153.3	192.5
Min. Support Thickness (inches)	p. 9-5	0.38	0.38	0.38
Shear Plate Shear Yield (kips)	J4-3	72.9	97.2	121.5
Shear Plate Shear Rupture (kips)	J4-4	83.2	110.9	138.7
Shear Plate Block Shear Rupture (kips)	J4-5	83.9	108.2	132.4
Beam Shear Yield (kips)	G2-1	159.3	159.3	159.3

Table 3.2: Single Plate Un-Factored Tensile Capacities per AISC 13th Edition Limit States [2].

Single Plate Ultimate Tensile Capacity				
Connection Limit State	**AISC 13th Equation**	**3 Bolt Shear Tab**	**4 Bolt Shear Tab**	**5 Bolt Shear Tab**
Single Bolt Shear Rupture (kips/bolt)	J3-1	26.5	26.5	26.5
Connecting Plate Single Bolt Tearout (kips/bolt)	J3-6b	35.7	35.7	35.7
Connecting Plate Single Bolt Bearing (kips/bolt)	J3-6b	48.9	48.9	48.9
Beam Web Single Bolt Tearout (kips/bolt)	J3-6b	32.0	32.0	32.0
Beam Web Single Bolt Bearing (kips/bolt)	J3-6b	43.9	43.9	43.9
Bolt Shear Rupture (kips)	J3-1	79.5	106.0	132.5
Connecting Plate Bolt Bearing (kips)	J3-6b	107.1	142.8	178.5
Beam Web Bolt Bearing (kips)	J3-6b	96.0	128.0	160.0
Weld Shear Rupture (kips)	J2-4	194.9	261.7	328.5
Base Metal Tensile Rupture (kips)	J4-2	190.3	255.6	320.8
Connecting Plate Tensile Yield (kips)	J4-1	121.5	162.0	202.5
Connecting Plate Tensile Rupture (kips)	J4-2	138.7	184.9	231.1
Connecting Plate Block Shear Rupture (kips)	J4-5	116.5	163.1	209.3
Beam Web Block Shear Rupture (kips)	J4-5	107.8	149.3	190.7

3.3 Experimental Setup

3.3.1 Test Assembly Overview

An overview of the experimental test setup is shown in Figure 3.5. Refer to Appendix C for design calculations of the test apparatus sub-assemblies. All sub-assemblies excluding the interior columns were designed to withstand all testing conducted for this research as well as the research of Friedman [22] and Johnson [23].

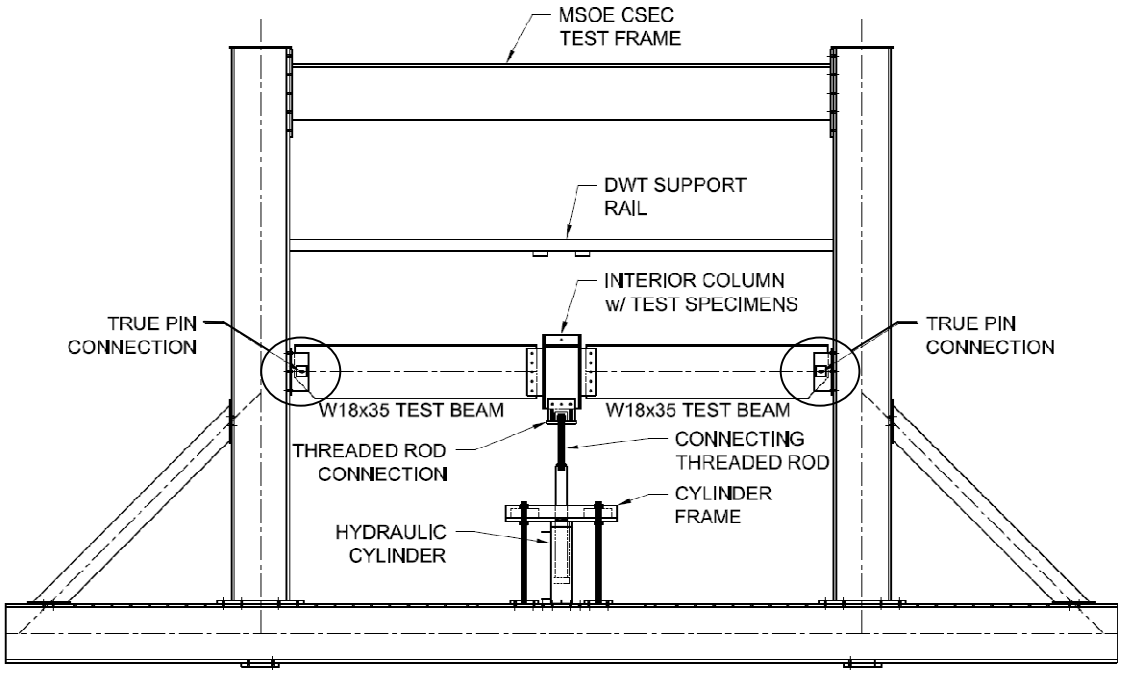

Figure 3.5: Test Assembly Overview.

3.3.2 Test Beam

The interior test specimens were connected by two symmetrical ASTM A992 W18X35 sections. The section size was selected because the interior web depth provided adequate clearance for five bolt connections while maintaining the one-half depth requirement required per the AISC 13th Edition Specification [2] for the three bolt connections. To ensure bolt bearing deformations were minimized at the test specimen

bolt hole locations, a 3/8 inch ASTM A36 web doubling plate was welded to the far side of the beam web with an all-around 1/4 inch E70XX fillet welds. The exterior beam ends were fabricated with one 1-5/16 inch diameter hole with one 3/8 inch thick ASTM A36 web doubling plate welded with a 5/16 inch E70XX three sided fillet weld on each side of the beam web to accommodate the true pin connection. The bottom beam flange was chamfered to prevent the possibility of the flange binding against the MSOE CSEC test frame during testing. Figure 3.6 shows the typical test beam configuration.

Figure 3.6: Typical Test Beam Configuration.

3.3.3 True Pin Connection

True pin connections were designed for the test beam connections to the MSOE CSEC test frame to limit the load transfer at the beam end to a unidirectional tensile force in line with the test beam strong axis. Doing so, the pin location was treated as a point of zero moment when developing the moment envelope for the tested connection. The pin connections consisted of a welded plate assembly connected to the test beam with a 1-1/4 inch diameter ASTM A490 bolt with the threads excluded. The assembly was bolted to the MSOE test frame with six 3/4 inch ASTM A325 bolts with the threads included. Figures 3.7 and 3.8 show the typical true pin connection assembly

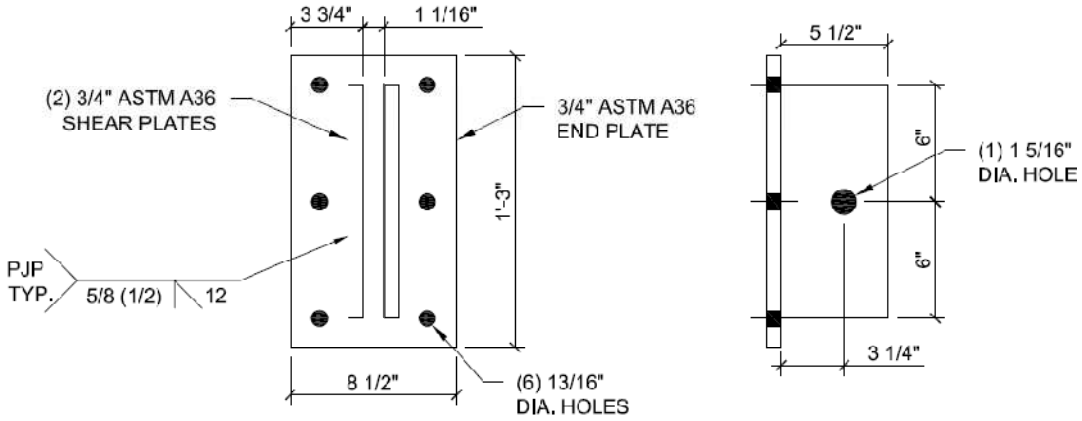

Figure 3.7: Exterior Beam End True Pin Connections.

Figure 3.8: Erected True Pin Connection.

3.3.4 Hydraulic Cylinder Frame

A hydraulic cylinder was utilized to impart vertical loads and displacements which simulated a controlled collapse of the interior column by retracting the threaded rod assembly connected to the interior column web. To provide the resistance which allowed the hydraulic cylinder to retract, a frame assembly was designed utilizing welded plates and threaded rods. The frame assembly also provided the housing for two load cells which were used to measure the load applied to the system. Shown in Figure 3.9, the

frame assembly was composed of a one inch ASTM A36 end plate reinforced with a pair of one inch ASTM A36 stiffener plates. The end plate was fabricated with a four inch diameter hole centered on the plate to allow the hydraulic cylinder to extend through the plate assembly. The hydraulic cylinder's outside collar was used as the end plate bearing surface.

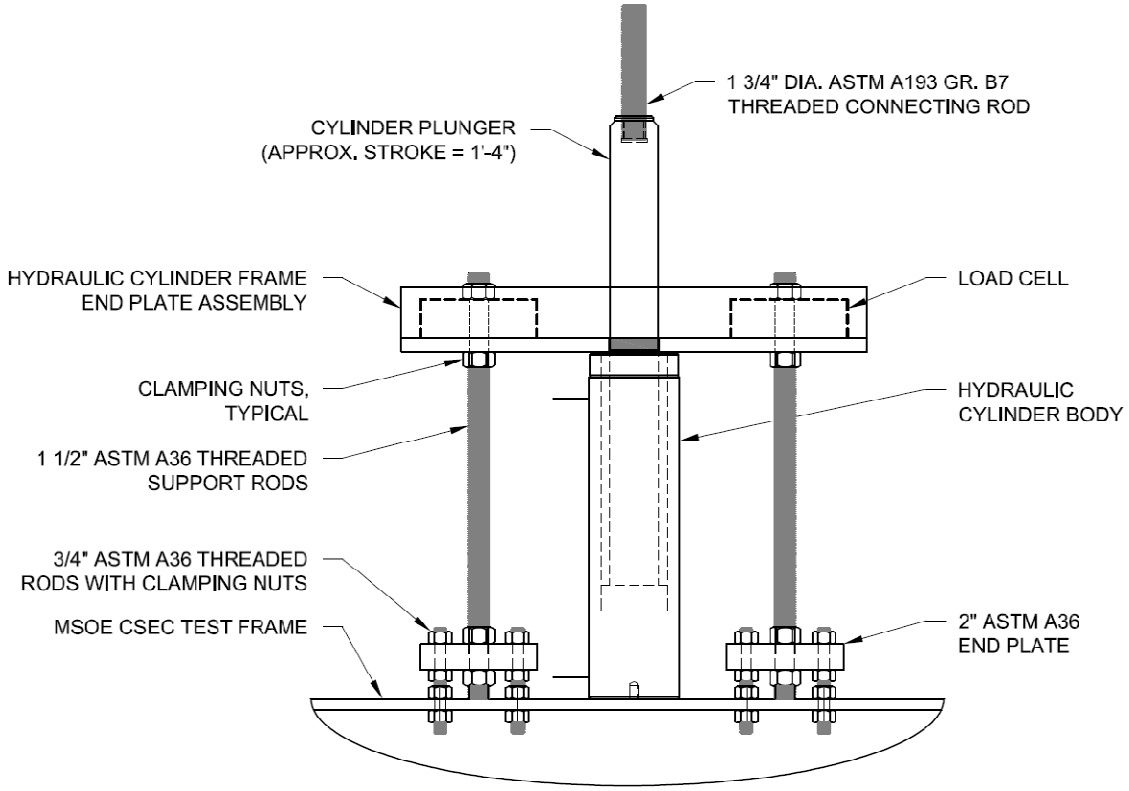

Figure 3.9: Hydraulic Cylinder Frame Assembly Overview.

The end plate assembly was required to be rigid enough to transfer the bearing force from the hydraulic cylinder to two 1 1/2 inch diameter ASTM A36 threaded rods. The threaded rods projected through a load cell and the end plate assembly. A threaded nut was used on each side of the load cell and end plate assembly providing a clamped support for the assembly. The threaded rods were extended down and attached to the MSOE CSEC test frame. The threaded rods passed through a two inch ASTM A36 end

plate where threaded nuts on each side of the end plated clamped the threaded rod in place. The end plates were then attached to the MSOE CSEC test frame with four 3/4 inch diameter ASTM A36 threaded rods. Two lateral supports were attached from the welded end plate assembly to the MSOE CSEC test frame to prevent lateral movements from occurring during the testing. Figure 3.10 shows the erected assembly of the hydraulic cylinder frame.

Figure 3.10: Hydraulic Cylinder Erected Condition.

3.3.5 Threaded Rod Connection

The hydraulic cylinder plunger was connected to the interior column by the use of a 1 3/4 inch diameter ASTM A193 Gr. B7 rod threaded into the hydraulic cylinder and clamped with two threaded nuts to a welded plate assembly. The welded assembly consisted of a one inch ASTM A36 end plate with two 1/2 inch ASTM A36 shear plates welded to the end plate face. Four 1/2 inch ASTM A36 stiffener plates were added to the welded joint to ensure the connection was rigid enough to withstand the hydraulic cylinder retraction. The welded assembly was connected to the interior column specimens

with three 3/4 inch diameter ASTM A325 bolts with the threads excluded. Figure 3.11 and Figure 3.12 depict the threaded rod connection assembly.

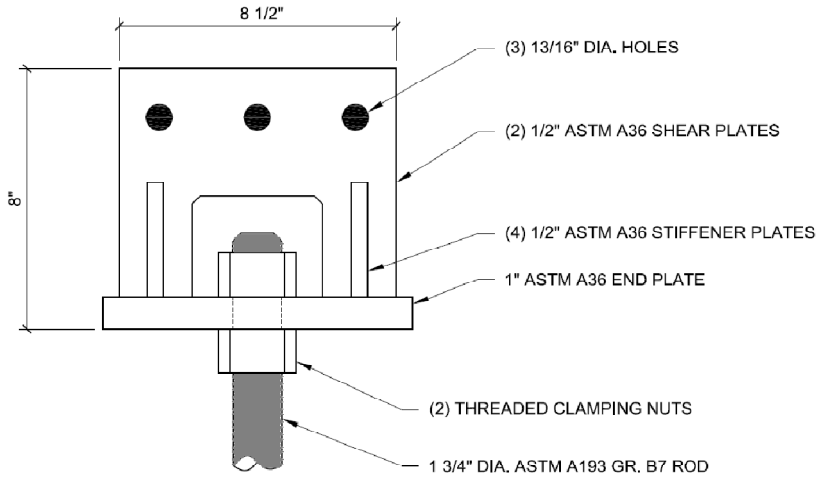

Figure 3.11: Threaded Rod Connection Overview.

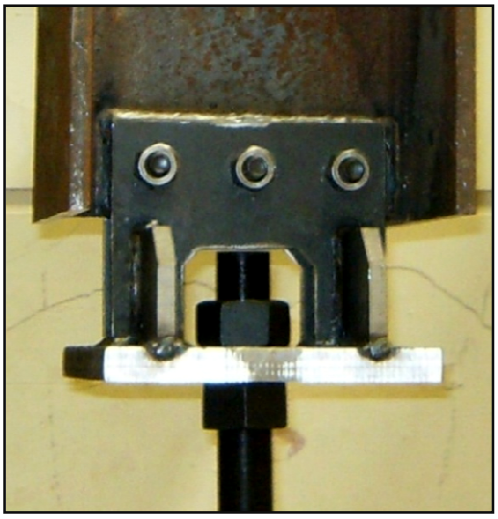

Figure 3.12: Threaded Rod Connection Erected Condition.

3.4 Experimental Instrumentation

The experimental data acquisition consisted of three primary components measuring the applied load, vertical deflection, and resulting strain in the test beams. Shown in Figure 3.9, the applied vertical shear load was provided by an ENERPAC® Model RR-10018 hydraulic cylinder capable of producing approximately eighteen inches

of vertical stroke with a 100 ton retraction capacity powered by a manually operated 64 ton capacity hydraulic pump. The applied force was measured by two Sensotec® Model 41-A530-01-03 loads cells each capable of measuring 50 tons with accurate measurement increments of fifty pounds of force. Shown in Figure 3.13, two Unimeasure® Model PA-30DS-L5M draw wire transducers (DWT) connected to a cold formed steel track were attached to the interior column flanges providing the vertical deflection measurements.

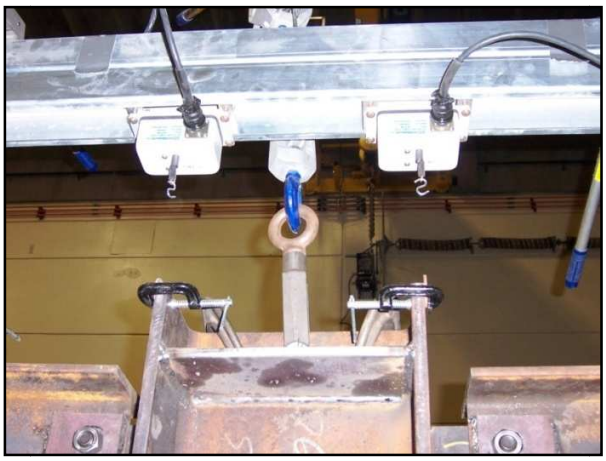

Figure 3.13: Draw Wire Transducer Placement.

Strain data were collected from eight 120 ohm, series EA-XX-125BT-120, strain gauges placed four feet from the center of the test apparatus. Shown in Figure 3.14, one strain gauge was centered on each flange with the remaining two strain gages placed at the beam section's quarter points.

Figure 3.14: Typical Strain Gage Placement on Test Beam.

Data readings from the load cells, DWT's, and strain gauges were transmitted to a National Instruments "DAQPad" Model 6020E, twelve bit data acquisition system. Readings were collected by a Compaq Armada Model E500 laptop computer with National Instruments "LabView" software for interface with the data acquisition system.

3.5 Experimental Safety

Due to the destructive nature of the experimental testing, safety of the researchers and MSOE CSEC laboratory equipment was of primary importance. A lexan containment cage was fabricated to contain bolt and plate fragments which sheared off during testing. To prevent the test beams and interior column specimens from crashing or propelling out of plane, three steel cable hand ratchets, or "comealongs," were attached from the MSOE test frame to each individual component. The cables were slacked to allow the full stroke of the hydraulic cylinder without interfering with the test process but provided a restraint in the event of a complete connection failure. The comealongs also aided in holding the positions of the test beams as the interior column specimens were switched between tests.

3.6 Experimental Procedure

Upon the arrival of the fabricated steel specimens from Germantown Iron and Steel based in Jackson, Wisconsin, the hydraulic cylinder, true pin connections, and cylinder frame were installed and secured to the MSOE CSEC test frame. The test beams were lifted into the test frame and attached to the true pin connections with a 1-1/4 inch ASTM A490 bolt. The bolt was only snug tightened to allow the beam end to freely

rotate. An additional nut was added to prevent the connection from loosening during the testing. The test beams were held in place with a comealong at each beam end.

Next, the experimental instrumentation was verified for accuracy. The load cells were independently verified for accuracy using an external MSOE CSEC laboratory small scale test frame. The two load cells were found accurate within 100 pounds of force or 0.1 percent error of the rated capacity. The load cells were then place in the hydraulic cylinder frame and secured with a plate washer and hand tightened threaded nut as shown in Figure 3.9. The DWT's were verified within 0.01 inches before being installed and secured in the fabricated cold-formed steel track. Finally, the strain gauges were verified to have 120 ohms of resistance before being wired to the data acquisition equipment.

With the instrumentation accuracy verified, the threaded rod connection was bolted to the interior column specimens. The interior column with the fabricated connection test specimens was then lifted into place with the MSOE CSEC laboratory overhead crane. The specimens were connected with snug tight bolts with one washer on the nut side. A comealong was attached to the interior column and the test system was leveled. The DWT's were then attached to the column flanges, a plaster white wash was applied to the near side connection face, and the lexan safety cage was secured. The hydraulic cylinder and threaded rod were extended and attached with two threaded nuts to the threaded rod connection. As is discussed in Chapter 4, the plaster white wash provided a real-time visual aid into the understanding of the load path(s), stress patterns, and material yielding which occurred during testing.

Upon verification that all test instrumentation was correctly attached, safety devices installed, and the plaster white wash had sufficiently dried, the testing was

conducted. The data acquisition system was set up to provide a real-time plot of force versus displacement to serve as a guide of the potential connection failure point as the hydraulic pump used to control the retraction of the hydraulic cylinder required manual operation. The pump was not capable of sustaining a steady state of force nor could the pump automatically apply force based on predetermined force or displacement increments. Therefore, load was slowly applied at steady increments based on the pump operator's discretion. As is shown in Chapter 4, the discretionary load increments caused non-uniformity in the plotted data; however, the validity of the collected data remained. Loading was continued until connection failure. The determination of the connection's failure was based on the sudden loss of force reported by the data acquisition system's real-time graph. The connection failure was visually verified as an obvious failure mode was evident simultaneous of the loss of force. Figure 3.15 shows a typical connection failure. Upon connection failure, the comealongs were tightened and the hydraulic ram was released. Observations and notes of the connection failure were taken, the connections were released, and the testing was repeated.

Figure 3.15: Typical Connection Failure Visual Verification.

Chapter 4

Experimental Results

4.1 Experimental Results Overview

The experimental results included within this chapter have been compiled to describe the four fundamental measurements observed during testing. A description of the applied shear, measured axial and moment forces, and measured beam end rotations have been compiled to describe the behavior and failure mechanisms of the three, four, and five bolt shear tab connections. Furthermore, a preliminary analysis method has been described to provide an initial step to determine the maximum bolt forces at the point of the maximum measured moment. The preliminary bolt force calculations have been used to validate the failure mode mechanism calculations provided for each test's failure mode.

4.2 Data Analysis Process

The following represents the analysis process utilized to synthesis the collected experimental data. The raw experimental data were converted to axial and flexural force utilizing three fundamental equations. First, the strain gage measurements at each time step for each strain gage were converted to stress using Hooke's Laws, shown as

$$\sigma_n = E * \mu^{-6} * 10^6 \quad (23)$$

where

σ_n = stress at strain gage 'n' in ksi,

E = Modulus of elasticity of steel equal to 29,000 ksi,

μ^{-6} = measured experimental microstrain.

These stress measurements represented the combined axial and flexure stress at the location of each strain gage as shown in Figure 3.14. The stress at any point of the beam section was evaluated as

$$\sigma_n = \frac{P}{A} \pm \frac{Mc_n}{I_x} \tag{24}$$

where

A = Cross sectional area of a W18X35 equal to 10.3 in.^{2},

c_n = Distance from strain gage 'n' to the neutral axis of the supported beam,

I_x = Strong axis moment of inertia of a W18X35 equal to 510 in.^{4},

P = Axial force in kips,

M = Flexural force in kip-inches.

To determine the axial and flexural forces in the supported beam at each time step, a system of simultaneous equations was derived using the stress measurements at two equidistant strain gages on opposing sides of the neutral axis of the supported beam. The collected data showed erroneous results were collected for strain gage 1 on the left supported beam and strain gage 6 on the right side supported beam. Because of this invalid data, strain gages 2 and 3 on the left supported beam and strain gages 5 and 8 on the right supported beam were used to determine the axial and flexural forces of the respective beams. Solving the stress equation of σ_2 for P yields

$$P = A(\sigma_2 + \frac{\mathrm{Mc_2}}{\mathrm{I_x}}). \tag{25}$$

Equation (25) is substituted for P into the stress equation of σ_3

$$\sigma_3 = \frac{A(\sigma_2 + \frac{\mathrm{Mc_2}}{\mathrm{I_x}})}{A} + \frac{\mathrm{Mc_3}}{\mathrm{I_x}}. \tag{26}$$

Setting c_2 equal to c_3 Equation (26) is simplified to

$$\sigma_3 = \sigma_2 + \frac{2\mathrm{Mc}}{\mathrm{I_x}}. \quad (27)$$

Solving for *M*, Equation (27) can be shown as

$$M = \frac{I_x(\sigma_3 - \sigma_2)}{2*c}. \quad (28)$$

Substituting Equation (27) for *M* in Equation (25), *P* can be simplified to

$$P = 0.5 * A * (\sigma_3 + \sigma_2). \quad (29)$$

Equation (28) and Equation (29) provide the flexure and axial forces in the left side supported beam at the strain gage location for each time step. Similarly, substituting in the right side stress values, the flexural force is shown as

$$M = \frac{I_x(\sigma_8 - \sigma_5)}{2c} \quad (30)$$

and the axial force is taken as

$$P = 0.5 * A * (\sigma_8 + \sigma_5). \quad (31)$$

The data at the strain gage locations were used to determine the forces at the bolt lines of the tested connections. The measured axial force at the strain gage location and the bolt line remained unchanged. The flexural forces were extrapolated from the forces at the strain gage locations using a simple triangular moment distribution model. Using the true pin connection at the exterior column connections as a point of zero moment, the slope of the moment distribution line was taken as

$$slope = \frac{M_x}{x} \quad (32)$$

where M_x is equal to the moment in kip-inches at any distance *x* away from the true pin connection in inches. Using the slope of the moment distribution line, a comparison of similar triangles at each time step yielded,

$$M_b = \frac{Mx_b}{x_{sg}} \quad (33)$$

where

M_b = flexural force at the bolt line in kip-inches,

M = flexural force at the strain gage location in kip-inches per Equation (28) and Equation (30),

x_{sg} = horizontal distance from the true pin connection to the strain gage location equal to 36.875 inches,

x_b = horizontal distance from the true pin connection to the bolt line of the tested connection equal to 74.625 inches.

The beam end rotation for each supported beam at each time step was determined using fundamental trigonometric properties. Using the vertical displacement data measured by the DWT's, the beam end rotation was determined by

$$\theta_n = \tan^{-1}\frac{x_f}{\Delta_n} \quad (34)$$

where

x_f = horizontal distance from the true pin to the supported column flange face equal to 78.375 inches,

θ_n = beam end rotation at time step 'n' in radians,

Δ_n= vertical deflection measured by DWT at time step 'n' in inches.

4.3 Experimental Results

The data analysis process provided in Section 4.2 has been used to evaluate the experimental data from the nine experimental tests performed. All data shown hereafter have been extracted using the process outlined in Section 4.2.

4.3.1 Test 3ST1

The failure mechanism for test 3ST1 was a bolt shear rupture failure of the third bolt of specimen 3STR1. Test 3ST1 was the only three bolt connection specimen to exhibit a bolt shear failure mode. This is believed to be caused by an initial alignment issue due to the fabricated misalignment of the second hole location in specimen 3STR1. The second bolt hole in the shear plate was manually reamed to provide proper fit-up tolerance prior to testing. The hole reaming process resulted in a non-uniform bearing surface at the second bolt location.

Shown in Figure 4.1, the bottom hole of specimens 3STR1 and 3STL1 exhibited large bolt bearing deformations while the second hole remained mainly undistorted. The bottom bolt holes exhibited small tears at the bolt bearing surface where the material had yielded and began to rupture in multiple locations around the radius of the bolt hole. While the plaster white wash was not available at the time of testing, the mill scale as shown in Figure 4.2 provided a good indication of the stress distribution near the bearing contact areas. A force couple in the bolts was evident as stress marks indicated the top bolt put a compressive force on the shear plate while the bottom bolt caused a tensile force. As shown in Figure 4.2, the bearing stress distributed at approximately a thirty degree angle from the horizontal centerline of the bolt holes. Furthermore, a substantial stress concentration was evident at the bottom edge of the shear plate where the formation of a tear had begun on specimen 3STR1.

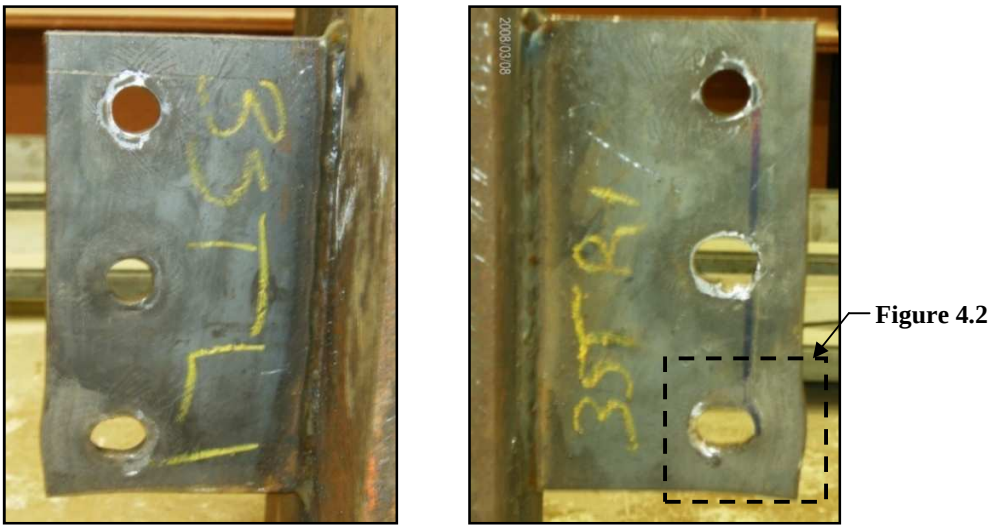

Figure 4.1: Test 3ST1 Connection Specimen Post-Test Condition.
a) Specimen 3STL1. b) Specimen 3STR1.

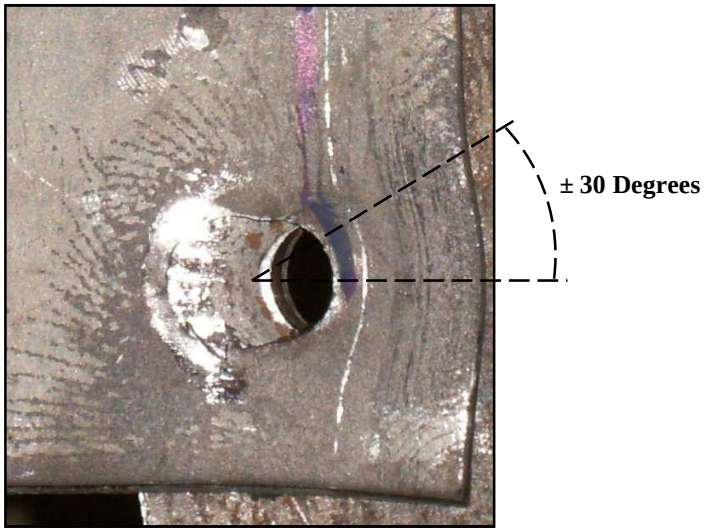

Figure 4.2: Specimen 3STR1 Stress Distribution at the Bottom Hole.

The force couple indicated by the stress marks in the mill scale of specimen 3STR1 was backed by the measured moment capacity. As the flexural stiffness of the connection was exceeded the tensile forces in the connection quickly increased until the point of the connection's failure. This behavior indicated the switch between flexure and catenary load paths in the connection. Figures 4.3 and 4.4 indicate the key characteristics measured during the experimental testing for specimens 3STR1 and 3STL1, respectively.

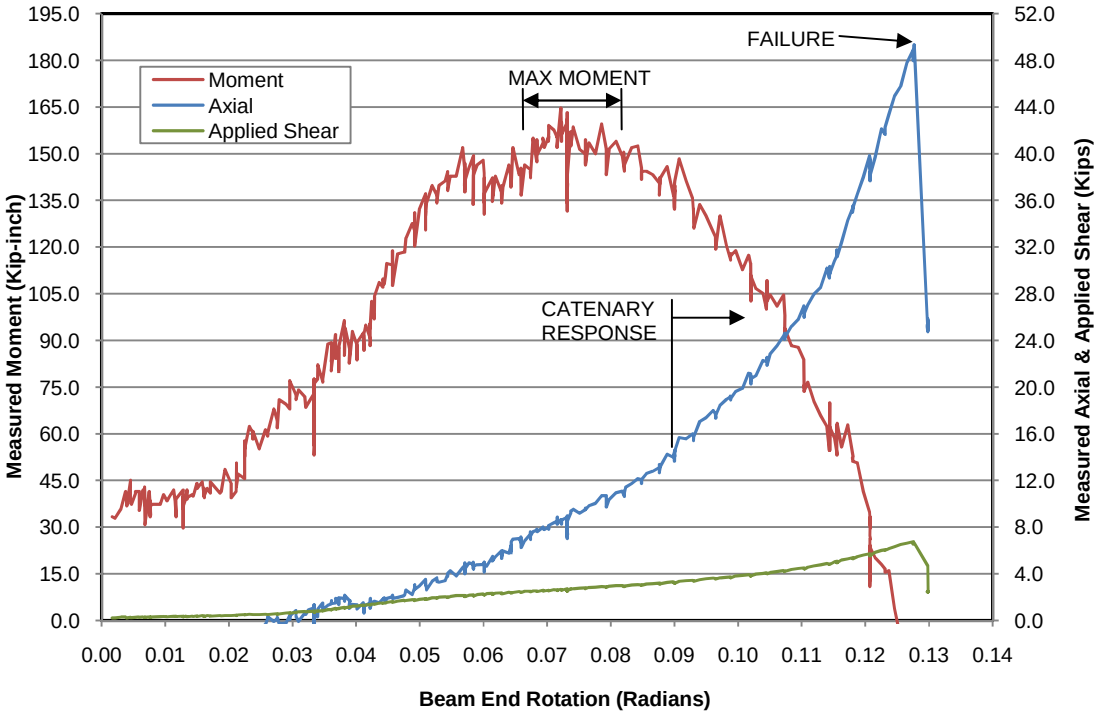

Figure 4.3: Specimen 3STR1 Bolt Line Forces versus Beam End Rotation.

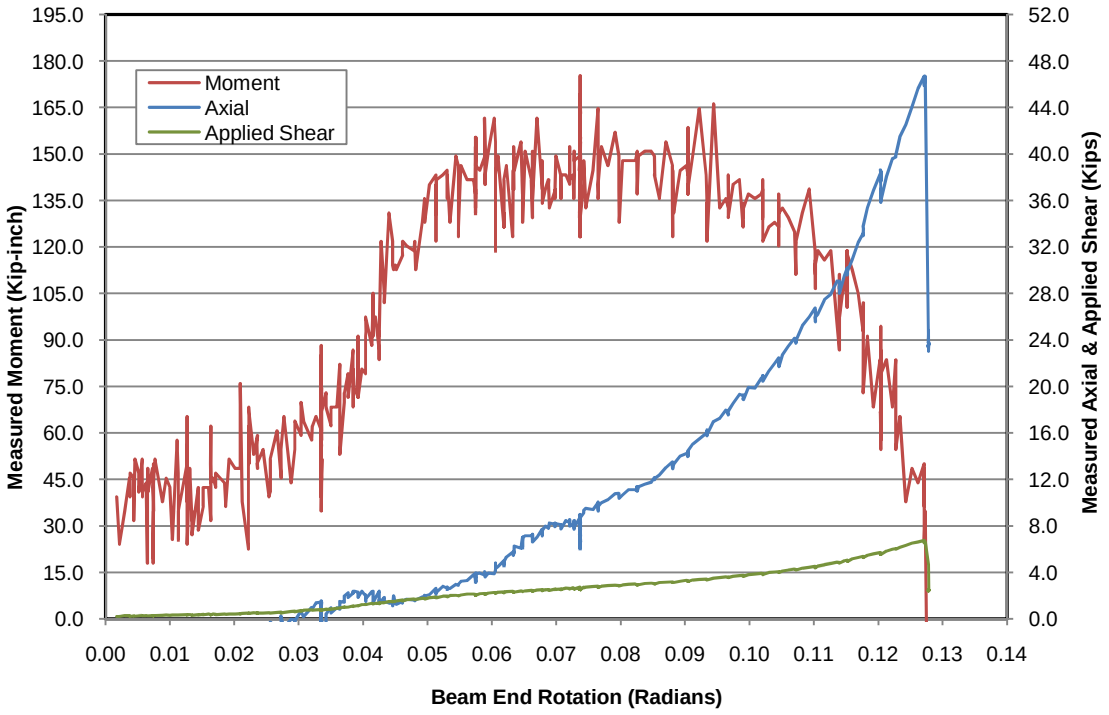

Figure 4.4: Specimen 3STL1 Bolt Line Forces versus Beam End Rotation.

4.3.2 Test 3ST2

The failure mechanism of test 3ST2 was due to a tension rupture failure at the bottom edge of specimen 3STR2. Shown in Figure 4.6(b), the shear plate unzipped along the bolt line from the bottom plate edge through the second bolt hole location. Specimens 3STR2 and 3STL2 also experienced large bolt bearing deformations in the bottom bolt hole in a thirty degree pattern similar to test 3ST1. Furthermore, the bottom bolts of each tested specimen experience large plastic shear deformations. Shown in Figure 4.5, the shear deformation in the bottom bolt of specimen 3STR2 reduced the bolt cross-sectional area by more than thirty percent.

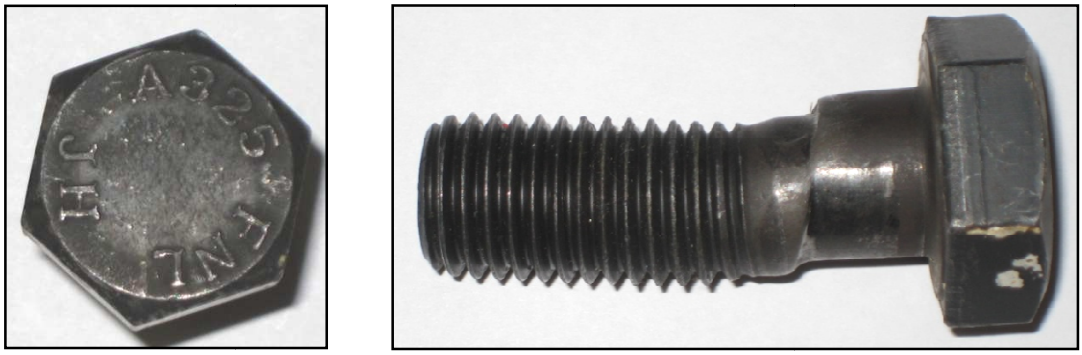

Figure 4.5: Typical Bolt Cross-Section Area Deformation.

The plaster white wash was not available at the time of testing; however, similar to test 3ST1, the mill scale provided a good indication of the key stress locations in the connection. A force couple in the bolts caused the top bolt to compress the shear plate while the bottom bolt imparted tensile forces on the shear plate. The top bolt and bolt holes of each specimen exhibit large scale plastic deformations. A large stress concentration was evident at the bottom plate edge where the connection failure occurred. As the bolt bearing deformations increased small ruptures around the radius of the bolt hole developed until the plate failed. Shown in Figure 4.7, the shear plate of specimen

3STR2 did not rupture completely along the bolt line as the shear plate's bottom edge had a distinct rupture pattern. The bottom edge had a sudden curved failure path approximately a 1/4 inch from the bottom edge of shear plate.

As the flexural stiffness of the connections was exceeded, the tensile forces in the connection quickly increased until the point of the connections failure. As shown in Figures 4.8 and 4.9, the load path mechanism shifted from flexure to catenary tensile force transfer near the point of maximum moment. The connection quickly gathered tensile forces until the rupture point of specimen 3STR2.

Figure 4.6: Test 3ST2 Connection Specimen Post-Test Condition.
a) Specimen 3STL2. b) Specimen 3STR2.

Figure 4.7: Specimen 3STR2 Rupture Source.

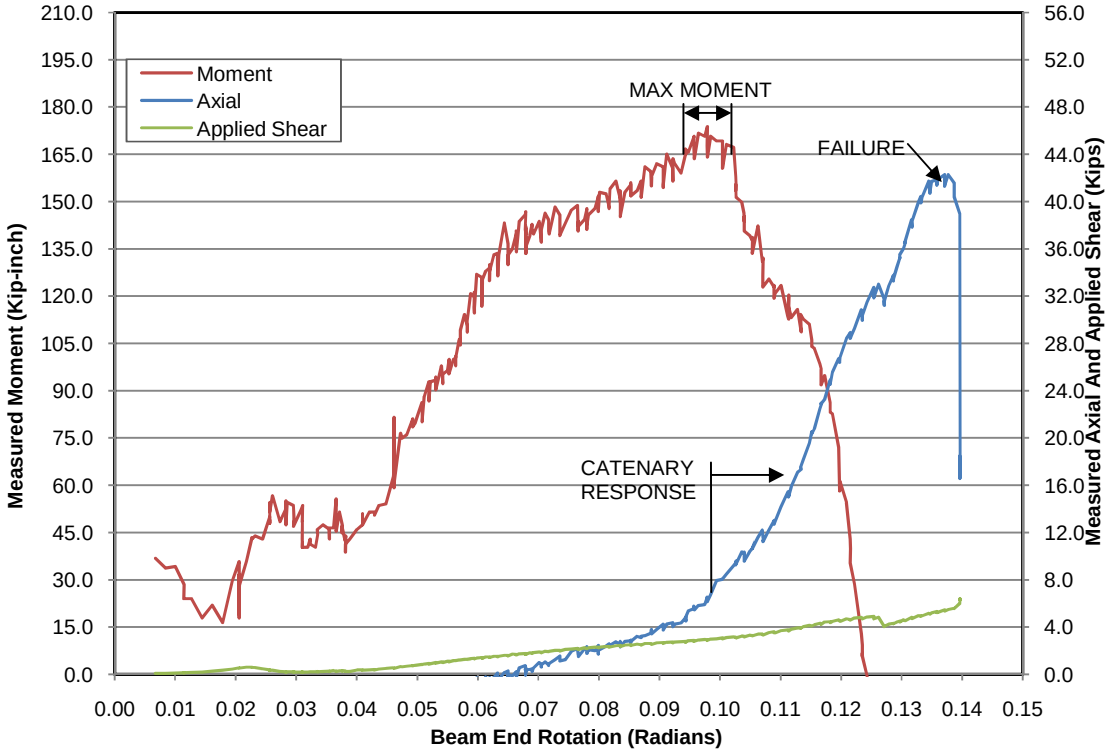

Figure 4.8: Specimen 3STR2 Bolt Line Forces versus Beam End Rotation.

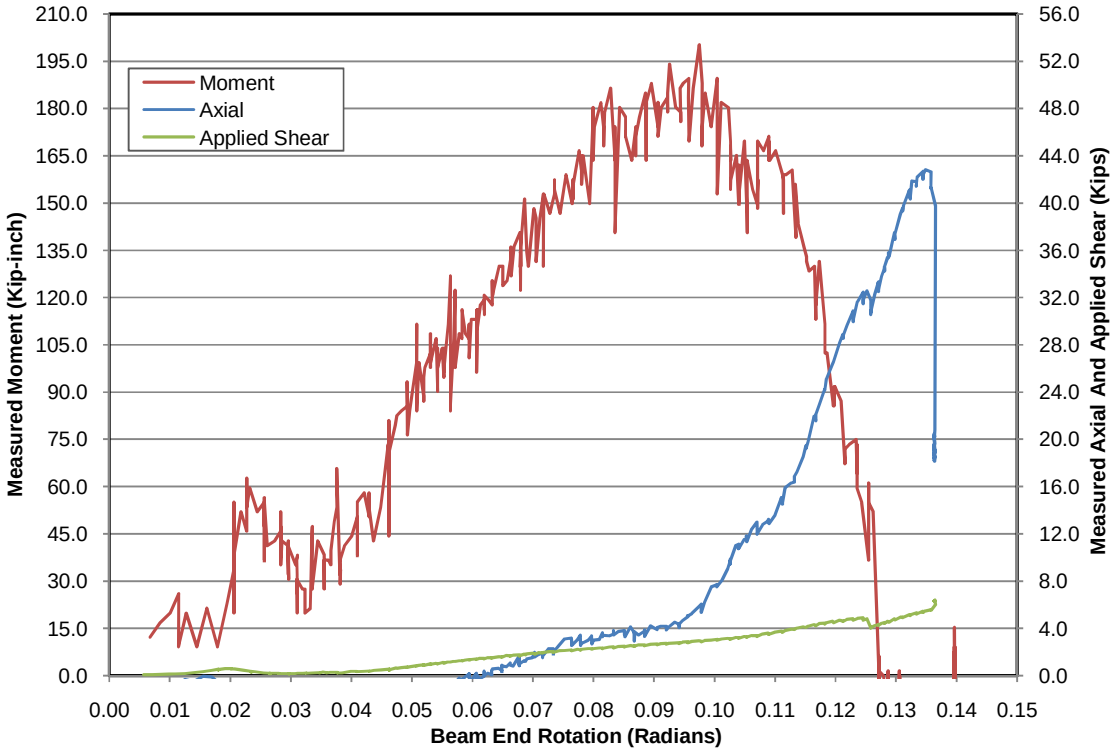

Figure 4.9: Specimen 3STL2 Bolt Line Forces versus Beam End Rotation.

4.3.3 Test 3ST3

Test 3ST3 experienced a similar failure mechanism as test 3ST2. Shown in Figure 4.10(b), a tensile rupture failure of the shear plate of specimen 3STR3 caused the plate to unzip along the bolt line. Large plastic bolt bearing deformations were exhibited in the shear plates of specimens 3STR3 and 3STL3 as well as a substantial reduction in the bottom bolt shear due to large plastic shear deformations. Similar to test 3ST2, the bottom hole of specimen 3STR2 had small ruptures along the radius of the hole cause by the elongation of the bolt hole. The failure point at the bottom plate edge also ruptured in a curved pattern approximately 1/4 inch from the plate edge.

Shown in Figures 4.11 and 4.12, the connection exhibited similar behavior as the previous three bolt shear tests where a transition in load path from flexure to catenary tension was evident.

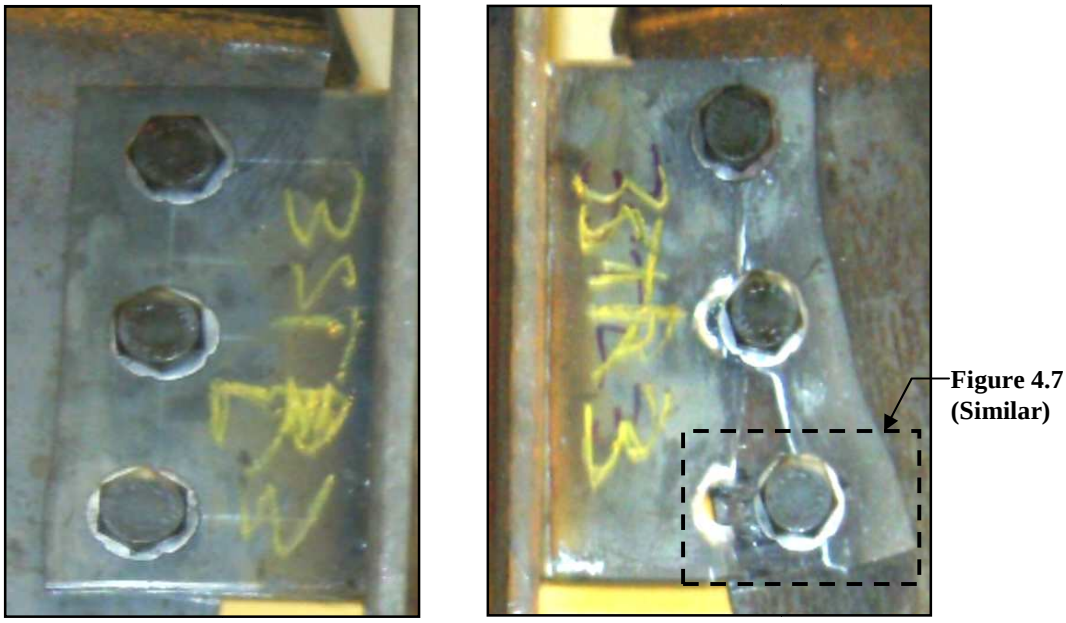

Figure 4.10: Test 3ST3 Connection Specimen Post-Test Condition.
a) Specimen 3STL3. b) Specimen 3STR3.

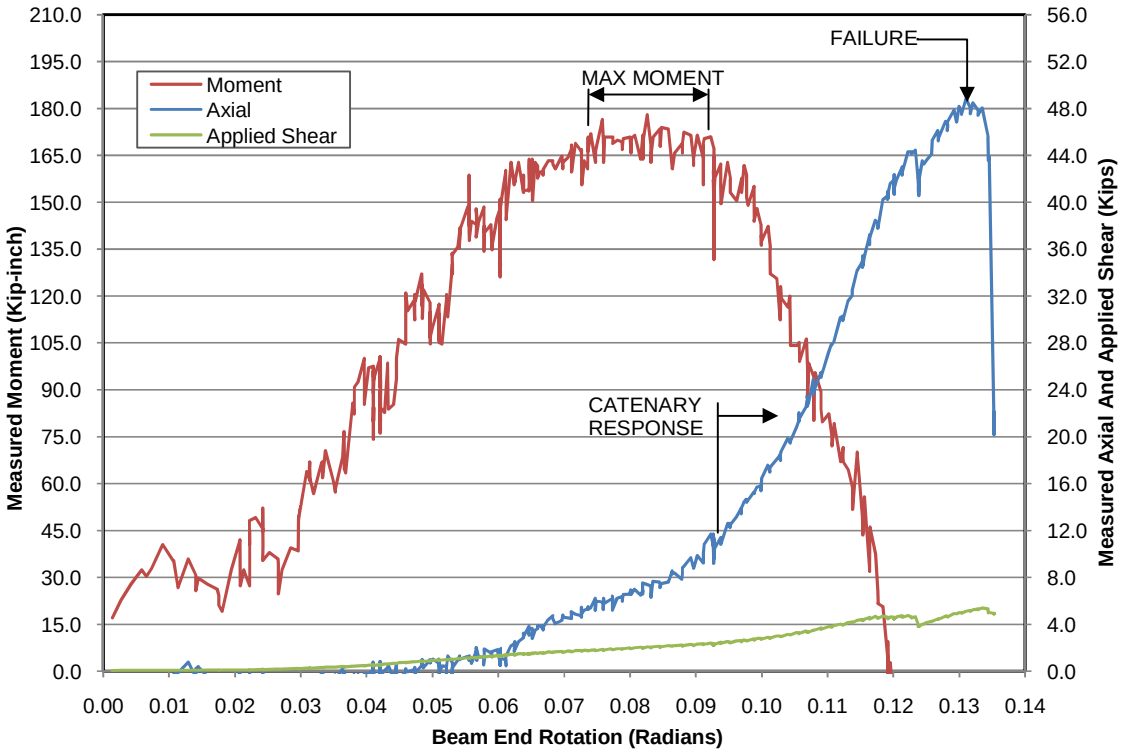

Figure 4.11: Specimen 3STR3 Bolt Line Forces versus Beam End Rotation.

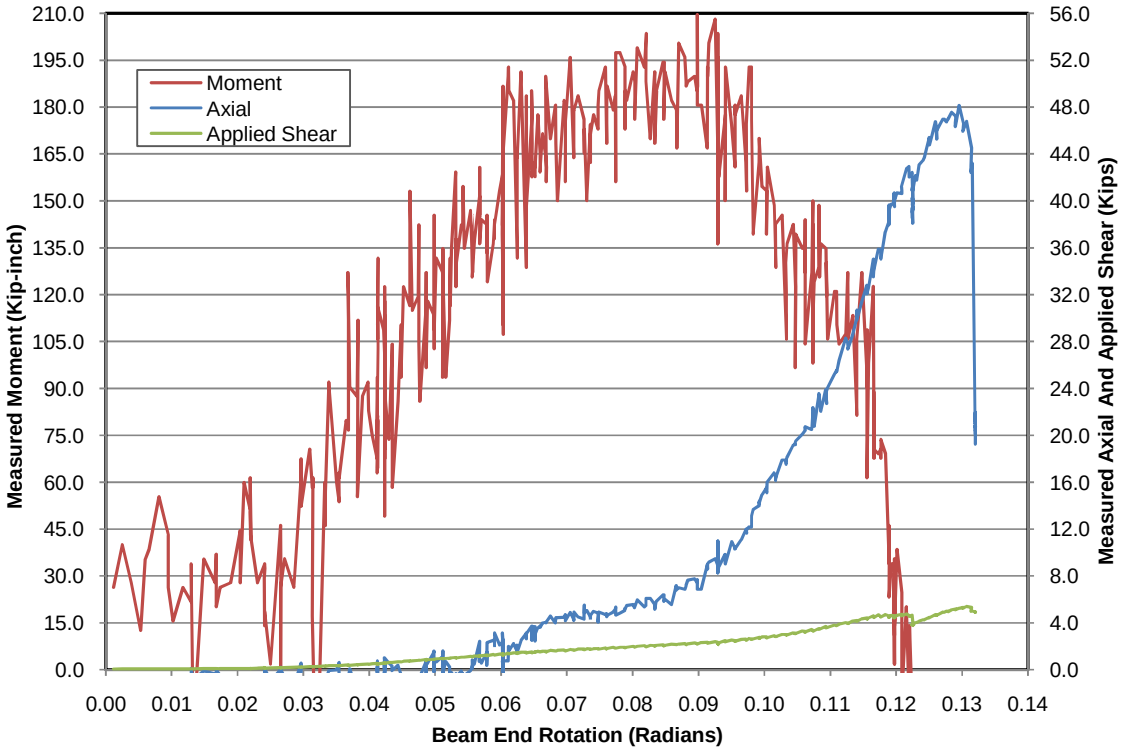

Figure 4.12: Specimen 3STL3 Bolt Line Forces versus Beam End Rotation.

4.3.4 Test 4ST1

Multiple failure mechanisms occurred during test 4ST1 leading to the connection's overall failure. Shown in Figures 4.13(a) and 4.13(b), a force couple similar to the three bolt tests was evident about the centroid of the bolt group in each specimen. The plaster white wash showed that the top and bottom bolts of specimens 4STR1 and 4STL1 provided a greater percentage of the connection's flexural resistance. As the tension forces in the fourth bolt increased, substantial bolt hole bearing deformations and bolt shear deformations occurred. The initial failure occurred in the shear plate of specimen 4STR1 as a localized block shear failure at the fourth bolt hole. Shown in Figure 4.14, the tension force generated by the flexural resistance of the shear tab caused a shear failure at approximately a thirty degree angle from the bolt hole's horizontal axis. Simultaneous to the shear failure, the plastic deformations of the bolt hole created a tear in the radius of the bolt hole due to a tension rupture failure of the shear plate. As Figure 4.14 shows, the tension failure of the plate caused a distinct failure shape near the bottom edge of the plate similar to the failures of tests 3ST1 and 3ST2. The tension failure appeared to be a brittle fracture of the tension plane as the plate material did not visibly deform in the tension zone prior to the block shear rupture.

The block shear failure of the fourth bolt hole location did not lead to the connections overall loss of strength. A secondary failure due to the bolt shear rupture of the third bolt of specimen 4STR1 lead to the connections inability to support the applied shear load. Though the fourth bolt hole location initially failed, the connection was still able to resist an increased shear load until the secondary bolt shear failure occurred.

Figures 4.15 and 4.16 show the connections develop catenary tensile forces as the connections reached their peak flexural resistance. Axial forces increased as plastic bearing deformations decreased the connections flexural resistance. As loading continued the load path for specimen 4STR1 became exclusively a tension only connection as the connections flexural stiffness was negligible.

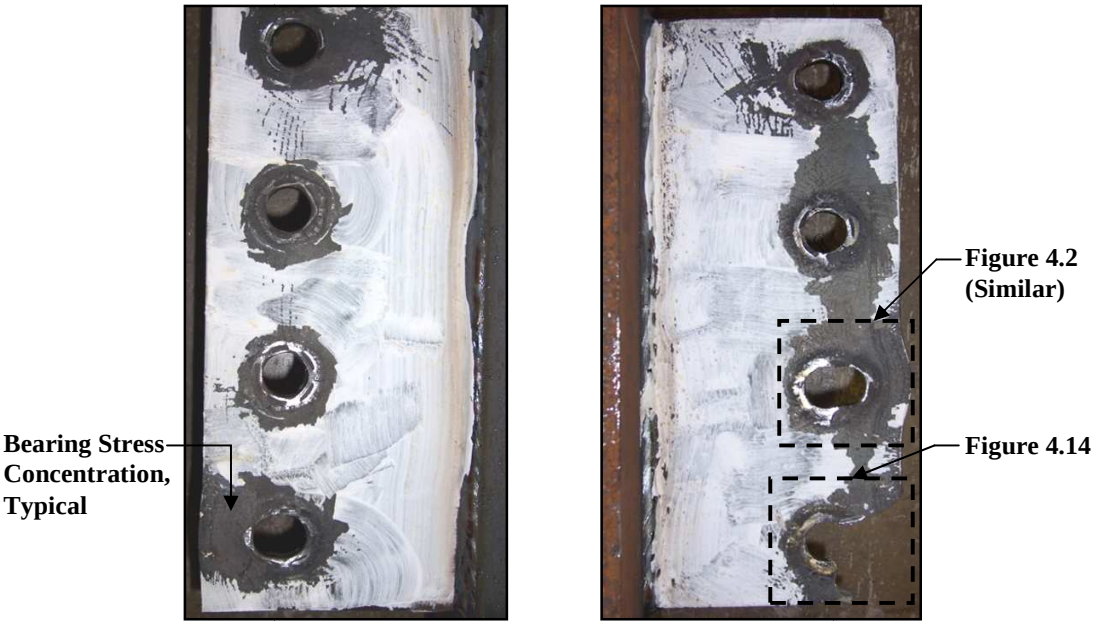

Figure 4.13: Test 4ST1 Connection Specimen Post-Test Condition.
a) Specimen 4STL1. b) Specimen 4STR1.

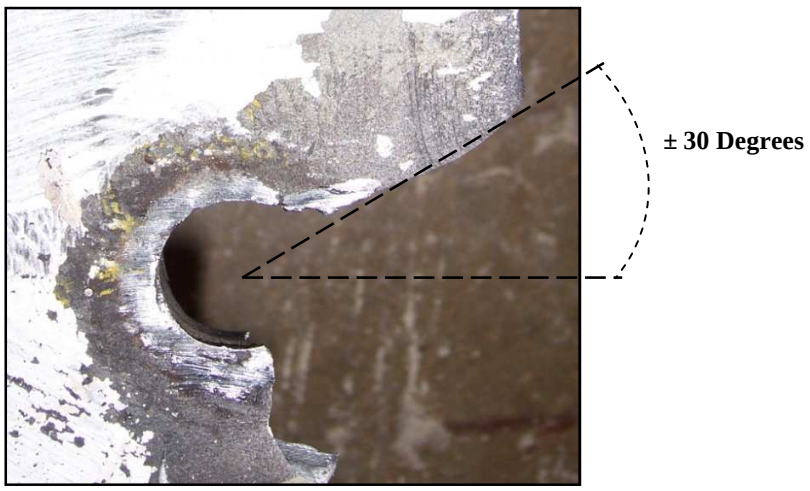

Figure 4.14: Specimen 4STR1 Initial Failure Mode.

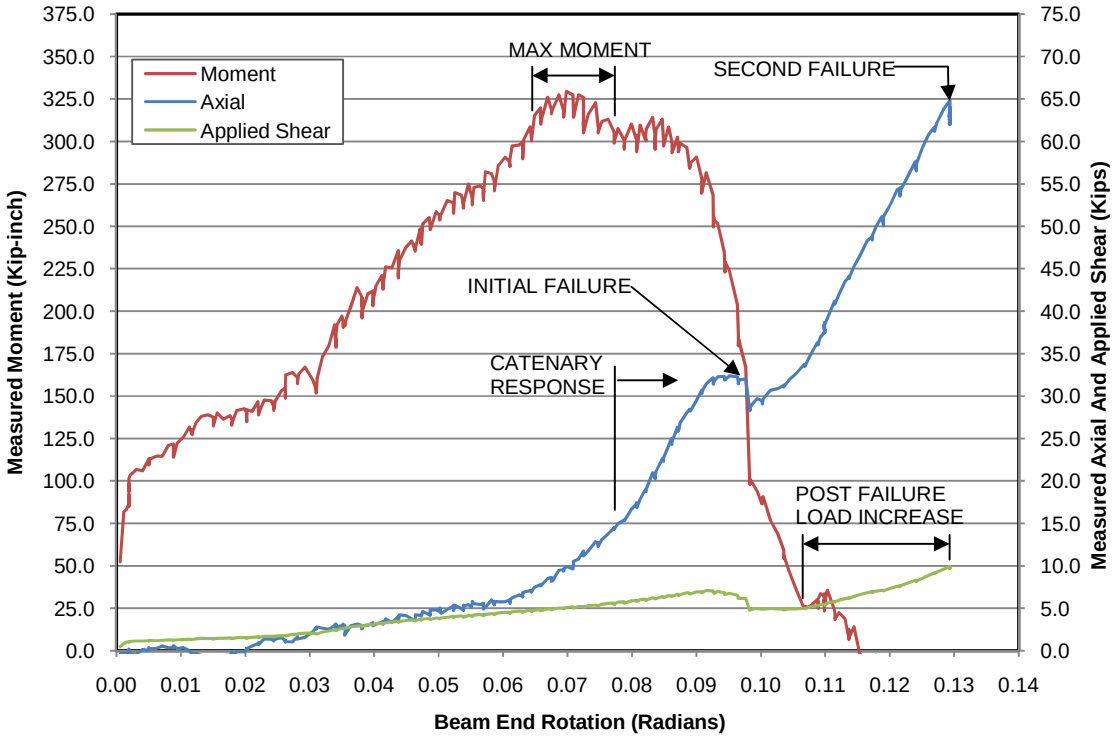

Figure 4.15: Specimen 4STR1 Bolt Line Forces versus Beam End Rotation.

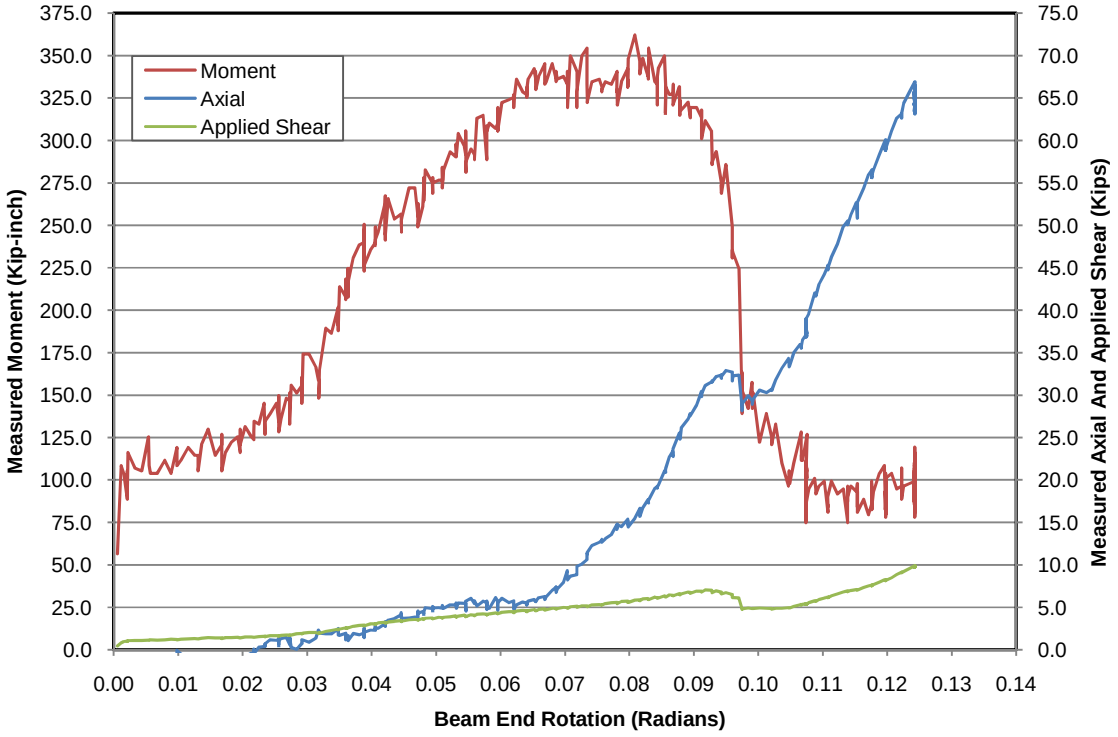

Figure 4.16: Specimen 4STL1 Bolt Line Forces versus Beam End Rotation.

4.3.5 Test 4ST2

The behavior of the connection specimens of test 4ST2 resembled the behavior of test 4ST1; however, the connection's failure mechanism differed. As shown in Figure 4.17(a) and Figure 4.17(b), the connection specimens exhibited a similar force couple as the previous tests as well as similar bolt hole bearing deformations of the bottom bolt holes of each specimen. However, the failure mechanism of test 4ST2 was due to the shear rupture of the bottom bolt of specimen 4STR2.

Shown in Figure 4.18, the load transfer of the bottom bolt of specimen 4STR2 was nearly identical to the behavior of specimen 4STR1. The shear force in the connection plate of specimen 4STR2 distributed at a similar thirty degree angle while the tension forces were evident along the bolt line. The bottom bolt hole showed evidence of the initiation of multiple rupture failures along shear and tension lines.

Figure 4.17: Test 4ST2 Connection Specimen Post-Test Condition.
a) Specimen 4STL2. b) Specimen 4STR2.

Shown in Figure 4.19 and Figure 4.20 the load path of test 4ST2 also resembled the behavior of test 4ST1 where the catenary tension forces increased as the connections reached and exceeded their flexural capacity. The specimens of test 4ST2 were able to resist an applied shear load after the initial bolt failure; however, the testing was stopped before a secondary failure mechanism could be established.

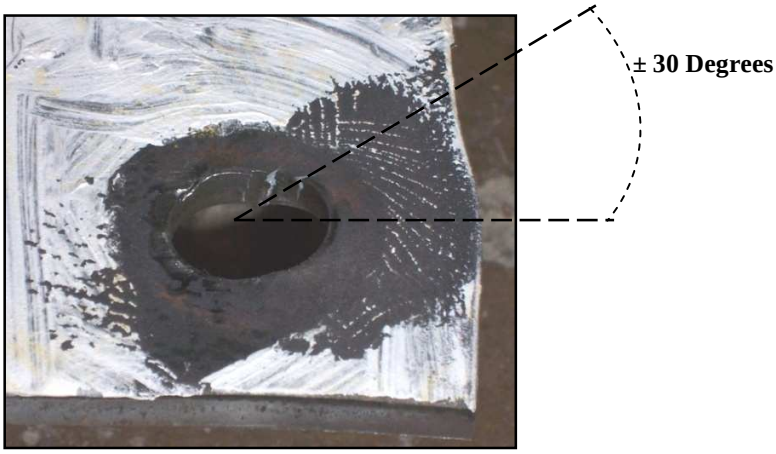

Figure 4.18: Bottom Hole Condition of Specimen 4STR2 Shear Plate.

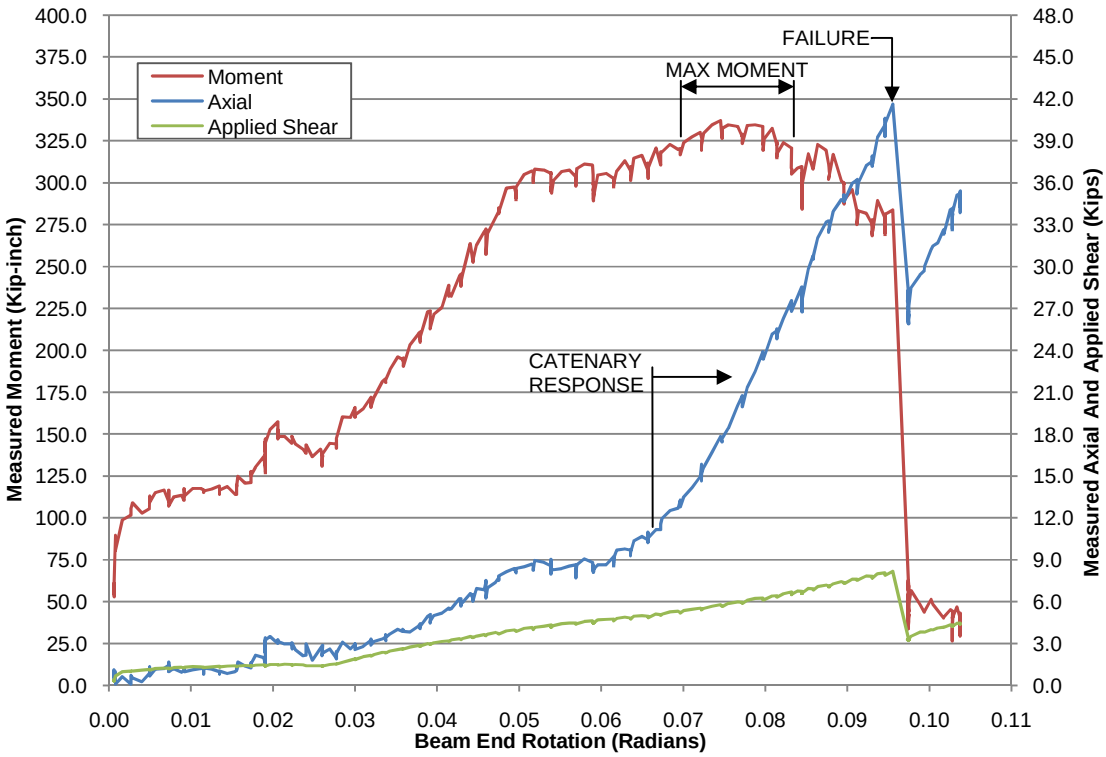

Figure 4.19: Specimen 4STR2 Bolt Line Forces versus Beam End Rotation.

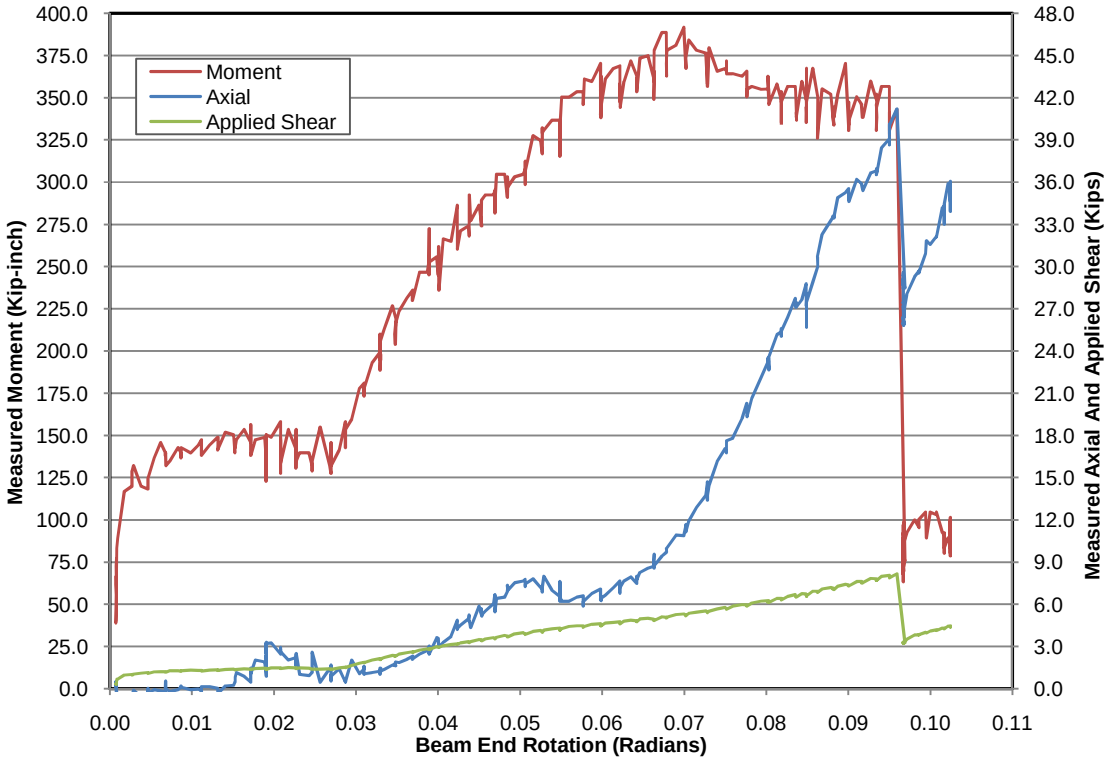

Figure 4.20: Specimen 4STL2 Bolt Line Forces versus Beam End Rotation.

4.3.6 Test 4ST3

Test 4ST3 exhibited a third type of failure mechanism for the four bolt shear tab tests. Similar to test 3ST2 and 3ST3, the shear plate of specimen 4STL3 failed due to a tension rupture failure at the bottom bolt hole. Shown in Figure 4.21(a) and Figure 4.21(b), the plastic deformations due to the tension side of the bolt force couple resembled the typical connection behavior exhibited by the previous tests. As the bolt bearing deformations in specimen 4STL3 increased, the plate developed small tears in the bolt hole radius near the connection bolt line leading to the tension rupture of the shear plate. Shown in Figure 4.22, the tension zone failure near the bottom edge of the shear plate of specimen 4STL3 matched the brittle rupture failure shape of similar tests which failed due to tension rupture and block shear rupture of the shear plate.

The load path of test 4ST3 was similar to the previous four bolt shear tab tests up to the point of failure. Shown in Figure 4.23 and Figure 4.24, the connections developed catenary tensile forces as the connection reached and exceeded their flexural capacity until specimen 4STL3 failed. After the initial failure, the connections continued to transfer axial loads however the connections were never able to reach the peak applied shear load as specimen 4STL3 began to unzip along the bolt line as the beam end rotated.

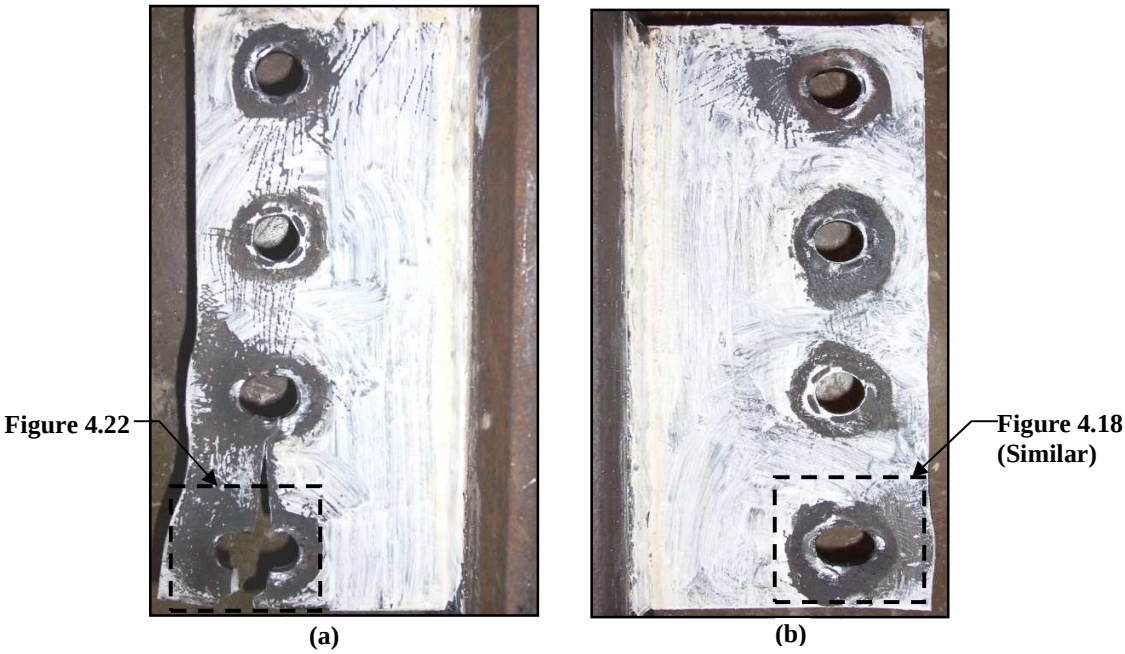

Figure 4.21: Test 4ST3 Connection Specimen Post-Test Condition.
a) Specimen 4STL3. b) Specimen 4STR3.

Figure 4.22: Specimen 4STL3 Bottom Hole Failure Mechanism.

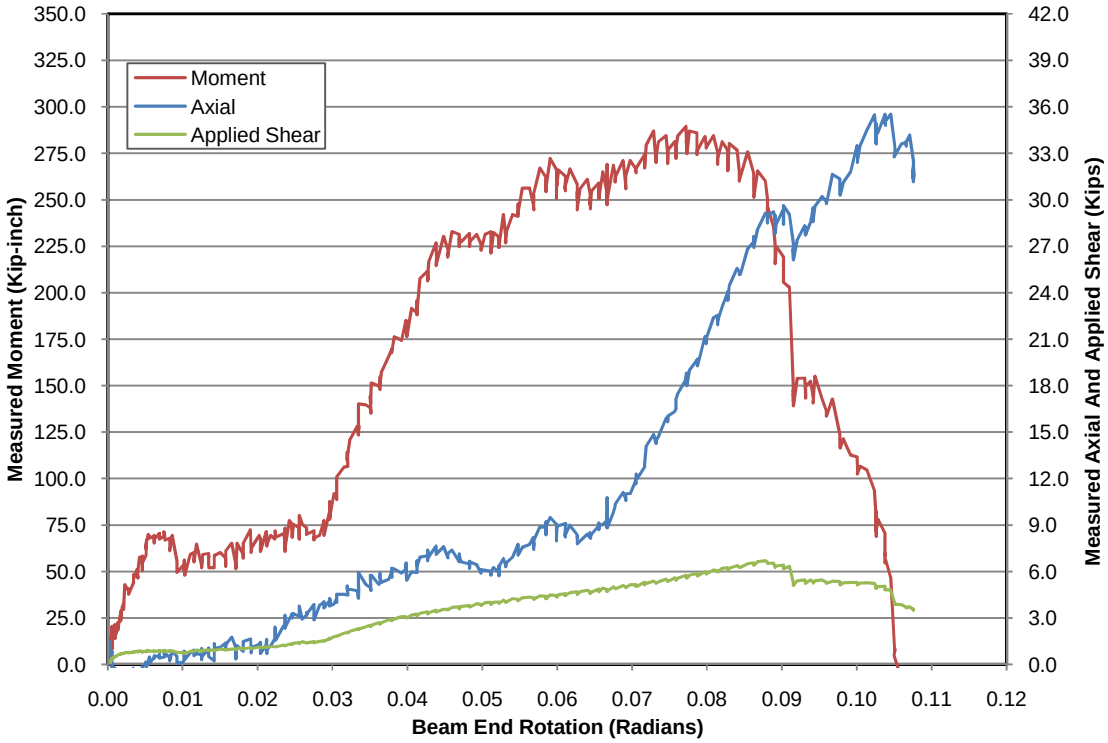

Figure 4.23: Specimen 4STR3 Bolt Line Forces versus Beam End Rotation.

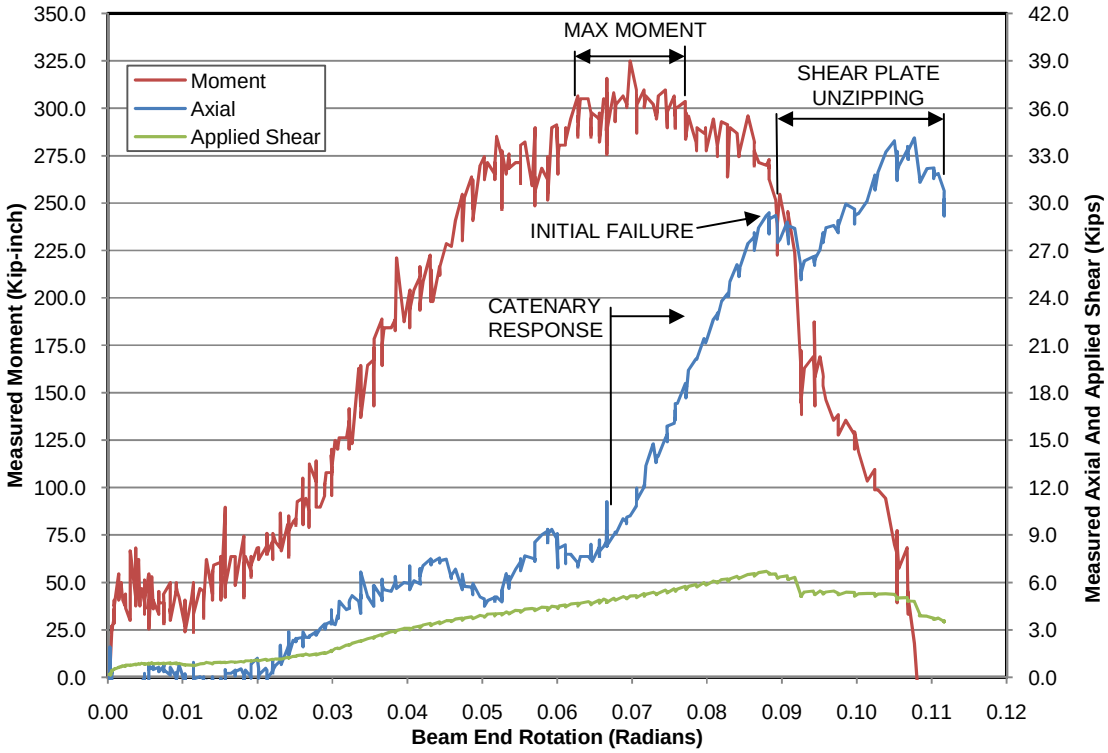

Figure 4.24: Specimen 4STL3 Bolt Line Forces versus Beam End Rotation.

4.3.7 Test 5ST1

Test 5ST1 exhibited similar behavior and multiple failure mechanisms as was noted during test 4ST1. Shown in Figure 4.25(a) and Figure 4.25(b), the initial load transfer was through the typical force couple observed in previous tests about the centroid of the bolt group. The connections' ductility was based on the connections' ability to withstand bolt hole bearing deformation and bolt shear deformation at the bottom bolt. The initial failure mechanism was a localized block shear failure in the shear plate of specimen 5STR1 caused by the tension component of the force couple at the bottom bolt. The plate failure replicated the failure of specimen 4STR1 with the shear failure at a thirty degree angle form horizontal and the tension failure occurring at the shear plate's bottom edge along the bolt line. The tension failure produced the typical curved failure path as a result of a brittle tension rupture at the radius of the bolt hole.

After the initial failure, the connection exhibited similar behavior as was seen during the four bolt shear tests. A secondary failure mode due to bolt shear rupture of the fourth bolt of specimen 5STR1 resulted in the connections' inability to support the applied shear load. The plaster white wash indicated the force at the third bolt location of specimen 5STR1 increased as the connection's behavior transformed into a four bolt connection. Similar to Figure 4.5, significant bolt shear deformations were observed in the top bolts of specimens 5STR1 and 5STL2 resulting in a reduction of nearly fifty percent of the bolts cross-sectional area.

The measured data collected for test 5ST1 were skewed due to an initial error in the test setup. As shown in Figure 4.26 and Figure 4.27, the collected data prior to approximately 0.06 radians were neglected as the hydraulic pump used to power the

hydraulic cylinder was incorrectly attached. During test 5ST1 it was discovered the hydraulic hoses had been reversed and were limiting the output capacity of the hydraulic pump. The error had not been noticed prior to the five bolt testing as the increased applied shear demand was not required for the three and four bolt tests. Test 5ST1 was stopped and the hydraulic lines were correctly attached to maximize the ability of the hydraulic pump. The testing and data collection were restarted after correcting the hydraulic connections. As Figure 4.26 and Figure 4.27 show, the data collected after restarting test 5ST1 indicated the testing was restarted near the connections maximum flexural capacity. While the collected data are skewed, the behavior after the connection reached its peak flexural capacity resembles the behavior of the four bolt tests. The connections' load path transferred from flexure to catenary tension after the initial block shear failure occurred. The axial forces increased until the second failure mechanism occurred resulting in specimen 5STR1's inability support to the applied shear.

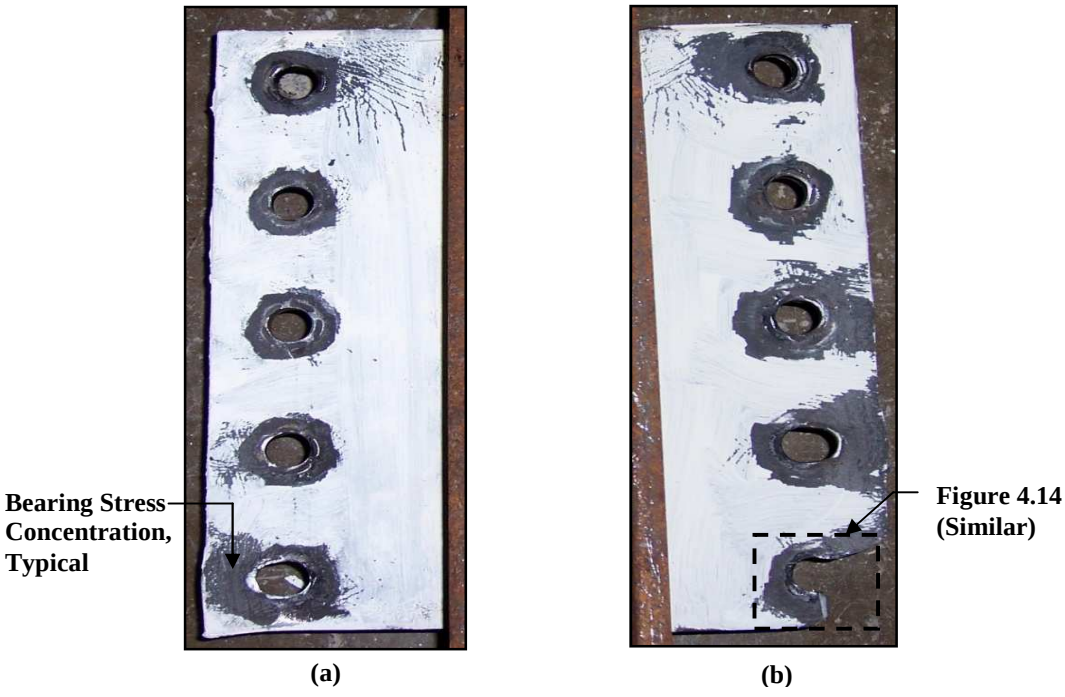

Figure 4.25: Test 5ST1 Connection Specimen Post-Test Condition.
a) Specimen 5STL1. b) Specimen 5STR1.

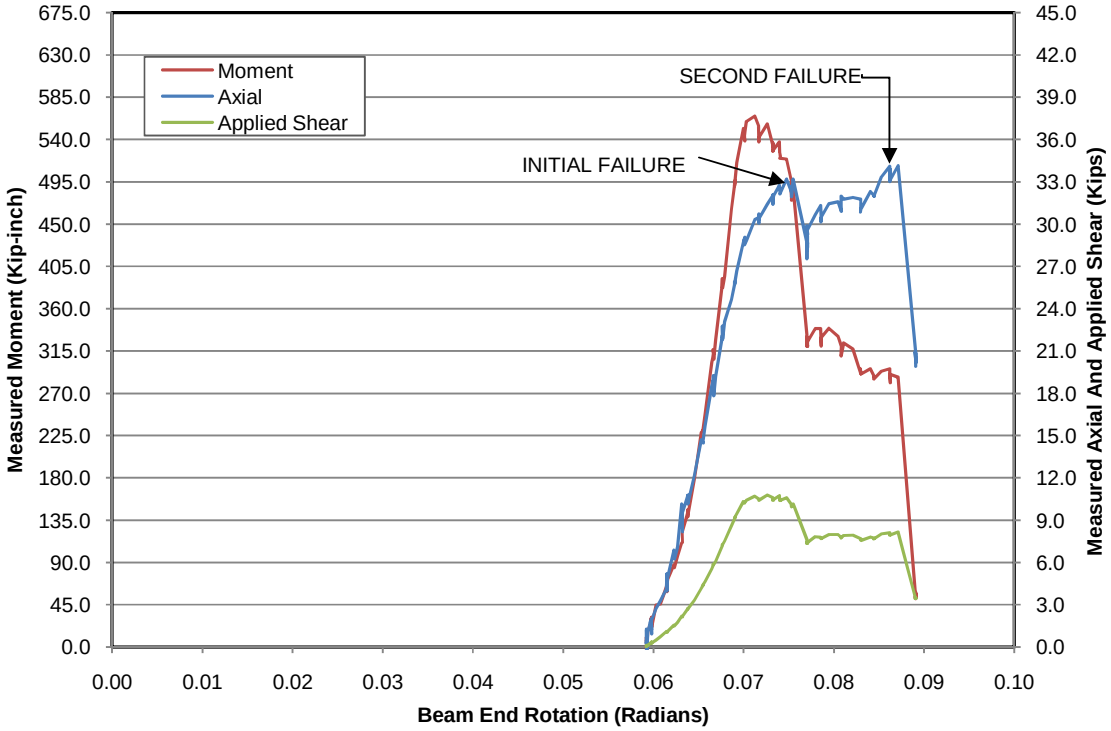

Figure 4.26: Specimen 5STR1 Bolt Line Forces versus Beam End Rotation.

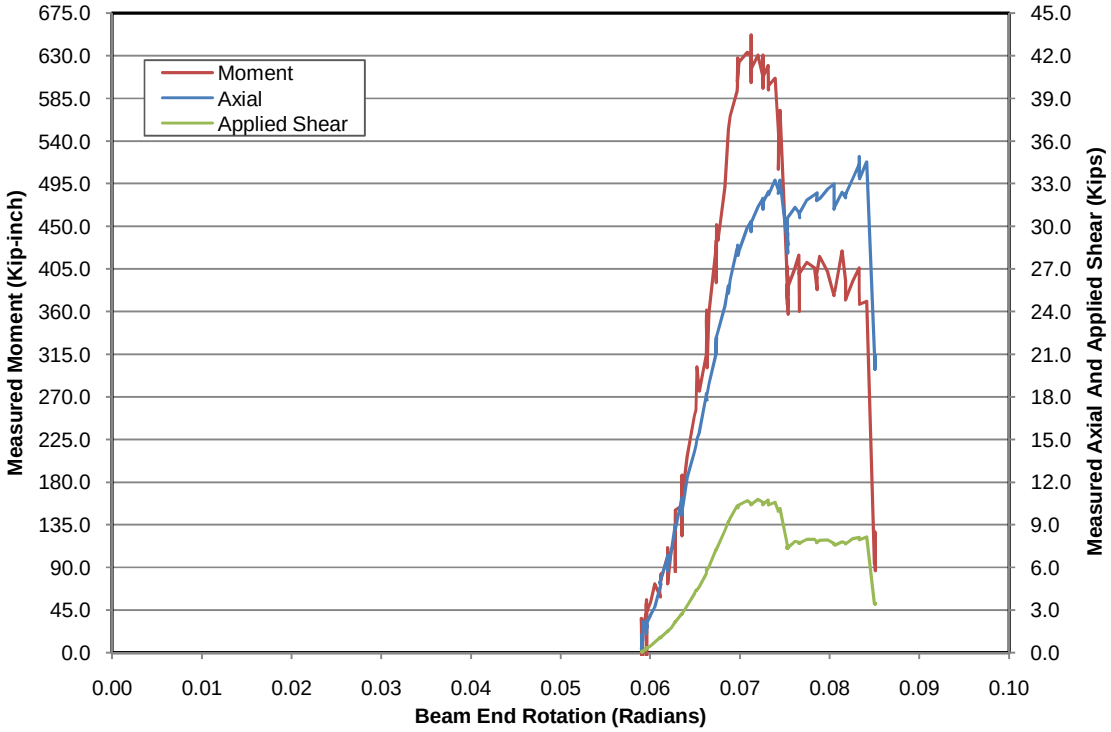

Figure 4.27: Specimen 5STL1 Bolt Line Forces versus Beam End Rotation.

4.3.8 Test 5ST2

The connection behavior and failure mechanisms of test 5ST2 were nearly identical to that noted during test 5ST1. The initial failure mechanism was a localized block shear rupture of the fifth bolt hole on the shear plate of specimen 5STR2 as a result of the tension component of the force couple generated by the flexural resistance of the connection. Shown in Figure 4.28(a) and Figure 4.28(b), the connections' ductility was based on the bolt hole bearing deformation and bolt shear deformation capacity of the connections. The shear and tension planes of the block shear failure in specimen 5STR2 were identical to those observed during the block shear failure of test 5ST2. Similarly, the secondary connection failure mechanism was due to bolt shear rupture failure of the fourth bolt of specimen 5STR2. The connection's behavior simulated the behavior observed during the four bolt tests with the third bolt transferring increased shear forces after the initial failure.

The collected data indicated the connections transferred more axial forces prior to the peak flexural capacity of the connection than noted during the three and four bolt tests. However, as shown in Figure 4.29 and Figure 4.30, the rate of increase in tension force transfer increased as the connections reached their flexural capacity. This behavior was similar to that observed during three and four bolt tests. Also, similar to tests 4ST1 and 4ST2, the connection was able to recover some of the applied shear load lost during the initial connection failure. The connections were not able to recover the maximum applied shear load observed prior to the second connection failure of specimen 5STR2.

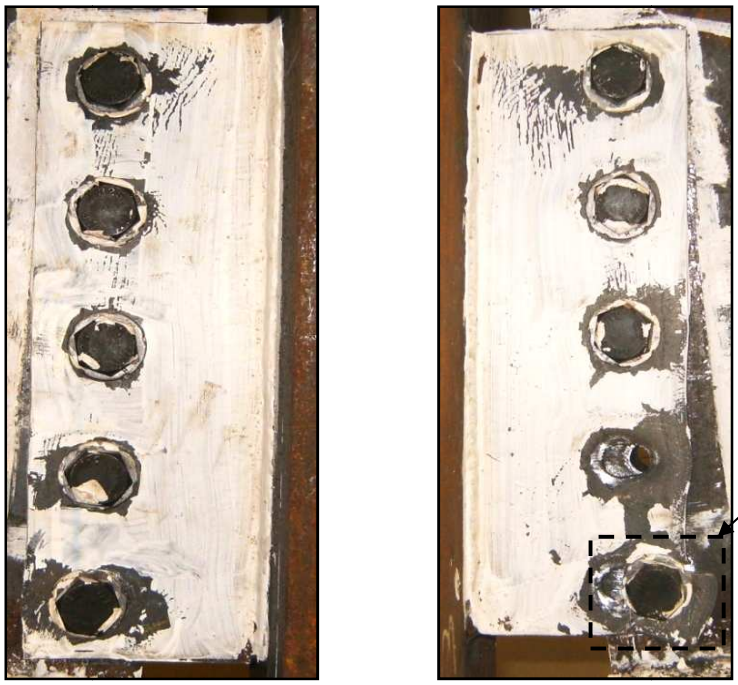

Figure 4.28: Test 5ST2 Connection Specimen Post-Test Condition.
a) Specimen 5STL2. b) Specimen 5STR2.

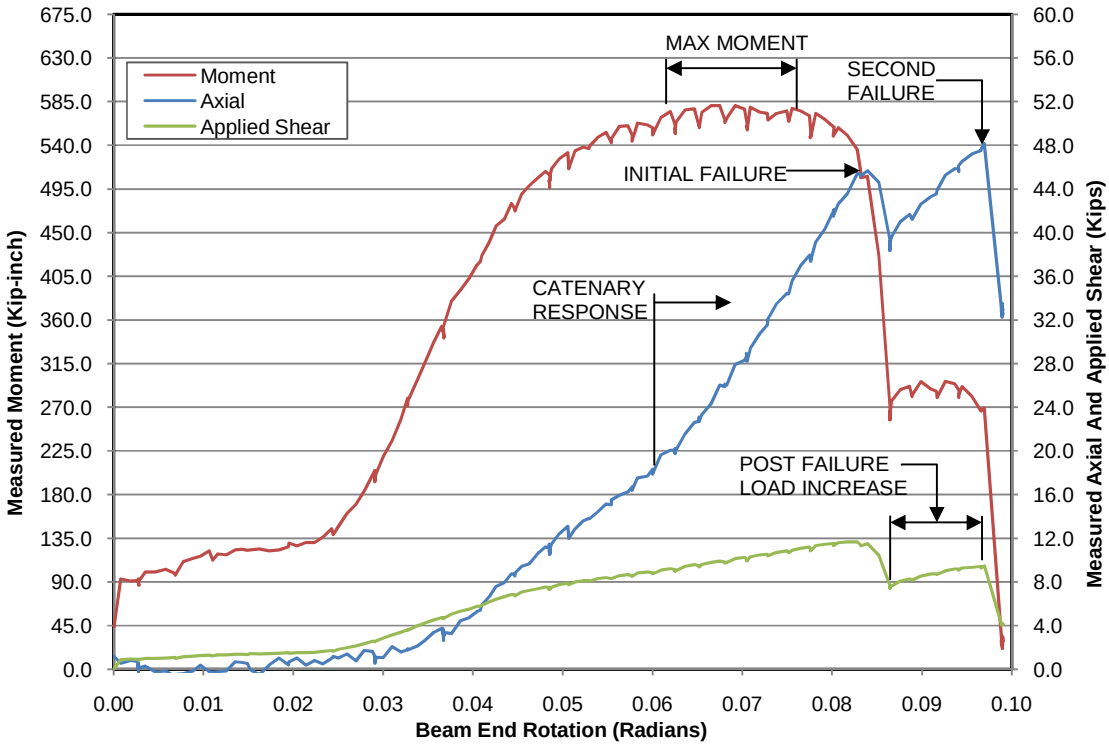

Figure 4.29: Specimen 5STR2 Bolt Line Forces versus Beam End Rotation.

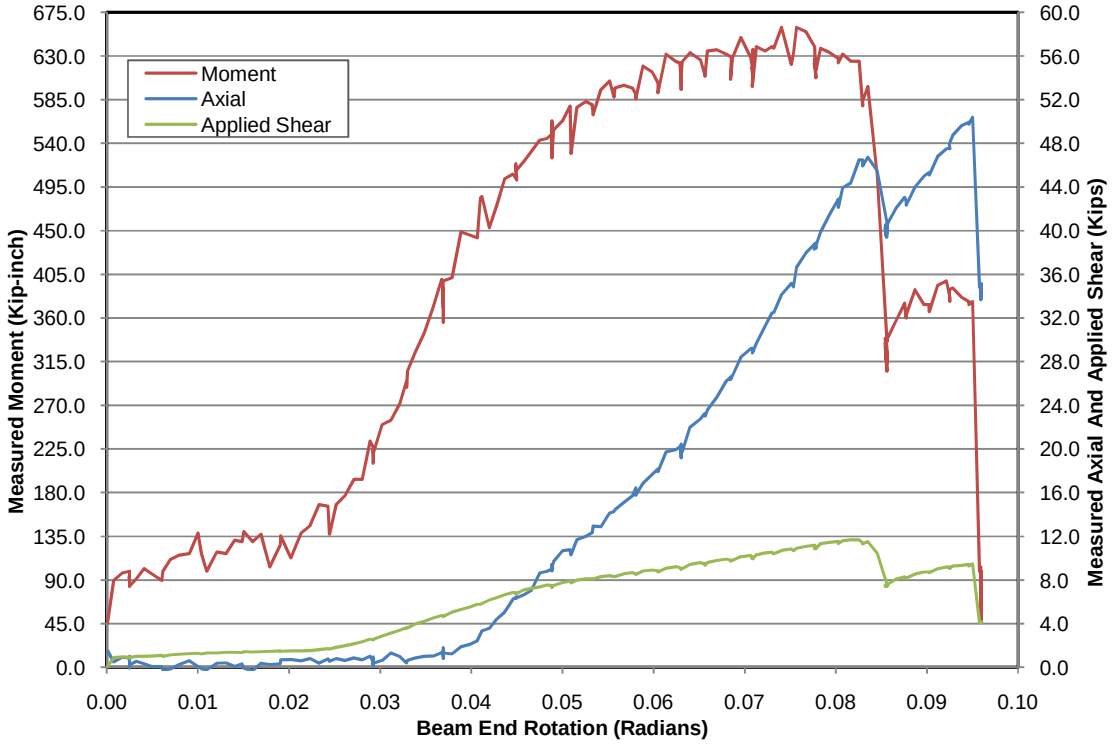

Figure 4.30: Specimen 5STL2 Bolt Line Forces versus Beam End Rotation.

4.3.9 Test 5ST3

Similar to the previous five bolt tests, test 5ST3 exhibited multiple failure mechanisms. However, the initial failure mechanism was due to tension rupture of the bottom bolt hole of specimen 5STL3 similar to the failure observed during test 4ST3. As with all previous tests, the initial force transfer was through the force couple generated by the flexural capacity of the connection about the centroid of the bolt group. Shown in Figure 4.31(a) and Figure 4.31(b), the tension component of the force couple caused significant bolt hole deformation and bolt shear deformation resulting in the formation of tears at the radius of the bolt holes. Similar to specimen 4STR3, the tears caused a brittle tension rupture failure near the bottom edge the shear plate.

Unlike previous tests where the initial tension rupture of the connection plate caused the connection to unzip, a secondary failure mechanism occurred in specimen 5STL3. Similar to the previous five bolt tests, the secondary failure was due to the bolt shear rupture of the fourth bolt of specimen 5STL3. Also, the connections' behavior after the initial failure resembled the behavior observed during the four bolt tests. Comparing Figure 4.31(a) to Figure 4.31(b), the plaster white wash indicated an increase in shear stress at the third and fourth bolt as a result of the initial failure of specimen 5STL3.

The load transfer mechanisms shown in Figure 4.32 and Figure 4.33 closely resemble the behavior observed during test 5ST2. The tension force transfer increased as the connection reached its flexural capacity. Furthermore, after the initial connection failure the flexural capacity was decreased to a level similar to the four bolt tests. As the applied shear increased, the measured axial force increased while the flexural capacity maintained nearly a steady level until the second failure of specimen 5STL3.

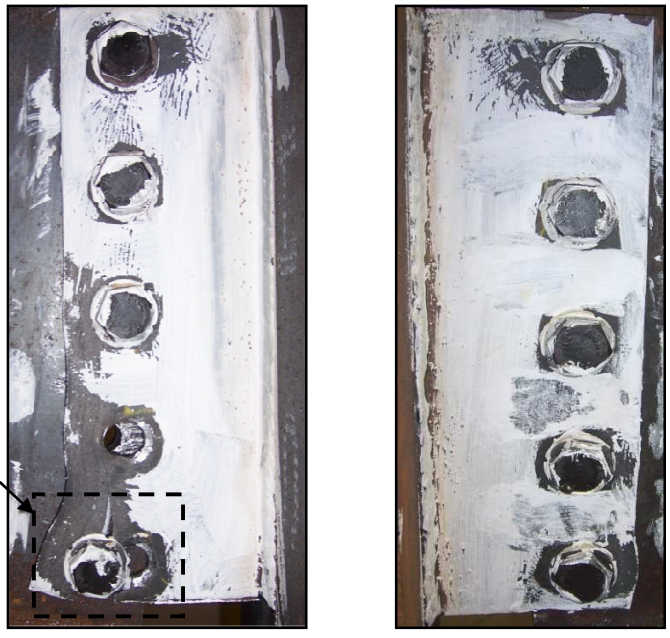

Figure 4.31: Test 5ST3 Connection Specimen Post-Test Condition.
a) Specimen 5STL3. b) Specimen 5STR3.

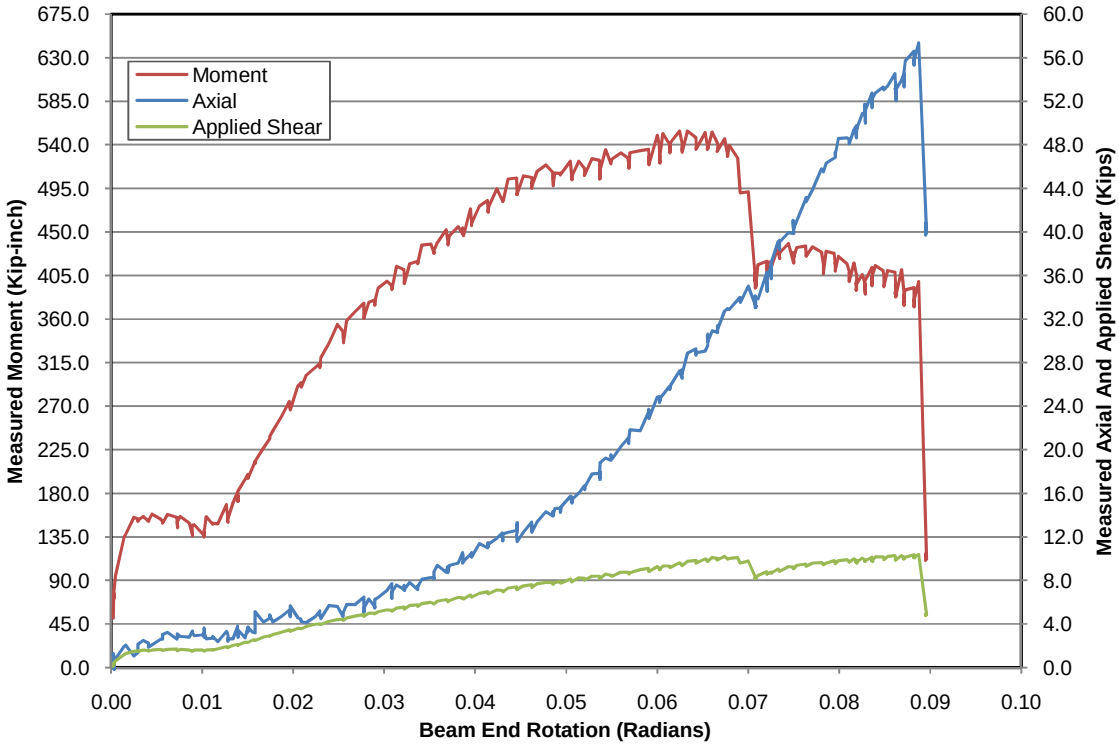

Figure 4.32: Specimen 5STR3 Bolt Line Forces versus Beam End Rotation.

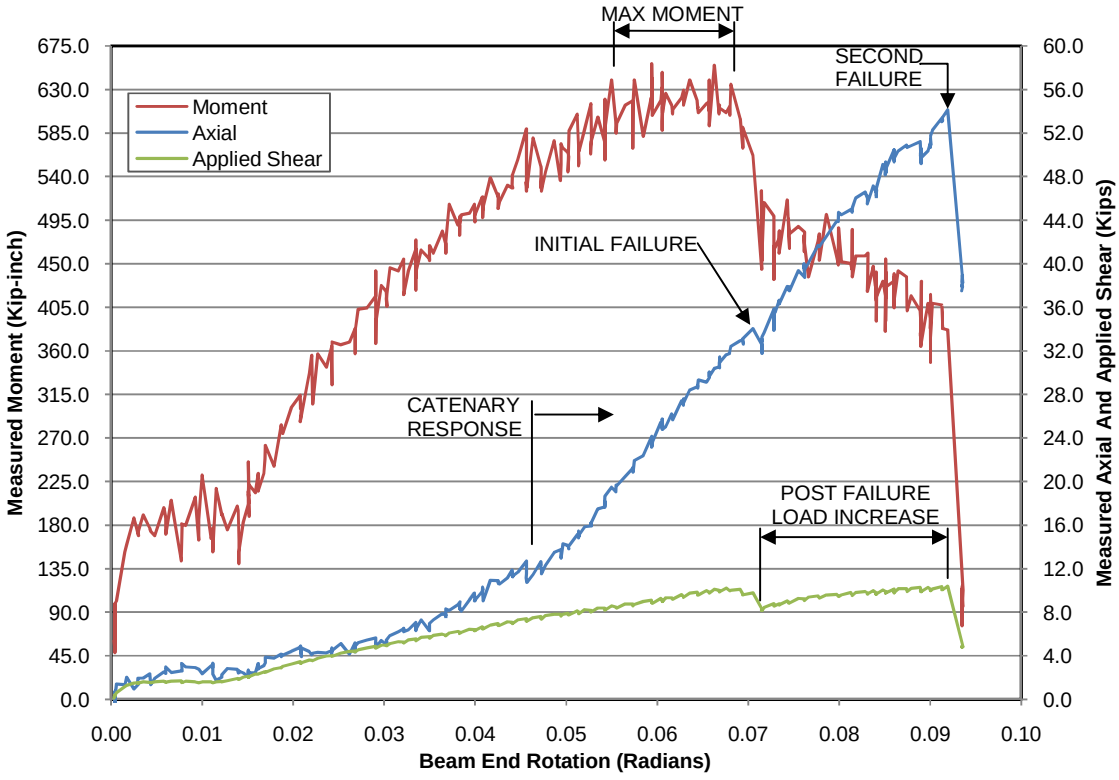

Figure 4.33: Specimen 5STL3 Bolt Line Forces versus Beam End Rotation.

4.3.10 Experimental Results Summary

The tested shear tab connections displayed similar behavioral characteristics when subjected to the simulated column collapse. The connections all exhibited measureable flexural capacity as well as the ability to utilize an alternative load path mechanism via catenary action. The collected data showed the rate of increase in catenary tensile forces increased as connections reached their maximum measured moment. Shown in Table 4.1, the connections' maximum measured flexural capacity and corresponding data measurements have been provided for each specimen. Due to the variability in the collected data, the reported values are based on a sampled average taken between extremes in the measured moments. The data range was based on the controlling connection specimen and applied to the opposing connection specimen's data.

Table 4.1: Specimen Bolt Line Forces at Approximate Maximum Measured Moment.

Test	Specimen	Applied Shear (Kips)	Measured Moment (Kip-Inch)	Measured Axial (Kips)	Beam End Rotation (Radians)
3ST1	3STR1	2.62	157.36	8.45	0.072
	3STL1	2.62	144.68	8.08	0.073
3ST2	3STR2	2.88	169.10	6.05	0.097
	3STL2	2.88	182.70	5.54	0.097
3ST3	3STR3	1.97	169.44	6.61	0.080
	3STL3	1.97	185.02	5.38	0.080
4ST1	4STR1	5.18	315.35	11.43	0.073
	4STL1	5.18	334.33	11.03	0.074
4ST2	4STR2	5.85	331.19	19.21	0.076
	4STL2	5.85	362.16	18.64	0.076
4ST3	4STR3	5.50	279.25	16.70	0.076
	4STL3	5.50	296.55	16.51	0.076
5ST1	5STR1	10.52	549.66	30.32	0.072
	5STL1	10.52	624.45	29.92	0.071
5ST2	5STR2	10.00	568.24	27.52	0.069
	5STL2	10.00	624.94	28.05	0.070
5ST3	5STR3	9.70	541.41	28.90	0.064
	5STL3	9.70	619.60	28.78	0.064

The experimental testing for the three, four, and five bolt shear tab connections produced three key failure mechanisms resulting from the two stages of load transfer exhibited during testing. These failures included bolt shear, localized block shear rupture, and tension rupture of the connection specimen's shear plate. Located in Table 4.2, the controlling limit states, bolt line forces, and beam end rotations have been assembled summarizing the numerical findings for the initial failure points for each specimen.

Table 4.2: Initial Failure Mechanism and Bolt Line Forces for the Tested Shear Tab Connections.

Test	Controlling Connection Specimen	Applied Shear (Kips)	Measured Moment (Kip-Inch)	Measured Axial (Kips)	Beam End Rotation (Radians)	Failure Mechanism
3ST1	3STR1[a]	6.76	Negligible	48.95	0.128	Bolt Shear Rupture
3ST2	3STR2	6.43	Negligible	42.29	0.137	Tension Rupture
3ST3	3STR3	5.41	Negligible	48.89	0.133	Tension Rupture
4ST1	4STR1	7.02	268.35	32.14	0.093	Block Shear Rupture
4ST2	4STR2	8.62	279.07	41.64	0.096	Bolt Shear Rupture
4ST3	4STL3	6.34	224.12	28.44	0.093	Tension Rupture
5ST1	5STR1[b]	10.59	494.72	33.21	0.075	Block Shear Rupture
5ST2	5STR2	11.69	535.81	45.44	0.083	Block Shear Rupture
5ST3	5STL3	10.22	606.15	34.04	0.071	Tension Rupture

[a] Initial connection misalignment lead to uneven bearing surface of the middle bolt in order to facilitate erection.

[b] Testing was interrupted due to initial reversal of hydraulic couplings.

The experimental testing revealed several connections had the robustness to continue transferring the applied shear load after an initial failure mechanism occurred. While not all connections exhibited the ability to overcome an initial failure, several connections were able to support a larger or nearly equal shear load as a result of the load path transition from flexure to catenary tension. The experimental summary of the connections' secondary failure mechanism and corresponding bolt line forces are shown in Table 4.3.

Table 4.3: Secondary Failure Mechanism and Bolt Line Forces for the Tested Shear Tab Connections.

Test	Controlling Connection	Applied Shear (Kips)	Measured Moment (Kip-Inch)	Measured Axial (Kips)	Beam End Rotation (Radians)	Failure Mechanism
3ST1	---[a]	---	---	---	---	---
3ST2	---[a]	---	---	---	---	---
3ST3	---[a]	---	---	---	---	---
4ST1	4STR1	9.93	Negligible	64.83	0.129	Bolt Shear Rupture
4ST2	---[b]	---	---	---	---	---
4ST3	---[c]	---	---	---	---	---
5ST1	5STR1	8.16	287.39	33.88	0.087	Bolt Shear Rupture
5ST2	5STR2	9.49	269.38	48.17	0.097	Bolt Shear Rupture
5ST3	5STL3	10.39	381.57	54.13	0.091	Bolt Shear Rupture

---[a] Secondary failure mechanism was not attainable due to the initial tension rupture failure.

---[b] Loading was not continued to the point of a secondary failure.

---[c] Initial tension rupture failure resulted in unzipping of shear plate. A secondary failure was not reached.

4.4 Statics Verification

An equilibrium analysis of the test system was conducted for each test to ensure reliable data were collected from the experimental instrumentation. The basis of the analysis was to verify the collected strain gage data corresponded well with the applied vertical shear load. The analysis was conducted during the linear force-rotation increase state which provided a location during test process in which a statically determinant system could be evaluated using fundamental statics principles. Using the free body diagram shown in Figure 4.34, the sum of forces and moments were solved for each test beam.

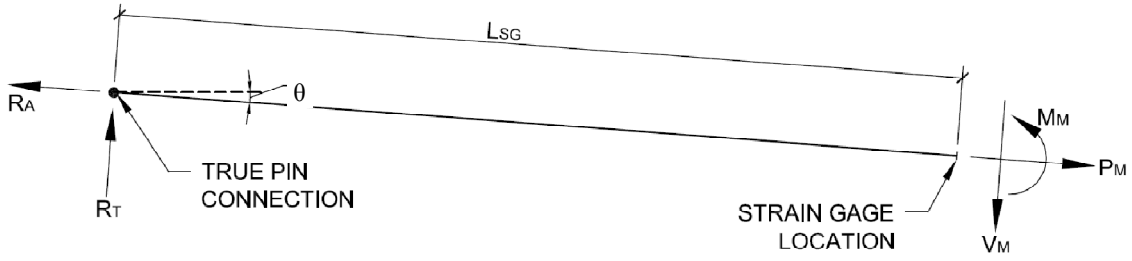

Figure 4.34: Free Body Diagram at the Strain Gage Location.

The horizontal reaction at the true pin connection R_A was set equal to the measured axial load P_M. The true pin vertical reaction was solved summing the moments about the strain gage location, shown as

$$R_T = \frac{M_M}{L_{SG}} \tag{35}$$

where

R_T = Vertical reaction at the true pin connection in kips,

M_M = Measured moment solved using Equations (28) and (30) in kip-inches,

L_{SG} = Distance from the true pin connection to the strain gage locations in inches.

The true pin connection reactions were solved for the vertical component of each reaction using fundamental trigonometric principles. Combining the vertical components of each force, the total vertical reaction was taken as

$$R_y = R_A \sin\theta + R_T \cos\theta \tag{36}$$

where

R_y = Vertical reaction at the true pin connection for side 'x' in kips,

θ = Measured beam end rotation in radians.

The summation of the vertical reactions for the left and right test beams were compared to the measured applied vertical shear load, V_{app}, to determine a percentage of error for each test. The comparisons for the nine experimental tests are shown in Table 4.4. The test data fell within a four percent margin of error with the exception of test 3ST3. As Figure 4.12 shows, the test data for specimen 3STL3 appeared to be an anomaly as the test data unexplainably showed severe spikes throughout the duration of

testing unlike the remaining tests. The accuracy of the data collected for specimen 3STL3 is questionable due to the inconsistency determined using the fundamental statics equations. The data collected for specimen 3STL3 have been noted but have not been evaluated in further sections of the current research as the failure of test 3ST3 was isolated to specimen 3STR3.

Table 4.4: Experimental Data Statics Verification.

Test		P_M (kips)	M_M (kip-inch)	θ (Radians)	V_x (kips)	V_{app} (kips)	Error (%)
3ST1	L	2.08	45.14	0.040	1.31	1.22	1.11
	R	1.13	41.41	0.040	1.17	1.22	
3ST2	L	2.69	80.86	0.080	2.40	2.24	1.43
	R	2.13	72.82	0.080	2.14	2.24	
3ST3	L	0.69	46.26	0.052	1.29	0.98	27.50
	R	0.45	51.80	0.051	1.42	0.98	
4ST1	L	2.31	116.37	0.040	3.24	3.05	1.26
	R	2.97	103.97	0.039	2.93	3.05	
4ST2	L	9.05	172.60	0.066	5.27	4.90	3.11
	R	10.75	152.84	0.066	4.84	4.90	
4ST3	L	9.09	143.31	0.060	4.42	4.41	3.84
	R	8.87	130.51	0.060	4.06	4.41	
5ST1[a]	L	---	---	---	---	---	---
	R						
5ST2	L	10.69	278.57	0.050	8.07	7.78	1.13
	R	12.43	260.12	0.050	7.66	7.78	
5ST3	L	15.00	274.03	0.051	8.19	7.98	1.25
	R	15.26	251.34	0.051	7.57	7.98	

[a] Data not evaluated due to invalid data collection prior to connection failure for test 5ST1.

4.5 Approximate Bolt Force Analysis

In an effort to better understand the effects of the combination of shear, tension, and moment on the tested shear tab connections, a bolt force analysis technique was developed which provided approximate bolt forces at the reported maximum moment. Providing an approximation of the individual bolt forces, limit states which occurred during testing could be approximated as well as the testing accuracy verified. The single bolt shear tests conducted by Kulak *et al.* [20] determined the ultimate bolt shear strength for ASTM A325 bolts as approximately 80.1 ksi. This test data served as a benchmark for the experimental testing. Based on ASTM A325 bolts with the threads excluded used during testing, the maximum experimental bolt shear expected was determined to be 35.4 kips.

The bolt force analysis independently analyzed the effects of the collected experimental data for shear, tension, and moment as well as the effects of the inherent eccentricities resulting from the connection's geometry. All forces were simplified to express units of magnitude for the primary orthogonal axes. The measured axial force was first simplified to force components using fundamental trigonometric principles before being evenly distributed to the connections bolts. The horizontal component of the measured axial force for each bolt was shown as

$$P_x = \frac{P_M * \cos\theta}{n} \tag{37}$$

and the vertical component was taken as

$$P_y = \frac{P_M * \sin\theta}{n}. \tag{38}$$

The bolt forces resulting from applied moments on the bolts were resolved using the Elastic and the Instantaneous Center of Rotation (ICOR) Method described in the

AISC 13TH Edition Specification [2]. The Elastic Method provided conservative bolt forces which did not correspond to reasonable bolt forces when compared to the benchmark maximum bolt shear capacity of 35.4 kips. Because of the conservative nature of the Elastic Method the ICOR method was used exclusively. Unlike the Elastic Method, the ICOR method takes into account the plastic shear deformations which occur in the bolt shank near failure loads. Based on experimental observations by Kulak *et al.* [20], the approximate maximum plastic shear deformation for ASTM A325 bolts with the threads excluded was equal to 0.34 inches. Kulak *et al.* [20] used this plastic deformation limit to construct a load-deformation relationship based on the ultimate shear strength and ultimate plastic deformation limits of a bolt shown as

$$R = R_{ult}(1 - e^{-10\Delta})^{0.55} \tag{39}$$

where

R = nominal shear strength of one bolt at deformation Δ, in kips,

R_{ult} = ultimate shear strength of one bolt in kips,

Δ = total bolt deformation equal to 0.34 inches,

e = natural logarithm equal to 2.71828…

The ICOR method was used to derive the bolt forces as a result of the measured moment and the eccentrically applied shear load. The bolt force analysis summaries for the maximum moments derived in Table 4.1 have been included in Appendix E. Shown in Figure 4.35, the measured moment, M_M, was resolved into bolt forces using a normalized unit shear force, V_{Norm}, applied at an eccentricity, *e*, equal to the measured moment in inches. Shown in Figure 4.36, the results of the ICOR method provided

component bolt forces, $F_{x,n,}$ and, $F_{y,n}$, rotated with respect to the angle, θ, along the line of action of the supported beam.

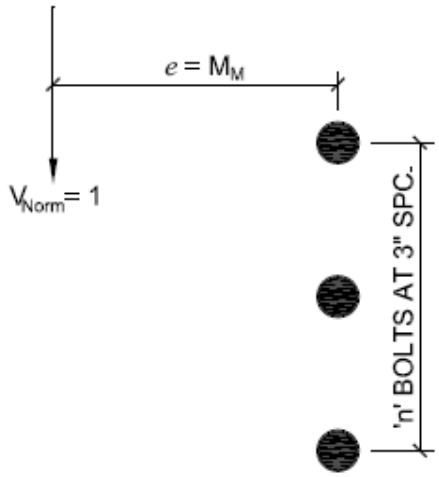

Figure 4.35: Measured Moment ICOR Model

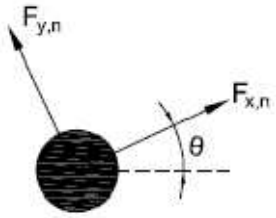

Figure 4.36: Measured Moment ICOR Model Bolt Component Forces.

The ICOR component bolt forces were transformed to orthogonal component forces using fundamental trigonometric principles. The horizontal force, $H_{mx,n}$, for each bolt in the connection was taken as

$$H_{mx,n} = \left(F_{x,n} \cos\theta\right) + \left(F_{y,n} \sin\theta\right). \quad (40)$$

The vertical bolt force, $H_{my,n}$, with respect to the orthogonal axis for each bolt in the connection was taken as

$$H_{my,n} = \left(F_{x,n} \sin\theta\right) + \left(F_{y,n} \sin\theta\right). \quad (41)$$

Using the normalized shear with a unit value of one, the vertical bolt force components for the measured moment analysis were omitted. Simplifying Equation (40), the horizontal bolt force was shown as

$$H_{mx,n} = \left(F_{x,n} \cos\theta\right) \tag{42}$$

and Equation (41) was simplified to

$$H_{my,n} = \left(F_{y,n} \sin\theta\right) \tag{43}$$

A second ICOR analysis was conducted for the eccentrically applied shear load. All experimental tests were conducted with an eccentricity equal to 3 1/2 inches from the face of the stub column flange face. The current provisions of the AISC 13th Edition Specification do not account for this eccentricity directly in the design of the shear tab connections as the BGAF used in the bolt shear capacities accounts for this eccentricity. The eccentrically applied shear load has been accounted for in this research based on the intent of determining the ultimate bolt shear forces. Using the 3 1/2 inch eccentricity, the ICOR method produced a horizontal shear force, $V_{mx,n}$, and a vertical shear force $V_{my,n}$, for each bolt in the connection with respect to the test system orthogonal axis. The summary of the second ICOR analysis is provided in Appendix E.

The bolt force analysis was conducted using the approximate maximum moment data provided in Table 4.1 for each test specimen. The bolt shear force, $V_{b\,max,n}$, for each bolt as a result of the approximate maximum moment was determined by summing the horizontal and vertical forces shown as

$$V_{b\,max,n} = \sqrt{\left(P_x + H_{mx,n} + V_{mx,n}\right)^2 + \left(P_y + H_{my,n} + V_{my,n}\right)^2}. \tag{44}$$

Figure 4.37 provides a summary of the bolt forces analyzed for each bolt in the tested connections. The bolt forces developed using Equation (44) are shown in Table

4.5. The forces represent the resulting shear force due to the connections maximum measured flexural capacity. Beyond this point the connections' load transfer transitioned from flexure to catenary action as a result of large plastic deformations in the plate and bolt cross sections. As shown in Table 4.5, the data analysis corresponded well with the benchmark maximum bolt shear capacity for the three and four bolt connections; however, the five bolt connections were consistently outside this range.

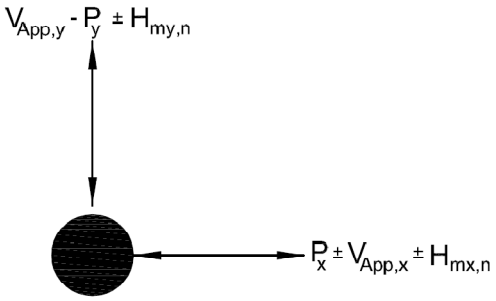

Figure 4.37: Bolt Analysis Bolt Force Summary.

Table 4.5: Bolt Shear Forces at Approximated Maximum Moment.

Test	Specimen	Maximum Bolt Forces (kips)[a]				
		Bolt 1	Bolt 2	Bolt 3	Bolt 4	Bolt 5
3ST1	3STR1	25.0	3.1	**30.7**	-	-
	3STL1	23.1	2.9	28.5	-	-
3ST2	3STR2	28.6	2.4	**32.6**	-	-
	3STL2	30.6	2.3	34.4	-	-
3ST3	3STR3	27.9	2.4	**32.3**	-	-
	3STL3	30.5	2.0	34.1	-	-
4ST1	4STR1	26.3	20.6	26.5	**32.1**	-
	4STL1	28.1	22.1	27.8	33.7	-
4ST2	4STR2	26.0	19.9	29.7	**35.6**	-
	4STL2	28.8	22.3	31.8	38.2	-
4ST3	4STR3	22.0	16.8	25.3	30.4	-
	4STL3	23.5	18.1	26.5	**31.8**	-
5ST1	5STR1	27.9	24.4	6.4	36.7	**40.1**
	5STL1	32.1	28.2	6.4	40.4	44.2
5ST2	5STR2	29.4	25.8	5.9	37.0	**40.5**
	5STL2	32.4	28.5	6.0	39.9	43.8
5ST3	5STR3	27.6	24.1	6.1	35.8	39.2
	5STL3	31.9	28.1	6.1	39.8	**43.5**

[a] Highlighted cells represent bolt shear forces for the failed specimens.

4.6 Preliminary Interaction Diagram

To evaluate the effects of the combination of shear, tension, and moment, an interaction diagram was developed to portray the controlling force components for the three, four, and five bolt connections. The interaction diagrams plotted the resultant vector of the applied shear and measured axial bolt line force, shown as

$$R_v = \sqrt{\left({V_{app}}^2 + {P_M}^2\right)}, \tag{45}$$

versus the maximum measured moment for the values tabulated in Table 4.1. A baseline linear interaction equation was developed using the benchmark maximum bolt shear capacity of 35.4 kips established by Kulak *et al.* [20] to develop the shear capacity and pure moment capacity of the bolted connection. The connection's maximum resultant shear capacity was taken as

$$R_{v,max} = 35.4 * n. \tag{46}$$

The maximum moment capacity, $M_{M,max}$, was determined as described in Section 4.5 using an ICOR analysis for an applied moment which developed the benchmark bolt shear force. The interaction equation was shown as

$$\frac{R_v}{R_{v,max}} + \frac{M_M}{M_{M,max}} \leq 1. \tag{47}$$

The linear interaction equation provided a conservative estimate of the maximum combined force interaction for the tested connections assuming bolt shear was the controlling limit state of the connection. However, as the testing showed, shear and tension rupture limit states controlled a majority of the tested connections. The connections were not able to develop the full shear capacity of the bolts prior to failure. As shown in Figure 4.38, the experimental data fell below the linear interaction diagram for the three and four bolt tests while the five bolt data fell outside the interaction line.

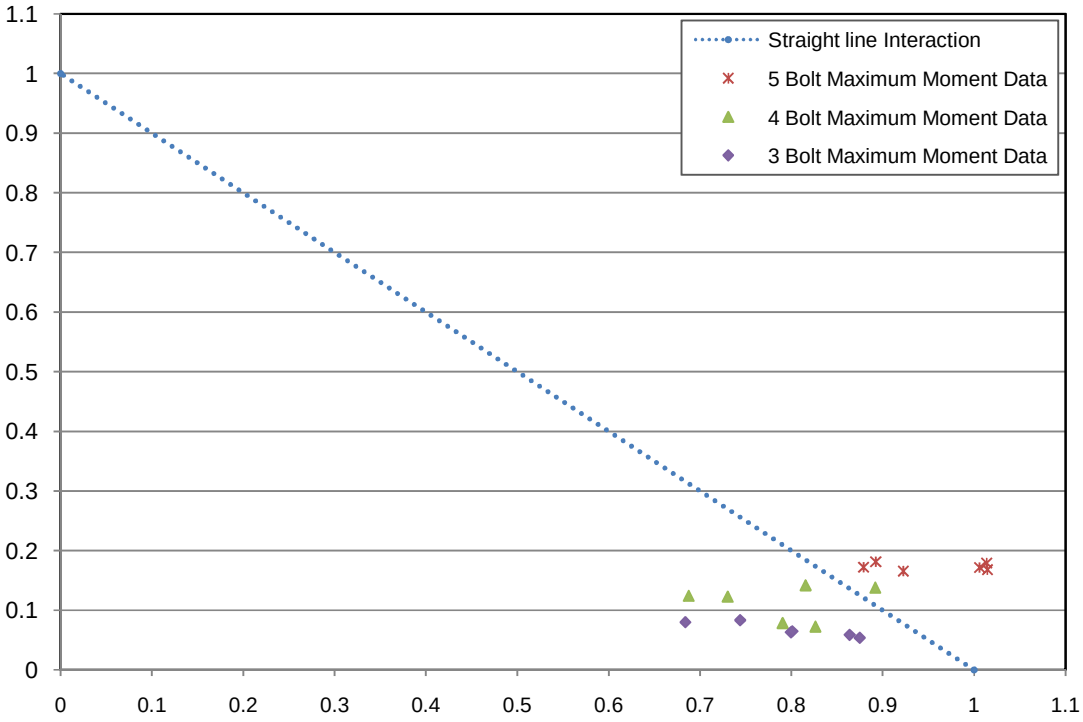

Figure 4.38: Shear Tab Interaction Diagram for Forces at the Maximum Measured Moment.

The linear interaction diagram provided insight into several key behavioral characteristics for the tested shear tab connections. The interaction diagram clearly shows the main force contribution to the connections was due to the flexural forces imparted as a result of the vertical deflection of the test specimens. Also, for the three and four bolt connections the use of a linear interaction diagram based on the shear capacity of the bolts provides an un-conservative limit for the connections. As shown in Table 4.5, the maximum bolt forces observed emulated Figure 4.38 and the failures observed during testing as the connections' primary failures were due to shear plate limit states. A more accurate interaction diagram may be produced using the shear plate limit states. However, as shown in Section 4.7, the observed limits states are not well represented by the design equations of the AISC 13th Edition Specification [2] as the specification limit states are based on direct shear or direct tension limits. Also, as Table 4.5 and Figure 4.38 show,

the five bolt connections fell outside the benchmark data as the measured maximum flexural capacity of the five bolt connections alone reached the maximum bolt capacity determined using the ICOR analysis for the applied moment only case.

4.7 Failure State Derivations

The failure limits states depicted in Section 4.3 included bolt shear rupture, localized block shear of the shear plate, and localized net tension rupture of the shear plate. The development of Equation (47) and the corresponding interaction diagram was based on the experimental data provided by Kulak *et al.* [20] which found the ultimate bolt shear strength for ASTM A325 bolts with the threads excluded from the shear plane to be equal to 35.4 kips. However, as shown in Table 4.2 seven of the nine tests conducted failed due to the shear plate limit states. The shear plate failure patterns do not follow the typical behavior for the design limit states provided by the AISC 13th Edition Specification [2] resulting in limit states which do not correspond well with the bolt forces in Table 4.5. The approximate connection limits states for the failures observed during testing have been calculated per the provisions of the AISC 13th Edition Specification [2] to show the variability which occurs when applying the specification limit states to the current testing. The complete calculations are provided in Appendix F.

The single bolt shear capacity was calculated using the specification capacity and compared to the experimental data determined by Kulak *et al.* [20]. Shown in Table 4.6, the unfactored AISC rated capacity for an ASTM A325 bolt with the threads excluded from the shear plane in single shear is twenty-five percent less than the ultimate capacity reported by Kulak *et al.* [20].

The shear plate net section rupture capacity was calculated using the Whitmore Section effective width criteria defined by Section 9 of the AISC 13th Edition Specification [2]. Shown in Figure 4.39, the Whitmore Section is based on spreading the bolt force from the edge of the plate thirty degrees each side of the line of force back to the bolt line.

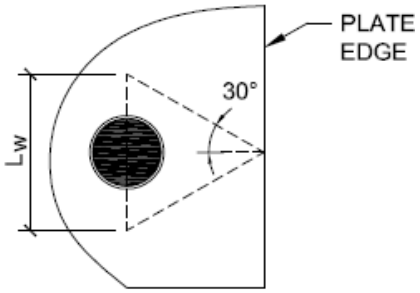

Figure 4.39: Whitmore Section Description.

Shown in Table 4.6, the Whitmore Section provides a largely conservative value for the localized net section capacity of the shear plate at the bottom bolt hole. By varying the Whitmore Section angle between thirty-five and forty degrees, the net section capacity can be increased to values which more closely correspond with the bolt forces determined in Section 4.5.

The bolt forces calculated for the connection which failed due to a localized block shear failure did not correspond well with the calculated capacity determined using the AISC 13th Edition Specification. Using the specification's block shear equation, the un-factored capacity for the failure path shown in Figure 4.40 was calculated to be 36.9 kips. This capacity does not correlate with the failure modes exhibited in three of the nine experimental tests as the specification capacity is greater than the benchmark single bolt shear capacity of 35.4 kips reported by Kulak *et al.* [20] as well as the calculated bolt forces per Table 4.5.

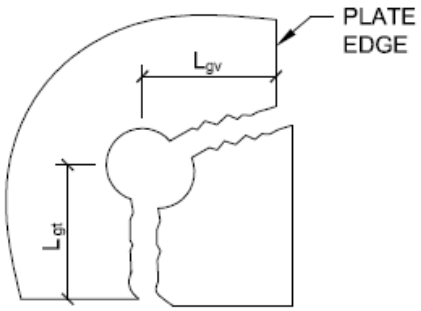

Figure 4.40: Typical Localized Block Shear Failure.

Table 4.6: Approximate Localized Shear Rupture Failure Comparisons.

Approximate Shear Plate Rupture Limit States	
Limit State	Capacity (Kips)
Single Bolt Shear Rupture Per AISC 13th Edition[a]	26.5
Single Bolt Shear Rupture Per Kulak Data[b]	35.4
Net Shear Rupture Per AISC 13th Edition Whitmore Length[a,c]	18.6
Modified Net Shear Rupture Using θ = 35 Degrees	26.6
Modified Net Shear Rupture Using θ = 40 Degrees	35.7
Localized Block Shear Rupture Per AISC 13th Edition[a]	36.9

[a] Capacity calculated per the previsions of the AISC 13th Edition Specification [2].
[b] Single bolt shear capacity per the experimental data reported by Kulak [20].
[c] Whitmore section based on a thirty degree load spread angle each side of the line of force.

Poor correlation exists between the shear plate calculated capacities per the AISC 13th Edition Specification [2], the experimental data provided by Kulak *et al.* [20], and the bolt forces reported in Section 4.5. The discrepancies indicate further investigation is required to determine shear plate capacities which more accurately define true limit states for shear tab connections subject to the combination of shear, tension, and flexure.

Chapter 5

Conclusions

5.1 Research Summary

The purpose of this research was to provide experimental observations and data describing the behavior of single plate "shear tab" simple shear connections subjected to extreme loading conditions caused by the loss of the primary supporting column. The testing sought to determine if shear tab connections had a measurable flexural capacity as well as determining if catenary tension could serve as a secondary load path mechanism. The experimental setup isolated the tested system to only evaluated connections without the contributions of a steel deck or concrete floor. The connections, designed per the "Conventional Configuration" provisions of the AISC 13th Edition Specification [2] for a shear only load application, were subjected to beam end rotations and tension forces not typical expected in gravity load only supporting members. The results of this research have provided insight into the behavior of shear tab connections subjected to extreme loading conditions as well as correlation to previous shear tab research.

5.2 Connection Response Summary

Collected data for the tested specimens' response to the simulated column failure provide three distinct phases of force-rotation behavior. The force-rotation behavior was minimal for the initial load application until the beam end rotation reached approximately 0.025 and 0.03 radians. Beyond 0.03 radians, a linear increase in the measured beam end moment and beam end rotation existed as the applied shear increased. As the connections' flexural capacity was achieved the relationship between the measured beam

end moment and the beam end rotation leveled off. With the flexural capacity leveling the measured tension forces increased until the initial connection failure occurred.

Three bolt connections displayed a more dramatic transition between a flexural and tension response indicating catenary action was an effective alternative load path for the applied shear load. At the peak of the measured moment, the tension forces increased as the measured moment dissipated. At the point of failure, the connections were primarily subjected to shear and tension only as the measured moment was negligible.

Four and five bolt connections displayed similar behavior as the three bolt connections however the transition from flexure to tension was not as significant. As the measured moment peaked, the measured tension forces increased. The measured moment dissipated slightly as the tension forces increased; however, at the connections' initial failure point, a measurable beam end moment and tension force existed. The four and five bolt connections indicated flexure and tension load paths existed; however, catenary tension was not the exclusive load path.

5.3 Rotational Ductility

The ductility mechanisms observed in the current research correspond well with previous research for shear tab connections; however, the rotational ductility magnitudes differed. Research by Richard *et al.* [5] and Astaneh *et al.* [7] determined the shear tab ductility was primarily based on the ability of the connections to undergo acceptable levels of plastic bolt shear deformations as well as bolt hole deformations. Tested connections in this research underwent similar plastic deformations in the shear plate and

bolts shanks. Significant plastic bolt bearing and bolt shear deformations eventually led to the rupture limits states observed during testing.

The tested connection's rotational magnitudes greatly differed from previous test data and assumed behavior reported in the current design specifications for the expected beam end rotation characteristics of simple connections subjected to gravity loads. As reported in the AISC 13th Edition Specification [2] based on experimentation conducted by Astaneh [7], the beam end rotations expected for simple shear connections near the initiation of failure was 0.03 radians. The influence of small applied shears and large measured moments and axial forces in the connections of this research resulted in beam end rotations at the initial failure point ranging from 0.133 radians to 0.076 radians for the three and five bolt connections, respectively. These beam end rotations were similar to those determined by the finite element analysis conducted by Sadek *et al.* [19]. However, this research suggests Sadek *et al.*'s [19] comparisons made to the research of FEMA-355D [17] are misleading as the controlling limit states determined by this research as well as Sadek *et al*. [19] were a result of bearing and tearout failures of the shear plate or beam web rather than bolt shear failures reported by FEMA-355D [17].

Ultimate beam end rotations at the initial failure loads also differed from previous research of shear tab connections subjected to similar large scale beam end rotations. The research provided in FEMA-355D [17] developed Equation (13) which suggested a maximum rotational ductility limit existed based on the ability for the shear tab connection to develop the full moment capacity of the connection bolts. Table 5.1 provides a comparison of the average rotational ductility observed during the current research versus the rotational limits established by the FEMA-355D provisions using

Equation (13). Table 5.1 shows the current research indicated the connection shear plates were not capable of developing the full moment capacity of the bolts in the connections as the shear plate limits controlled the connections capacity. While the three bolt connections rotational data fell within FEMA-355D standard deviation, the limits stated for the validity of Equation (13) were not met due to the controlling shear plate limits.

Table 5.1: Theoretical versus Experimental Beam End Rotation Limits.

Rotational Ductility Limits (Radians)			
Bolts	Equation (13) Theoretical Limits[a]		Experimentally Observed Limits
	Maximum	Minimum	
3	0.137	0.120	0.133
4	0.123	0.113	0.094
5	0.109	0.105	0.076

[a] Limits established by research reported per FEMA-355D [17].

5.4 Connection Failure Modes

Based on the configurations of the specimens tested, three limit states controlled the ultimate capacity of the connections. Failures due to bolt shear, localized net section tensile rupture, and localized block shear rupture were observed at the bottom bolt location. Previous research conducted by Kulak *et al.* [20] provided benchmark data for the ultimate shear capacity of the bolts used in this research. The bolt force analysis conducted for the test data of the three and four bolt connections fell within the benchmark bolt shear data developed by Kulak *et al.* indicating a good correlation existed with the analysis method and the observed failure states. However, the five bolt analysis yielded maximum bolt forces which were consistently greater than the maximum bolt shear benchmark value. This discrepancy indicates further research is required to determine the validity of the proposed bolt force analysis method.

The experimental research confirmed the conservative nature inherent in the bolt shear capacities provided by the current provisions of the AISC 13th Edition Specification [2]. As reported by Baldwin Metzger [3], the BGAF used in the current provisions allows for non-uniform bolt stresses occurring in certain types of connections. The specification bolt shear values are greater than twenty-five percent less than forces calculated in this research and the experimental values reported by Kulak *et al.* [20]. This research agrees with the conservative nature of the specification for connection design; however, investigation into existing structure's robustness and reserve capacity may be hindered using the specifications limits. Further research is required to determine the extent the conservative bolt shear values has on deeper shear tab connections as well as different types of connections.

The plate rupture limits observed during testing were not well represented by the current design equations provided by the AISC 13th Edition Specification. The Whitmore Section analysis conducted for the limit state of net tension rupture suggested an increase force spread angle between thirty-five and forty degrees provided plate capacities which better fit the collected data. The localized block shear calculation for the bottom bolt hole provided plate capacities greater than the bench mark bolt shear capacity. The poor correlation between the observed failure modes and calculated bolt forces, maximum bolt shear data reported by Kulak *et al.* [20], and the limit state equations provided by the AISC 13th Edition Specification [2] suggests further research is required to validate design equations for the plate capacities incorporating tension and shear forces. Further research developing equations for the plate rupture limit states will also verify the validity of the suggested ICOR bolt force analysis.

5.5 Data Validity

The data collection for the current research included measurements of applied load, vertical displacement, and strain. A manually operated hydraulic pump was utilized to power the hydraulic cylinder used for the applied shear load due to limitations of the MSOE CSEC facility. The reported results indicated some variability in the collected data existed as the rate of load application was based on the discretion of the pump operator. Spikes in the graphical data indicated variability existed in the application of the applied shear load; however, consistency was observed between the plotted data throughout the duration of the experimental testing. Further testing would benefit from the use of a hydraulic pump capable of sustaining a steady rate of force or displacement to reduce the peaks and variability between collected data time steps.

The experimental strain gage data indicated two of eight strain gages reported invalid results. One strain gage from each side of the test system providing inconsistent data was eliminated from the data analysis. The loss of the strain gages did not void the tests as only two strain gages from each side of the system were required to extrapolate the system results. However, the ability to map the stress diagrams along the cross section of the supported beams using four points of data was not achieved. The left side beam data were consistently greater in magnitude and more variable than the right side data. The location of the valid strain gages were believed to be the reason for this inconsistency. The valid strain gage readings for the left side were at the quarter points of the beam cross section compared to the right side strain gages at the flange faces which provided more consistent data. Further testing would benefit from multiple strain gages placed at each flange face as well as more strain gages placed within web of the

supported beam profile to increase the probability of collecting valid data as well as increasing the ability to map the stress distribution within the supported beam cross section.

Despite the variability of the collected data due to the inaccuracies of experimental measurement devices, the experimental data validity was verified by an equilibrium analysis indicating the data were within a four percent margin of error when compared to fundamental statics principles. The analysis was conducted within the linear range of the force-rotation relationship to assure significant plastic deformations would not skew the analysis. One irregularity was observed in a three bolt test resulting in greater than twenty percent error as a result of large scale variability in the collected data. Future experimentation would benefit from implementing a more precise hydraulic pump as well as an increase in the number of strain gages.

5.6 Overall Connection Performance

The shear tab connections' overall performance showed the ability to withstand measureable unexpected forces from those specifically considered per the design equations of the AISC 13th Edition Specification [2]. Average flexural capacities generally ignored by current design standards of 165 kip-inches, 320 kip-inches, 580 kip-inches were measured for the three, four, and five bolt connections, respectively. Significant tensile forces were also developed in the connections up to the point of failure. All tested connections yielded due to the flexural forces developed as a result of vertical deflection and ruptured as a result tension or the combination of tension and flexure. All connection failures were due to rupture failures of the bottom bolt and/or bolt

hole. The gross section as well as the shear plate to column flange weld did not show signs of damage.

The connections appeared to have the inherent robustness to transfer flexural and axial forces not accounted for in the original connection design. However the three, four, and five bolt test systems were only capable of achieving an applied shear load ranging from 7.5 to 9 percent of the un-factored connection design strength. The connections designed to withstand gravity loads were not able to bridge over the column failure using catenary forces exclusively prior to failure. Some evidence existed of the five bolt connections ability to recover from the initial failure mode and support less than a one percent increase in applied shear load. However, the data were limited and would benefit from future research.

5.7 Suggested Future Research

The design of shear tab connections per the AISC 13th Edition Specification [2] has been based on previous research which analyzed the connection's characteristic behavior when subjected to gravity loads and typical beam end rotations. Much time and effort has been spent understanding the shear tab's intended behavior. Yet, research into the connection's behavior when subjected to the combination of shear, tension, and moment as a result of extreme loading scenarios has largely been unreported. While a few analytical studies have been conducted few experimental tests have been conducted to verify these studies.

As of today, the New York City Building Code is one of the first United States building codes incorporating structural integrity parameters for steel connections. Under

the 2008 *New York City Construction Code* [23], simple shear connections are required to have a tensile capacity equal to the shear capacity but not combined. Specifically for shear tab connections, the tensile capacity is required to be equal to the bearing capacity of the plate or supported web with bolt hole deformations not a consideration. While a step in the right direction, this requirement may create un-conservative designs. Without looking at the interaction of the shear and tensile forces this blanket requirement, while well intended, may not be the solution for structural integrity design in simple shear connections.

The current research has provided a step in the broad idea of inherent robustness of steel framed structures. The current research was isolated to one connection along a planar two bay frame without influences of a steel deck and concrete floor. Future experimental research exploring the benefits of three-dimensional framing systems with deeper connections, different diameter and grades of bolts, and thicker shear plates would provide a more expansive understanding of a steel framed building's response to the loss of a supporting column. Future research is suggested to refine the bolt force analysis technique utilized in the current research as to develop limit state capacity equations for the combination of localized shear and tension forces in the shear plate. Additional benefits of a non-composite and composite steel deck and concrete floor system are suggested for future analytical and experimental research. Increasing the complexity of the flooring system may better determine a steel framed structures response to unexpected forces. Doing so, future research may provide a more complete understanding of current and future structures ability to withstand extreme loading conditions.

References

[1] Segui, William T. 2003. *LRFD Steel Design 3rd Edition.* Pacific Grove, California: Thomson Learning, Inc.

[2] American Institute of Steel Construction (AISC). 2005. *Manual of Steel Construction 13th Edition.* Chicago, IL.

[3] Baldwin Metzger, Kirsten A. 2006. "Experimental Verification of a New Single Plate Shear Connection Design Model." Master's Thesis, Virginia Polytechnic Institute.

[4] DeStefano, Jim P.E. November 2006. "Detailing to Prevent Progressive Collapse." *STRUCTURE Magazine.* Vol. XX (11), pp. 66-67

[5] Richard, Ralph M., Paul E. Gillett, James D. Kriegh, and Brett A. Lewis. 1980. "The Analysis and Design of Single Plate Framing Connections." *American Institute of Steel Construction: Engineering Journal.* Vol. 17 (2), pp. 38-51.

[6] Lipson, S.L. "Single Angle and Single Plate Beam Framing Connections." *Proceedings of the Canadian Structural Engineering Conference.* 1968. Toronto, Ontario: pp. 141-162

[7] Astaneh, Abolhassan, Steven M. Call, and Kurt M. McMullion. 1989. "Design of Single Plate Shear Connections." *American Institute of Steel Construction: Engineering Journal.* Vol. 26 (1), pp. 21-32.

[8] American Institute of Steel Construction (AISC). 2001. *Manual of Steel Construction 3rd Edition LRFD.* Chicago, IL.

[9] Astaneh, Abolhassan, and M. Nadar. 1989. "Design of Tee Framing Shear Connections." *American Institute of Steel Construction: Engineering Journal.* Vol. 26 (1), pp. 9-20.

[10] American Institute of Steel Construction (AISC). 1980. *Manual of Steel Construction 8th Edition ASD.* Chicago, IL.

[11] Creech, D. 2005. "Behavior of Single Plate Shear Connections with Rigid and Flexible Supports." Master's Thesis, North Carolina State University.

[12] Hewitt, Christopher M. October 2006. "Simple Shear Connections." *Modern Steel Construction.* Vol. 11 (10), pp. 51-53.

[13] Goel, Subhash C. 1986. "Combined Shear and Tension Stresses." *American Institute of Steel Construction: Engineering Journal.* Vol. 23(3), pp. 124-125.

[14] Tamboli, Akbar R. “Simple Beam connections under shear and axial loads.” 1999. *Handbook of Structural Steel Connection Design and Details*. New York: McGraw-Hill, pp. 159-164

[15] Guravich, Susan J., and John L. Dawe. 2006. “Simple Beam Connections in Combined Shear and Tension.” *Canadian Journal of Civil Engineering.* Vol. 33 (4), pp. 357-372.

[16] Canadian Standards Association. 2001. *Limit States Design of Steel Structures.* Standard CAN/CSA-S16-01. Toronto, Ontario.

[17] Federal Emergency Management Agency (FEMA). September 2000. *State of the Art Report on Connection Performance.* FEMA-355D. Richmond, California: SAC Joint Venture, California Universities for Research in Earthquake Engineering.

[18] Girhammar, Ulf Arne. 1980. “Behavior of Bolted Beam-Column Connections under Catenary Action in Damaged Steel Structures: D12.” *Swedish Council for Building Research.* University of Lulea: Lulea, Sweden.

[19] Sadek, Fahim, Sherif El-Tawil, H.S. Lew. 2008. “Robustness of Composite Floor Systems with Shear Connections: Modeling, Simulation, and Evaluation.” *Journal of Structural Engineering.* Vol. 134 (11), pp. 1717-1724.

[20] Kulak, Geoffrey L., John W. Fisher, John H. A. Struik. 2001. *Guide to Design Criteria for Bolted and Riveted Joints*. 2nd ed. Chicago, Illinois: American Institute of Steel Construction.

[21] Friedman, Adam. 2009. “Axial, Shear, and Moment Interaction of WT Connections.” Working Paper, Milwaukee School of Engineering: Milwaukee, Wisconsin.

[22] Johnson, Mathew. 2009. “Axial, Shear and Moment Interaction of Single Angle Connections.” Working Paper, Milwaukee School of Engineering: Milwaukee, Wisconsin.

[23] New York City Department of Buildings. July 2008. New York City Construction Codes. Chapter 22, Section BC 2213: *Structural Integrity Requirements*. [Internet, WWW, PDF]. *Available:* Available in .PDF format; *Address:* http://www.nyc.gov/html/dob/downloads/pdf/cc_chapter22.pdf. [Accessed: 6 November 2007].

Appendix A

"Conventional Configuration" Shear Tab Calculations

The following calculations represent the specific criterion and design procedure presented in the 2005 AISC 13th Edition Specification for the design of single plate shear connections under the "Conventional Configuration" limitations. These calculations represent the expected capacities for the tested three, four, and five bolt shear tab connection subjected to vertical shear only. These calculations have been used to predict an expected maximum applied load level required to ensure a defined failure mechanism is known during experimental testing. The calculations and page number references shown throughout pertain to the 2005 AISC 13th Edition Specification[1]. The calculations have been carried out without the use of the specified safety factors as the analytical ultimate connection capacities are pertinent to the current research. Detailed calculations have been provided for the tested three bolt shear tab connection. A summary of the ultimate shear connection capacities for the three, four, and five bolt connections is shown in Table A-2.

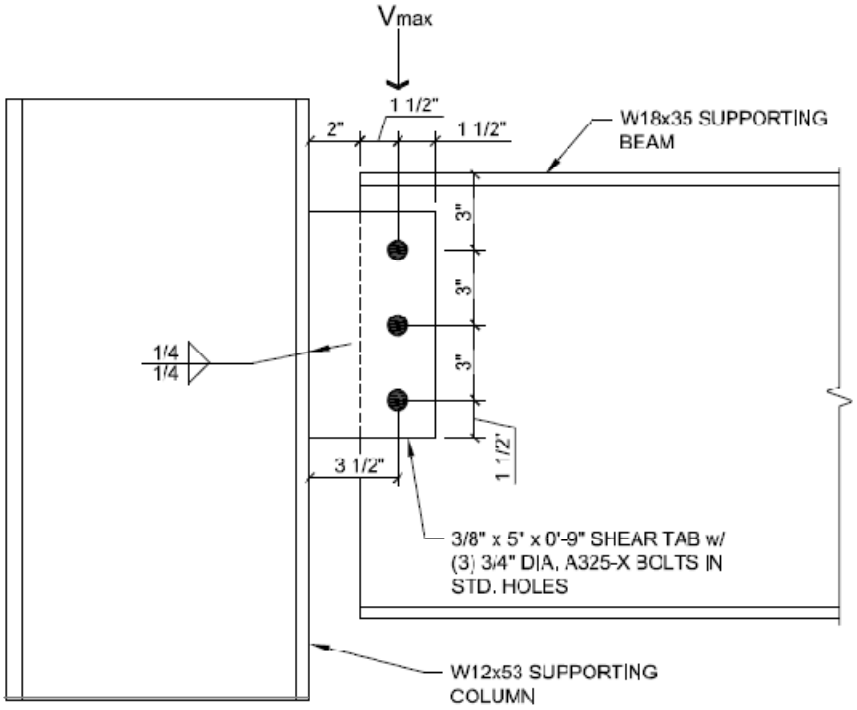

Figure A-1: Typical Three Bolt Shear Tab Connection "Conventional Configuration".

[1] American Institute of Steel Construction (AISC). 2005. *Manual of Steel Construction 13th Edition*. Chicago, IL.

A.1 Connection Material Properties.

Table A-1: Connection Material Properties

	Yield Strength	Rupture Strength	t_{pl} / t_{web} / t_{flange}
Shear Plate	36 ksi	58 ksi	0.375 in
W18x35	50 ksi	65 ksi	0.3 in
W12x53	50 ksi	65 ksi	0.575 in

A.2 "Conventional Configuration" Geometric Requirements (p.10-101).

a. The connection is limited to one column of bolts with the number of bolts, *n*, less than or equal to twelve bolts in the connection.

$$n = 3, 4, 5 \text{ bolts}$$

b. Distance from weld line to bolt line, *a*, less than or equal to 3 1/2 in.

$$a = 3\ 1/2\text{in.}$$

c. Standard or Horizontal Short Slotted Holes only.

d. The horizontal edge distance, $L_{eh,}$ from the center of the bolt hole to the edge of the connecting plate and beam web must be greater than twice the diameter of the bolt.

$$L_{eh} = 1\ 1/2\text{in.}$$

e. The vertical edge distance, L_{ev}, from the center of the bolt hole to the edge of the connecting plate must be equal to or greater than 1 1/4 in. for 3/4 in. diameter bolts.

$$L_{ev} = 1\ 1/2\text{in.}$$

f. Either the thickness of the connecting plate, t_{pl}, or beam web, t_w, must be thicker than one half the diameter of the bolt plus one-sixteenth of an inch.

$$t_{max} = 0.5(0.75\text{in.}) + 0\ .0625\text{in.} = 0.4375\text{in.}$$
$$t_{pl} = 0.375\text{in.} \quad t_w = 0.3\text{in.}$$

g. The minimum weld thickness, $t_{w,min}$, must be equal to or greater than 5/8 $t_{pl.}$

$$t_{w,min} = 0.625 * 0.375$$
$$t_{w,min} = 0.25\text{in.}$$

A.3 Bolt Shear Rupture Capacity (Eq. J3-1).

$$R_n = n * F_n * A_b$$
$$R_n = (3)*(60\ \text{ksi})*\frac{\pi(0.75\ \text{in})^2}{4}$$
$$R_n = 79.5\ \text{kips}$$

A.4 Weld Shear Rupture Capacity (Eq. J2-4).

$$R_n = 0.6 * F_{exx} * \frac{\sqrt{2}}{2} * t_w * l_w * 2$$
$$R_n = 0.6*(70\text{ksi})*\frac{\sqrt{2}}{2}*(0.25\text{in})*(9\text{in}-0.25\text{in})*2$$
$$R_n = 129.9\ \text{kips}$$

A.5 Connecting Plate Base Metal Shear Rupture (Eq. J4-4).

$$R_n = 0.6 * F_u * A_{nv}$$
$$R_n = 0.6*(58\ \text{ksi})*(0.375\text{in})*(9\text{in}-0.25\text{in})$$
$$R_n = 114.2\ \text{kips}$$

A.6 Supporting Column Flange Rupture Strength (p. 9-5).

$$t_{fl,\,min} = \frac{0.6*F_{exx}*\frac{\sqrt{2}}{2}*t_w*2}{06*F_u}$$
$$t_{fl,\,min} = \frac{0.6*(70\text{ksi})*\frac{\sqrt{2}}{2}*(0.25\text{in})*2}{06*(65\text{ksi})}$$
$$t_{fl,\,min} = 0.381\text{in}.$$

A.7 Connecting Plate Shear Yielding (Eq. J4-3).

$$R_n = 0.6 * F_y * A_g$$
$$R_n = (0.6)*(36\text{ksi})*(9\text{in})*(0.375\text{in})$$
$$R_n = 72.9\ \text{kips}$$

A.8 Connecting Plate Shear Rupture (Eq. J4-4).

$$R_n = 0.6 * F_u * A_{nv}$$
$$A_{nv} = t_{pl} * (l_{pl} - (n * (d_b + 0.125in))$$
$$A_{nv} = (0.375\text{in})*(9-(3*(0.75\text{in}+0.125\text{in}))$$
$$A_{nv} = 2.39\text{in}^2$$
$$R_n = (0.6)*(58\text{ksi})*(2.39\text{in}^2)$$
$$R_n = 83.2\ \text{kips}$$

A.9 Connecting Plate Bolt Bearing (Eq. J3-6b).

$$r_n = 1.5 * L_c * t * F_u \leq 3.0 * d_b * t * F_u$$
$$L_c = L_{ev} - 0.5 * (d_b + 0.0625\text{in})$$
$$L_c = 1.5\text{in} - 0.5*(0.75 + 0.0625\text{in})$$
$$L_c = 1.094\ \text{in}$$
$$r_n = (1.5*(1.094\text{in})*(0.375\text{in})*(58\text{ksi}))$$
$$\leq (3.0*(0.75\text{in})*(0.375\text{in})*(58\text{ksi}))$$
$$r_n = 35.7\text{kips} \leq 48.9\text{kips}$$
$$R_n = 35.7\text{kips} + 2*(48.9\text{kips})$$
$$R_n = 133.6\ \text{kips}$$

A.10 Supporting Beam Web Bolt Bearing (Eq. J3-6b).

$$r_n = 1.5 * L_c * t * F_u \leq 3.0 * d_b * t * F_u$$
$$L_c = \text{N/A}$$
$$r_n = (3.0*(0.75\text{in})*(0.3\text{in})*(65\text{ksi}))$$
$$r_n = 43.9\text{kips}$$
$$R_n = 3*(43.9\text{kips})$$
$$R_n = 131.6\ \text{kips}$$

A.11 Connecting Plate Block Shear Rupture (Eq. J4-5).

$$R_n = U_{bs} * F_u * A_{nt} + min\ (0.6 * F_y * A_{gv}, 0.6 * F_u * A_{nv})$$
$$A_{gv} = t_{pl}*(L_{pl} - L_{ev})$$
$$A_{gv} = 0.375\text{in}*(9\text{in} - 1.5\text{in})$$
$$A_{gv} = 2.81\ \text{in}^2$$
$$A_{nv} = t_{pl} * (L_{pl} - L_{ev} - ((n - .05) * (d_b + 0.125in)))$$
$$A_{nv} = 0.375\text{in}*(9\text{in} - 1.5\text{in} - ((3 - 0.5)*(0.75\text{in} + 0.125\text{in})))$$
$$A_{nv} = 1.99\ \text{in}^2$$
$$A_{nt} = t_{pl} * (L_{eh} - (0.5 * (d_b + 0.125in)))$$
$$A_{nt} = 0.375\text{in}*(1.5\text{in} - (0.5*(0.75\text{in} + 0.125\text{in})))$$
$$A_{nt} = 0.398\ \text{in}^2$$
$$U_{bs} = 1.0$$
$$R_n = (1.0*58\text{ksi}*0.398\text{in}^2)$$
$$+\min((0.6*36\text{ksi}*2.81\text{in}^2), (0.6*58\text{ksi}*1.99\text{in}^2))$$
$$R_n = 83.9\ \text{kips}$$

A.12 Supporting Beam Shear Yield (Eq. G2-1).

$$R_n = 0.6 * F_y * A_w * C_v$$
$$R_n = (0.6)*(50\text{ksi})*(17.7\text{in})*(0.3\text{in})*(1.0)$$
$$R_n = 159.3\ \text{kips}$$

Table A-2: Ultimate Shear Capacities for Three, Four, and Five Bolt Shear Tab Connections.

Single Plate "Conventional Configuration" Ultimate Shear Capacity				
Connection Limit State	**AISC 13th Equation**	**3 Bolt Shear Tab**	**4 Bolt Shear Tab**	**5 Bolt Shear Tab**
Single Bolt Shear Rupture (kips/bolt)	J3-1	26.5	26.5	26.5
Shear Plate Single Bolt Tearout (kips/bolt)	J3-6b	35.7	35.7	35.7
Shear Plate Single Bolt Bearing (kips/bolt)	J3-6b	48.9	48.9	48.9
Beam Web Single Bolt Tearout (kips/bolt)	J3-6b	-	-	-
Beam Web Single Bolt Bearing (kips/bolt)	J3-6b	43.9	43.9	43.9
Bolt Shear Rupture (kips)	J3-1	79.5	106.0	132.5
Shear Plate Bolt Bearing (kips)	J3-6b	133.6	182.4	231.4
Beam Web Bolt Bearing (kips)	J3-6b	131.6	175.6	219.5
Weld Shear Rupture (kips)	J2-4	129.9	174.4	219.0
Base Metal Shear Rupture (kips)	J4-4	114.2	153.3	192.5
Min. Support Thickness (inches)	p. 9-5	0.38	0.38	0.38
Shear Plate Shear Yield (kips)	J4-3	72.9	97.2	121.5
Shear Plate Shear Rupture (kips)	J4-4	83.2	110.9	138.7
Shear Plate Block Shear Rupture (kips)	J4-5	83.9	108.2	132.4
Beam Shear Yield (kips)	G2-1	159.3	159.3	159.3

Appendix B

Single Plate "Hanger" Connection Calculations

The following calculations represent an idealized situation in which the shear tab connection designed per Appendix A is subjected to an unexpected tensile force. These calculations represent the expected capacities for the tested three, four, and five bolt shear tab connections subjected to a perpendicular tensile force only. These calculations have been used to predict an expected maximum catenary force required to ensure a defined failure mechanism is known during experimental testing. The calculations and page number references shown throughout pertain to the 2005 AISC 13th Edition Specification[1]. The calculations have been carried out without the use of the specified safety factors as the analytical ultimate connection capacities are pertinent to the current research. Detailed calculations have been provided for the tested three bolt shear tab connection. A summary of the ultimate shear connection capacities for the three, four, and five bolt connections is shown in Table B-2.

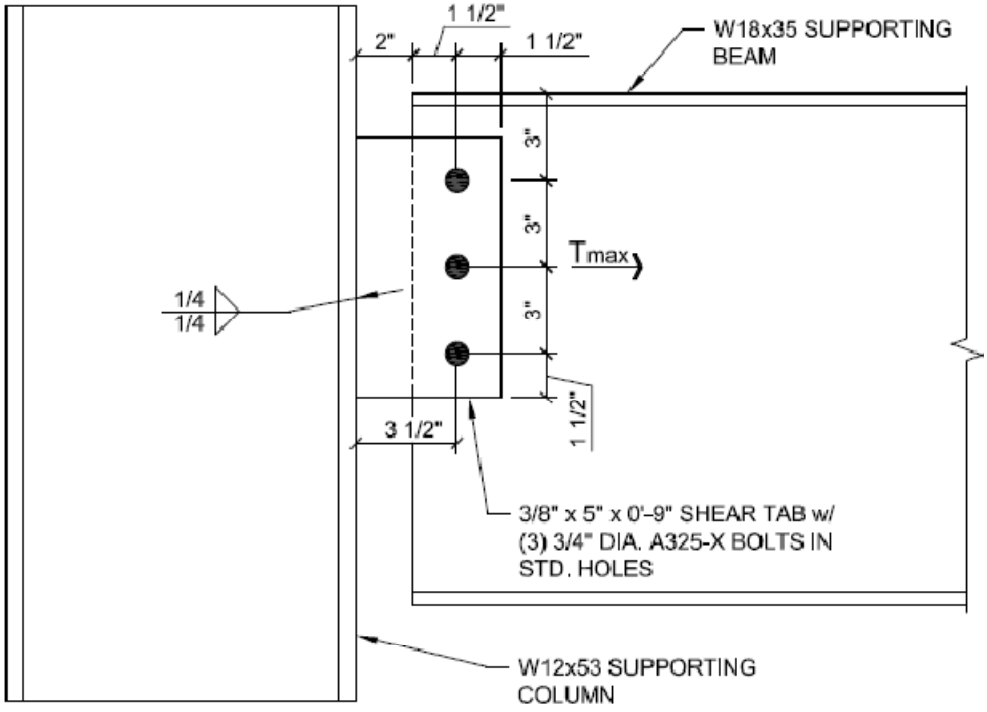

Figure B-1: Typical Three Bolt Shear Tab Connection Configuration – Tension Case.

[1] American Institute of Steel Construction (AISC). 2005. *Manual of Steel Construction 13th Edition*. Chicago, IL.

B.1 Connection Material Properties.

Table B-1: Connection Material Properties.

	Yield Strength	Rupture Strength	t_{pl} / t_{web} / t_{flange}
Shear Plate	36 ksi	58 ksi	0.375 in
W18x35	50 ksi	65 ksi	0.3 in
W12x53	50 ksi	65 ksi	0.575 in

B.2 Geometric Requirements.

Refer to the Appendix A Section A.2 for the geometric considerations required for the connection shown in Figure B-1.

B.3 Bolt Shear Rupture Capacity (Eq. J3-1).

$$R_n = n * F_n * A_b$$
$$R_n = (3)*(60\ \text{ksi})*\frac{\pi(0.75\ \text{in})^2}{4}$$
$$R_n = 79.5\ \text{kips}$$

B.4 Weld Tensile Rupture Capacity (Eq. J2-4 & J2-5).

$$R_n = F_w * A_w$$
$$F_w = 0.6*F_{EXX}*(1.0+0.5*\sin^{1.5}\theta)$$
$$F_w = 0.6*(70\text{ksi})*(1.0+0.5*\sin^{1.5}(90))$$
$$F_w = 63.0\text{ksi}$$
$$R_n = (63\text{ksi})*\frac{\sqrt{2}}{2}*(0.25\text{in})*(9\text{in-}0.25\text{in})*2$$
$$R_n = 194.9\ \text{kips}$$

B.5 Connecting Plate Base Metal Tensile Rupture (Eq. J4-2).

$$R_n = F_u * A_e$$
$$R_n = (58\ \text{ksi})*(0.375\text{in})*(9\text{in-}0.25\text{in})$$
$$R_n = 190.3\ \text{kips}$$

B.6 Connecting Plate Tensile Yielding (Eq. J4-1).

$$R_n = F_y * A_g$$
$$R_n = (36\text{ksi})*(9\text{in})*(0.375\text{in})$$
$$R_n = 121.5\ \text{kips}$$

B.7 Connecting Plate Tensile Rupture (Eq. J4-2).

$R_n = F_u * A_e$
$A_e = A_e * U$
$A_e = (0.375in)*(9-(3*(0.75in+0.125in))*(1.0)$
$A_e = 2.39in^2$
$R_n = (58ksi)*(2.39in^2)$
$R_n = 138.7$ kips

B.8 Connecting Plate Bolt Bearing (Eq. J3-6b).

$r_n = 1.5 * L_c * t_{pl} * F_u \leq 3.0 * d_b * t_{pl} * F_u$
$L_c = L_{ev} - 0.5 * (d_b + 0.0625in)$
$L_c = 1.5in-0.5*(0.75+0.0625in)$
$L_c = 1.094$ in
$r_n = (1.5*(1.094in)*(0.375in)*(58ksi))$
$\leq(3.0*(0.75in)*(0.375in)*(58ksi))$
$r_n = 35.7kips \leq 48.9kips$
$R_n = 3*(35.7kips)$
$R_n = 107.1$ kips

B.9 Supporting Beam Web Bolt Bearing (Eq. J3-6b).

$r_n = 1.5 * L_c * t_w * F_u \leq 3.0 * d_b * t_w * F_u$
$L_c = L_{ev} - 0.5 * (d_b + 0.0625in)$
$L_c = 1.5in-0.5*(0.75+0.0625in)$
$L_c = 1.094$ in
$r_n =(1.5*(1.094in)*(0.3in)*(65ksi))$
$\leq(3.0*(0.75in)*(0.3in)*(65ksi))$
$r_n = 32.0kips \leq 43.9kips$
$R_n = 3*(32.0kips)$
$R_n = 96.0$ kips

B.10 Connecting Plate Block Shear Rupture (Eq. J4-5).

$R_n = U_{bs} * F_u * A_{nt} + min\ (0.6 * F_y * A_{gv}, 0.6 * F_u * A_{nv})$
$A_{gv} = 2 * t_{pl} * L_{ev}$
$A_{gv} = 2*(0.375in)*(1.5in)$
$A_{gv} = 1.13in^2$
$A_{nv} = 2 * t_{pl} * (L_{ev} - (0.5) * (d_b + 0.125in))$
$A_{nv} = 2* 0.375in*(1.5in-(0.5)*(0.75in+0.125in))$
$A_{nv} = 0.8$ in^2
$A_{nt} = t_{pl} * (L_{pl} - (n-1) * (d_b + 0.125in) - 2 * L_{ev})$
$A_{nt} = 0.375in*(9in-(3-1)*(0.75in+0.125in)-2*(1.5in))$
$A_{nt} = 1.59$ in^2
$U_{bs} = 1.0$

$$R_n = (1.0*58ksi*1.59in^2) + \min((0.6*36ksi*1.13in^2), (0.6*58ksi*0.8in^2))$$
$$R_n = 116.52 \text{ kips}$$

B.11 Supporting Beam Web Block Shear Rupture (Eq. J4-5).

$$R_n = U_{bs} * F_u * A_{nt} + min\,(0.6 * F_y * A_{gv}, 0.6 * F_u * A_{nv})$$
$$A_{gv} = 2 * t_w * L_{ev}$$
$$A_{gv} = 2*(0.3in)*(1.5in)$$
$$A_{gv} = 0.9in^2$$
$$A_{nv} = 2 * t_w * (L_{ev} - (0.5) * (d_b + 0.125in))$$
$$A_{nv} = 2*\ 0.3in*(1.5in-(0.5)*(0.75in+0.125in))$$
$$A_{nv} = 0.64\ in^2$$
$$A_{nt} = t_w * ((n-1) * s) - (n-1) * (d_b + 0.125in)$$
$$A_{nt} = 0.3in*((3-1)*3in)-(3-1)*(0.75in+0.125in))$$
$$A_{nt} = 1.28\ in^2$$
$$U_{bs} = 1.0$$
$$R_n = (1.0*65ksi*1.28in^2) + \min((0.6*50ksi*0.9in^2), (0.6*65ksi*0.64in^2))$$
$$R_n = 107.8 \text{ kips}$$

Table B-2: Ultimate Tensile Capacities for Three, Four, and Five Bolt Single Plate Connections.

Single Plate Ultimate Tensile Capacity				
Connection Limit State	AISC 13th Equation	3 Bolt Shear Tab	4 Bolt Shear Tab	5 Bolt Shear Tab
Single Bolt Shear Rupture (kips/bolt)	J3-1	26.5	26.5	26.5
Connecting Plate Single Bolt Tearout (kips/bolt)	J3-6b	35.7	35.7	35.7
Connecting Plate Single Bolt Bearing (kips/bolt)	J3-6b	48.9	48.9	48.9
Beam Web Single Bolt Tearout (kips/bolt)	J3-6b	32.0	32.0	32.0
Beam Web Single Bolt Bearing (kips/bolt)	J3-6b	43.9	43.9	43.9
Bolt Shear Rupture (kips)	J3-1	79.5	106.0	132.5
Connecting Plate Bolt Bearing (kips)	J3-6b	107.1	142.8	178.5
Beam Web Bolt Bearing (kips)	J3-6b	96.0	128.0	160.0
Weld Shear Rupture (kips)	J2-4	194.9	261.7	328.5
Base Metal Tensile Rupture (kips)	J4-2	190.3	255.6	320.8
Connecting Plate Tensile Yield (kips)	J4-1	121.5	162.0	202.5
Connecting Plate Tensile Rupture (kips)	J4-2	138.7	184.9	231.1
Connecting Plate Block Shear Rupture (kips)	J4-5	116.5	163.1	209.3
Beam Web Block Shear Rupture (kips)	J4-5	107.8	149.3	190.7

Appendix C

Test Frame Component Design

The following represents the verification and design conducted for the design of the of the test frame apparatuses. All design calculations and design equations included in Appendix C are based on the AISC 13th Edition Specification[1] using the LRFD design equations. Refer to Appendix D for the design shop drawings referenced in the following design calculations for all dimensions and material grades.

C.1 True Pin Connection

A true pin connection was designed for the exterior beam to column connections to ensure a point of zero moment existed in the test system. This was accomplished by using one 1 1/4 inch diameter ASTM A490 bolt with the threads excluded from the shear plane at each end. The connection was designed for a combined shear force, *V*, of 60 kips and a tensile force, *T*, of 110 kips.

C.1.1 Bolt Design Shear Load

$$V_{max} = \sqrt{V^2 + T^2}$$

$$\mathrm{V_{max}} = \sqrt{(60\ \mathrm{kips})^2 + (110\ \mathrm{kips})^2}$$

$$\mathrm{V_{max}} = 126\ \mathrm{kips}$$

C.1.2 "Pin" Bolt Shear Design

From Table 7-1 of the *AISC 13th Edition Steel Construction Manual*, a 1 1/4 inch diameter ASTM A490 X bolt in double shear is adequate for 138 kips.

$$\phi R_n = 138\ \mathrm{kips} > 126\ \mathrm{kips}$$

$\therefore$ Bolt has adequate capacity.

[1] American Institute of Steel Construction (AISC). 2005. *Manual of Steel Construction 13th Edition*. Chicago, IL.

C.1.3 Beam Web Bearing and Tearout Strength (J3-6a)

$$R_n = 1.2L_c tF_u \leq 2.4dtF_u$$

$$\mathrm{R_n} = (1.2)[2.25\text{ in.} - (0.5)(1.25\text{ in.} + 0.0625\text{ in.})]\mathrm{t_w}(58\text{ ksi})$$

$$\leq (2.4)(1.25\text{ in.})\mathrm{t_w}(58\text{ ksi})$$

$$\mathrm{R_n} = 111\mathrm{t_w} \leq 174\mathrm{t_w}$$

$$\phi\mathrm{R_n} = 126\text{ kips} = (0.75) * (111) * \mathrm{t_w}$$

$$\therefore \mathrm{t_{w\,min}} = 1.51\text{ in.}$$

Two 3/4 inch ASTM A36 doubler Plates were required on each side of the beam web. Similarly, two 3/4 inch extended plates are required for the connection from the pin to the end plate.

C.1.4 End Plate Web Bearing and Tearout Strength (J3-6a)

Top Bolts:

$$R_n = 1.2L_c tF_u \leq 2.4dtF_u$$

$$\mathrm{R_n} = (1.2)[1.5\text{in.} - (0.5)(0.75\text{in.} + 0.0625\text{ in.})]\mathrm{t_{ep}}(58\text{ ksi})$$

$$\leq (2.4)(0.75\text{ in.})\mathrm{t_{ep}}(58\text{ ksi})$$

$$\mathrm{R_n} = 76.1\mathrm{t_{ep}} \leq 104\mathrm{t_{ep}}$$

∴ Therefore tearing is the controlling portion of the equation.

Other Bolts:

$$R_n = 1.2L_c tF_u \leq 2.4dtF_u$$

$$\mathrm{R_n} = (1.2)[6.0\text{ in.} - (0.75\text{in.} + 0.0625\text{ in.})]\mathrm{t_{ep}}(58\text{ ksi})$$

$$\leq (2.4)(0.75\text{ in.})\mathrm{t_{ep}}(58\text{ ksi}) = 104\mathrm{t_{ep}}$$

$$\mathrm{R_n} = 361\mathrm{t_{ep}} \leq 104\mathrm{t_{ep}}$$

∴ Therefore bearing is the controlling portion of the equation.

$$\phi\mathrm{R_n} = 126\text{ kips} = (0.75)[(2\text{ bolts} * 76.1\mathrm{t_{ep}}) + (4\text{ bolts} * 104\mathrm{t_{ep}})]$$

$$\therefore \mathrm{t_{ep\,min}} = 0.295\text{ in.}$$

A minimum 3/4 inch ASTM A36 end plate was used to match the thickness of the extended shear plates.

C.1.5 End Plate Bolts in Shear and Tension (J3-2)

$$\phi R_n = \phi F'_{nt} A_b$$

$$F'_{nt} = 1.3F_{nt} - \frac{F_{nt}}{\phi F_{nt}} f_v \leq F_{nt}$$

$$\mathrm{F'_{nt}} = 1.3(90\text{ ksi}) - \frac{(90\text{ ksi})}{(0.75)(48\text{ ksi})}\left(\frac{60\text{ kips}}{6\text{ bolts}\times 0.442\text{ in.}^2}\right) \leq (90\text{ ksi})$$

$$\mathrm{F'_{nt}} = 60.4\text{ ksi} \leq 90\text{ ksi}$$

$$\phi \mathrm{R_n} = (0.75)[(60.4\text{ ksi})(6\text{ bolts} * 0.442\text{ in.}^2)]$$

$$\phi \mathrm{R_n} = 120\text{ kips} > 110\text{ kips}$$

∴ The end plate bolts are adequate for the applied tension.

C.1.6 Block Shear of Endplate (J4-5)

$$\phi R_n = \varphi\left[0.6F_u A_{nv} + U_{bs} F_u A_{nt} \leq 0.6F_y A_{gv} + U_{bs} F_u A_{nt}\right]$$

$$L_{gv} = 13.5\text{ in.}$$

$$A_{gv} = 5.06\text{ in.}^2$$

$$L_{nv} = [13.5\text{ in.} - (2.5)(0.75\text{in.} + 0.125\text{ in.})] = 11.3\text{ in.}$$

$$A_{nv} = 4.24\text{ in.}^2$$

$$L_{nt} = [1.5\text{ in.} - (0.5)(0.75\text{in.} + 0.125\text{ in.})] = 2.13\text{ in.}$$

$$A_{nt} = 0.799\text{ in.}^2$$

$$\phi \mathrm{R_n} = \phi\left[0.6\mathrm{F_u A_{nv}} + \mathrm{U_{bs} F_u A_{nt}} \leq 0.6\mathrm{F_y A_{gv}} + \mathrm{U_{bs} F_u A_{nt}}\right]$$

$$\mathrm{U_{bs} F_u A_{nt}} = (1.0)(58\text{ ksi})(0.799\text{ in.}^2) = 46.3\text{ kips}$$

$$0.6\mathrm{F_u A_{nv}} = (0.6)(58\text{ ksi})(4.24\text{ in.}^2) = 148\text{ kips}$$

$$0.6\mathrm{F_y A_{gv}} = (0.6)(36\text{ ksi})(5.06\text{ in.}^2) = 109\text{ kips}$$

∴ Shear yielding controls

$$\phi \mathrm{R_n} = (0.75)[109\text{ kips} + 46.3\text{ kips}] = 116\text{ kips} > 126\text{ kips}$$

$$\phi \mathrm{R_n} = 116\text{ kips} > 90\text{ kips}$$

∴ The end plate has adequate shear capacity.

C.1.7 Extended Plate Flexure Checks (F2-1)

The design moment is based on the eccentricity of the pin to the end plate.

$$M_u = V \times distance\ to\ end\ plate$$

$$\mathrm{M_u} = (60\ \mathrm{kips})(3.25\ \mathrm{in.})$$

$$\mathrm{M_u} = 195\ \mathrm{kip\text{-}in.}$$

Assuming the end connection's outside plates are 3/4 inch thick from bearing and tearout section, the flexural capacity of the extended plates is shown.

$$\phi M_n = \phi F_y Z_x$$

$$Z_x = \frac{bd^2}{4}$$

$$\mathrm{Z_x} = \frac{(0.75\mathrm{in.})(12\ \mathrm{in.})^2}{4} = 27.0\ \mathrm{in.}^3$$

$$\phi\mathrm{M_n} = (0.9)[(2)(36\ \mathrm{ksi})(27.0\ \mathrm{in.}^3)]$$

$$\phi\mathrm{M_n} = 1750\ \mathrm{kip\text{-}in.} > 195\ kip\text{-}in$$

∴ Plate has adequate capacity.

C.1.8 End Plate Shear Yielding (J4-3)

$$\phi R_n = \phi 0.6 F_y A_g$$

$$\phi\mathrm{R_n} = (1.0)[(0.6)(36\ \mathrm{ksi})(12\ \mathrm{in.} \times 0.75\ \mathrm{in.})]$$

$$\phi\mathrm{R_n} = 194\ \mathrm{kips} > 60\ \mathrm{kips}$$

∴ The end plate has adequate capacity.

C.1.9 End Plate Shear Rupture (J4-4)

$$\phi R_n = \phi 0.6 F_u A_{nv}$$

$$\phi\mathrm{R_n} = (0.75)[(0.6)(58\ \mathrm{ksi})(12\ \mathrm{in.} * 0.75\ \mathrm{in.})]$$

$$\phi\mathrm{R_n} = 235\ \mathrm{kips} > 60\ \mathrm{kips}$$

∴ The end plate has adequate capacity.

C.1.10 End Plate Prying

To check whether prying action was a concern for this connection, Section 9 from the *AISC 13th Edition Steel Construction Manual* was used.

$$T_{bolt} = 110\ \mathrm{kips}/6\ \mathrm{bolts} = 18.3\ \mathrm{kips}$$

$$b' = \left(b - \frac{d_b}{2}\right) = \left(2.75 \text{ in.} - \frac{0.75 \text{ in.}}{2}\right) = 2.38 \text{ in.}$$

$$p = 6.0 \text{ in.}$$

$$t_{min} = \sqrt{\frac{4.44 T_{bolt} b'}{p F_u}}$$

$$\mathrm{t_{min}} = \sqrt{\frac{4.44(18.3 \text{ kips})(2.38 \text{ in.})}{(6 \text{ in.})(58 \text{ ksi})}}$$

$$\mathrm{t_{min}} = 0.745 \text{ in.} < 0.75\ in.\ (Thickness\ of\ End\ Plate)$$

∴ Prying does not control the end plate design.

C.1.11 Weld Design (J2-4)

Due to limited weld access, a partial penetration weld was designed to secure the side plates of the end connection to end plate.

Tension Capacity

$$\phi R_n = \phi 0.6 F_{exx} A_w$$

$$\phi \mathrm{R_n} = (0.8)[0.6(70 \text{ ksi})(12\text{in})(0.5\text{in.})(2)(0.5)]$$

$$\phi \mathrm{R_n} = 202 \text{ kips} > 110 \text{ kips}$$

∴ Weld has adequate tensile capacity.

Shear Capacity

$$\phi R_n = \phi 0.6 F_{exx} A_e$$

$$\phi \mathrm{R_n} = (0.75)[0.6(70 \text{ ksi})(6 \text{ in.}^2)]$$

$$\phi R_n = 189 \text{ kips} > 60 \text{ kips}$$

∴ Weld has adequate capacity.

Combined Force Capacity:

$$\phi R_n = \sqrt{V^2 + T^2}$$

$$\phi \mathrm{R_n} = \sqrt{(189 \text{ kips})^2 + (202 \text{ kips})^2}$$

$$\phi \mathrm{R_n} = 277 \text{ kips} > 126 \text{ kips}$$

∴ Weld has adequate capacity.

C1.12 MSOE CSEC Test Frame Flange Local Buckling (J10-1)

$$\phi R_n = \phi 6.25 {t_f}^2 F_{yf}$$

$$\phi R_n = (0.9)[(6.25)(0.94 \text{ in.})^2(50 \text{ ksi})]$$

$$\phi \mathrm{R_n} = 248 \text{ kips} > 55 \text{ kips}$$

∴ Flange has adequate capacity.

C1.13 Web Local Yielding:

$$\phi R_n = \phi(5k + N) F_{yw} t_w$$

$$\phi \mathrm{R_n} = (1.0)[\{(5)(1.34 \text{ in.}) + 12 \text{ in.}\}(50 \text{ ksi})(0.890 \text{ in.})]$$

$$\phi \mathrm{R_n} = 551 \text{ kips} > 55 \text{ kips}$$

∴ Web has adequate capacity.

C.2 Design of Hydraulic Ram Base Connection

A secondary apparatus was constructed to secure the hydraulic ram to the MSOE CSEC test frame. The assembly provided the restraint which prevented the ram from kicking out or excessively moving during the testing. The connection was designed for an ultimate tensile force the hydraulic ram was rated for equal to 100 kips. The overall ram support apparatus consists of an upper and lower section. Shown in Appendix D, the lower section provided a base connection for the 1 3/4 inch ASTM A36 threaded rods.

C2.1 Connecting Bolts Ultimate Design Load

$$T_{ult/bolt} = 100 \text{ kips}/2 \text{ sides} / 4 \text{ bolts} = 12.5 \text{ kips /bolt}$$

C2.2 Bolt Tensile Strength (J3-1)

$$\phi r_n = \phi F_n A_b$$

$$\phi r_n = (0.75)[(90 \text{ ksi})(0.442 \text{ in.})^2]$$

$$\phi r_n = 29.8 \text{ kips/bolt} > 12.5 \text{ kips/bolt}$$

∴ The bolts have adequate capacity.

C2.3 Threaded Rod Ultimate Tensile Load

$$T_{ult/rod} = 100 \text{ kips}/2 \text{ sides} = 50 \text{ kips/rod}$$

C2.4 Threaded Rod Tensile Yielding (D2-1)

$$\phi P_n = \phi_t F_y A_b$$

$$\phi P_n = (0.9)[(36 \text{ ksi})(1.77 \text{ in.}^2)]$$

$$\phi P_n = 57.2 \text{ kips} > 50 \text{ kips}$$

$\therefore$ The threaded rods are adequate.

C2.5 Threaded Rod Tensile Rupture Strength (J3-1)

$$\phi P_n = \phi F_n A_b$$

$$F_n = 0.75 F_u$$

$$\phi P_n = (0.75)\left[(0.75)(58 \text{ ksi})\left(\frac{\pi}{2} * (1.5\text{in.})^2\right)\right]$$

$$\phi \mathrm{P_n} = 57.6 \text{ kips} > 50.0 \text{ kips}$$

$\therefore$ The threaded rods are adequate.

C2.6 Thread Tensile Strength in Bottom Plates

The initial design of the threaded rods shown in Appendix D intended the treaded rods to be threaded into their respective base plates. Due to a fabrication variance from the shop drawings, the threaded rods were instead bolted through the plate. Because the original pieces were sized to prevent stripping or pullout of the threads, it was found that the same sizes were adequate for the final set-up.

C2.7 Base Plate Prying:

The minimum base plate thickness ensuring prying action would not control the connection was based on Section 9 from the *AISC 13th Edition Steel Construction Manual*.

$$T_{bolt} = 50 \text{ kips}/4 \text{ bolts} = 12.5 \text{ kips}$$

$$b' = \left(b - \frac{d_b}{2}\right) = \left(2.75 \text{ in.} - \frac{0.75 \text{ in.}}{2}\right) = 2.38 \text{ in.}$$

$$p = 6.0 \text{ in.}$$

$$t_{min} = \sqrt{\frac{4.44 T_{bolt} b'}{p F_u}}$$

$$t_{min} = \sqrt{\frac{4.44(12.5 \text{ kips})(2.38 \text{ in.})}{(6 \text{ in.})(58 \text{ ksi})}}$$

$$t_{min} = 0.62 \text{ in.} < 1.0 \text{ in}$$

∴ Prying is not a concern using one inch base plates.

C.3 Design of Hydraulic Ram Upper Connection.

The upper portion of the hydraulic ram support provided the vertical and lateral restraint for the hydraulic ram. As shown in Appendix D, the apparatus also provided the support for the load cells.

C3.1 Statics Summary

The top plate was designed to resist a load applied at the center of the plate with a maximum force of 100 kips. The two threaded rods designed in Section C.3 provided the simple supports. With a centrally located point load of 100 kips, the bending moment is

$$M_{max} = \frac{Pl}{4}$$

$$M_{max} = \frac{(100 \text{ kips})(24 \text{ in.})}{4}$$

$$M_{max} = 600 \text{ kip-in.}$$

C3.2 Flexural Yielding of Built-Up Top Plate Section (F9-2)

$$\phi M_n = \phi M_p = \phi F_y Z_x \leq 1.6 M_y$$

$$\phi M_n = (0.9)[(36 \text{ ksi})(23 \text{ in.}^3)] \leq (1.6)(600 \text{ kip-in})$$

$$\phi M_n = 745 \text{ kip-in} \leq 960 \text{ kip-in}$$

$$\phi M_n = 745 \text{ kip-in} > 600 \text{ kip-in}$$

∴ The built-up section has adequate flexural capacity.

C3.3 Lateral-Torsional Buckling of Built-up Section (Stems in Tension) (F9-4)

$$\phi M_n = \phi M_{cr} = \phi \frac{\pi \sqrt{EI_y GJ}}{L_b} \left[B + \sqrt{1 + B^2}\right]$$

$$B = \pm 2.3 \left(\frac{d}{L_b}\right) \sqrt{\frac{I_y}{J}}$$

$$B = 2.3\left(\frac{5\text{ in.}}{24\text{ in.}}\right)\sqrt{\frac{679\text{ in.}^4}{4\text{ in.}^4}}$$

$$B = 6.24$$

$$\phi M_n = (0.9)\left[\frac{\pi\sqrt{(29000\text{ ksi})(679\text{ in.}^4)(11500\text{ ksi})(4\text{ in.}^4)}}{(24\text{ in.}^4)}\left[6.24+\sqrt{1+6.24^2}\right]\right]$$

$$\phi M_n = 1.41\text{ x }10^6\text{ kip-in} \gg 600\text{ kip-in}$$

∴ Lateral torsional buckling does not control.

C3.4 Flange Local Buckling of Built-up Section Tees (F9-6)

Check to see if section is compact

$$\frac{b}{t} = \frac{12\text{ in.}}{1\text{ in.}} = 12$$

$$\lambda_r = 1.49\sqrt{\frac{E}{F_y}} = 1.49\sqrt{\frac{(29000\text{ ksi})}{(36\text{ ksi})}} = 42 > 12$$

∴ Section is noncompact.

$$F_{cr} = F_y\left(1.19 - 0.50\left(\frac{b_f}{2t_f}\right)\sqrt{\frac{F_y}{E}}\right)$$

$$F_{cr} = (36)\left(1.19 - 0.50\left(\frac{(12\text{ in.})}{2(1\text{ in.})}\right)\sqrt{\frac{(36\text{ ksi})}{(29000\text{ ksi})}}\right)$$

$$F_{cr} = 39\text{ ksi}$$

$$\phi M_n = \phi F_{cr} S_{xc}$$

$$\phi M_n = (0.9)[(39\text{ ksi})(34\text{ in.}^3)]$$

$$\phi M_n = 1193\text{ kip-in} > 600\text{ kip-in}$$

∴ Built-up section has adequate capacity.

C3.5 Stiffener Weld Demand

$$V_{max} = \frac{M_{max}}{2d}$$

$$V_{max} = \frac{600\text{ kip-in}}{2(2.5\text{ in.})}$$

$$V_{max} = 120\text{ kips}$$

$$V_{max/stiff} = 120\text{ kips}/2\text{ Stiffeners} = 60\text{ kips/stiffener}$$

C3.6 Stiffener Plate Weld Design (J2-3)

$$\phi R_n = \phi F_w A_w$$

$$F_w = 0.6F_{exx}$$

$$\phi \mathrm{R_n} = (0.75)\left[0.6(70\text{ ksi})\left(2\text{ welds} * 36\text{ in.} * \frac{\sqrt{2}}{2} * \frac{5}{16}\text{in.}\right)\right]$$

$$\phi \mathrm{R_n} = 500\text{ kips} > 60\ kips$$

∴ Weld has adequate capacity.

C3.7 Base Metal Shear Yielding (J4-3)

$$\phi R_n = \phi 0.6F_y A_g$$

$$\phi \mathrm{R_n} = (1.0)[0.6(36\text{ ksi})(36\text{ in.} * 1\text{ in.})]$$

$$\phi \mathrm{R_n} = 778\text{ kips} > 60\ kips$$

∴ Weld has adequate capacity.

C3.8 *Base Metal Shear Rupture (J4-4)*

$$\phi R_n = \varphi 0.6F_u A_{nv}$$

$$\phi \mathrm{R_n} = (0.75)[0.6(58\text{ ksi})(36\text{ in.} * 1\text{ in.})]$$

$$\phi \mathrm{R_n} = 940\text{ kips} > 60\text{ kips}$$

∴ Weld has adequate capacity. Use 5/16” fillet welds.

C3.9 Plate Apparatus Deflection

$$\Delta_{max} = \frac{l}{240}$$

$$\Delta_{\mathrm{max}} = \frac{24\text{ in.}}{240}$$

$$\Delta_{\mathrm{max}} = 0.10\text{ in.}$$

$$\Delta = \frac{Pl^3}{48EI}$$

$$\Delta = \frac{(100\text{ kips})(24\text{ in.})^3}{(48)(29000\text{ ksi})(45.3\text{ in.}^4)}$$

$$\Delta = 0.02\text{ in.} < 0.10\ in.$$

∴ The section will not deflect more than the limit allowed.

B.4 Design of the Threaded Rod Connection

A bolted clevis-type connection was designed to provide the link between the test specimen column stubs and the hydraulic cylinder. The connection also provided a support location for the threaded rod extended out of the hydraulic cylinder. The connection was designed for an ultimate applied load of 100 kips based on the hydraulic cylinder's rated capacity. The following represents the design calculations conducted verifying the connection capacity. Refer to Appendix D for all dimensions and sizes not shown.

C4.1 Threaded Rod Tensile Yield Strength (D2-1)

The threaded rod connecting the hydraulic cylinder to the column stub connection was designed as a 1-3/4 inch diameter ASTM A572 Grade 60 rod.

$$\phi P_n = \phi F_y A_b$$

$$\phi P_n = (0.9)[(60 \text{ ksi})(2.41 \text{ in.}^2)]$$

$$\phi P_n = 129 \text{ kips} > 100 \; kips$$

$\therefore$ Threaded rod has adequate capacity

C4.2 Threaded Rod Tensile Rupture Strength (J3-1)

$$\phi P_n = \phi F_n A_b$$

$$F_n = \; 0.75 F_u$$

$$\phi \mathrm{P_n} = (0.75)[(0.75)(75 \text{ ksi})]$$

$$\phi P_n = 101.5 \text{ kips} \; > 100 \text{ kips}$$

$\therefore$ Threaded rod has adequate capacity.

C4.3 Threaded Rod Connection Bolt Shear

From Table 7-1 of the *AISC 13th Edition Steel Construction Manual*, a 3/4 inch diameter A325 X bolt in double shear is adequate for 39.8 kips.

$$\phi \mathrm{R_n} = (39.8 \text{ kips/bolt}) * \; 3 \text{ bolts}$$

$$\phi \mathrm{R_n} = 119.4 \text{ kips} > 100 \; kips$$

$\therefore$ Bolts have adequate capacity.

C4.4 Clevis Bearing/Tearout Strength (J3-6a)

$$R_n = 1.2L_c tF_u \leq 2.4dtF_u$$

$$\mathrm{R_n} = (1.2)[1.5\text{ in.} - (0.5)(0.75\text{ in.} + 0.0625\text{ in.})](2)(0.5\text{in.})(58\text{ ksi})$$

$$\leq (2.4)(0.75\text{ in.})(2)(0.5\text{ in.})(58\text{ ksi})$$

$$\mathrm{R_n} = 76.1\text{ kips} \leq 104\text{ kips}$$

∴ Therefore tearout is the controlling portion of the equation.

$$\phi\mathrm{R_n} = (0.75)[76.1\text{ kips} * 3\text{ bolts}]$$

$$\phi\mathrm{R_n} = 171\text{ kips} > 100\ kips$$

∴ The Clevis plates are adequate in bearing and tearout.

C4.5 Specimen Column Stub Bearing/Tearout Strength (J3-6a)

$$R_n = 1.2L_c tF_u \leq 2.4dtF_u$$

$$\mathrm{R_n} = (1.2)[1.5\text{ in.} - (0.5)(0.75\text{ in.} + 0.0625\text{ in.})](0.26\text{ in.})(65\text{ ksi})$$

$$\leq (2.4)(0.75\text{ in.})(0.26\text{ in.})(65\text{ ksi})$$

$$\mathrm{R_n} = 22.2\text{ kips} \leq 30.4\text{ kips}$$

∴ Therefore tearout is the controlling portion of the equation.

$$\phi R_n = (0.75)[22.2\text{ kips} * 3\text{ bolts}]$$

$$\phi R_n = 49.9\text{ kips} < 100\text{ kips}$$

∴ W12 column stub web is not adequate in bearing and tearout.

A1/2 inch ASTM A36 web doubling plate is required at each side of the W12X26 column sub web. Doing so, the column web connection is adequate by inspection as the thickness of the web is greater than the thickness of the clevis connecting plates calculated per *C4.4.*

C4.6 Clevis Plates Block Shear (J4-5)

Case 1: “L” shape rupture path

$$\phi R_n = \phi\left[0.6F_u A_{nv} + U_{bs}F_u A_{nt} \leq 0.6F_y A_{gv} + U_{bs}F_u A_{nt}\right]$$

$$L_{gv} = 1.5\text{ in.}$$

$$A_{gv} = 0.75\text{ in.}^2$$

$$L_{nv} = [1.5\text{ in.} - (0.5)(0.75\text{in.} + 0.125\text{ in.})] = 1.06\text{ in.}$$

$A_{nv} = 0.53 \text{ in.}^2$

$L_{nt} = [7.25 \text{ in.} - (2.5)(0.75\text{in.} + 0.125 \text{ in.})] = 2.64 \text{ in.}$

$A_{nt} = 2.53 \text{ in.}^2$

$\mathrm{U_{bs}F_uA_{nt}} = (1.0)(58 \text{ ksi})(2.53 \text{ in.}^2) = 147 \text{ kips}$

$0.6\mathrm{F_uA_{nv}} = (0.6)(58 \text{ ksi})(0.53 \text{ in.}^2) = 18.4 \text{ kips}$

$0.6\mathrm{F_yA_{gv}} = (0.6)(36 \text{ ksi})(0.75 \text{ in.}^2) = 16.2 \text{ kips}$

$\therefore$ Therefore with yielding controlling

$\phi\mathrm{R_n} = (0.75)(2)[16.2 \text{ kips} + 147 \text{ kips}]$

$\phi\mathrm{R_n} = 244\text{kips} > 100 \text{ kips}$

Case 2: "C" shaped rupture path

$\phi R_n = \phi\left[0.6F_uA_{nv} + U_{bs}F_uA_{nt} \leq 0.6F_yA_{gv} + U_{bs}F_uA_{nt}\right]$

$L_{gv} = 3.0 \text{ in.}$

$A_{gv} = 1.5 \text{ in.}^2$

$L_{nv} = [3.0 \text{ in.} - (1.0)(0.75\text{in.} + 0.125 \text{ in.})] = 2.13 \text{ in.}$

$A_{nv} = 1.06 \text{ in.}^2$

$L_{nt} = [6.0 \text{ in.} - (2.0)(0.75\text{in.} + 0.125 \text{ in.})] = 4.25 \text{ in.}$

$A_{nt} = 2.13 \text{ in.}^2$

$\mathrm{U_{bs}F_uA_{nt}} = (1.0)(58 \text{ ksi})(2.13 \text{ in.}^2) = 123 \text{ kips}$

$0.6\mathrm{F_uA_{nv}} = (0.6)(58 \text{ ksi})(1.06 \text{ in.}^2) = 36.9 \text{ kips}$

$0.6\mathrm{F_yA_{gv}} = (0.6)(36 \text{ ksi})(1.5 \text{ in.}^2) = 32.4 \text{ kips}$

$\therefore$ Therefore with yielding controlling

$\phi\mathrm{R_n} = (0.75)[32.4 \text{ kips} + 123 \text{ kips}]$

$\phi\mathrm{R_n} = 234\text{kips} > 100 \text{ kips}$

$\therefore$ Plate has adequate capacity.

C4.6 Column Stub Web Block Shear Rupture

Similar to the bearing check per *C4.5*, the addition of the web doubling plates assures the block shear capacity of the column stub web is adequate.

C4.7 Clevis Plate Tension Yielding (J4-1)

$$\phi R_n = \phi F_y A_g$$

$$\phi \mathrm{R_n} = (1.0)[(36\ \mathrm{ksi})(2\ \mathrm{sides} * 2\ \mathrm{pieces} * 2.25\ \mathrm{in.} * 0.5\ \mathrm{in.})]$$

$$\phi \mathrm{R_n} = 146\ \mathrm{kips} > 100\ kips$$

∴ Plate has adequate capacity.

C4.8 Clevis Plate Tensile Rupture (J4-2)

$$\phi R_n = \phi F_u A_e$$

$$\phi \mathrm{R_n} = (0.75)\left[(58\ \mathrm{ksi})(2 * (8.5\ \mathrm{in.} - (3)(.0875\ \mathrm{in.})) * 0.5\ \mathrm{in.})\right]$$

$$\phi R_n = 256\ \mathrm{kips} > 100\ \mathrm{kips}$$

∴ Plate has adequate capacity.

C4.9 Clevis Plate Weld Design (J2-3)

$$\phi R_n = \phi F_w A_w$$

$$F_w = 0.6 F_{EXX}$$

$$\phi \mathrm{R_n} = (0.75)(0.6)(70\mathrm{ksi})(2.25\mathrm{in.})(2)(4)(0.25)\left(\frac{\sqrt{2}}{2}\right)$$

$$\phi \mathrm{R_n} = 100.2\mathrm{kips} > 100\ \mathrm{kips}$$

∴ Use 1/4 inch fillet welds on each side (4 total) of clevis plates.

C4.10 Clevis Plate Base Metal Rupture (J2-2)

$$\phi R_n = \phi 0.6 F_u A_{BM}$$

$$\phi \mathrm{R_n} = (0.75)[(0.6)(58\ \mathrm{ksi})(2)(2)(0.5\mathrm{in.})(2.25\mathrm{in.})]$$

$$\phi \mathrm{R_n} = 117.5\ \mathrm{kips} > 100\ \mathrm{kips}$$

∴ Base metal has adequate capacity.

C4.11 Flexural Demand on Base Plate of Clevis Apparatus

Assuming a point load of 100 kips at the center of the threaded rod connection bottom plate, the connection was analyzed to ensure the base plate had sufficient flexural capacity to span between the openings in the clevis plates.

$$M_u = \frac{P_u L}{4}$$

$$\mathrm{M_u} = \frac{(100\mathrm{kips})(4.25\mathrm{in.})}{4}$$

$$\mathrm{M_u} = 106.3\ \mathrm{kip\text{-}in}$$

C4.12 Flexural Yielding Capacity of Clevis Apparatus Base Plate (F2-1)

$$\phi M_n = \phi F_y Z_x$$

$$Z_x = \frac{bd^2}{4}$$

$$\mathrm{Z_x} = \frac{(10\mathrm{in.})(1.25\mathrm{in.})^2}{4}$$

$$\mathrm{Z_x} = 3.9\ \mathrm{in.}^3$$

$$\phi \mathrm{M_n} = (0.9)(36\mathrm{ksi})(3.9\mathrm{in.}^3)$$

$$\phi \mathrm{M_n} = 126.6\mathrm{kip\text{-}in} > 106.3\mathrm{kip\text{-}in}$$

$\therefore$ The base plate has adequate capacity.

Appendix D

Test Apparatus Shop Drawings

The following represents the shop drawings developed for the fabrication of the test apparatuses required for testing. The materials and fabrication was donated by AISC certified Germantown Iron and Steel based in Jackson, Wisconsin. Figure D-1 provides an erection drawing referencing the particular shop drawing piece marks.

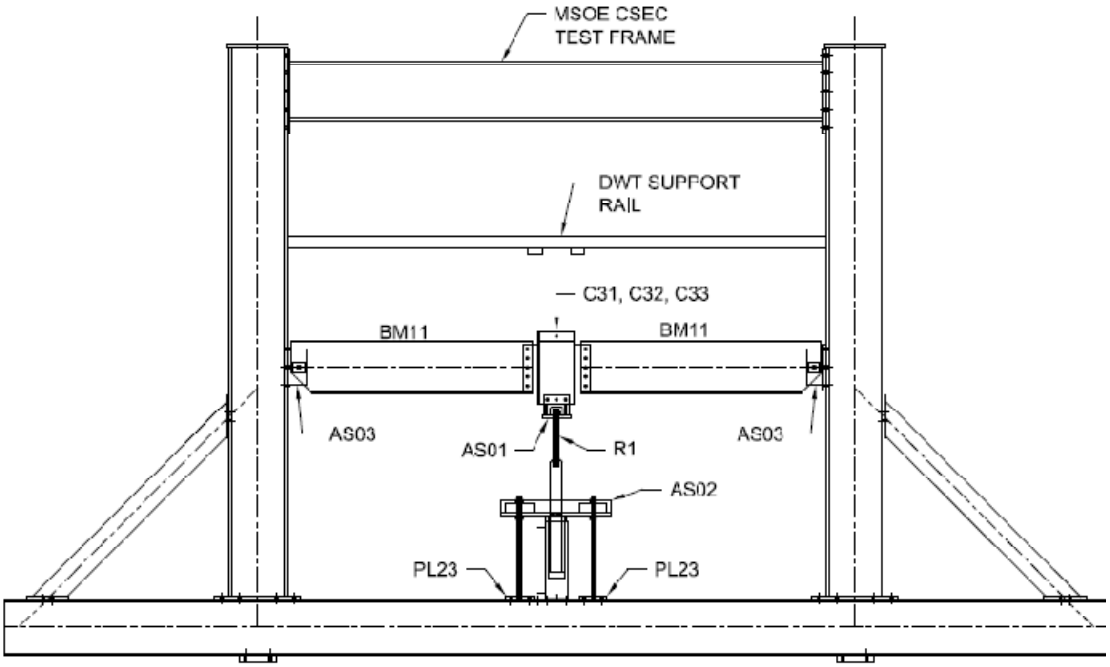

Figure D-1: Test Setup Erection Drawing.

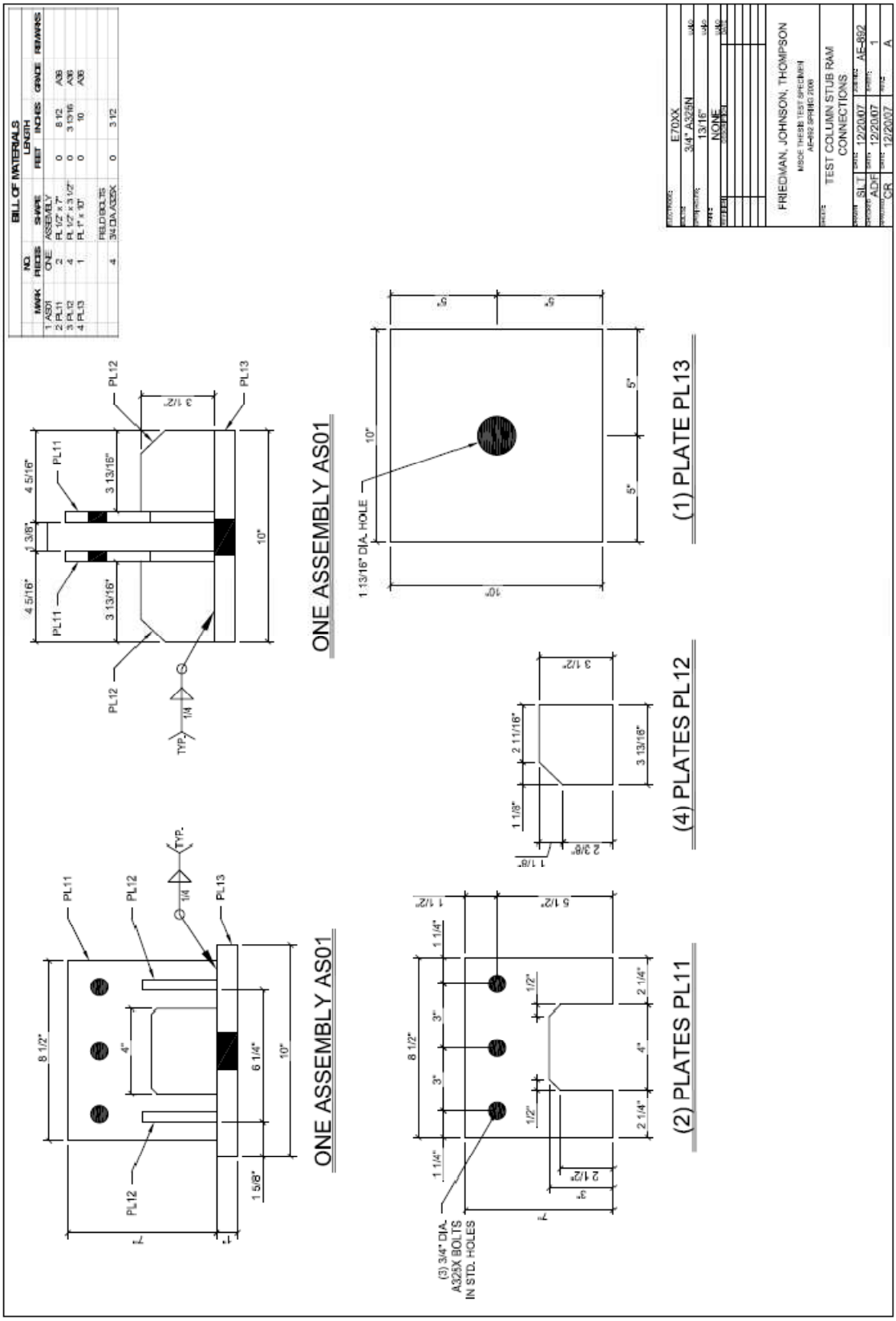
BILL OF MATERIALS
MARK
NO. PIECES
SHAPE
LENGTH FEET
LENGTH INCHES
GRADE
REMARKS
1 AS01 ONE ASSEMBLY
2 PL11 2 PL 1/2" x 7" 0 8 1/2 A36
3 PL12 4 PL 1/2" x 3 1/2" 0 3 13/16 A36
4 PL13 1 PL 1" x 10" 0 10 A36
FIELD BOLTS
4 3/4 DIA A325X 0 3 1/2
E70XX
3/4" A325N
13/16"
NONE
FRIEDMAN, JOHNSON, THOMPSON
MSCE THESIS TEST SPECIMEN
AE-892 SPRING 2008
TEST COLUMN STUB RAM CONNECTIONS
SLT 12/20/07
ADF 12/20/07
CR 12/20/07
AE-892
1
A
PL11
PL12
PL13
4 5/16"
1 3/8"
3 13/16"
3 1/2"
10"
TYP.
1/4
ONE ASSEMBLY AS01
8 1/2"
4"
6 1/4"
1 5/8"
(1) PLATE PL13
1 13/16" DIA. HOLE
5"
(4) PLATES PL12
2 11/16"
1 1/8"
2 3/8"
(2) PLATES PL11
1 1/4"
3"
1/2"
2 1/4"
5 1/2"
2 1/2"
(3) 3/4" DIA. A325X BOLTS IN STD. HOLES

ONE ASSEMBLY AS02

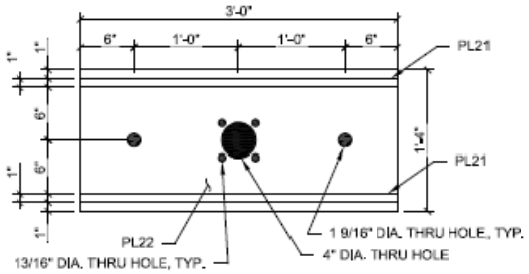

ONE ASSEMBLY AS02

BILL OF MATERIALS							
	MARK	NO. PIECES	SHAPE	LENGTH FEET	LENGTH INCHES	GRADE	REMARKS
1	AS02	ONE	ASSEMBLY				
2	PL21	2	PL 1" x 4'	3	0	A36	
3	PL22	1	PL 1" x 1'-4"	3	0	A36	
4							
5	PL23	2	PL 1" x 8 1/2"	0	9	A36	
6	R1	1	1 3/4" DIA - 12	1	6	A572	Fy = 60ksi Fu = 75ksi
8			FIELD BOLTS				
9		8	3/4 DIA A325N	0	3		HD WASH
10		4	3/4 DIA A325N	0	2		HD WASH

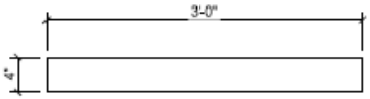

(2) PLATES PL21

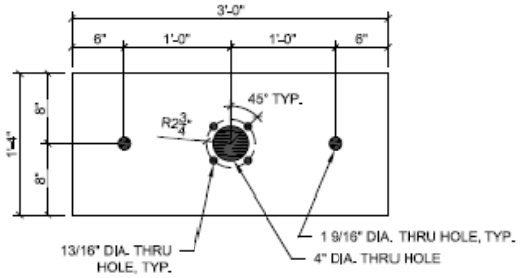

(1) PLATE PL22

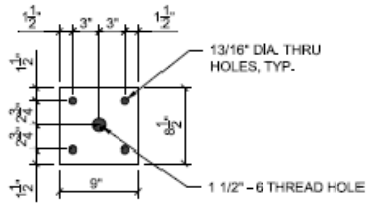

(2) PLATES PL23

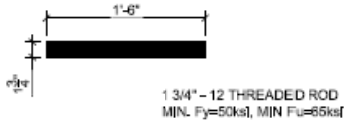

(1) ROD R1

ELECTRODE:	E70XX
BOLTS:	3/4" A325N
SPACING ROUTE:	13/16"
PLATE:	NONE
REVISIONS	DESCRIPTION / DATE

FRIEDMAN, JOHNSON, THOMPSON

MSOE THESIS TEST SPECIMEN
AE-892 SPRING 2008

TEST RAM CONNECTION

DRAWN	SLT	DATE 12/20/07	JOB NO. AE-892
CHECKED	ADF	DATE 12/20/07	SHEET NO. 2
APPROVED	CR	DATE 12/20/07	REV. A

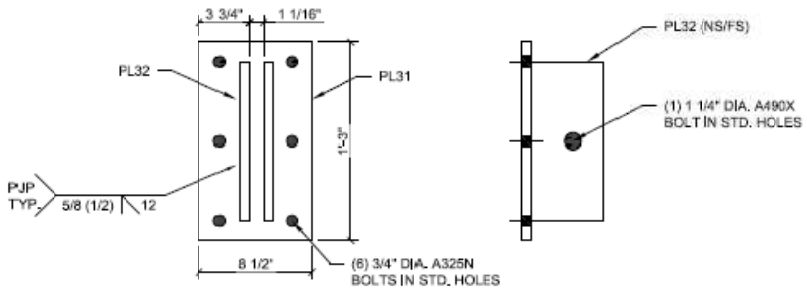

(2) ASSEMBLIES AS03

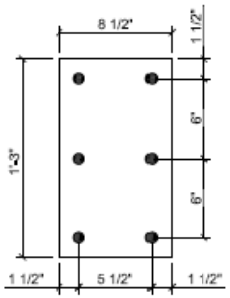

(2) PLATES PL31

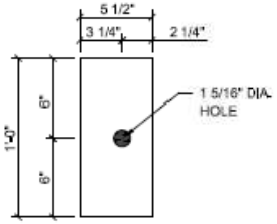

(4) PLATES PL32

BILL OF MATERIALS

	MARK	NO. PIECES	SHAPE	LENGTH FEET	LENGTH INCHES	GRADE	REMARKS
1	AS03	TWO	ASSEMBLY				
2	PL31	2	PL 3/4" x 8 1/2"	1	3	A36	
3	PL32	4	PL 3/4" x 5 1/2"	1	0	A36	
4							
5			FIELD BOLTS				
6		12	3/4 DIA A325N	0	3		

ELECTRODES	E70XX
BOLTS	3/4" A325N
SPACERS	13/16"
PLATES	NONE

FRIEDMAN, JOHNSON, THOMPSON

MSCE THESIS TEST SPECIMEN
AE-892 SPRING 2008

TEST ASSEMBLY
TRUE PIN CONNECTION

DRAWN	SLT	DATE 12/20/07	JOB NO. AE-892
CHECKED	ADF	DATE 12/20/07	SHEET 3
APPROVED	CR	DATE 12/20/07	REV'S A

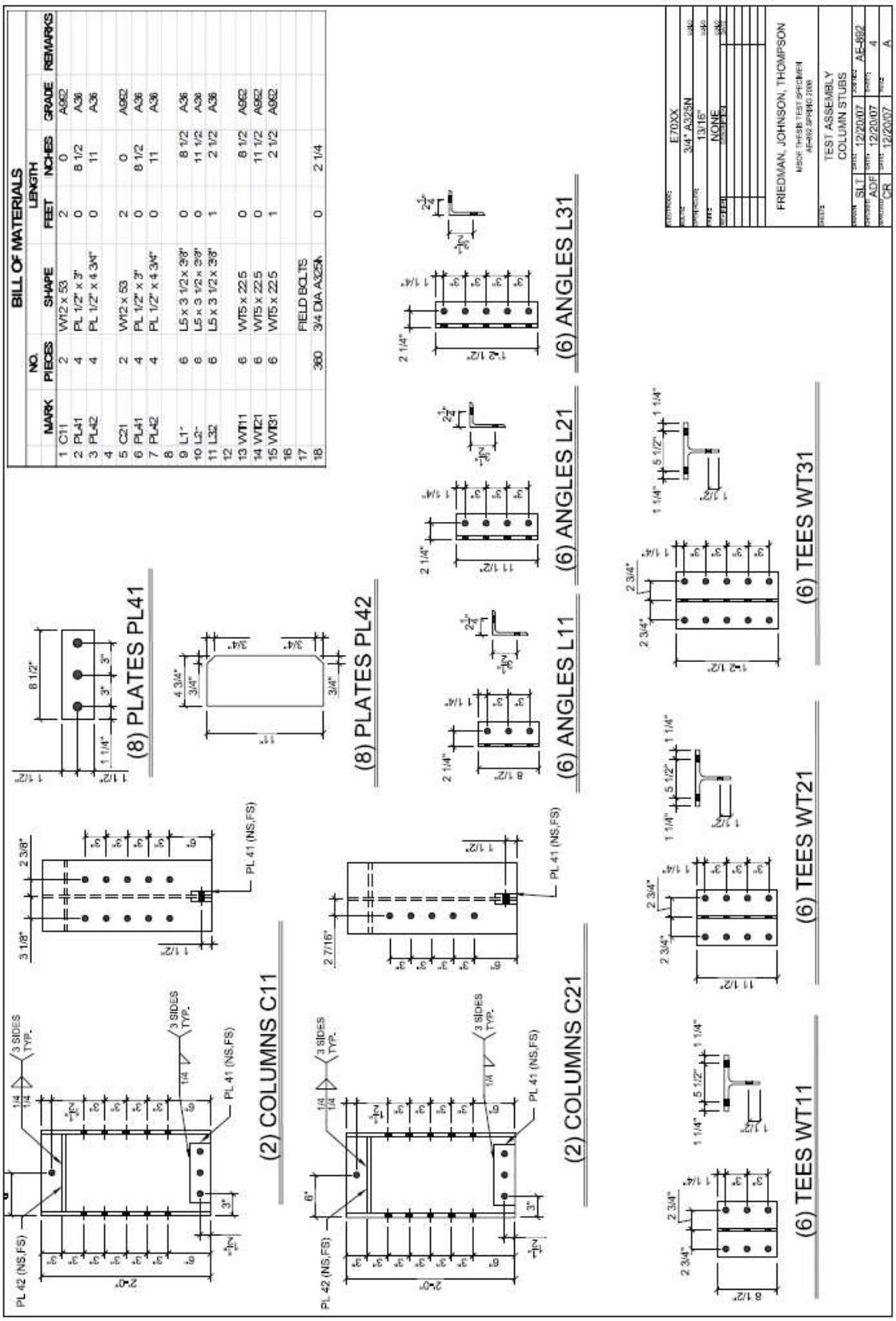
BILL OF MATERIALS
NO. LENGTH
MARK PIECES SHAPE FEET INCHES GRADE REMARKS
1 C11 2 W12 x 53 2 0 A992
2 PL41 4 PL 1/2" x 3" 0 8 1/2 A36
3 PL42 4 PL 1/2" x 4 3/4" 0 11 A36
5 C21 2 W12 x 53 2 0 A992
6 PL41 4 PL 1/2" x 3" 0 8 1/2 A36
7 PL42 4 PL 1/2" x 4 3/4" 0 11 A36
9 L1" 6 L5 x 3 1/2 x 3/8" 0 8 1/2 A36
10 L2" 6 L5 x 3 1/2 x 3/8" 0 11 1/2 A36
11 L32 6 L5 x 3 1/2 x 3/8" 1 2 1/2 A36
13 WT11 6 WT5 x 22.5 0 8 1/2 A992
14 WT21 6 WT5 x 22.5 0 11 1/2 A992
15 WT31 6 WT5 x 22.5 1 2 1/2 A992
17 FIELD BOLTS
18 360 3/4 DIA A325N 0 2 1/4
(8) PLATES PL41
(8) PLATES PL42
(2) COLUMNS C11
(2) COLUMNS C21
(6) ANGLES L11
(6) ANGLES L21
(6) ANGLES L31
(6) TEES WT11
(6) TEES WT21
(6) TEES WT31
PL 42 (NS,FS)
PL 41 (NS,FS)
3 SIDES TYP.
E70XX
3/4" A325N
13/16"
NONE
FRIEDMAN, JOHNSON, THOMPSON
TEST ASSEMBLY
COLUMN STUBS
SLT 12/20/07
ADF 12/20/07
CR 12/20/07
AE-892
4
A

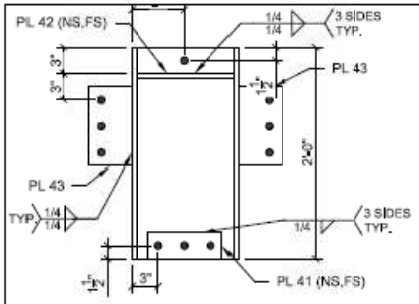

(3) COLUMNS C31

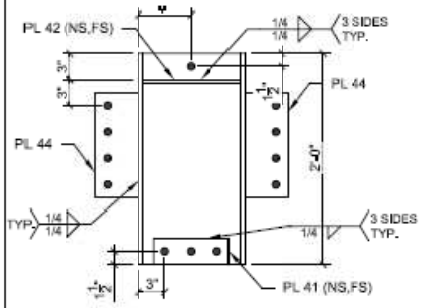

(3) COLUMNS C32

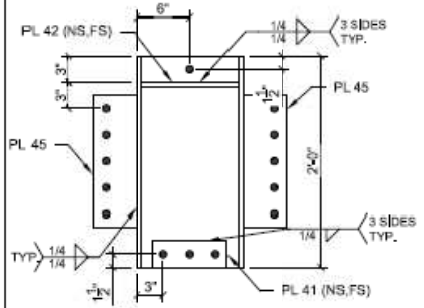

(3) COLUMNS C33

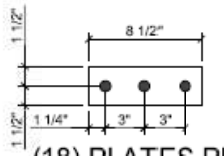

(18) PLATES PL41

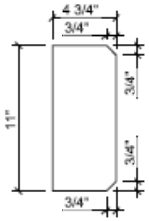

(18) PLATES PL42

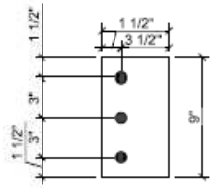

(6) PLATES PL43

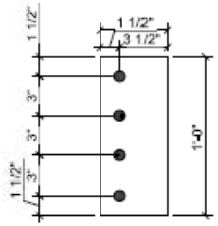

(6) PLATES PL44

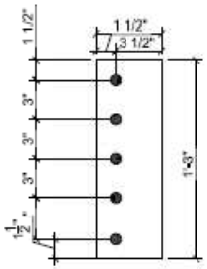

(6) PLATES PL45

BILL OF MATERIALS

	MARK	NO. PIECES	SHAPE	LENGTH FEET	LENGTH INCHES	GRADE	REMARKS
1	C31	3	W12 x 53	2	0	A992	
2	PL41	6	PL 1/2" x 3"	0	8 1/2	A36	
3	PL42	6	PL 1/2" x 4 3/4"	0	11	A36	
4	PL43	6	PL 3/8" x 5"	0	9	A36	
5							
6	C32	3	W12 x 53	2	0	A992	
7	PL41	6	PL 1/2" x 3"	0	8 1/2	A36	
8	PL42	6	PL 1/2" x 4 3/4"	0	11	A36	
9	PL44	6	PL 3/8" x 5"	1	0	A36	
10							
11	C32	3	W12 x 53	2	0	A992	
12	PL41	6	PL 1/2" x 3"	0	8 1/2	A36	
13	PL42	6	PL 1/2" x 4 3/4"	0	11	A36	
14	PL45	6	PL 3/8" x 5"	1	3	A36	
15							
16		72	3/4 DIA A325N	0	2 1/4		

ELECTRODE:	E70XX
BOLTS:	3/4" A325N
SPECIAL HOLES:	13/16"
PAINT:	NONE
WELDED BY:	

FRIEDMAN, JOHNSON, THOMPSON

MSCE THESIS TEST SPECIMEN
AE-892 SPRING 2008

TEST ASSEMBLY
COLUMN STUBS

DRAWN: SLT	DATE: 12/20/07	JOB NO.: AE-892	
CHECKED: ADF	DATE: 12/20/07	SHEET: 5	
APPROVED: CR	DATE: 12/20/07	REV: A	

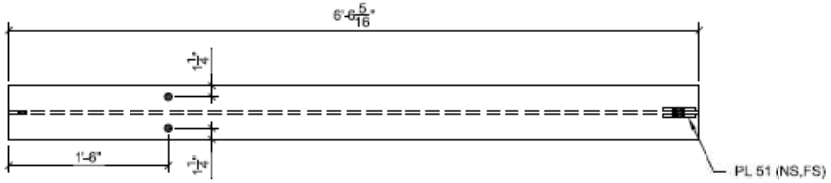

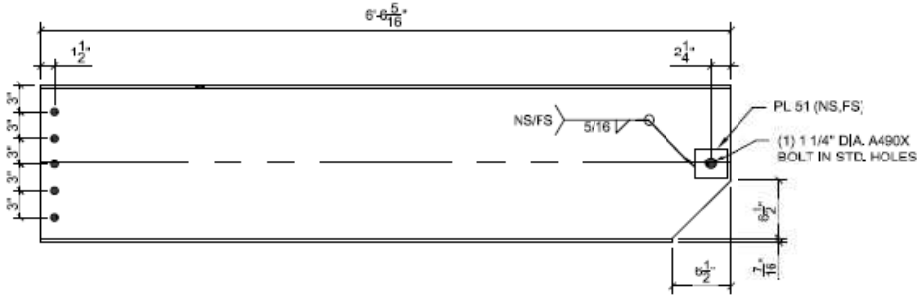

(2) BEAMS BM11

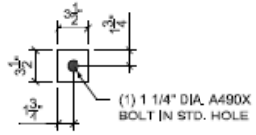

(4) PLATES PL51

BILL OF MATERIALS

	MARK	NO. PIECES	SHAPE	LENGTH FEET	LENGTH INCHES	GRADE	REMARKS
1	B11	2	W18 x 35	6	6 5/16	A992	
2							
3	PL51	4	PL 3/8" x 3 1/2"	0	3 1/2	A36	
4							
5			FIELD BOLTS				
6		2	1 1/4 DIA A490X	0	3		

ELECTRODES	E70XX
BOLTS	3/4" A325N
PLATE THICKNESS	13/16"
PAINT	NONE

FRIEDMAN, JOHNSON, THOMPSON

MSE THESIS TEST SPECIMEN
AE-892 SPRING 2008

TEST ASSEMBLY
BEAM ASSEMBLY

DRAWN	SLT	DATE 12/20/07	JOB NO. AE-892
CHECKED	ALH	DATE 12/20/07	SHEET NO. 5
APPROVED	CR	DATE 12/20/07	REV. A

Appendix E

Bolt Force Development

The following provides the Instantaneous Center of Rotation (ICOR) bolt force analysis conducted for the experimental tests. The ICOR method was implemented for two cases of applied moments about the bolt group of each connection including the measured moment and the eccentrically applied shear load. The data collected at the tested specimens' approximate maximum moment were used for the analysis. The ICOR analysis was conducted as described per the *AISC 13TH Edition Specification.*[1]

[1] American Institute of Steel Construction (AISC). 2005. *Manual of Steel Construction 13th Edition*. Chicago, IL.

ICOR BOLT SHEAR STRENGTH ANALYSIS

Test: **3ST1**

Specimen: **3STR1**

Bolt Location w/r to Neutral Axis of Beam			
Bolt	Location	Bolt	Location
# of Bolts	3.0	3	-3.0
1	3.0	4	-
2	0.0	5	-

Collected Data At Maximum			
V_{app} (Kips)	M_M (Kip-Inch)	P_M (Kips)	θ (Radians)
2.623	157.364	8.453	0.072

Maximum Bolt Forces - Ultimate Method				
Bolt 1	Bolt 2	Bolt 3	Bolt 4	Bolt 5
25.01	3.05	30.67	-	-

Bolt Force Summary For I.C.O.R for Moment only Case Normalized to Primary Axis Due to Beam										Bolt Force Summary For I.C.O.R for Shear Only										Axial Force Per	
Bolt 1		Bolt 2		Bolt 3		Bolt 4		Bolt 5		Bolt 1		Bolt 2		Bolt 3		Bolt 4		Bolt 5		Axial	Axial Shear
$H_{mx,1}$	$H_{my,1}$	$H_{mx,2}$	$H_{my,2}$	$H_{mx,3}$	$H_{my,3}$	$H_{mx,4}$	$H_{my,4}$	$H_{mx,5}$	$H_{my,5}$	$V_{mx,1}$	$V_{my,1}$	$V_{mx,2}$	$V_{my,2}$	$V_{mx,3}$	$V_{my,3}$	$V_{mx,4}$	$V_{my,4}$	$V_{mx,5}$	$V_{my,5}$	P_x	P_y
-26.24	-1.90	0.00	0.00	26.24	1.90	0.00	0.00	0.00	0.00	-1.53	0.61	0.00	1.40	1.53	0.61	0.00	0.00	0.00	0.00	2.81	-0.20

Measured Moment Analysis

rox = 0.002 roy = 0.000 ro = 0.002

Row	Column	Bolt (y,n)	xcg	xi	ycg	yi	di	Di	Ri	Fy Ri * xi / di	M R di	Fx Ri * yi / d	Sign Multiplier	Fx kip	Fy kip
1	1	1	0.00	-0.002	3.00	3.000	3.000	0.340	0.982	-0.001	2.945	-0.982	-1	-26.31	0.02
2	1	1	0.00	-0.002	0.00	0.000	0.002	0.000	0.036	-0.036	0.000	0.000	-1	0.00	0.96
3	1	1	0.00	-0.002	-3.00	-3.000	3.000	0.340	0.982	-0.001	2.945	0.982	-1	26.31	0.02
4	1	0	0.00	0.000	0.00	0.000	0.000	0.000	0.000	0.000	0.000	0.000	0	0.00	0.00
5	1	0	0.00	0.000	0.00	0.000	0.000	0.000	0.000	0.000	0.000	0.000	0	0.00	0.00
						d max =	3.0000	S	2.00	-0.04	5.89	0.00		0.00	1.00

Measured Moment ICOR		
e (in)	Vnorm (kips)	Rotation (radians)
157.36	1.00	0.07

Total deformation on a bolt D max 0.34 n
Distance to I.C.O.R. ro 0.002 n
Eccentricity ex 157.36 n
e 157.36 n
Coefficient C 0.037

sqrt[Fx^2 + Fy^2] = 0.0373
M/(e + ro) = 0.0374
C = 0.0374
-0.0001

Bolt Forces Due to Measured Moment Normalised for Beam Rotation

Bolt 1		Bolt 2		Bolt 3		Bolt 4		Bolt 5	
$H_{mx,1}$	$H_{my,1}$	$H_{mx,2}$	$H_{my,2}$	$H_{mx,3}$	$H_{my,3}$	$H_{mx,4}$	$H_{my,4}$	$H_{mx,5}$	$H_{my,5}$
-26.2437	-1.9017	0.0000	0.0000	26.2437	1.9017	0.0000	0.0000	0.0000	0.0000

Applied Shear Analysis

rox = 1.200 roy = 0.000 ro = 1.200

Row	Column	Bolt (y,n)	xcg	xi	ycg	yi	di	Di	Ri	Fy Ri * xi / di	M R di	Fx Ri * yi / d	Sign Multiplier	Fx kip	Fy kip
1	1	1	0.00	-1.200	3.00	3.000	3.231	0.340	0.982	-0.365	3.171	-0.911	-1	-1.53	0.61
2	1	1	0.00	-1.200	0.00	0.000	1.200	0.126	0.833	-0.833	1.000	0.000	-1	0.00	1.40
3	1	1	0.00	1.200	3.00	3.000	3.231	0.340	0.982	0.365	3.171	0.911	1	1.53	0.61
4	1	0	0.00	0.000	0.00	0.000	0.000	0.000	0.000	0.000	0.000	0.000	0	0.00	0.00
5	1	0	0.00	0.000	0.00	0.000	0.000	0.000	0.000	0.000	0.000	0.000	0	0.00	0.00
						d max =	3.2312	S	2.80	-1.56	7.34	0.00		0.00	2.62

Eccentric Shear ICOR		
e (in)	Vapp (kips)	Rotation (radians)
3.50	2.62	0.07

Total deformation on a bolt D max 0.34 n
Distance to I.C.O.R. ro 1.200 n
Eccentricity ex 3.50 n
e 3.50 n
Coefficient C 1.562

sqrt[Fx^2 + Fy^2] = 1.5621
M/(e + ro) = 1.5622
C = 1.5622
0.0000

Bolt Forces Due to Eccenctric Shear Normalised for Beam Rotation

Bolt 1		Bolt 2		Bolt 3		Bolt 4		Bolt 5	
$V_{mx,1}$	$V_{my,1}$	$V_{mx,2}$	$V_{my,2}$	$V_{mx,3}$	$V_{my,3}$	$V_{mx,4}$	$V_{my,4}$	$V_{mx,5}$	$V_{my,5}$
-1.5302	0.6122	0.0000	1.3986	1.5302	0.6122	0.0000	0.0000	0.0000	0.0000

ICOR BOLT SHEAR STRENGTH ANALYSIS

Test: **3ST1**

Specimen: **3STL1**

Bolt Location w/r to Neutral Axis of Beam			
Bolt	Location	Bolt	Location
# of Bolts	3.0	3	-3.0
1	3.0	4	-
2	0.0	5	-

Collected Data At Maximum			
V_{app} (Kips)	M_M (Kip-inch)	P_M (Kips)	θ (Radians)
2.623	144.682	8.077	0.073

Maximum Bolt Forces - Ultimate Method				
Bolt 1	Bolt 2	Bolt 3	Bolt 4	Bolt 5
23.08	2.94	28.50	-	-

Bolt Force Summary For I.C.O.R for Moment only Case Normalized to Primary Axis Due to Beam End										Bolt Force Summary For I.C.O.R for Shear Only										Axial Force Per	
Bolt 1		Bolt 2		Bolt 3		Bolt 4		Bolt 5		Bolt 1		Bolt 2		Bolt 3		Bolt 4		Bolt 5		Axial	Axial Shear
$H_{mx,1}$	$H_{my,1}$	$H_{mx,2}$	$H_{my,2}$	$H_{mx,3}$	$H_{my,3}$	$H_{mx,4}$	$H_{my,4}$	$H_{mx,5}$	$H_{my,5}$	$V_{mx,1}$	$V_{my,1}$	$V_{mx,2}$	$V_{my,2}$	$V_{mx,3}$	$V_{my,3}$	$V_{mx,4}$	$V_{my,4}$	$V_{mx,5}$	$V_{my,5}$	P_x	P_y
-24.20	-1.77	0.00	0.00	24.20	1.77	0.00	0.00	0.00	0.00	-1.53	0.61	0.00	1.40	1.53	0.61	0.00	0.00	0.00	0.00	2.69	-0.20

Measured Moment Analysis

rox = 0.002 roy = 0.000 ro = 0.002

Row	Column	bolt (y,n)	xcg	xi	ycg	yi	di	Di	Ri	Fy Ri * xi / di	M Ri di	Fx Ri * yi / di	Sign Multiplier	Fx kip	Fy kip
1	1	1	0.00	-0.002	3.00	3.000	3.000	0.340	0.982	-0.001	2.945	-0.982	-1	-24.26	0.02
2	1	1	0.00	-0.002	0.00	0.000	0.002	0.000	0.039	-0.039	0.000	0.000	-1	0.00	0.96
3	1	1	0.00	-0.002	-3.00	-3.000	3.000	0.340	0.982	-0.001	2.945	0.982	-1	24.26	0.02
4	1	0	0.00	0.000	0.00	0.000	0.000	0.000	0.000	0.000	0.000	0.000	0	0.00	0.00
5	1	0	0.00	0.000	0.00	0.000	0.000	0.000	0.000	0.000	0.000	0.000	0	0.00	0.00
						d max =	3.0000	S	2.00	-0.04	5.89	0.00		0.00	1.00

Measured Moment ICOR		
e (in)	Vnorm (kips)	Rotation (radians)
144.68	1.00	0.07

Total deformation on a bolt	D max	0.34	in
Distance to I.C.O.R.	ro	0.002	in
Eccentricity	ex	144.68	in
	e	144.68	in
Coefficient	C	0.041	

sqrt[Fx^2 + Fy^2] = 0.0405
M/(e + ro) = 0.0407
C = 0.0407
-0.0002

Bolt Forces Due to Measured Moment Normalised for Beam Rotation									
Bolt 1		Bolt 2		Bolt 3		Bolt 4		Bolt 5	
$H_{mx,1}$	$H_{my,1}$	$H_{mx,2}$	$H_{my,2}$	$H_{mx,3}$	$H_{my,3}$	$H_{mx,4}$	$H_{my,4}$	$H_{mx,5}$	$H_{my,5}$
-24.1978	-1.7653	0.0000	0.0000	24.1978	1.7653	0.0000	0.0000	0.0000	0.0000

Applied Shear Analysis

rox = 1.200 roy = 0.000 ro = 1.200

Row	Column	bolt (y,n)	xcg	xi	ycg	yi	di	Di	Ri	Fy Ri * xi / di	M Ri di	Fx Ri * yi / di	Sign Multiplier	Fx kip	Fy kip
1	1	1	0.00	-1.200	3.00	3.000	3.231	0.340	0.982	-0.365	3.171	-0.911	-1	-1.53	0.61
2	1	1	0.00	-1.200	0.00	0.000	1.200	0.126	0.833	-0.833	1.000	0.000	-1	0.00	1.40
3	1	1	0.00	-1.200	-3.00	-3.000	3.231	0.340	0.982	-0.365	3.171	0.911	-1	1.53	0.61
4	1	0	0.00	0.000	0.00	0.000	0.000	0.000	0.000	0.000	0.000	0.000	0	0.00	0.00
5	1	0	0.00	0.000	0.00	0.000	0.000	0.000	0.000	0.000	0.000	0.000	0	0.00	0.00
						d max =	3.2312	S	2.80	-1.56	7.34	0.00		0.00	2.62

Eccentric Shear ICOR		
e (in)	Vapp (kips)	Rotation (radians)
3.50	2.62	0.07

Total deformation on a bolt	D max	0.34	in
Distance to I.C.O.R.	ro	1.200	in
Eccentricity	ex	3.50	in
	e	3.50	in
Coefficient	C	1.562	

sqrt[Fx^2 + Fy^2] = 1.5621
M/(e + ro) = 1.5622
C = 1.5622
0.0000

Bolt Forces Due to Eccentric Shear Normalised for Beam Rotation									
Bolt 1		Bolt 2		Bolt 3		Bolt 4		Bolt 5	
$V_{mx,1}$	$V_{my,1}$	$V_{mx,2}$	$V_{my,2}$	$V_{mx,3}$	$V_{my,3}$	$V_{mx,4}$	$V_{my,4}$	$V_{mx,5}$	$V_{my,5}$
-1.5302	0.6122	0.0000	1.3986	1.5302	0.6122	0.0000	0.0000	0.0000	0.0000

ICOR BOLT SHEAR STRENGTH ANALYSIS

Test: **3ST2**

Specimen: **3STR2**

Bolt Location w/r to Neutral Axis of Beam			
Bolt	Location	Bolt	Location
# of Bolts	3.0	*3*	-3.0
1	3.0	*4*	-
2	0.0	*5*	-

Collected Data At Maximum			
V_{app} (Kips)	M_M (Kip-Inch)	P_M (Kips)	θ (Radians)
2.876	169.096	6.051	0.097

Maximum Bolt Forces - Ultimate Method				
Bolt 1	Bolt 2	Bolt 3	Bolt 4	Bolt 5
28.55	2.41	32.64	-	-

Bolt Force Summary For I.C.O.R for Moment only Case Normalized to Primary Axis Due to Beam End										Bolt Force Summary For I.C.O.R for Shear Only										Axial Force Per	
Bolt 1		Bolt 2		Bolt 3		Bolt 4		Bolt 5		Bolt 1		Bolt 2		Bolt 3		Bolt 4		Bolt 5		Axial	Axial Shear
$H_{mx,1}$	$H_{my,1}$	$H_{mx,2}$	$H_{my,2}$	$H_{mx,3}$	$H_{my,3}$	$H_{mx,4}$	$H_{my,4}$	$H_{mx,5}$	$H_{my,5}$	$V_{mx,1}$	$V_{my,1}$	$V_{mx,2}$	$V_{my,2}$	$V_{mx,3}$	$V_{my,3}$	$V_{mx,4}$	$V_{my,4}$	$V_{mx,5}$	$V_{my,5}$	P_x	P_y
-28.79	-2.80	0.00	0.00	28.79	2.80	0.00	0.00	0.00	0.00	-1.68	0.67	0.00	1.53	1.68	0.67	0.00	0.00	0.00	0.00	2.01	-0.20

Measured Moment Analysis

rox = 0.002 roy = 0.000 ro = 0.002

Row	Column	bolt (y,n)	xcg	xi	ycg	yi	di	Di	Ri	Fi * xi / di	Ri di	Fi * yi / di	Sign Multiplier	Fx kip	Fy kip
1	1	1	0.00	-0.002	3.00	3.000	3.000	0.340	0.982	-0.001	2.945	-0.982	-1	-28.92	0.02
2	1	1	0.00	-0.002	0.00	0.000	0.002	0.000	0.033	-0.033	0.000	0.000	-1	0.00	0.97
3	1	1	0.00	-0.002	-3.00	-3.000	3.000	0.340	0.982	-0.001	2.945	0.982	-1	28.92	0.02
4	1	0	0.00	0.000	0.00	0.000	0.000	0.000	0.000	0.000	0.000	0.000	0	0.00	0.00
5	1	0	0.00	0.000	0.00	0.000	0.000	0.000	0.000	0.000	0.000	0.000	0	0.00	0.00
						d max =	3.0000	S	2.00	-0.03	5.89	0.00		0.00	1.00

Measured Moment ICOR		
e (in)	Vnorm (kips)	Rotation (radians)
169.10	1.00	0.10

Total deformation on a bolt D max 0.34 in
Distance to I.C.O.R. ro 0.002 in
Eccentricity ex 169.10 in
e 169.10 in
Coefficient C 0.035

sqrt[Fx^2 + Fy^2] = 0.0339
M/(e + ro) = 0.0348
C = 0.0348
-0.0009

Bolt Forces Due to Measured Moment Normalised for Beam Rotation

Bolt 1		Bolt 2		Bolt 3		Bolt 4		Bolt 5	
$H_{mx,1}$	$H_{my,1}$	$H_{mx,2}$	$H_{my,2}$	$H_{mx,3}$	$H_{my,3}$	$H_{mx,4}$	$H_{my,4}$	$H_{mx,5}$	$H_{my,5}$
-28.7855	-2.8017	0.0000	0.0000	28.7855	2.8017	0.0000	0.0000	0.0000	0.0000

Applied Shear Analysis

rox = 1.200 roy = 0.000 ro = 1.200

Row	Column	bolt (y,n)	xcg	xi	ycg	yi	di	Di	Ri	Fi * xi / di	Ri di	Fi * yi / di	Sign Multiplier	Fx kip	Fy kip
1	1	1	0.00	-1.200	3.00	3.000	3.231	0.340	0.982	-0.365	3.171	-0.911	-1	-1.68	0.67
2	1	1	0.00	-1.200	0.00	0.000	1.200	0.126	0.833	-0.833	1.000	0.000	-1	0.00	1.53
3	1	1	0.00	-1.200	-3.00	-3.000	3.231	0.340	0.982	-0.365	3.171	0.911	-1	1.68	0.67
4	1	0	0.00	0.000	0.00	0.000	0.000	0.000	0.000	0.000	0.000	0.000	0	0.00	0.00
5	1	0	0.00	0.000	0.00	0.000	0.000	0.000	0.000	0.000	0.000	0.000	0	0.00	0.00
						d max =	3.2312	S	2.80	-1.56	7.34	0.00		0.00	2.88

Eccentric Shear ICOR		
e (in)	Vapp (kips)	Rotation (radians)
3.50	2.88	0.10

Total deformation on a bolt D max 0.34 in
Distance to I.C.O.R. ro 1.200 in
Eccentricity ex 3.50 in
e 3.50 in
Coefficient C 1.562

sqrt[Fx^2 + Fy^2] = 1.5621
M/(e + ro) = 1.5622
C = 1.5622
0.0000

Bolt Forces Due to Eccenctric Shear Normalised for Beam Rotation

Bolt 1		Bolt 2		Bolt 3		Bolt 4		Bolt 5	
$V_{mx,1}$	$V_{my,1}$	$V_{mx,2}$	$V_{my,2}$	$V_{mx,3}$	$V_{my,3}$	$V_{mx,4}$	$V_{my,4}$	$V_{mx,5}$	$V_{my,5}$
-1.6774	0.6712	0.0000	1.5332	1.6774	0.6712	0.0000	0.0000	0.0000	0.0000

ICOR BOLT SHEAR STRENGTH ANALYSIS

Test: **3ST2**

Specimen: **3STL2**

Bolt Location w/r to Neutral Axis of Beam			
Bolt	Location	Bolt	Location
# of Bolts	3.0	*3*	-3.0
1	3.0	*4*	-
2	0.0	*5*	-

Collected Data At Maximum			
V_{app} (Kips)	M_M (Kip-Inch)	P_M (Kips)	θ (Radians)
2.876	182.702	5.537	0.097

Maximum Bolt Forces - Ultimate Method				
Bolt 1	Bolt 2	Bolt 3	Bolt 4	Bolt 5
30.63	2.28	34.38	-	-

Bolt Force Summary For I.C.O.R for Moment only Case Normalized to Primary Axis Due to Beam End										Bolt Force Summary For I.C.O.R for Shear Only										Axial Force Per	
Bolt 1		Bolt 2		Bolt 3		Bolt 4		Bolt 5		Bolt 1		Bolt 2		Bolt 3		Bolt 4		Bolt 5		Axial	Axial Shear
$H_{mx,1}$	$H_{my,1}$	$H_{mx,2}$	$H_{my,2}$	$H_{mx,3}$	$H_{my,3}$	$H_{mx,4}$	$H_{my,4}$	$H_{mx,5}$	$H_{my,5}$	$V_{mx,1}$	$V_{my,1}$	$V_{mx,2}$	$V_{my,2}$	$V_{mx,3}$	$V_{my,3}$	$V_{mx,4}$	$V_{my,4}$	$V_{mx,5}$	$V_{my,5}$	P_x	P_y
-30.69	-2.98	0.00	0.00	30.69	2.98	0.00	0.00	0.00	0.00	-1.68	0.67	0.00	1.53	1.68	0.67	0.00	0.00	0.00	0.00	1.84	-0.18

Measured Moment Analysis

rox = 0.002 roy = 0.000 ro = 0.002

Row	Column	bolt (y,n)	xcg	xi	ycg	yi	di	Di	Ri	Fy Ri * xi / di	M Ri di	Fx Ri * yi / di	Sign Multiplier	Fx kip	Fy kip
1	1	1	0.00	-0.002	3.00	3.000	3.000	0.340	0.982	-0.001	2.945	-0.982	-1	-30.84	0.02
2	1	1	0.00	-0.002	0.00	0.000	0.002	0.000	0.031	-0.031	0.000	0.000	-1	0.00	0.97
3	1	1	0.00	-0.002	-3.00	-3.000	3.000	0.340	0.982	-0.001	2.945	0.982	-1	30.84	0.02
4	1	0	0.00	0.000	0.00	0.000	0.000	0.000	0.000	0.000	0.000	0.000	0	0.00	0.00
5	1	0	0.00	0.000	0.00	0.000	0.000	0.000	0.000	0.000	0.000	0.000	0	0.00	0.00
						d max =	3.0000	S	1.99	-0.03	5.89	0.00		0.00	1.00

Measured Moment ICOR		
e (in)	Vnorm (kips)	Rotation (radians)
182.70	1.00	0.10

Total deformation on a bolt D max 0.34 in
Distance to I.C.O.R. ro 0.002 in
Eccentricity ex 182.70 in
e 182.70 in
Coefficient C 0.032

sqrt[Fx^2 + Fy^2] = 0.0318
M/(e + ro) = 0.0322
C = 0.0322
-0.0004

Bolt Forces Due to Measured Moment Normalised for Beam Rotation									
Bolt 1		Bolt 2		Bolt 3		Bolt 4		Bolt 5	
$H_{mx,1}$	$H_{my,1}$	$H_{mx,2}$	$H_{my,2}$	$H_{mx,3}$	$H_{my,3}$	$H_{mx,4}$	$H_{my,4}$	$H_{mx,5}$	$H_{my,5}$
-30.6911	-2.9830	0.0000	0.0000	30.6911	2.9830	0.0000	0.0000	0.0000	0.0000

Applied Shear Analysis

rox = 1.200 roy = 0.000 ro = 1.200

Row	Column	bolt (y,n)	xcg	xi	ycg	yi	di	Di	Ri	Fy Ri * xi / di	M Ri di	Fx Ri * yi / di	Sign Multiplier	Fx kip	Fy kip
1	1	1	0.00	-1.200	3.00	3.000	3.231	0.340	0.982	-0.365	3.171	-0.911	-1	-1.68	0.67
2	1	1	0.00	-1.200	0.00	0.000	1.200	0.126	0.833	-0.833	1.000	0.000	-1	0.00	1.53
3	1	1	0.00	-1.200	-3.00	-3.000	3.231	0.340	0.982	-0.365	3.171	0.911	-1	1.68	0.67
4	1	0	0.00	0.000	0.00	0.000	0.000	0.000	0.000	0.000	0.000	0.000	0	0.00	0.00
5	1	0	0.00	0.000	0.00	0.000	0.000	0.000	0.000	0.000	0.000	0.000	0	0.00	0.00
						d max =	3.2312	S	2.80	-1.56	7.34	0.00		0.00	2.88

Eccentric Shear ICOR		
e (in)	Vapp (kips)	Rotation (radians)
3.50	2.88	0.10

Total deformation on a bolt D max 0.34 in
Distance to I.C.O.R. ro 1.200 in
Eccentricity ex 3.50 in
e 3.50 in
Coefficient C 1.562

sqrt[Fx^2 + Fy^2] = 1.5621
M/(e + ro) = 1.5622
C = 1.5622
0.0000

Bolt Forces Due to Eccenctric Shear Normalised for Beam Rotation									
Bolt 1		Bolt 2		Bolt 3		Bolt 4		Bolt 5	
$V_{mx,1}$	$V_{my,1}$	$V_{mx,2}$	$V_{my,2}$	$V_{mx,3}$	$V_{my,3}$	$V_{mx,4}$	$V_{my,4}$	$V_{mx,5}$	$V_{my,5}$
-1.6774	0.6712	0.0000	1.5332	1.6774	0.6712	0.0000	0.0000	0.0000	0.0000

ICOR BOLT SHEAR STRENGTH ANALYSIS

Test: 3ST3

Specimen: 3STR3

Bolt Location w/r to Neutral Axis of Beam			
Bolt	Location	Bolt	Location
# of Bolts	3.0	3	-3.0
1	3.0	4	-
2	0.0	5	-

Collected Data At Maximum			
V_{app} (Kips)	M_M (Kip-Inch)	P_M (Kips)	θ (Radians)
1.965	169.444	6.607	0.080

Maximum Bolt Forces - Ultimate Method				
Bolt 1	Bolt 2	Bolt 3	Bolt 4	Bolt 5
27.90	2.36	32.32	-	-

Bolt Force Summary For I.C.O.R for Moment only Case Normalized to Primary Axis Due to Beam End										Bolt Force Summary For I.C.O.R for Shear Only										Axial Force Per	
Bolt 1		Bolt 2		Bolt 3		Bolt 4		Bolt 5		Bolt 1		Bolt 2		Bolt 3		Bolt 4		Bolt 5		Axial	Axial Shear
$H_{mx,1}$	$H_{my,1}$	$H_{mx,2}$	$H_{my,2}$	$H_{mx,3}$	$H_{my,3}$	$H_{mx,4}$	$H_{my,4}$	$H_{mx,5}$	$H_{my,5}$	$V_{mx,1}$	$V_{my,1}$	$V_{mx,2}$	$V_{my,2}$	$V_{mx,3}$	$V_{my,3}$	$V_{mx,4}$	$V_{my,4}$	$V_{mx,5}$	$V_{my,5}$	P_x	P_y
-28.88	-2.32	0.00	0.00	28.88	2.32	0.00	0.00	0.00	0.00	-1.15	0.46	0.00	1.05	1.15	0.46	0.00	0.00	0.00	0.00	2.20	-0.18

Measured Moment Analysis

rox = 0.002 roy = 0.000 ro = 0.002

Row	Column	bolt (y,n)	xcg	xi	ycg	yi	di	Di	Ri	Fy Ri * xi / di	M Ri di	Fx Ri * yi / di	Sign Multiplier	Fx kip	Fy kip
1	1	1	0.00	-0.002	3.00	3.000	3.000	0.340	0.982	-0.001	2.946	-0.982	-1	28.87	0.02
2	1	1	0.00	-0.002	0.00	0.000	0.002	0.000	0.033	-0.033	0.000	0.000	-1	0.00	0.97
3	1	1	0.00	-0.002	-3.00	-3.000	3.000	0.340	0.982	-0.001	2.945	0.982	-1	28.87	0.02
4	1	0	0.00	0.000	0.00	0.000	0.000	0.000	0.000	0.000	0.000	0.000	0	0.00	0.00
5	1	0	0.00	0.000	0.00	0.000	0.000	0.000	0.000	0.000	0.000	0.000	0	0.00	0.00
						d max =	3.0000	S	2.00	-0.03	5.89	0.00		0.00	1.00

Measured Moment ICOR		
e (in)	Vnorm (kips)	Rotation (radians)
169.44	1.00	0.08

Total deformation on a bolt D max 0.34 in
Distance to I.C.O.R. ro 0.002 in
Eccentricity ex 169.44 in
e 169.44 in
Coefficient C 0.035

sqrt[Fx^2 + Fv^2] = 0.0339
M/(e + ro) = 0.0348
C = 0.0348
-0.0009

Bolt Forces Due to Measured Moment Normalised for Beam Rotation

Bolt 1		Bolt 2		Bolt 3		Bolt 4		Bolt 5	
$H_{mx,1}$	$H_{my,1}$	$H_{mx,2}$	$H_{my,2}$	$H_{mx,3}$	$H_{my,3}$	$H_{mx,4}$	$H_{my,4}$	$H_{mx,5}$	$H_{my,5}$
-28.8766	-2.3243	0.0000	0.0000	28.8766	2.3243	0.0000	0.0000	0.0000	0.0000

Applied Shear Analysis

rox = 1.200 roy = 0.000 ro = 1.200

Row	Column	bolt (y,n)	xcg	xi	ycg	yi	di	Di	Ri	Fy Ri * xi / di	M Ri di	Fx Ri * yi / di	Sign Multiplier	Fx kip	Fy kip
1	1	1	0.00	-1.200	3.00	3.000	3.231	0.340	0.982	-0.365	3.171	-0.911	-1	-1.15	0.46
2	1	1	0.00	-1.200	0.00	0.000	1.200	0.126	0.833	-0.833	1.000	0.000	-1	0.00	1.05
3	1	1	0.00	-1.200	-3.00	-3.000	3.231	0.340	0.982	-0.365	3.171	0.911	-1	1.15	0.46
4	1	0	0.00	0.000	0.00	0.000	0.000	0.000	0.000	0.000	0.000	0.000	0	0.00	0.00
5	1	0	0.00	0.000	0.00	0.000	0.000	0.000	0.000	0.000	0.000	0.000	0	0.00	0.00
						d max =	3.2312	S	2.80	-1.56	7.34	0.00		0.00	1.97

Eccentric Shear ICOR		
e (in)	Vapp (kips)	Rotation (radians)
3.50	1.97	0.08

Total deformation on a bolt D max 0.34 in
Distance to I.C.O.R. ro 1.200 in
Eccentricity ex 3.50 in
e 3.50 in
Coefficient C 1.562

sqrt[Fx^2 + Fy^2] = 1.5621
M/(e + ro) = 1.5622
C = 1.5622
0.0000

Bolt Forces Due to Eccenctric Shear Normalised for Beam Rotation

Bolt 1		Bolt 2		Bolt 3		Bolt 4		Bolt 5	
$V_{mx,1}$	$V_{my,1}$	$V_{mx,2}$	$V_{my,2}$	$V_{mx,3}$	$V_{my,3}$	$V_{mx,4}$	$V_{my,4}$	$V_{mx,5}$	$V_{my,5}$
-1.1463	0.4586	0.0000	1.0477	1.1463	0.4586	0.0000	0.0000	0.0000	0.0000

ICOR BOLT SHEAR STRENGTH ANALYSIS

Test: 3ST3

Specimen: 3STL3

Bolt Location w/r to Neutral Axis of Beam			
Bolt	Location	Bolt	Location
# of Bolts	3.0	3	-3.0
1	3.0	4	-
2	0.0	5	-

Collected Data At Maximum			
V_{app} (Kips)	M_M (Kip-Inch)	P_M (Kips)	θ (Radians)
1.965	185.023	5.376	0.080

Maximum Bolt Forces - Ultimate Method				
Bolt 1	Bolt 2	Bolt 3	Bolt 4	Bolt 5
30.52	2.00	34.13	-	-

Bolt Force Summary For I.C.O.R for Moment only Case Normalized to Primary Axis Due to Beam End										Bolt Force Summary For I.C.O.R for Shear Only										Axial Force Per	
Bolt 1		Bolt 2		Bolt 3		Bolt 4		Bolt 5		Bolt 1		Bolt 2		Bolt 3		Bolt 4		Bolt 5		Axial	Axial Shear
$H_{mx,1}$	$H_{my,1}$	$H_{mx,2}$	$H_{my,2}$	$H_{mx,3}$	$H_{my,3}$	$H_{mx,4}$	$H_{my,4}$	$H_{mx,5}$	$H_{my,5}$	$V_{mx,1}$	$V_{my,1}$	$V_{mx,2}$	$V_{my,2}$	$V_{mx,3}$	$V_{my,3}$	$V_{mx,4}$	$V_{my,4}$	$V_{mx,5}$	$V_{my,5}$	P_x	P_y
-31.09	-2.51	0.00	0.00	31.09	2.51	0.00	0.00	0.00	0.00	-1.15	0.46	0.00	1.05	1.15	0.46	0.00	0.00	0.00	0.00	1.79	-0.14

Measured Moment Analysis

rox = 0.002 roy = 0.000 ro = 0.002

Row	Column	bolt (y,n)	xcg	xi	ycg	yi	di	Di	Ri	Fy Ri * xi / di	M Ri di	Fx Ri * yi / di	Sign Multiplier	Fx kip	Fy kip
1	1	1	0.00	-0.002	3.00	3.000	3.000	0.340	0.982	-0.001	2.945	-0.982	-1	-31.19	0.02
2	1	1	0.00	-0.002	0.00	0.000	0.002	0.000	0.030	-0.030	0.000	0.000	-1	0.00	0.97
3	1	1	0.00	-0.002	-3.00	-3.000	3.000	0.340	0.982	0.001	2.945	0.982	1	31.19	0.02
4	1	0	0.00	0.000	0.00	0.000	0.000	0.000	0.000	0.000	0.000	0.000	0	0.00	0.00
5	1	0	0.00	0.000	0.00	0.000	0.000	0.000	0.000	0.000	0.000	0.000	0	0.00	0.00
						d max =	3.0000	S	1.99	-0.03	5.89	0.00		0.00	1.00

Measured Moment ICOR		
e (in)	Vnorm (kips)	Rotation (radians)
185.02	1.00	0.08

Total deformation on a bolt	D max	0.34	in
Distance to I.C.O.R.	ro	0.002	in
Eccentricity	ex	185.02	in
	e	185.02	in
Coefficient	C	0.082	

sqrt[Fx^2 + Fy^2] =	0.0315
M/(e + ro) =	0.0318
C =	0.0318
	-0.0004

Bolt Forces Due to Measured Moment Normalised for Beam Rotation									
Bolt 1		Bolt 2		Bolt 3		Bolt 4		Bolt 5	
$H_{mx,1}$	$H_{my,1}$	$H_{mx,2}$	$H_{my,2}$	$H_{mx,3}$	$H_{my,3}$	$H_{mx,4}$	$H_{my,4}$	$H_{mx,5}$	$H_{my,5}$
-31.0852	-2.5052	0.0000	0.0000	31.0852	2.5052	0.0000	0.0000	0.0000	0.0000

Applied Shear Analysis

rox = 1.200 roy = 0.000 ro = 1.200

Row	Column	bolt (y,n)	xcg	xi	ycg	yi	di	Di	Ri	Fy Ri * xi / di	M Ri di	Fx Ri * yi / di	Sign Multiplier	Fx kip	Fy kip
1	1	1	0.00	-1.200	3.00	3.000	3.231	0.340	0.982	-0.365	3.171	-0.911	-1	-1.15	0.46
2	1	1	0.00	-1.200	0.00	0.000	1.200	0.126	0.833	-0.833	1.000	0.000	-1	0.00	1.05
3	1	1	0.00	-1.200	-3.00	-3.000	3.231	0.340	0.982	-0.365	3.171	0.911	-1	1.15	0.46
4	1	0	0.00	0.000	0.00	0.000	0.000	0.000	0.000	0.000	0.000	0.000	0	0.00	0.00
5	1	0	0.00	0.000	0.00	0.000	0.000	0.000	0.000	0.000	0.000	0.000	0	0.00	0.00
						d max =	3.2312	S	2.80	-1.56	7.34	0.00		0.00	1.97

Eccentric Shear ICOR		
e (in)	Vapp (kips)	Rotation (radians)
3.50	1.97	0.08

Total deformation on a bolt	D max	0.34	in
Distance to I.C.O.R.	ro	1.200	in
Eccentricity	ex	3.50	in
	e	3.50	in
Coefficient	C	1.562	

sqrt[Fx^2 + Fy^2] =	1.5621
M/(e + ro) =	1.5622
C =	1.5622
	0.0000

Bolt Forces Due to Eccenctric Shear Normalised for Beam Rotation									
Bolt 1		Bolt 2		Bolt 3		Bolt 4		Bolt 5	
$V_{mx,1}$	$V_{my,1}$	$V_{mx,2}$	$V_{my,2}$	$V_{mx,3}$	$V_{my,3}$	$V_{mx,4}$	$V_{my,4}$	$V_{mx,5}$	$V_{my,5}$
-1.1463	0.4586	0.0000	1.0477	1.1463	0.4586	0.0000	0.0000	0.0000	0.0000

ICOR BOLT SHEAR STRENGTH ANALYSIS

Test: **4ST1**

Specimen: **4STR1**

Bolt Location w/r to Neutral Axis of Beam			
Bolt	Location	Bolt	Location
# of Bolts	4.0	*3*	-1.5
1	4.5	*4*	-4.5
2	1.5	*5*	-

Collected Data At Maximum			
V_{app} (Kips)	M_M (Kip-Inch)	P_M (Kips)	θ (Radians)
5.183	315.351	11.430	0.073

Maximum Bolt Forces - Ultimate Method				
Bolt 1	Bolt 2	Bolt 3	Bolt 4	Bolt 5
26.31	**20.64**	**26.51**	**32.10**	-

Bolt Force Summary For I.C.O.R for Moment only Case Normalized to Primary Axis Due to Beam End										Bolt Force Summary For I.C.O.R for Shear Only										Axial Force Per	
Bolt 1		Bolt 2		Bolt 3		Bolt 4		Bolt 5		Bolt 1		Bolt 2		Bolt 3		Bolt 4		Bolt 5		Axial	Axial Shear
$H_{mx,1}$	$H_{my,1}$	$H_{mx,2}$	$H_{my,2}$	$H_{mx,3}$	$H_{my,3}$	$H_{mx,4}$	$H_{my,4}$	$H_{mx,5}$	$H_{my,5}$	$V_{mx,1}$	$V_{my,1}$	$V_{mx,2}$	$V_{my,2}$	$V_{mx,3}$	$V_{my,3}$	$V_{mx,4}$	$V_{my,4}$	$V_{mx,5}$	$V_{my,5}$	P_x	P_y
-27.43	-1.99	-22.56	-1.64	22.56	1.64	27.43	1.99	0.00	0.00	-1.71	0.99	-0.92	1.60	0.92	1.60	1.71	0.99	0.00	0.00	2.85	-0.21

Measured Moment Analysis

rox = 0.024 roy = 0.000 ro = 0.024

Row	Column	bolt (y,n)	xcg	xi	ycg	yi	di	Di	Ri	Fy Ri * xi / di	M Ri di	Fx Ri * yi / di	Sign Multiplier	Fx kip	Fy kip
1	1	1	0.00	-0.024	4.50	4.500	4.500	0.340	0.982	-0.005	4.417	-0.981	-1	-27.50	0.14
2	1	1	0.00	-0.024	1.50	1.500	1.500	0.113	0.808	-0.013	1.212	-0.808	-1	-22.62	0.36
3	1	1	0.00	-0.024	-1.50	-1.500	1.500	0.113	0.808	-0.013	1.212	0.808	-1	22.62	0.36
4	1	1	0.00	-0.024	-4.50	-4.500	4.500	0.340	0.982	-0.005	4.417	0.981	-1	27.50	0.14
5	1	0	0.00	0.000	0.00	0.000	0.000	0.000	0.000	0.000	0.000	0.000	0	0.00	0.00
						d max =	4.5001	S	3.58	-0.04	11.26	0.00		0.00	1.00

Measured Moment ICOR		
e (in)	Vnorm (kips)	Rotation (radians)
315.35	1.00	0.07

Total deformation on a bolt D max 0.34 in
Distance to I.C.O.R. ro 0.024 in
Eccentricity ex 315.35 in
e 315.35 in
Coefficient C 0.036

sqrt[Fx^2 + Fy^2] = 0.0357
M/(e + ro) = 0.0357
C = 0.0357
0.0000

Bolt Forces Due to Measured Moment Normalised for Beam Rotation									
Bolt 1		Bolt 2		Bolt 3		Bolt 4		Bolt 5	
$H_{mx,1}$	$H_{my,1}$	$H_{mx,2}$	$H_{my,2}$	$H_{mx,3}$	$H_{my,3}$	$H_{mx,4}$	$H_{my,4}$	$H_{mx,5}$	$H_{my,5}$
-27.4258	-1.9942	-22.5644	######	22.5644	1.6408	27.4258	1.9942	0.0000	0.0000

Applied Shear Analysis

rox = 2.604 roy = 0.000 ro = 2.604

Row	Column	bolt (y,n)	xcg	xi	ycg	yi	di	Di	Ri	Fy Ri * xi / di	M Ri di	Fx Ri * yi / di	Sign Multiplier	Fx kip	Fy kip
1	1	1	0.00	-2.604	4.50	4.500	5.199	0.340	0.982	-0.492	5.103	-0.850	-1	-1.71	0.99
2	1	1	0.00	-2.604	1.50	1.500	3.005	0.197	0.920	-0.797	2.766	-0.459	-1	-0.92	1.60
3	1	1	0.00	-2.604	-1.50	-1.500	3.005	0.197	0.920	-0.797	2.766	0.459	-1	0.92	1.60
4	1	1	0.00	-2.604	-4.50	-4.500	5.199	0.340	0.982	-0.492	5.103	0.850	-1	1.71	0.99
5	1	0	0.00	0.000	0.00	0.000	0.000	0.000	0.000	0.000	0.000	0.000	0	0.00	0.00
						d max =	5.1992	S	3.80	-2.58	15.74	0.00		0.00	5.18

Eccentric Shear ICOR		
e (in)	Vapp (kips)	Rotation (radians)
3.50	5.18	0.07

Total deformation on a bolt D max 0.34 in
Distance to I.C.O.R. ro 2.604 in
Eccentricity ex 3.50 in
e 3.50 in
Coefficient C 2.578

sqrt[Fx^2 + Fy^2] = 2.5782
M/(e + ro) = 2.5782
C = 2.5782
0.0000

Bolt Forces Due to Eccentric Shear Normalised for Beam Rotation									
Bolt 1		Bolt 2		Bolt 3		Bolt 4		Bolt 5	
$V_{mx,1}$	$V_{my,1}$	$V_{mx,2}$	$V_{my,2}$	$V_{mx,3}$	$V_{my,3}$	$V_{mx,4}$	$V_{my,4}$	$V_{mx,5}$	$V_{my,5}$
-1.7079	0.9884	-0.9235	1.6033	0.9235	1.6033	1.7079	0.9884	0.0000	0.0000

ICOR BOLT SHEAR STRENGTH ANALYSIS

Test: 4ST1

Specimen: 4STL1

Bolt Location w/r to Neutral Axis of Beam			
Bolt	Location	Bolt	Location
# of Bolts	4.0	3	-1.5
1	4.5	4	-4.5
2	1.5	5	-

Collected Data At Maximum			
V_{app} (Kips)	M_M (Kip-Inch)	P_M (Kips)	θ (Radians)
5.183	334.328	11.027	0.074

Maximum Bolt Forces - Ultimate Method				
Bolt 1	Bolt 2	Bolt 3	Bolt 4	Bolt 5
28.07	22.10	27.77	33.66	-

Bolt Force Summary For I.C.O.R for Moment only Case Normalized to Primary Axis Due to Beam End										Bolt Force Summary For I.C.O.R for Shear Only										Axial Force Per	
Bolt 1		Bolt 2		Bolt 3		Bolt 4		Bolt 5		Bolt 1		Bolt 2		Bolt 3		Bolt 4		Bolt 5		Axial	Axial Shear
$H_{mx,1}$	$H_{my,1}$	$H_{mx,2}$	$H_{my,2}$	$H_{mx,3}$	$H_{my,3}$	$H_{mx,4}$	$H_{my,4}$	$H_{mx,5}$	$H_{my,5}$	$V_{mx,1}$	$V_{my,1}$	$V_{mx,2}$	$V_{my,2}$	$V_{mx,3}$	$V_{my,3}$	$V_{mx,4}$	$V_{my,4}$	$V_{mx,5}$	$V_{my,5}$	P_x	P_y
-29.07	-2.14	-23.92	-1.76	23.92	1.75	29.07	2.14	0.00	0.00	-1.71	0.99	-0.92	1.60	0.92	1.60	1.71	0.99	0.00	0.00	2.75	-0.20

Measured Moment Analysis

rox = 0.022 roy = 0.000 ro = 0.022

Row	Column	bolt (y,n)	xcg	xi	ycg	yi	di	Di	Ri	Fy Ri * xi / di	M Ri di	Fx Ri * yi / di	Sign Multiplier	Fx kip	Fy kip
1	1	1	0.00	-0.022	4.50	4.500	4.500	0.340	0.982	-0.005	4.417	-0.981	-1	-29.15	0.14
2	1	1	0.00	-0.022	1.50	1.500	1.500	0.113	0.808	-0.012	1.212	-0.808	-1	-23.99	0.36
3	1	1	0.00	-0.022	-1.50	-1.500	1.500	0.113	0.808	-0.012	1.212	0.808	-1	23.99	0.36
4	1	1	0.00	-0.022	-4.50	-4.500	4.500	0.340	0.982	-0.005	4.417	0.981	-1	29.15	0.14
5	1	0	0.00	0.000	0.00	0.000	0.000	0.000	0.000	0.000	0.000	0.000	0	0.00	0.00
						d max =	4.5001	S	3.58	-0.03	11.26	0.00		0.00	1.00

Measured Moment ICOR		
e (in)	Vnorm (kips)	Rotation (radians)
334.33	1.00	0.07

Total deformation on a bolt D max 0.34 in
Distance to I.C.O.R. ro 0.022 in
Eccentricity ex 334.33 in
e 334.33 in
Coefficient C 0.034

sqrt[Fx^2 + Fy^2] = 0.0337
M/(e + ro) = 0.0337
C = 0.0337
0.0000

Bolt Forces Due to Measured Moment Normalised for Beam Rotation									
Bolt 1		Bolt 2		Bolt 3		Bolt 4		Bolt 5	
$H_{mx,1}$	$H_{my,1}$	$H_{mx,2}$	$H_{my,2}$	$H_{mx,3}$	$H_{my,3}$	$H_{mx,4}$	$H_{my,4}$	$H_{mx,5}$	$H_{my,5}$
-29.0739	-2.1424	-23.9206	######	23.9206	1.7627	29.0739	2.1424	0.0000	0.0000

Applied Shear Analysis

rox = 2.604 roy = 0.000 ro = 2.604

Row	Column	bolt (y,n)	xcg	xi	ycg	yi	di	Di	Ri	Fy Ri * xi / di	M Ri di	Fx Ri * yi / di	Sign Multiplier	Fx kip	Fy kip
1	1	1	0.00	-2.604	4.50	4.500	5.199	0.340	0.982	-0.492	5.103	-0.850	-1	-1.71	0.99
2	1	1	0.00	-2.604	1.50	1.500	3.005	0.197	0.920	-0.797	2.766	-0.459	-1	-0.92	1.60
3	1	1	0.00	-2.604	-1.50	-1.500	3.005	0.197	0.920	-0.797	2.766	0.459	-1	0.92	1.60
4	1	1	0.00	-2.604	-4.50	-4.500	5.199	0.340	0.982	-0.492	5.103	0.850	-1	1.71	0.99
5	1	0	0.00	0.000	0.00	0.000	0.000	0.000	0.000	0.000	0.000	0.000	0	0.00	0.00
						d max =	5.1992	S	3.80	-2.58	15.74	0.00		0.00	5.18

Eccentric Shear ICOR		
e (in)	Vapp (kips)	Rotation (radians)
3.50	5.18	0.07

Total deformation on a bolt D max 0.34 in
Distance to I.C.O.R. ro 2.604 in
Eccentricity ex 3.50 in
e 3.50 in
Coefficient C 2.578

sqrt[Fx^2 + Fy^2] = 2.5782
M/(e + ro) = 2.5782
C = 2.5782
0.0000

Bolt Forces Due to Eccenctric Shear Normalised for Beam Rotation									
Bolt 1		Bolt 2		Bolt 3		Bolt 4		Bolt 5	
$V_{mx,1}$	$V_{my,1}$	$V_{mx,2}$	$V_{my,2}$	$V_{mx,3}$	$V_{my,3}$	$V_{mx,4}$	$V_{my,4}$	$V_{mx,5}$	$V_{my,5}$
-1.7079	0.9884	-0.9235	1.6033	0.9235	1.6033	1.7079	0.9884	0.0000	0.0000

ICOR BOLT SHEAR STRENGTH ANALYSIS

Test: 4ST2

Specimen: 4STR2

Bolt Location w/r to Neutral Axis of Beam			
Bolt	Location	Bolt	Location
# of Bolts	4.0	3	-1.5
1	4.5	4	-4.5
2	1.5	5	-

Collected Data At Maximum			
Vapp (Kips)	MM (Kip-Inch)	PM (Kips)	θ (Radians)
5.850	331.193	19.206	0.076

Maximum Bolt Forces - Ultimate Method				
Bolt 1	Bolt 2	Bolt 3	Bolt 4	Bolt 5
25.98	19.95	29.70	35.63	-

Bolt Force Summary For I.C.O.R for Moment only Case Normalized to Primary Axis Due to Beam End										Bolt Force Summary For I.C.O.R for Shear Only										Axial Force Per	
Bolt 1		Bolt 2		Bolt 3		Bolt 4		Bolt 5		Bolt 1		Bolt 2		Bolt 3		Bolt 4		Bolt 5		Axial	Axial Shear
$H_{mx,1}$	$H_{my,1}$	$H_{mx,2}$	$H_{my,2}$	$H_{mx,3}$	$H_{my,3}$	$H_{mx,4}$	$H_{my,4}$	$H_{mx,5}$	$H_{my,5}$	$V_{mx,1}$	$V_{my,1}$	$V_{mx,2}$	$V_{my,2}$	$V_{mx,3}$	$V_{my,3}$	$V_{mx,4}$	$V_{my,4}$	$V_{mx,5}$	$V_{my,5}$	P_x	P_y
-28.80	-2.19	-23.69	-1.81	23.69	1.81	28.80	2.19	0.00	0.00	-1.93	1.12	-1.04	1.81	1.04	1.81	1.93	1.12	0.00	0.00	4.79	-0.36

Measured Moment Analysis

rox = 0.022 roy = 0.000 ro = 0.022

Row	Column	bolt (y,n)	xcg	xi	ycg	yi	di	Di	Ri	Fy Ri * xi / di	M Ridi	Fx Ri * yi / di	Sign Multiplier	Fx kip	Fy kip
1	1	1	0.00	-0.022	4.50	4.500	4.500	0.340	0.982	-0.005	4.417	-0.981	-1	-28.88	0.14
2	1	1	0.00	-0.022	1.50	1.500	1.500	0.113	0.808	-0.012	1.212	-0.808	-1	-23.76	0.36
3	1	1	0.00	-0.022	-1.50	-1.500	1.500	0.113	0.808	-0.012	1.212	0.808	-1	23.76	0.36
4	1	1	0.00	-0.022	-4.50	-4.500	4.500	0.340	0.982	-0.005	4.417	0.981	-1	28.88	0.14
5	1	0	0.00	0.000	0.00	0.000	0.000	0.000	0.000	0.000	0.000	0.000	0	0.00	0.00
						di max =	4.5001	S	3.58	-0.03	11.26	0.00		0.00	1.00

Measured Moment ICOR		
e (in)	Vnorm (kips)	Rotation (radians)
331.19	1.00	0.08

Total deformation on a bolt D max 0.34 in
Distance to I.C.O.R. ro 0.022 in
Eccentricity ex 331.19 in
e 331.19 in
Coefficient C 0.034

sqrt[Fx^2 + Fy^2] = 0.0340
M/(e + ro) = 0.0340
C = 0.0340
0.0000

Bolt Forces Due to Measured Moment Normalised for Beam Rotation

Bolt 1		Bolt 2		Bolt 3		Bolt 4		Bolt 5	
$H_{mx,1}$	$H_{my,1}$	$H_{mx,2}$	$H_{my,2}$	$H_{mx,3}$	$H_{my,3}$	$H_{mx,4}$	$H_{my,4}$	$H_{mx,5}$	$H_{my,5}$
-28.7959	-2.1945	-23.6918	######	23.6918	1.8055	28.7959	2.1945	0.0000	0.0000

Applied Shear Analysis

rox = 2.604 roy = 0.000 ro = 2.604

Row	Column	bolt (y,n)	xcg	xi	ycg	yi	di	Di	Ri	Fy Ri * xi / di	M Ridi	Fx Ri * yi / di	Sign Multiplier	Fx kip	Fy kip
1	1	1	0.00	-2.604	4.50	4.500	5.199	0.340	0.982	-0.492	5.103	-0.850	-1	-1.93	1.12
2	1	1	0.00	-2.604	1.50	1.500	3.005	0.197	0.920	-0.797	2.766	-0.459	-1	-1.04	1.81
3	1	1	0.00	2.604	1.50	-1.500	3.005	0.197	0.920	0.797	2.766	0.459	1	1.04	1.81
4	1	1	0.00	-2.604	-4.50	-4.500	5.199	0.340	0.982	-0.492	5.103	0.850	-1	1.93	1.12
5	1	0	0.00	0.000	0.00	0.000	0.000	0.000	0.000	0.000	0.000	0.000	0	0.00	0.00
						di max =	5.1992	S	3.80	-2.58	15.74	0.00		0.00	5.85

Eccentric Shear ICOR		
e (in)	Vapp (kips)	Rotation (radians)
3.50	5.85	0.08

Total deformation on a bolt D max 0.34 in
Distance to I.C.O.R. ro 2.604 in
Eccentricity ex 3.50 in
e 3.50 in
Coefficient C 2.578

sqrt[Fx^2 + Fy^2] = 2.5782
M/(e + ro) = 2.5782
C = 2.5782
0.0000

Bolt Forces Due to Eccentric Shear Normalised for Beam Rotation

Bolt 1		Bolt 2		Bolt 3		Bolt 4		Bolt 5	
$V_{mx,1}$	$V_{my,1}$	$V_{mx,2}$	$V_{my,2}$	$V_{mx,3}$	$V_{my,3}$	$V_{mx,4}$	$V_{my,4}$	$V_{mx,5}$	$V_{my,5}$
-1.9274	1.1154	-1.0422	1.8094	1.0422	1.8094	1.9274	1.1154	0.0000	0.0000

ICOR BOLT SHEAR STRENGTH ANALYSIS

Test: 4ST2

Specimen: 4STL2

Bolt Location w/r to Neutral Axis of Beam			
Bolt	Location	Bolt	Location
# of Bolts	4.0	*3*	-1.5
1	4.5	*4*	-4.5
2	1.5	*5*	-

Collected Data At Maximum			
V_{app} (Kips)	M_M (Kip-Inch)	P_M (Kips)	θ (Radians)
5.850	362.158	18.639	0.076

Maximum Bolt Forces - Ultimate Method				
Bolt 1	Bolt 2	Bolt 3	Bolt 4	Bolt 5
28.82	22.31	31.78	38.19	-

Bolt Force Summary For I.C.O.R for Moment only Case Normalized to Primary Axis Due to Beam End										Bolt Force Summary For I.C.O.R for Shear Only										Axial Force Per	
Bolt 1		Bolt 2		Bolt 3		Bolt 4		Bolt 5		Bolt 1		Bolt 2		Bolt 3		Bolt 4		Bolt 5		Axial	Axial Shear
$H_{mx,1}$	$H_{my,1}$	$H_{mx,2}$	$H_{my,2}$	$H_{mx,3}$	$H_{my,3}$	$H_{mx,4}$	$H_{my,4}$	$H_{mx,5}$	$H_{my,5}$	$V_{mx,1}$	$V_{my,1}$	$V_{mx,2}$	$V_{my,2}$	$V_{mx,3}$	$V_{my,3}$	$V_{mx,4}$	$V_{my,4}$	$V_{mx,5}$	$V_{my,5}$	P_x	P_y
-31.49	-2.41	-25.91	-1.98	25.91	1.98	31.49	2.41	0.00	0.00	-1.93	1.12	-1.04	1.81	1.04	1.81	1.93	1.12	0.00	0.00	4.65	-0.36

Measured Moment Analysis

rox = 0.021 roy = 0.000 ro = 0.021

Row	Column	bolt (y,n)	xcg	xi	ycg	yi	di	Di	Ri	Fy Ri * xi / di	M Ri di	Fx Ri * yi / di	Sign Multiplier	Fx kip	Fy kip
1	1	1	0.00	-0.021	4.50	4.500	4.500	0.340	0.982	-0.004	4.417	-0.981	-1	-31.58	0.14
2	1	1	0.00	-0.021	1.50	1.500	1.500	0.113	0.808	-0.011	1.212	-0.808	-1	-25.98	0.36
3	1	1	0.00	-0.021	-1.50	-1.500	1.500	0.113	0.808	-0.011	1.212	0.808	-1	25.98	0.36
4	1	1	0.00	-0.021	-4.50	-4.500	4.500	0.340	0.982	-0.004	4.417	0.981	-1	31.58	0.14
5	1	0	0.00	0.000	0.00	0.000	0.000	0.000	0.000	0.000	0.000	0.000	0	0.00	0.00
						d max =	4.5000	S	3.58	-0.03	11.26	0.00		0.00	1.00

Measured Moment ICOR		
e (in)	Vnorm (kips)	Rotation (radians)
362.16	1.00	0.08

Total deformation on a bolt	D max	0.34	in
Distance to I.C.O.R.	ro	0.021	in
Eccentricity	ex	362.16	in
	e	362.16	in
Coefficient	C	0.031	

sqrt[Fx^2 + Fy^2] = 0.0311
M/(e + ro) = 0.0311
C = 0.0311
0.0000

Bolt Forces Due to Measured Moment Normalised for Beam Rotation									
Bolt 1		Bolt 2		Bolt 3		Bolt 4		Bolt 5	
$H_{mx,1}$	$H_{my,1}$	$H_{mx,2}$	$H_{my,2}$	$H_{mx,3}$	$H_{my,3}$	$H_{mx,4}$	$H_{my,4}$	$H_{mx,5}$	$H_{my,5}$
-31.4883	-2.4125	-25.9073	######	25.9073	1.9849	31.4883	2.4125	0.0000	0.0000

Applied Shear Analysis

rox = 2.604 roy = 0.000 ro = 2.604

Row	Column	bolt (y,n)	xcg	xi	ycg	yi	di	Di	Ri	Fy Ri * xi / di	M Ri di	Fx Ri * yi / di	Sign Multiplier	Fx kip	Fy kip
1	1	1	0.00	-2.604	4.50	4.500	5.199	0.340	0.982	-0.492	5.103	-0.850	-1	-1.93	1.12
2	1	1	0.00	-2.604	1.50	1.500	3.005	0.197	0.920	-0.797	2.766	-0.459	-1	-1.04	1.81
3	1	1	0.00	-2.604	-1.50	-1.500	3.005	0.197	0.920	-0.797	2.766	0.459	-1	1.04	1.81
4	1	1	0.00	-2.604	-4.50	-4.500	5.199	0.340	0.982	-0.492	5.103	0.850	-1	1.93	1.12
5	1	0	0.00	0.000	0.00	0.000	0.000	0.000	0.000	0.000	0.000	0.000	0	0.00	0.00
						d max =	5.1992	S	3.80	-2.58	15.74	0.00		0.00	5.85

Eccentric Shear ICOR		
e (in)	Vapp (kips)	Rotation (radians)
3.50	5.85	0.08

Total deformation on a bolt	D max	0.34	in
Distance to I.C.O.R.	ro	2.604	in
Eccentricity	ex	3.50	in
	e	3.50	in
Coefficient	C	2.578	

sqrt[Fx^2 + Fy^2] = 2.5782
M/(e + ro) = 2.5782
C = 2.5782
0.0000

Bolt Forces Due to Eccenctric Shear Normalised for Beam Rotation									
Bolt 1		Bolt 2		Bolt 3		Bolt 4		Bolt 5	
$V_{mx,1}$	$V_{my,1}$	$V_{mx,2}$	$V_{my,2}$	$V_{mx,3}$	$V_{my,3}$	$V_{mx,4}$	$V_{my,4}$	$V_{mx,5}$	$V_{my,5}$
-1.9274	1.1154	-1.0422	1.8094	1.0422	1.8094	1.9274	1.1154	0.0000	0.0000

ICOR BOLT SHEAR STRENGTH ANALYSIS

Test: 4ST3

Specimen: 4STR3

Bolt Location w/r to Neutral Axis of Beam			
Bolt	Location	Bolt	Location
# of Bolts	4.0	3	-1.5
1	4.5	4	-4.5
2	1.5	5	-

Collected Data At Maximum			
V_{app} (Kips)	M_M (Kip-Inch)	P_M (Kips)	θ (Radians)
5.504	279.251	16.704	0.076

Maximum Bolt Forces - Ultimate Method				
Bolt 1	Bolt 2	Bolt 3	Bolt 4	Bolt 5
21.96	16.79	25.29	30.37	-

Bolt Force Summary For I.C.O.R for Moment only Case Normalized to Primary Axis Due to Beam End										Bolt Force Summary For I.C.O.R for Shear Only										Axial Force Per	
Bolt 1		Bolt 2		Bolt 3		Bolt 4		Bolt 5		Bolt 1		Bolt 2		Bolt 3		Bolt 4		Bolt 5		Axial	Axial Shear
$H_{mx,1}$	$H_{my,1}$	$H_{mx,2}$	$H_{my,2}$	$H_{mx,3}$	$H_{my,3}$	$H_{mx,4}$	$H_{my,4}$	$H_{mx,5}$	$H_{my,5}$	$V_{mx,1}$	$V_{my,1}$	$V_{mx,2}$	$V_{my,2}$	$V_{mx,3}$	$V_{my,3}$	$V_{mx,4}$	$V_{my,4}$	$V_{mx,5}$	$V_{my,5}$	P_x	P_y
-24.28	-1.84	-19.98	-1.51	19.98	1.51	24.28	1.84	0.00	0.00	-1.81	1.05	-0.98	1.70	0.98	1.70	1.81	1.05	0.00	0.00	4.16	-0.32

Measured Moment Analysis

rox = 0.027 roy = 0.000 ro = 0.027

Row	Column	bolt (y,n)	xcg	xi	ycg	yi	di	Di	Ri	Fy Ri * xi / di	Mi Ri di	Fx Ri * yi / di	Sign Multiplier	Fx kip	Fy kip
1	1	1	0.00	-0.027	4.50	4.500	4.500	0.340	0.982	-0.006	4.417	-0.981	-1	-24.35	0.14
2	1	1	0.00	-0.027	1.50	1.500	1.500	0.113	0.808	-0.014	1.212	-0.807	-1	-20.03	0.36
3	1	1	0.00	-0.027	-1.50	-1.500	1.500	0.113	0.808	-0.014	1.212	0.807	-1	20.03	0.36
4	1	1	0.00	-0.027	-4.50	-4.500	4.500	0.340	0.982	-0.006	4.417	0.981	-1	24.35	0.14
5	1	0	0.00	0.000	0.00	0.000	0.000	0.000	0.000	0.000	0.000	0.000	0	0.00	0.00
						d max =	4.5001	S	3.58	-0.04	11.26	0.00		0.00	1.00

Measured Moment ICOR		
e (in)	Vnorm (kips)	Rotation (radians)
279.25	1.00	0.08

Total deformation on a bolt D max 0.34 in
Distance to I.C.O.R. ro 0.027 in
Eccentricity ex 279.25 in
e 279.25 in
Coefficient C 0.040

sqrt[Fx^2 + Fy^2] = 0.0403
M/(e + ro) = 0.0403
C = 0.0403
0.0000

Bolt Forces Due to Measured Moment Normalised for Beam Rotation

Bolt 1		Bolt 2		Bolt 3		Bolt 4		Bolt 5	
$H_{mx,1}$	$H_{my,1}$	$H_{mx,2}$	$H_{my,2}$	$H_{mx,3}$	$H_{my,3}$	$H_{mx,4}$	$H_{my,4}$	$H_{mx,5}$	$H_{my,5}$
-24.2814	-1.8389	-19.9769	#######	19.9769	1.5129	24.2814	1.8389	0.0000	0.0000

Applied Shear Analysis

rox = 2.604 roy = 0.000 ro = 2.604

Row	Column	bolt (y,n)	xcg	xi	ycg	yi	di	Di	Ri	Fy Ri * xi / di	Mi Ri di	Fx Ri * yi / di	Sign Multiplier	Fx kip	Fy kip
1	1	1	0.00	-2.604	4.50	4.500	5.199	0.340	0.982	-0.492	5.103	-0.850	-1	-1.81	1.05
2	1	1	0.00	-2.604	1.50	1.500	3.005	0.197	0.920	-0.797	2.766	-0.459	-1	-0.98	1.70
3	1	1	0.00	-2.604	-1.50	-1.500	3.005	0.197	0.920	-0.797	2.766	0.459	-1	0.98	1.70
4	1	1	0.00	-2.604	-4.50	-4.500	5.199	0.340	0.982	-0.492	5.103	0.850	-1	1.81	1.05
5	1	0	0.00	0.000	0.00	0.000	0.000	0.000	0.000	0.000	0.000	0.000	0	0.00	0.00
						d max =	5.1992	S	3.80	-2.58	15.74	0.00		0.00	5.50

Eccentric Shear ICOR		
e (in)	Vapp (kips)	Rotation (radians)
3.50	5.50	0.08

Total deformation on a bolt D max 0.34 in
Distance to I.C.O.R. ro 2.604 in
Eccentricity ex 3.50 in
e 3.50 in
Coefficient C 2.578

sqrt[Fx^2 + Fy^2] = 2.5782
M/(e + ro) = 2.5782
C = 2.5782
0.0000

Bolt Forces Due to Eccentric Shear Normalised for Beam Rotation

Bolt 1		Bolt 2		Bolt 3		Bolt 4		Bolt 5	
$V_{mx,1}$	$V_{my,1}$	$V_{mx,2}$	$V_{my,2}$	$V_{mx,3}$	$V_{my,3}$	$V_{mx,4}$	$V_{my,4}$	$V_{mx,5}$	$V_{my,5}$
-1.8137	1.0495	-0.9807	1.7026	0.9807	1.7026	1.8137	1.0495	0.0000	0.0000

ICOR BOLT SHEAR STRENGTH ANALYSIS

Test: 4ST3

Specimen: 4STL3

Bolt Location w/r to Neutral Axis of Beam			
Bolt	Location	Bolt	Location
# of Bolts	4.0	3	-1.5
1	4.5	4	-4.5
2	1.5	5	-

Collected Data At Maximum			
V_{app} (Kips)	M_M (Kip-Inch)	P_M (Kips)	θ (Radians)
5.504	296.546	16.508	0.076

Maximum Bolt Forces - Ultimate Method				
Bolt 1	Bolt 2	Bolt 3	Bolt 4	Bolt 5
23.51	18.08	26.48	31.83	-

Bolt Force Summary For I.C.O.R for Moment only Case Normalized to Primary Axis Due to Beam End										Bolt Force Summary For I.C.O.R for Shear Only										Axial Force Per	
Bolt 1		Bolt 2		Bolt 3		Bolt 4		Bolt 5		Bolt 1		Bolt 2		Bolt 3		Bolt 4		Bolt 5		Axial	Axial Shear
$H_{mx,1}$	$H_{my,1}$	$H_{mx,2}$	$H_{my,2}$	$H_{mx,3}$	$H_{my,3}$	$H_{mx,4}$	$H_{my,4}$	$H_{mx,5}$	$H_{my,5}$	$V_{mx,1}$	$V_{my,1}$	$V_{mx,2}$	$V_{my,2}$	$V_{mx,3}$	$V_{my,3}$	$V_{mx,4}$	$V_{my,4}$	$V_{mx,5}$	$V_{my,5}$	P_x	P_y
-25.79	-1.95	-21.21	-1.61	21.21	1.61	25.79	1.95	0.00	0.00	-1.81	1.05	-0.98	1.70	0.98	1.70	1.81	1.05	0.00	0.00	4.12	-0.31

Measured Moment Analysis

rox = 0.025 roy = 0.000 ro = 0.025

Row	Column	bolt (y,n)	xcg	xi	ycg	yi	di	Di	Ri	Fy Ri * xi / di	M Ri di	Fx Ri * yi / di	Sign Multiplier	Fx kip	Fy kip
1	1	1	0.00	-0.025	4.50	4.500	4.500	0.340	0.982	-0.005	4.417	-0.981	-1	-25.86	0.14
2	1	1	0.00	-0.025	1.50	1.500	1.500	0.113	0.808	-0.014	1.212	-0.808	-1	-21.27	0.36
3	1	1	0.00	-0.025	-1.50	-1.500	1.500	0.113	0.808	-0.014	1.212	0.808	-1	21.27	0.36
4	1	1	0.00	-0.025	-4.50	-4.500	4.500	0.340	0.982	-0.005	4.417	0.981	-1	25.86	0.14
5	1	0	0.00	0.000	0.00	0.000	0.000	0.000	0.000	0.000	0.000	0.000	0	0.00	0.00
						d max =	4.5001	S	3.58	-0.04	11.26	0.00		0.00	1.00

Measured Moment ICOR		
e (in)	Vnurm (kips)	Rotation (radians)
296.55	1.00	0.08

Total deformation on a bolt D max 0.34 in
Distance to I.C.O.R. ro 0.025 in
Eccentricity ex 296.55 in
e 296.55 in
Coefficient C 0.038

sqrt[Fx^2 + Fy^2] = 0.0380
M/(e + ro) = 0.0380
C = 0.0380
0.0000

Bolt Forces Due to Measured Moment Normalised for Beam Rotation

Bolt 1		Bolt 2		Bolt 3		Bolt 4		Bolt 5	
$H_{mx,1}$	$H_{my,1}$	$H_{mx,2}$	$H_{my,2}$	$H_{mx,3}$	$H_{my,3}$	$H_{mx,4}$	$H_{my,4}$	$H_{mx,5}$	$H_{my,5}$
-25.7850	-1.9508	-21.2143	######	21.2143	1.6050	25.7850	1.9508	0.0000	0.0000

Applied Shear Analysis

rox = 2.604 roy = 0.000 ro = 2.604

Row	Column	bolt (y,n)	xcg	xi	ycg	yi	di	Di	Ri	Fy Ri * xi / di	M Ri di	Fx Ri * yi / di	Sign Multiplier	Fx kip	Fy kip
1	1	1	0.00	-2.604	4.50	4.500	5.199	0.340	0.982	-0.492	5.103	-0.850	-1	-1.81	1.05
2	1	1	0.00	-2.604	1.50	1.500	3.005	0.197	0.920	-0.797	2.766	-0.459	-1	-0.98	1.70
3	1	1	0.00	-2.604	-1.50	-1.500	3.005	0.197	0.920	-0.797	2.766	0.459	-1	0.98	1.70
4	1	1	0.00	-2.604	-4.50	-4.500	5.199	0.340	0.982	-0.492	5.103	0.850	-1	1.81	1.05
5	1	0	0.00	0.000	0.00	0.000	0.000	0.000	0.000	0.000	0.000	0.000	0	0.00	0.00
						d max =	5.1992	S	3.80	-2.58	15.74	0.00		0.00	5.50

Eccentric Shear ICOR		
e (in)	Vapp (kips)	Rotation (radians)
3.50	5.50	0.08

Total deformation on a bolt D max 0.34 in
Distance to I.C.O.R. ro 2.604 in
Eccentricity ex 3.50 in
e 3.50 in
Coefficient C 2.578

sqrt[Fx^2 + Fy^2] = 2.578.2
M/(e + ro) = 2.578.2
C = 2.578.2
0.0000

Bolt Forces Due to Eccentric Shear Normalised for Beam Rotation

Bolt 1		Bolt 2		Bolt 3		Bolt 4		Bolt 5	
$V_{mx,1}$	$V_{my,1}$	$V_{mx,2}$	$V_{my,2}$	$V_{mx,3}$	$V_{my,3}$	$V_{mx,4}$	$V_{my,4}$	$V_{mx,5}$	$V_{my,5}$
-1.8137	1.0495	-0.9807	1.7026	0.9807	1.7026	1.8137	1.0495	0.0000	0.0000

ICOR BOLT SHEAR STRENGTH ANALYSIS

Test: 5ST1

Specimen: 5STR1

Bolt Location w/r to Neutral Axis of Beam			
Bolt	Location	Bolt	Location
# of Bolts	5.0	3	0.0
1	6.0	4	-3.0
2	3.0	5	-6.0

Collected Data At Maximum			
Vapp (Kips)	MM (Kip-Inch)	PM (Kips)	θ (Radians)
10.518	549.660	30.315	0.072

Maximum Bolt Forces - Ultimate Method				
Bolt 1	Bolt 2	Bolt 3	Bolt 4	Bolt 5
27.91	24.37	6.45	36.67	40.14

Bolt Force Summary For I.C.O.R for Moment only Case Normalized to Primary Axis Due to Beam End										Bolt Force Summary For I.C.O.R for Shear Only										Axial Force Per	
Bolt 1		Bolt 2		Bolt 3		Bolt 4		Bolt 5		Bolt 1		Bolt 2		Bolt 3		Bolt 4		Bolt 5		Axial	Axial Shear
$H_{mx,1}$	$H_{my,1}$	$H_{mx,2}$	$H_{my,2}$	$H_{mx,3}$	$H_{my,3}$	$H_{mx,4}$	$H_{my,4}$	$H_{mx,5}$	$H_{my,5}$	$V_{mx,1}$	$V_{my,1}$	$V_{mx,2}$	$V_{my,2}$	$V_{mx,3}$	$V_{my,3}$	$V_{mx,4}$	$V_{my,4}$	$V_{mx,5}$	$V_{my,5}$	P_x	P_y
-31.65	-2.27	-28.86	-2.07	0.00	0.00	28.86	2.07	31.65	2.27	-2.29	1.67	-1.55	2.26	0.00	2.66	1.55	2.26	2.29	1.67	6.05	-0.43

Measured Moment Analysis

rox = 0.003 roy = 0.000 ro = 0.003

Row	Column	bolt (y,n)	xcg	xi	ycg	yi	di	Di	Ri	Fy Ri * xi / di	M Ri di	Fx Ri * yi / di	Sign Multiplier	Fx kip	Fy kip
1	1	1	0.00	-0.003	6.00	6.000	6.000	0.340	0.982	0.000	5.889	-0.982	-1	-31.73	0.01
2	1	1	0.00	-0.003	3.00	3.000	3.000	0.170	0.895	-0.001	2.685	-0.895	-1	-28.94	0.03
3	1	1	0.00	-0.003	0.00	0.000	0.003	0.000	0.028	-0.028	0.000	0.000	-1	0.00	0.92
4	1	1	0.00	-0.003	-3.00	-3.000	3.000	0.170	0.895	-0.001	2.685	0.895	-1	28.94	0.03
5	1	1	0.00	-0.003	-6.00	-6.000	6.000	0.340	0.982	0.000	5.889	0.982	-1	31.73	0.01
						d max =	6.0000	S	3.78	-0.03	17.15	0.00		0.00	1.00

Measured Moment ICOR		
e (in)	Vnorm (kips)	Rotation (radians)
549.66	1.00	0.07

Total deformation on a bolt D max 0.34 in
Distance to I.C.O.R. ro 0.003 in
Eccentricity ex 549.66 in
e 549.66 in
Coefficient C 0.031

sqrt[Fx^2 + Fy^2] = 0.0309
M/(e + ro) = 0.0312
C = 0.0312
-0.0003

Bolt Forces Due to Measured Moment Normalised for Beam Rotation

Bolt 1		Bolt 2		Bolt 3		Bolt 4		Bolt 5	
$H_{mx,1}$	$H_{my,1}$	$H_{mx,2}$	$H_{my,2}$	$H_{mx,3}$	$H_{my,3}$	$H_{mx,4}$	$H_{my,4}$	$H_{mx,5}$	$H_{my,5}$
-31.6510	-2.2696	-28.8609	######	0.0000	0.0000	28.8609	2.0696	31.6510	2.2696

Applied Shear Analysis

rox = 4.364 roy = 0.000 ro = 4.364

Row	Column	bolt (y,n)	xcg	xi	ycg	yi	di	Di	Ri	Fy Ri * xi / di	M Ri di	Fx Ri * yi / di	Sign Multiplier	Fx kip	Fy kip
1	1	1	0.00	-4.364	6.00	6.000	7.419	0.340	0.982	-0.577	7.282	-0.794	-1	-2.29	1.67
2	1	1	0.00	-4.364	3.00	3.000	5.296	0.243	0.950	-0.783	5.033	-0.538	-1	-1.55	2.26
3	1	1	0.00	-4.364	0.00	0.000	4.364	0.200	0.923	-0.923	4.029	0.000	-1	0.00	2.66
4	1	1	0.00	-4.364	-3.00	-3.000	5.296	0.243	0.950	-0.783	5.033	0.538	-1	1.55	2.26
5	1	1	0.00	-4.364	-6.00	-6.000	7.419	0.340	0.982	-0.577	7.282	0.794	-1	2.29	1.67
						d max =	7.4194	S	4.79	-3.64	28.66	0.00		0.00	10.52

Eccentric Shear ICOR		
e (in)	Vapp (kips)	Rotation (radians)
3.50	10.52	0.07

Total deformation on a bolt D max 0.34 in
Distance to I.C.O.R. ro 4.364 in
Eccentricity ex 3.50 in
e 3.50 in
Coefficient C 3.644

sqrt[Fx^2 + Fy^2] = 3.6443
M/(e + ro) = 3.6443
C = 3.6443
0.0000

Bolt Forces Due to Eccentric Shear Normalised for Beam Rotation

Bolt 1		Bolt 2		Bolt 3		Bolt 4		Bolt 5	
$V_{mx,1}$	$V_{my,1}$	$V_{mx,2}$	$V_{my,2}$	$V_{mx,3}$	$V_{my,3}$	$V_{mx,4}$	$V_{my,4}$	$V_{mx,5}$	$V_{my,5}$
-2.2909	1.6664	-1.5539	2.2606	0.0000	2.6644	1.5539	2.2606	2.2909	1.6664

ICOR BOLT SHEAR STRENGTH ANALYSIS

Test: 5ST1

Specimen: 5STL1

Bolt Location w/r to Neutral Axis of Beam			
Bolt	Location	Bolt	Location
# of Bolts	5.0	*3*	0.0
1	6.0	*4*	-3.0
2	3.0	*5*	-6.0

Collected Data At Maximum			
V_{app} (Kips)	M_M (Kip-Inch)	P_M (Kips)	θ (Radians)
10.518	624.452	29.919	0.071

Maximum Bolt Forces - Ultimate Method				
Bolt 1	Bolt 2	Bolt 3	Bolt 4	Bolt 5
32.14	28.22	6.37	40.37	44.21

Bolt Force Summary For I.C.O.R for Moment only Case Normalized to Primary Axis Due to Beam End										Bolt Force Summary For I.C.O.R for Shear Only										Axial Force Per	
Bolt 1		Bolt 2		Bolt 3		Bolt 4		Bolt 5		Bolt 1		Bolt 2		Bolt 3		Bolt 4		Bolt 5		Axial	Axial Shear
$H_{mx,1}$	$H_{my,1}$	$H_{mx,2}$	$H_{my,2}$	$H_{mx,3}$	$H_{my,3}$	$H_{mx,4}$	$H_{my,4}$	$H_{mx,5}$	$H_{my,5}$	$V_{mx,1}$	$V_{my,1}$	$V_{mx,2}$	$V_{my,2}$	$V_{mx,3}$	$V_{my,3}$	$V_{mx,4}$	$V_{my,4}$	$V_{mx,5}$	$V_{my,5}$	P_x	P_y
-35.79	-2.55	-32.64	-2.32	0.00	0.00	32.64	2.32	35.79	2.55	-2.29	1.67	-1.55	2.26	0.00	2.66	1.55	2.26	2.29	1.67	5.97	-0.43

Measured Moment Analysis

rox = 0.002 roy = 0.000 ro = 0.002

Row	Column	bolt (y,n)	xcg	xi	ycg	yi	di	Di	Ri	Fy Ri * xi / di	M Ri di	Fx Ri * yi / di	Sign Multiplier	Fx kip	Fy kip
1	1	1	0.00	-0.002	6.00	6.000	6.000	0.340	0.982	0.000	5.889	-0.982	-1	-35.88	0.01
2	1	1	0.00	-0.002	3.00	3.000	3.000	0.170	0.895	-0.001	2.685	-0.895	-1	-32.72	0.02
3	1	1	0.00	-0.002	0.00	0.000	0.002	0.000	0.025	-0.025	0.000	0.000	-1	0.00	0.93
4	1	1	0.00	-0.002	-3.00	-3.000	3.000	0.170	0.895	-0.001	2.685	0.895	-1	32.72	0.02
5	1	1	0.00	-0.002	-6.00	-6.000	6.000	0.340	0.982	0.000	5.889	0.982	-1	35.88	0.01
						d max =	6.0000	S	3.78	-0.03	17.15	0.00		0.00	1.00

Measured Moment ICOR		
e (in)	Vnorm (kips)	Rotation (radians)
624.45	1.00	0.07

Total deformation on a bolt	D max	0.34	in
Distance to I.C.O.R.	ro	0.002	in
Eccentricity	ex	624.45	in
	e	624.45	in
Coefficient	C	0.027	

sqrt[Fx^2 + Fy^2] = 0.0274
M/(e + ro) = 0.0275
C = 0.0275
-0.0001

Bolt Forces Due to Measured Moment Normalised for Beam Rotation									
Bolt 1		Bolt 2		Bolt 3		Bolt 4		Bolt 5	
$H_{mx,1}$	$H_{my,1}$	$H_{mx,2}$	$H_{my,2}$	$H_{mx,3}$	$H_{my,3}$	$H_{mx,4}$	$H_{my,4}$	$H_{mx,5}$	$H_{my,5}$
-35.7904	-2.5492	-32.6354	######	0.0000	0.0000	32.6354	2.3245	35.7904	2.5492

Applied Shear Analysis

rox = 4.364 roy = 0.000 ro = 4.364

Row	Column	bolt (y,n)	xcg	xi	ycg	yi	di	Di	Ri	Fy Ri * xi / di	M Ri di	Fx Ri * yi / di	Sign Multiplier	Fx kip	Fy kip
1	1	1	0.00	-4.364	6.00	6.000	7.419	0.340	0.982	-0.577	7.282	-0.794	-1	-2.29	1.67
2	1	1	0.00	-4.364	3.00	3.000	5.296	0.243	0.950	-0.783	5.033	-0.538	-1	-1.55	2.26
3	1	1	0.00	-4.364	0.00	0.000	4.364	0.200	0.923	-0.923	4.029	0.000	-1	0.00	2.66
4	1	1	0.00	-4.364	-3.00	-3.000	5.296	0.243	0.950	-0.783	5.033	0.538	-1	1.55	2.26
5	1	1	0.00	-4.364	-6.00	-6.000	7.419	0.340	0.982	-0.577	7.282	0.794	-1	2.29	1.67
						d max =	7.4194	S	4.79	-3.64	28.66	0.00		0.00	10.52

Eccentric Shear ICOR		
e (in)	Vapp (kips)	Rotation (radians)
3.50	10.52	0.07

Total deformation on a bolt	D max	0.34	in
Distance to I.C.O.R.	ro	4.364	in
Eccentricity	ex	3.50	in
	e	3.50	in
Coefficient	C	3.644	

sqrt[Fx^2 + Fy^2] = 3.6443
M/(e + ro) = 3.6443
C = 3.6443
0.0000

Bolt Forces Due to Eccenctric Shear Normalised for Beam Rotation									
Bolt 1		Bolt 2		Bolt 3		Bolt 4		Bolt 5	
$V_{mx,1}$	$V_{my,1}$	$V_{mx,2}$	$V_{my,2}$	$V_{mx,3}$	$V_{my,3}$	$V_{mx,4}$	$V_{my,4}$	$V_{mx,5}$	$V_{my,5}$
-2.2909	1.6664	-1.5539	2.2606	0.0000	2.6644	1.5539	2.2606	2.2909	1.6664

ICOR BOLT SHEAR STRENGTH ANALYSIS

Test: 5ST2

Specimen: 5STR2

Bolt Location w/r to Neutral Axis of Beam			
Bolt	Location	Bolt	Location
# of Bolts	5.0	3	0.0
1	6.0	4	-3.0
2	3.0	5	-6.0

Collected Data At Maximum			
V_{app} (Kips)	M_M (Kip-Inch)	P_M (Kips)	θ (Radians)
9.997	568.237	27.525	0.069

Maximum Bolt Forces - Ultimate Method				
Bolt 1	Bolt 2	Bolt 3	Bolt 4	Bolt 5
29.38	25.79	5.90	36.97	40.50

Bolt Force Summary For I.C.O.R for Moment only Case Normalized to Primary Axis Due to Beam End										Bolt Force Summary For I.C.O.R for Shear Only										Axial Force Per	
Bolt 1		Bolt 2		Bolt 3		Bolt 4		Bolt 5		Bolt 1		Bolt 2		Bolt 3		Bolt 4		Bolt 5		Axial	Axial Shear
$H_{mx,1}$	$H_{my,1}$	$H_{mx,2}$	$H_{my,2}$	$H_{mx,3}$	$H_{my,3}$	$H_{mx,4}$	$H_{my,4}$	$H_{mx,5}$	$H_{my,5}$	$V_{mx,1}$	$V_{my,1}$	$V_{mx,2}$	$V_{my,2}$	$V_{mx,3}$	$V_{my,3}$	$V_{mx,4}$	$V_{my,4}$	$V_{mx,5}$	$V_{my,5}$	P_x	P_y
-32.68	-2.27	-29.80	-2.07	0.00	0.00	29.80	2.07	32.68	2.27	-2.18	1.58	-1.48	2.15	0.00	2.53	1.48	2.15	2.18	1.58	5.49	-0.38

Measured Moment Analysis — rox = 0.003, roy = 0.000, ro = 0.003

Row	Column	bolt (y,n)	xcg	xi	ycg	yi	di	Di	Ri	Fy	M	Fx	Sign	Fx	Fy
										Ri * xi / di	Ri di	Ri * yi / di	Multiplier	kip	kip
1	1	1	0.00	-0.003	6.00	6.000	6.000	0.340	0.982	0.000	5.889	-0.982	-1	-32.76	0.01
2	1	1	0.00	-0.003	3.00	3.000	3.000	0.170	0.895	-0.001	2.685	-0.895	-1	-29.87	0.03
3	1	1	0.00	-0.003	0.00	0.000	0.003	0.000	0.028	-0.028	0.000	0.000	-1	0.00	0.92
4	1	1	0.00	-0.003	-3.00	-3.000	3.000	0.170	0.895	-0.001	2.685	0.895	-1	29.87	0.03
5	1	1	0.00	-0.003	-6.00	-6.000	6.000	0.340	0.982	0.000	5.889	0.982	-1	32.76	0.01
						d max =	6.0000	S	3.78	-0.03	17.15	0.00		0.00	1.00

Measured Moment ICOR		
e (in)	Vnorm (kips)	Rotation (radians)
568.24	1.00	0.07

Total deformation on a bolt — D max = 0.34 in
Distance to I.C.O.R. — ro = 0.003 in
Eccentricity — ex = 568.24 in
e = 568.24 in
Coefficient — C = 0.030

sqrt[Fx^2 + Fy^2] = 0.0300
M/(e + ro) = 0.0302
C = 0.0302
0.0002

Bolt Forces Due to Measured Moment Normalised for Beam Rotation									
Bolt 1		Bolt 2		Bolt 3		Bolt 4		Bolt 5	
$H_{mx,1}$	$H_{my,1}$	$H_{mx,2}$	$H_{my,2}$	$H_{mx,3}$	$H_{my,3}$	$H_{mx,4}$	$H_{my,4}$	$H_{mx,5}$	$H_{my,5}$
-32.6798	-2.2723	-29.7990	######	0.0000	0.0000	29.7990	2.0720	32.6798	2.2723

Applied Shear Analysis — rox = 4.364, roy = 0.000, ro = 4.364

Row	Column	bolt (y,n)	xcg	xi	ycg	yi	di	Di	Ri	Fy	M	Fx	Sign	Fx	Fy
										Ri * xi / di	Ri di	Ri * yi / di	Multiplier	kip	kip
1	1	1	0.00	-4.364	6.00	6.000	7.419	0.340	0.982	-0.577	7.282	-0.794	-1	-2.18	1.58
2	1	1	0.00	-4.364	3.00	3.000	5.296	0.243	0.950	-0.783	5.033	-0.538	-1	-1.48	2.15
3	1	1	0.00	-4.364	0.00	0.000	4.364	0.200	0.923	-0.923	4.029	0.000	-1	0.00	2.53
4	1	1	0.00	-4.364	-3.00	-3.000	5.296	0.243	0.950	-0.783	5.033	0.538	-1	1.48	2.15
5	1	1	0.00	-4.364	-6.00	-6.000	7.419	0.340	0.982	-0.577	7.282	0.794	-1	2.18	1.58
						d max =	7.4194	S	4.79	-3.64	28.66	0.00		0.00	10.00

Eccentric Shear ICOR		
e (in)	Vapp (kips)	Rotation (radians)
3.50	10.00	0.07

Total deformation on a bolt — D max = 0.34 in
Distance to I.C.O.R. — ro = 4.364 in
Eccentricity — ex = 3.50 in
e = 3.50 in
Coefficient — C = 3.644

sqrt[Fx^2 + Fy^2] = 3.6443
M/(e + ro) = 3.6443
C = 3.6443
0.0000

Bolt Forces Due to Eccentric Shear Normalised for Beam Rotation									
Bolt 1		Bolt 2		Bolt 3		Bolt 4		Bolt 5	
$V_{mx,1}$	$V_{my,1}$	$V_{mx,2}$	$V_{my,2}$	$V_{mx,3}$	$V_{my,3}$	$V_{mx,4}$	$V_{my,4}$	$V_{mx,5}$	$V_{my,5}$
-2.1773	1.5837	-1.4769	2.1485	0.0000	2.5323	1.4769	2.1485	2.1773	1.5837

ICOR BOLT SHEAR STRENGTH ANALYSIS

Test: 5ST2

Specimen: 5STL2

Bolt Location w/r to Neutral Axis of Beam			
Bolt	Location	Bolt	Location
# of Bolts	5.0	*3*	0.0
1	6.0	*4*	-3.0
2	3.0	*5*	-6.0

Collected Data At Maximum			
V_{app} (Kips)	M_M (Kip-Inch)	P_M (Kips)	θ (Radians)
9.997	624.939	28.050	0.070

Maximum Bolt Forces - Ultimate Method				
Bolt 1	Bolt 2	Bolt 3	Bolt 4	Bolt 5
32.43	28.55	5.99	39.94	43.75

Bolt Force Summary For I.C.O.R for Moment only Case Normalized to Primary Axis Due to Beam End										Bolt Force Summary For I.C.O.R for Shear Only										Axial Force Per	
Bolt 1		Bolt 2		Bolt 3		Bolt 4		Bolt 5		Bolt 1		Bolt 2		Bolt 3		Bolt 4		Bolt 5		Axial	Axial Shear
$H_{mx,1}$	$H_{my,1}$	$H_{mx,2}$	$H_{my,2}$	$H_{mx,3}$	$H_{my,3}$	$H_{mx,4}$	$H_{my,4}$	$H_{mx,5}$	$H_{my,5}$	$V_{mx,1}$	$V_{my,1}$	$V_{mx,2}$	$V_{my,2}$	$V_{mx,3}$	$V_{my,3}$	$V_{mx,4}$	$V_{my,4}$	$V_{mx,5}$	$V_{my,5}$	P_x	P_y
-35.82	-2.50	-32.66	-2.28	0.00	0.00	32.66	2.28	35.82	2.50	-2.18	1.58	-1.48	2.15	0.00	2.53	1.48	2.15	2.18	1.58	5.60	-0.39

Measured Moment Analysis

rox = 0.002 roy = 0.000 ro = 0.002

Row	Column	bolt (y,n)	xcg	xi	ycg	yi	di	Di	Ri	Fy Ri * xi / di	M Ri di	Fx Ri * yi / di	Sign Multiplier	Fx kip	Fy kip
1	1	1	0.00	-0.002	6.00	6.000	6.000	0.340	0.982	0.000	5.889	-0.982	-1	-35.91	0.01
2	1	1	0.00	-0.002	3.00	3.000	3.000	0.170	0.895	-0.001	2.685	-0.895	-1	-32.74	0.02
3	1	1	0.00	-0.002	0.00	0.000	0.002	0.000	0.025	-0.025	0.000	0.000	-1	0.00	0.93
4	1	1	0.00	-0.002	-3.00	-3.000	3.000	0.170	0.895	-0.001	2.685	0.895	-1	32.74	0.02
5	1	1	0.00	-0.002	-6.00	-6.000	6.000	0.340	0.982	0.000	5.889	0.982	-1	35.91	0.01
						d max =	6.0000	S	3.78	-0.03	17.15	0.00		0.00	1.00

Measured Moment ICOR		
e (in)	Vnorm (kips)	Rotation (radians)
624.94	1.00	0.07

Total deformation on a bolt	D max	0.34	in
Distance to I.C.O.R.	ro	0.002	in
Eccentricity	ex	624.94	in
	e	624.94	in
Coefficient	C	0.027	

sqrt[Fx^2 + Fy^2] = 0.0273
M/(e + ro) = 0.0274
C = 0.0274
-0.0001

Bolt Forces Due to Measured Moment Normalised for Beam Rotation									
Bolt 1		Bolt 2		Bolt 3		Bolt 4		Bolt 5	
$H_{mx,1}$	$H_{my,1}$	$H_{mx,2}$	$H_{my,2}$	$H_{mx,3}$	$H_{my,3}$	$H_{mx,4}$	$H_{my,4}$	$H_{mx,5}$	$H_{my,5}$
-35.8208	-2.5046	-32.6631	######	0.0000	0.0000	32.6631	2.2838	35.8208	2.5046

Applied Shear Analysis

rox = 4.364 roy = 0.000 ro = 4.364

Row	Column	bolt (y,n)	xcg	xi	ycg	yi	di	Di	Ri	Fy Ri * xi / di	M Ri di	Fx Ri * yi / di	Sign Multiplier	Fx kip	Fy kip
1	1	1	0.00	-4.364	6.00	6.000	7.419	0.340	0.982	-0.577	7.282	-0.794	-1	-2.18	1.58
2	1	1	0.00	-4.364	3.00	3.000	5.296	0.243	0.950	-0.783	5.033	-0.538	-1	-1.48	2.15
3	1	1	0.00	-4.364	0.00	0.000	4.364	0.200	0.923	-0.923	4.029	0.000	-1	0.00	2.53
4	1	1	0.00	-4.364	-3.00	-3.000	5.296	0.243	0.950	-0.783	5.033	0.538	-1	1.48	2.15
5	1	1	0.00	-4.364	-6.00	-6.000	7.419	0.340	0.982	-0.577	7.282	0.794	-1	2.18	1.58
						d max =	7.4194	S	4.79	-3.64	28.66	0.00		0.00	10.00

Eccentric Shear ICOR		
e (in)	Vapp (kips)	Rotation (radians)
3.50	10.00	0.07

Total deformation on a bolt	D max	0.34	in
Distance to I.C.O.R.	ro	4.364	in
Eccentricity	ex	3.50	in
	e	3.50	in
Coefficient	C	3.644	

sqrt[Fx^2 + Fy^2] = 3.6443
M/(e + ro) = 3.6443
C = 3.6443
0.0000

Bolt Forces Due to Eccenctric Shear Normalised for Beam Rotation									
Bolt 1		Bolt 2		Bolt 3		Bolt 4		Bolt 5	
$V_{mx,1}$	$V_{my,1}$	$V_{mx,2}$	$V_{my,2}$	$V_{mx,3}$	$V_{my,3}$	$V_{mx,4}$	$V_{my,4}$	$V_{mx,5}$	$V_{my,5}$
-2.1773	1.5837	-1.4769	2.1485	0.0000	2.5323	1.4769	2.1485	2.1773	1.5837

ICOR BOLT SHEAR STRENGTH ANALYSIS

Test: 5ST3

Specimen: 5STR3

Bolt Location w/r to Neutral Axis of Beam			
Bolt	Location	Bolt	Location
# of Bolts	5.0	*3*	0.0
1	6.0	*4*	-3.0
2	3.0	*5*	-6.0

Collected Data At Maximum			
V_{app} (Kips)	M_M (Kip-Inch)	P_M (Kips)	θ (Radians)
9.703	541.415	28.901	0.064

Maximum Bolt Forces - Ultimate Method				
Bolt 1	Bolt 2	Bolt 3	Bolt 4	Bolt 5
27.57	24.13	6.13	35.84	39.22

Bolt Force Summary For I.C.O.R for Moment only Case Normalized to Primary Axis Due to Beam End										Bolt Force Summary For I.C.O.R for Shear Only										Axial Force Per	
Bolt 1		Bolt 2		Bolt 3		Bolt 4		Bolt 5		Bolt 1		Bolt 2		Bolt 3		Bolt 4		Bolt 5		Axial	Axial Shear
$H_{mx,1}$	$H_{my,1}$	$H_{mx,2}$	$H_{my,2}$	$H_{mx,3}$	$H_{my,3}$	$H_{mx,4}$	$H_{my,4}$	$H_{mx,5}$	$H_{my,5}$	$V_{mx,1}$	$V_{my,1}$	$V_{mx,2}$	$V_{my,2}$	$V_{mx,3}$	$V_{my,3}$	$V_{mx,4}$	$V_{my,4}$	$V_{mx,5}$	$V_{my,5}$	P_x	P_y
-31.21	-2.01	-28.46	-1.83	0.00	0.00	28.46	1.83	31.21	2.01	-2.11	1.54	-1.43	2.09	0.00	2.46	1.43	2.09	2.11	1.54	5.77	-0.37

Measured Moment Analysis

rox = 0.003 roy = 0.000 ro = 0.003

Row	Column	bolt (y,n)	xcg	xi	ycg	yi	di	Di	Ri	Fy Ri * xi / di	M Ri di	Fx Ri * yi / di	Sign Multiplier	Fx kip	Fy kip
1	1	1	0.00	-0.003	6.00	6.000	6.000	0.340	0.982	0.000	5.889	-0.982	-1	-31.28	0.01
2	1	1	0.00	-0.003	3.00	3.000	3.000	0.170	0.895	-0.001	2.685	-0.895	-1	-28.52	0.03
3	1	1	0.00	-0.003	0.00	0.000	0.003	0.000	0.029	-0.029	0.000	0.000	-1	0.00	0.92
4	1	1	0.00	-0.003	-3.00	-3.000	3.000	0.170	0.895	-0.001	2.685	0.895	-1	28.52	0.03
5	1	1	0.00	-0.003	-6.00	-6.000	6.000	0.340	0.982	0.000	5.889	0.982	-1	31.28	0.01
						d max =	6.0000	S	3.78	-0.03	17.15	0.00		0.00	1.00

Measured Moment ICOR		
e (in)	Vnorm (kips)	Rotation (radians)
541.41	1.00	0.06

Total deformation on a bolt D max 0.34 in
Distance to I.C.O.R. ro 0.003 in
Eccentricity ex 541.41 in
e 541.41 in
Coefficient C 0.032

sqrt[Fx^2 + Fy^2] = 0.0314
M/(e + ro) = 0.0317
C = 0.0317
-0.0003

Bolt Forces Due to Measured Moment Normalised for Beam Rotation									
Bolt 1		Bolt 2		Bolt 3		Bolt 4		Bolt 5	
$H_{mx,1}$	$H_{my,1}$	$H_{mx,2}$	$H_{my,2}$	$H_{mx,3}$	$H_{my,3}$	$H_{mx,4}$	$H_{my,4}$	$H_{mx,5}$	$H_{my,5}$
-31.2129	-2.0098	-28.4614	######	0.0000	0.0000	28.4614	1.8326	31.2129	2.0098

Applied Shear Analysis

rox = 4.364 roy = 0.000 ro = 4.364

Row	Column	bolt (y,n)	xcg	xi	ycg	yi	di	Di	Ri	Fy Ri * xi / di	M Ri di	Fx Ri * yi / di	Sign Multiplier	Fx kip	Fy kip
1	1	1	0.00	-4.364	6.00	6.000	7.419	0.340	0.982	-0.577	7.282	-0.794	-1	-2.11	1.54
2	1	1	0.00	-4.364	3.00	3.000	5.296	0.243	0.950	-0.783	5.033	-0.538	-1	-1.43	2.09
3	1	1	0.00	-4.364	0.00	0.000	4.364	0.200	0.923	-0.923	4.029	0.000	-1	0.00	2.46
4	1	1	0.00	-4.364	-3.00	-3.000	5.296	0.243	0.950	-0.783	5.033	0.538	-1	1.43	2.09
5	1	1	0.00	-4.364	-6.00	-6.000	7.419	0.340	0.982	-0.577	7.282	0.794	-1	2.11	1.54
						d max =	7.4194	S	4.79	-3.64	28.66	0.00		0.00	9.70

Eccentric Shear ICOR		
e (in)	Vapp (kips)	Rotation (radians)
3.50	9.70	0.06

Total deformation on a bolt D max 0.34 in
Distance to I.C.O.R. ro 4.364 in
Eccentricity ex 3.50 in
e 3.50 in
Coefficient C 3.644

sqrt[Fx^2 + Fy^2] = 3.6443
M/(e + ro) = 3.6443
C = 3.6443
0.0000

Bolt Forces Due to Eccenctric Shear Normalised for Beam Rotation									
Bolt 1		Bolt 2		Bolt 3		Bolt 4		Bolt 5	
$V_{mx,1}$	$V_{my,1}$	$V_{mx,2}$	$V_{my,2}$	$V_{mx,3}$	$V_{my,3}$	$V_{mx,4}$	$V_{my,4}$	$V_{mx,5}$	$V_{my,5}$
-2.1134	1.5373	-1.4335	2.0854	0.0000	2.4580	1.4335	2.0854	2.1134	1.5373

ICOR BOLT SHEAR STRENGTH ANALYSIS

Test: 5ST3

Specimen: 5STL3

Bolt Location w/r to Neutral Axis of Beam			
Bolt	Location	Bolt	Location
# of Bolts	5.0	3	0.0
1	6.0	4	-3.0
2	3.0	5	-6.0

Collected Data At Maximum			
V_{app} (Kips)	M_M (Kip-Inch)	P_M (Kips)	θ (Radians)
9.703	619.605	28.775	0.064

Maximum Bolt Forces - Ultimate Method				
Bolt 1	Bolt 2	Bolt 3	Bolt 4	Bolt 5
31.93	28.10	6.11	39.76	43.53

Bolt Force Summary For I.C.O.R for Moment only Case Normalized to Primary Axis Due to Beam End										Bolt Force Summary For I.C.O.R for Shear Only										Axial Force Per	
Bolt 1		Bolt 2		Bolt 3		Bolt 4		Bolt 5		Bolt 1		Bolt 2		Bolt 3		Bolt 4		Bolt 5		Axial	Axial Shear
$H_{mx,1}$	$H_{my,1}$	$H_{mx,2}$	$H_{my,2}$	$H_{mx,3}$	$H_{my,3}$	$H_{mx,4}$	$H_{my,4}$	$H_{mx,5}$	$H_{my,5}$	$V_{mx,1}$	$V_{my,1}$	$V_{mx,2}$	$V_{my,2}$	$V_{mx,3}$	$V_{my,3}$	$V_{mx,4}$	$V_{my,4}$	$V_{mx,5}$	$V_{my,5}$	P_x	P_y
-35.54	-2.29	-32.40	-2.09	0.00	0.00	32.40	2.09	35.54	2.29	-2.11	1.54	-1.43	2.09	0.00	2.46	1.43	2.09	2.11	1.54	5.74	-0.37

Measured Moment Analysis

rox = 0.002 roy = 0.000 ro = 0.002

Row	Column	bolt (y,n)	xcg	xi	ycg	yi	di	Di	Ri	Fy Ri * xi / di	M Ri di	Fx Ri * yi / di	Sign Multiplier	Fx kip	Fy kip
1	1	1	0.00	-0.002	6.00	6.000	6.000	0.340	0.982	0.000	5.889	-0.982	-1	-35.61	0.01
2	1	1	0.00	-0.002	3.00	3.000	3.000	0.170	0.895	-0.001	2.685	-0.895	-1	-32.47	0.02
3	1	1	0.00	-0.002	0.00	0.000	0.002	0.000	0.025	-0.025	0.000	0.000	-1	0.00	0.93
4	1	1	0.00	-0.002	-3.00	-3.000	3.000	0.170	0.895	-0.001	2.685	0.895	-1	32.47	0.02
5	1	1	0.00	-0.002	-6.00	-6.000	6.000	0.340	0.982	0.000	5.889	0.982	-1	35.61	0.01
						di max =	6.0000	S	3.78	-0.03	17.15	0.00		0.00	1.00

Measured Moment ICOR		
e (in)	Vnorm (kips)	Rotation (radians)
619.60	1.00	0.06

Total deformation on a bolt	D max	0.34	in
Distance to I.C.O.R.	ro	0.002	in
Eccentricity	ex	619.60	in
	e	619.60	in
Coefficient	C	0.028	

sqrt[Fx^2 + Fy^2] = 0.0276
M/(e + ro) = 0.0277
C = 0.0277
-0.0001

Bolt Forces Due to Measured Moment Normalised for Beam Rotation

Bolt 1		Bolt 2		Bolt 3		Bolt 4		Bolt 5	
$H_{mx,1}$	$H_{my,1}$	$H_{mx,2}$	$H_{my,2}$	$H_{mx,3}$	$H_{my,3}$	$H_{mx,4}$	$H_{my,4}$	$H_{mx,5}$	$H_{my,5}$
-35.5368	-2.2947	-32.4042	######	0.0000	0.0000	32.4042	2.0924	35.5368	2.2947

Applied Shear Analysis

rox = 4.364 roy = 0.000 ro = 4.364

Row	Column	bolt (y,n)	xcg	xi	ycg	yi	di	Di	Ri	Fy Ri * xi / di	M Ri di	Fx Ri * yi / di	Sign Multiplier	Fx kip	Fy kip
1	1	1	0.00	-4.364	6.00	6.000	7.419	0.340	0.982	-0.577	7.282	-0.794	-1	-2.11	1.54
2	1	1	0.00	-4.364	3.00	3.000	5.296	0.243	0.950	-0.783	5.033	-0.538	-1	-1.43	2.09
3	1	1	0.00	-4.364	0.00	0.000	4.364	0.200	0.923	-0.923	4.029	0.000	-1	0.00	2.46
4	1	1	0.00	-4.364	-3.00	-3.000	5.296	0.243	0.950	-0.783	5.033	0.538	-1	1.43	2.09
5	1	1	0.00	-4.364	-6.00	-6.000	7.419	0.340	0.982	-0.577	7.282	0.794	-1	2.11	1.54
						di max =	7.4194	S	4.79	-3.64	28.66	0.00		0.00	9.70

Eccentric Shear ICOR		
e (in)	Vapp (kips)	Rotation (radians)
3.50	9.70	0.06

Total deformation on a bolt	D max	0.34	in
Distance to I.C.O.R.	ro	4.364	in
Eccentricity	ex	3.50	in
	e	3.50	in
Coefficient	C	3.644	

sqrt[Fx^2 + Fy^2] = 3.6443
M/(e + ro) = 3.6443
C = 3.6443
0.0000

Bolt Forces Due to Eccenctric Shear Normalised for Beam Rotation

Bolt 1		Bolt 2		Bolt 3		Bolt 4		Bolt 5	
$V_{mx,1}$	$V_{my,1}$	$V_{mx,2}$	$V_{my,2}$	$V_{mx,3}$	$V_{my,3}$	$V_{mx,4}$	$V_{my,4}$	$V_{mx,5}$	$V_{my,5}$
-2.1134	1.5373	-1.4335	2.0854	0.0000	2.4580	1.4335	2.0854	2.1134	1.5373

Appendix F

Approximate Shear Tab Limit State Capacities

The following calculations represent the approximate limit states evaluated for the shear tab specimen's various rupture failures which were reported during the experimental testing. All equation references within this appendix refer to the AISC 13th Edition Specification[1]. The connection capacities have been calculated without the use of any specified safety factors as to provide a comparison of ultimate capacities versus experimental data.

F.1 Bolt Shear Rupture (J3-1)

$$R_n = F_n A_b$$
$$\mathrm{R_n} = (60\ \mathrm{ksi}) * \left(\frac{\pi(0.75\ in)^2}{4}\right)$$
$$\mathrm{R_n} = 26.5\ \mathrm{kips}$$

F.2 Bolt Shear Rupture

The following calculations represent the bolt shear rupture capacity as reported per the experimental testing of Kulak *et al.*[2]. The average shear rupture stress was reported as 80.1 ksi for an ASTM A325 bolt.

$$R_n = F_n A_b$$
$$\mathrm{R_n} = (80.1\ \mathrm{ksi}) * \left(\frac{\pi(0.75\ in)^2}{4}\right)$$
$$\mathrm{R_n} = 35.4\ \mathrm{kips}$$

F.2 Net Tension Rupture

The net shear rupture calculation is based on the Whitmore Section described in Part 9 of the AISC 13th Edition Specification.

$$R_n = F_u A_n$$
$$L_w = 2L_h \tan 30$$
$$\mathrm{L_w} = (2)(1.5) \tan 30$$
$$\mathrm{L_w} = 1.732\mathrm{in}.$$

---

[1] American Institute of Steel Construction (AISC). 2005. *Manual of Steel Construction 13th Edition*. Chicago, IL.

[2] Kulak, Geoffrey L., John W. Fisher, John H. A. Struik. 2001. *Guide to Design Criteria for Bolted and Riveted Joints*. 2nd ed. Chicago, Illinois: American Institute of Steel Construction.

$$L_n = L_w - (d_b + 0.125\text{in.})$$
$$L_n = 1.732 - (0.75\text{in.} + 0.125\text{in.})$$
$$L_n = 0.857\text{in.}$$
$$R_n = (58\text{ksi})(0.857\text{in.})(0.375\text{in})$$
$$R_n = 18.64 \text{ kips}$$

F.3 Alternative Net Tension Rupture

The Whitmore Section in Section F.2 has been modified using a range of angles varying from thirty-five to forty degrees to provide a range of capacities.

F.3.1 Alternative Angle of Thirty-five Degrees

$$R_n = F_u A_n$$
$$L_w = 2L_h \tan 35$$
$$L_w = (2)(1.5) \tan 35$$
$$L_w = 2.1\text{in.}$$
$$L_n = L_w - (d_b + 0.125\text{in.})$$
$$L_n = 2.1 - (0.75\text{in.} + 0.125\text{in.})$$
$$L_n = 1.23\text{in.}$$
$$R_n = (58\text{ksi})(1.23\text{in.})(0.375\text{in})$$
$$R_n = 26.6 \text{ kips}$$

F.3.1 Alternative Angle of Forty Degrees

$$R_n = F_u A_n$$
$$L_w = 2L_h \tan 40$$
$$L_w = (2)(1.5) \tan 40$$
$$L_w = 2.52\text{in.}$$
$$L_n = L_w - (d_b + 0.125\text{in.})$$
$$L_n = 2.52 - (0.75\text{in.} + 0.125\text{in.})$$
$$L_n = 1.64\text{in.}$$
$$R_n = (58\text{ksi})(1.64\text{in.})(0.375\text{in})$$
$$R_n = 35.7 \text{ kips}$$

F.4 Localized Block Shear Rupture (J4-5)

$$R_n = U_{bs}F_uA_{nt} + 0.6F_uA_{nv}$$

$$A_{nv} = t_{pl}(L_{ev} - (0.5)(d_b + 0.125in.))$$

A_{nv} =(0.375in.)(1.5in-(0.5)*(0.75in.+0.125in.))

A_{nv}= 0.398 in.^{2}

$$A_{nt} = t_{pl}(L_{ev} - (0.5)(d_b + 0.125in.))$$

A_{nt} = (0.375in.)(1.5in.-(0.5)(0.75in.+0.125in.))

A_{nt} = 0.398 in.^{2}

U_{bs} = 1.0

R_n = (1.0*58ksi*0.398in.^{2})+ (0.6*58ksi*0.398in.^{2})

R_n = 36.9 kips

Appendix G

Experimental Data

The experimental data recorded for this research are available upon request. Contact the Milwaukee School of Engineering campus library for further information on how to obtain access to the experimental data.

Structural Engineering

Capstone Report Approval Form

Master of Science in Structural Engineering – MSST

Milwaukee School of Engineering

This capstone report, entitled "Axial, Shear, and Moment Interaction of Single Plate "Shear Tab" Connections," submitted by the student Scott L. Thompson, has been approved by the following committee:

Faculty Advisor: _____ Date: _____

Christopher Raebel

Faculty Member: _____ Date: _____

Dr. Richard DeVries

Faculty Member: _____ Date: _____

Dr. Hans-Peter Huttelmaier